Chiral perturbation theory for generalized parton distributions and baryon distribution amplitudes

DISSERTATION
ZUR ERLANGUNG DES DOKTORGRADES
DER NATURWISSENSCHAFTEN (DR. RER. NAT.)
DER FAKULTÄT FÜR PHYSIK

DER UNIVERSITÄT REGENSBURG

vorgelegt von

Philipp Wein

aus

Regensburg

im Jahr 2016

Promotionsgesuch eingereicht am: 06.05.2016
Die Arbeit wurde angeleitet von: Prof. Dr. Andreas Schäfer

Prüfungsausschuss:

Vorsitzender:	Prof. Dr. Josef Zweck
1. Gutachter:	Prof. Dr. Andreas Schäfer
2. Gutachter:	Prof. Dr. Vladimir M. Braun
weiterer Prüfer:	Prof. Dr. Ferdinand Evers

Abstract

In this thesis we apply low-energy effective field theory to the first moments of generalized parton distributions and to baryon distribution amplitudes, which are both highly relevant for the parametrization of the nonperturbative part in hard processes. These quantities yield complementary information on hadron structure, since the former treat hadrons as a whole and, thus, give information about the (angular) momentum carried by an entire parton species on average, while the latter parametrize the momentum distribution within an individual Fock state. By performing one-loop calculations within covariant baryon chiral perturbation theory, we obtain sensible parametrizations of the quark mass dependence that are ideally suited for the subsequent analysis of lattice QCD data.

Contents

CHAPTER 1

Introduction

Aside from gravitational effects, the dynamics of elementary particles are described by the Standard Model of particle physics, which comprises electromagnetic, weak and strong interactions mediated by gauge bosons. Electromagnetic and weak effects are, actually, remnants of an underlying unified electroweak theory [1–3], whose spontaneous breaking via the Higgs mechanism [4] gives rise to one massless gauge boson (the photon), which is the gauge boson of quantum electrodynamics (QED), and three massive gauge bosons ($W^{\pm}$ and Z^0), the exchange of which generates the weak force. The strong interaction due to gluon exchange is described by quantum chromodynamics (QCD), which is a Yang–Mills theory [5], i.e., a non-Abelian gauge theory, based on SU(3) gauge symmetry. The corresponding conserved charges are called colors: red, green and blue. In contrast to the Abelian case also the agent of the interaction itself is a color-charge carrier, which leads to gluon self-interaction via the three- and four-gluon vertices. The probably most important consequence of this behavior is that the beta function, which describes the running of the coupling constant, can be negative depending on the number of colors N_c and flavors N_f. In particular for $N_c = 3$ the one-loop beta function is negative as long as $N_f \leq 16$ which is the case for QCD, where $N_f = 6$. Therefore, the strong coupling decreases with increasing four-momentum squared allowing for a perturbative treatment of QCD effects, and, eventually, leads to the asymptotic freedom of quarks and gluons. However, to a large extent the complexity and richness of QCD effects is a consequence of its strong coupling at low energies, where the opposite is the case: the coupling becomes large, denying a perturbative treatment, and the microscopic degrees of freedom (quarks and gluons) are confined to directly observable, colorless hadrons. Even very hard processes with large momentum transfer and relevant distances much smaller than the size of a hadron are influenced by the low-scale dynamics, since all measurements take place after hadronization.

The disentanglement of the short and long range contributions to hard processes is the basic concept behind QCD factorization [6–10], where one rewrites the cross section (in case of inclusive processes) or the scattering amplitude (in case of exclusive reactions) as a convolution of a hard

scattering kernel and a soft part parametrizing the low-energy dynamics. The process-dependent hard scattering part is accessible by perturbation theory in the strong coupling α_s using the usual diagrammatic techniques. The soft part consists of universal, process-independent functions that resolve the inner hadron structure and are intrinsically nonperturbative quantities. Both the hard and the soft parts depend on the factorization scale. The scale dependence is determined by evolution equations. The most prominent example are the DGLAP equations [11–13], which govern the evolution of parton distribution functions (PDFs) relevant in inclusive deep inelastic scattering (DIS). The exact physical cross section has to be independent of the factorization scale. However, in practice one finds that the perturbative expansion is most efficient if one chooses a factorization scale of the order of the large momentum scale of the process (cf., e.g., ref. [14]).

The functions which parametrize the nonperturbative part of the scattering in different experimental setups provide us with manifold information about the internal hadron structure. For instance, ordinary form factors (FFs) are relevant in elastic scattering processes (e.g., $e^- p \to e^- p$) and encode information about the charge distribution. In contrast, the PDFs mentioned above are needed in inclusive deep inelastic reactions, e.g., $e^- p \to e^- X$, where X is not measured and can contain a large number of hadrons and leptons. They can be interpreted as the probability density to find a parton carrying a fraction x of the longitudinal momentum of the parent hadron. As depicted schematically in figure 1.1, these seemingly unrelated concepts are subsumed by generalized parton distributions [15–18] (GPDs, also known as nonforward or off-forward parton distributions), which are relevant for the description of exclusive processes, like deeply virtual Compton scattering (DVCS: $\gamma^*(q)p(p) \to \gamma(q')p(p')$) and deeply virtual meson production (DVMP: e.g., $\gamma^*(q)p(p) \to \rho^0(q')p(p')$). On one hand, in the forward limit $\Delta = p' - p \to 0$, where the initial and final state baryon have the same momentum, GPDs reduce to ordinary PDFs. On the other hand one obtains the usual form factor if one integrates over all momentum fractions x. However, GPDs contain a surplus of information: e.g., the first x-moments of the chiral-even GPDs provide the total angular momentum carried by a specific parton species (for details see chapter 3). Therefore, both experimental measurement and numerical calculation of GPDs provide an important ingredient for the solution of the proton spin puzzle posed by the seminal measurement by the European Muon Collaboration (EMC) [19]. Contrary to the prevalent expectation the latter showed that only a small fraction of the proton spin is composed of the spin of the constituent quarks, which (heuristically) means that the remainder has to originate from the orbital angular momentum of the partons and the gluon spin.

All the nonperturbative functions described in the last paragraph have in common that they parametrize the hadron as a whole, i.e., they do not discriminate between different Fock states. However, in hard exclusive processes with a wide scattering angle and very large momentum transfer between the initial and the final state hadron, only the first few Fock states are relevant (see, e.g., ref. [9]). The heuristic explanation is, that each parton has to change its direction to form an intact hadron in the final state, which requires the exchange of a highly virtual gluon. In this kinematic situation, the relevant nonperturbative functions are distribution amplitudes [8–10] (DAs), which determine how the longitudinal hadron momentum is distributed amongst the

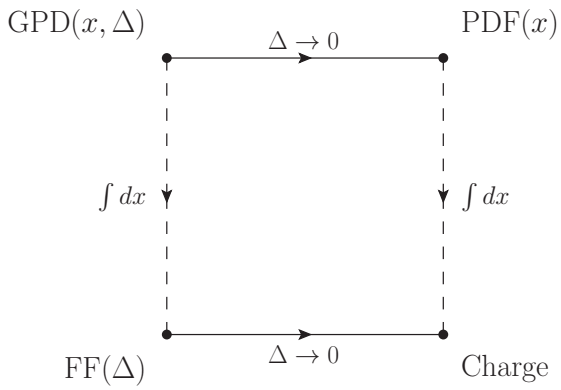

Figure 1.1: As depicted in this schematic diagram, generalized parton distributions unify the seemingly unrelated concepts of form factors and parton distribution functions. All of these functions are independent of the transverse momentum (which is integrated out). One could add a third dimension to this picture by showing also the relation to transverse momentum dependent distribution functions (see, e.g., ref. [20]).

partons within a specific Fock state. The leading contribution for octet baryons are three-quark DAs which will be treated in chapter 4. At asymptotically large momentum transfer (generalized) form factors can be calculated as a convolution of a hard scattering kernel with the distribution amplitudes for the incoming and outgoing hadron. As the momentum transfer decreases, the expansion in Fock states becomes less and less meaningful since one would have to take into account an increasing number of states. Yet, even in such less extreme kinematic situations one can establish a connection between form factors and distribution amplitudes by using light-cone sum rules [21–24], as demonstrated in ref. [25].

Pinning down the functions describing the nonperturbative part from experimental measurements is a highly nontrivial task, since the quantities of interest (e.g., DAs or GPDs) appear in convolutions with a hard scattering kernel. Especially in the exclusive channels one faces the additional difficulty that the final state phase space is very small, and that reactions with a small number of hadrons in the final state are power-suppressed at high momentum transfer. Therefore, statistics for such processes are poor and one needs very high luminosities to obtain exact measurements. Hence, complementary input and guidance from theoretical tools that can be applied in the nonperturbative regime and allow us to narrow down the set of possible models and parametrizations is of vital importance. One option for this task are QCD (or SVZ) sum rules [26–28], where one calculates correlation functions perturbatively, by approximating the full QCD vacuum in terms of a few vacuum condensates, which parametrize the relevant nonperturbative part. Based on the assumption of quark-hadron duality (cf., e.g., ref. [29]) the results can be matched to dispersive integrals over (modeled) hadronic spectral densities. Being computationally cheap, sum rules are even nowadays the most efficient tool to obtain a first qualitative insight into the nonperturbative dynamics. However, mainly due to the approximate description of the vacuum, they suffer from systematic errors which are hard to estimate, but are typically assumed to be $\sim 10\% - 30\%$ depending on the considered quantity. Another method

that can treat nonperturbative quantities is lattice QCD (see, e.g., ref. [30] for an introduction). It is based on the numerical evaluation of the path integral on a finite, discretized, Euclidean spacetime using Monte-Carlo importance sampling. Its first formulation in the seventies [31] was mainly driven by the desire to gain a better qualitative understanding of quark confinement. However, reflecting the (still ongoing) vast hardware and algorithmic development, lattice QCD is metamorphosing into a multi-purpose and high-precision tool in particle physics. In particular simple observables, like hadron masses, can be computed with unprecedented precision (including isospin breaking and QED effects; see ref. [32]). Obvious systematic uncertainties of lattice QCD are discretization and finite volume effects. Others originate from operator renormalization, scale setting and excited state contributions. The latter are particularly relevant for three-point functions, where the distances from the source to the insertion and from the insertion to the sink are relatively small. In addition to that one has to extrapolate the results to the physical point, since most simulations are carried out at unphysically large quark masses, which is computationally cheaper.

Having control over the various systematic uncertainties is a crucial ingredient to obtain reliable quantitative results. Here chiral perturbation theory (ChPT) comes into play, since it allows us to describe the quark mass dependence and also the leading finite volume dependence, which can be traced back to pions "traveling around the box".[1] ChPT is the unique effective field theory (EFT) that reproduces all relevant symmetry properties and symmetry breaking patterns of QCD in the low-energy regime (cf. section 2.1). The calculation of the studied matrix elements within the effective field theory helps to find sensible parametrizations for the low-scale dynamics. E.g., understanding the implications of flavor symmetry and its breaking can be seen as a necessary prerequisite for a successful analysis of lattice data on baryon octet DAs (cf. chapter 4). Additionally, in cases where one already has data points at physical quark masses, ChPT may serve as a tool to spot possible systematic errors (see ref. [33], where such an analysis has been carried out for $\langle x \rangle^{u-d}$ with the help of the results presented in chapter 3).

Let us give a short outline of this work. It consist of two separate projects, which are presented in chapters 3 and 4. Both projects are in large part based on the same theoretical framework, which is set up in chapter 2. Chapter 3 is dedicated to the calculation of the first moments of nucleon generalized parton distributions by the use of two-flavor covariant baryon ChPT. The calculation is carried out at full one-loop accuracy (i.e., all orders that do not yet contain two-loop contributions are taken into account), and thus can be seen as an extension of ref. [34]. Section 3.6 contains a preliminary analysis of QCDSF and RQCD lattice data with two light, mass-degenerate dynamical quark flavors. In chapter 4 we present a baryon ChPT study of baryon octet three-quark DAs to leading one-loop accuracy, which is based on our experience with nucleon wave function normalization constants [35, 36] and with the first and the second moments of nucleon DAs (cf. ref. [37]). However, it exceeds the latter in two central aspects. First, since the calculation is carried out for nonlocal three-quark operators, we obtain results for the complete DAs instead of single moments. Second, we use three (instead of two)

[1] In simulations one usually uses periodic boundary conditions in spatial directions.

quark flavors, which allows us to understand the role of flavor symmetry and flavor symmetry breaking. The results are tailor-made for the analysis of CLS lattice data with $N_f = 2 + 1$ dynamical quark flavors presented in section 4.6. Both main chapters are structured similarly: after an introductory overview, we review the decomposition of the relevant matrix elements in terms of (generalized) form factors and distribution amplitudes, respectively. Next, we perform the operator construction within the effective theory, outline the calculation within baryon chiral perturbation theory (BChPT) and present its results. Finally, we show the application to lattice data and give a summary. We conclude this work and give a short outlook in chapter 5.

CHAPTER 2

Basic concepts

In this chapter we provide the theoretical setup for this work by compiling the relevant textbook knowledge. Section 2.1 contains an exposition of chiral perturbation theory as a low-energy effective field theory for QCD. The properties of the fields under discrete symmetry transformations, which are relevant for the construction of operators within the effective theory, are discussed in section 2.2. Fierz transformations, which are needed for the construction of baryon interpolating currents in chapter 4, are explained in section 2.3.

2.1 Low-energy effective theory for QCD

Due to the confinement of partons to colorless hadrons neither free quarks nor free gluons can appear in the intial and final states of scattering experiments. Therefore, any useful interpretation of QCD cross sections or correlation functions relies on our understanding of the effective (hadronic) degrees of freedom. As will be explained in detail in this section, the observed hadron spectrum indicates that the approximate global chiral symmetry of QCD is broken spontaneously, which yields nearly massless pseudo Goldstone bosons. Owing to a systematic power counting scheme established in ref. [38], the associated effective theory (namely ChPT) can treat the dynamics of the hadron fields perturbatively in the low-energy region. Following a top-down approach, we start our discussion of chiral perturbation theory with an analysis of the QCD Lagrangian, its symmetries and, in cases where it is necessary, their breaking. In doing so, we will take special care of chiral symmetry breaking, since it plays the most important role in the derivation of the effective theory.

2.1.1 Quantum chromodynamics

As already mentioned in the introduction, QCD is a SU(3) gauge theory formulated in terms of $N_c \times N_f = 3 \times 6$ quark and $N_c^2 - 1 = 8$ gluon fields. The quark fields $q_\alpha^{a,i}$ are massive spin $\frac{1}{2}$ fermions (with masses m_a) and carry color ($i = 1, 2, 3$), flavor ($a = u, d, s, c, b, t$) and

Dirac ($\alpha = 1, \ldots, 4$) indices. The gluon fields A^I_μ are massless spin 1 gauge bosons. Being vector fields they carry a Lorentz index ($\mu = 0, \ldots, 3$) in addition to their color index ($I = 1, \ldots, 8$). Using the usual summation convention for Lorentz indices and the Dirac slash notation[1] the gauge-invariant Lagrangian density of QCD has the form[2]

$$\begin{aligned}\mathcal{L}_{\text{QCD}} &= \sum_a \sum_{i,j} \sum_{\alpha,\beta} \bar{q}^{a,i}_\alpha \big(i\not{D}^{ij}_{\alpha\beta} - m_a \delta^{ij}\delta_{\alpha\beta}\big) q^{a,j}_\beta - \tfrac{1}{2}\,\text{tr}_\text{c}\big\{F_{\mu\nu}F^{\mu\nu}\big\} \\ &\equiv \sum_a \bar{q}^a \big(i\not{D} - m_a\big) q^a - \tfrac{1}{2}\,\text{tr}_\text{c}\big\{F_{\mu\nu}F^{\mu\nu}\big\}\ ,\end{aligned} \tag{2.1}$$

where $\bar{q} = q^\dagger\gamma^0$ and tr_c denotes a trace in color space. The second line shows the usual abbreviated form in which color and Dirac indices (and sums over them) are implicit. In perturbative QCD the Lagrangian is usually supplemented with a gauge fixing and (using the wording of [14]) a gauge compensating term in order to remove unphysical degrees of freedom (see the brief discussion below). In eq. (2.1) the gluon fields are hidden within the covariant derivative

$$D_\mu = \partial_\mu + igA_\mu\ , \tag{2.2}$$

and the gluon field strength tensor

$$F_{\mu\nu} = \partial_\mu A_\nu - \partial_\nu A_\mu + ig[A_\mu, A_\nu] = -\frac{i}{g}[D_\mu, D_\nu]\ , \tag{2.3}$$

where g is the strong coupling constant, and A_μ is a 3×3 matrix containing the gluon fields: $A_\mu = \sum_I A^I_\mu t^I$. The t^I are the eight generators of SU(3) related to the Gell-Mann matrices given in appendix A.2 by $t^I = \lambda^I/2$. They obey the commutation relation

$$[t^I, t^J] = i\sum_K f^{IJK} t^K\ , \tag{2.4}$$

which determines the associated structure constants f^{IJK} (see also eq. (A.7)).

One can easily verify that the Lagrangian (2.1) is invariant under the local gauge transformation in color space

$$q(x) \to U(x)q(x)\ , \tag{2.5a}$$

$$A_\mu(x) \to U(x)A_\mu(x)U^\dagger(x) + \frac{i}{g}\big(\partial_\mu U(x)\big)U^\dagger(x)\ , \tag{2.5b}$$

with $U(x) \equiv \exp\big(i\sum_I \theta^I(x)t^I\big)$. To be able to use standard diagrammatic methods (based on the path integral quantization) for the perturbative calculation of loop corrections, one has to remove unphysical degrees of freedom corresponding to gauge-copies of the same physical field configuration (otherwise one cannot write down a gluon propagator). This can be achieved by fixing a gauge with the Faddeev–Popov method [41], where one adds a gauge fixing term and a gauge compensating term to the Lagrangian. The latter contains the ghost fields and does

[1] $\not{a} \equiv a_\mu\gamma^\mu$, where γ^μ are Dirac matrices; cf. appendix A.3.

[2] The QCD Lagrangian and the discussion of its symmetries are part of nearly every quantum field theory textbook. See, e.g., refs. [14, 39, 40].

only affect non-Abelian theories, since it decouples from the theory in the Abelian case. In the modified Lagrangian gauge invariance is superseded by BRST invariance [42, 43]. Anticipating that our subsequent discussions are not affected by the peculiarities of gauge fixing, we content ourselves with two concluding remarks on the issue: first, gauge invariant operators are automatically BRST invariant (see, e.g., ref. [14]), and, second, gauge fixing is not necessary in nonperturbative lattice QCD as long as one restricts oneself to the calculation of gauge invariant quantities.

As most relativistic quantum field theories, QCD contains ultraviolet divergences, which have to be made well-defined by the choice of a regulator. In lattice QCD, e.g., the finite lattice spacing itself is the regulator, since it acts as a momentum cutoff. Within perturbative QCD one usually uses dimensional regularization [44],[3] since it preserves all relevant symmetries throughout the calculation. After the regularization one uses the freedom to rescale the field variables and the parameters of the theory in such a way that all divergences are canceled. This procedure is known as renormalization. The condition that the divergences have to cancel, however, does not completely fix the finite numerical values of intermediate results. This ambiguity can be overcome by the definition of a so-called subtraction scheme, where the modified minimal subtraction ($\overline{\text{MS}}$) scheme [46] is without doubt the most popular choice in perturbative QCD. The definition of a subtraction scheme necessarily involves the introduction of an unphysical scale, whose meaning is directly clear for a cutoff regularization, where it corresponds to the choice of a specific cutoff, but is less intuitive for dimensional regularization (see, e.g., ref. [44]). It should be noted that the exact results for physical observables (say, e.g., a DVCS cross section) have to be scheme and scale independent, while the field theoretical ingredients (in case of DVCS: generalized parton distributions and the hard scattering kernel) are not. In practice, however, it has been shown (cf., e.g., ref. [14]) that the perturbative expansion yields the most precise results if one chooses the renormalization scale in the vicinity of the (large) scale of the process (the virtuality of the exchanged photon in case of DVCS; see, e.g., ref. [18]). A more technical description of the regularization and renormalization procedure will be given in section 2.1.5, where we will discuss its application to chiral perturbation theory.

The Lagrangian (2.1) is (individually) invariant under time reversal ($\mathcal{T}$), charge conjugation ($\mathcal{C}$) and parity ($\mathcal{P}$) transformation. Actually this is not a fundamental condition from the theory side, and the possible occurrence of the so-called theta term (a product of the gluon field strength tensor and its dual $\propto F_{\mu\nu}\tilde{F}^{\mu\nu} = F_{\mu\nu}\epsilon^{\mu\nu\rho\sigma}F_{\rho\sigma}$) has been explored in the literature. It would be a suitable source for strong $\mathcal{CP}$ violation, since it breaks the symmetries under time reversal and space inversion. However, the experimental upper bounds on this term from measurements of the neutron dipole moment are so strict (see, e.g., ref. [47]) that it can be safely ignored in most calculations.

[3] A didactically valuable presentation of dimensional regularization applied to classical electrostatics can be found in ref. [45].

Table 2.1: The table shows the electric charge (in units of the positive elementary charge e) and the quark masses obtained from fits to experimental data taken from ref. [48]. The light quark masses of u, d and s quarks are given at the $\overline{\text{MS}}$ scale $\mu = 2$ GeV. The masses of the heavy quarks are given at the $\overline{\text{MS}}$ scale which equals their own mass. Note that these masses are strongly scheme and scale dependent. E.g., the top mass obtained from a pole-mass definition yields a value that lies roughly 13 GeV higher.

q	mass	charge
u	$2.3^{+0.7}_{-0.5}$ MeV	$+\frac{2}{3}e$
d	$4.8^{+0.5}_{-0.3}$ MeV	$-\frac{1}{3}e$
c	1275 ± 25 MeV	$+\frac{2}{3}e$
s	95 ± 5 MeV	$-\frac{1}{3}e$
t	160^{+5}_{-4} GeV	$+\frac{2}{3}e$
b	4.18 ± 0.03 GeV	$-\frac{1}{3}e$

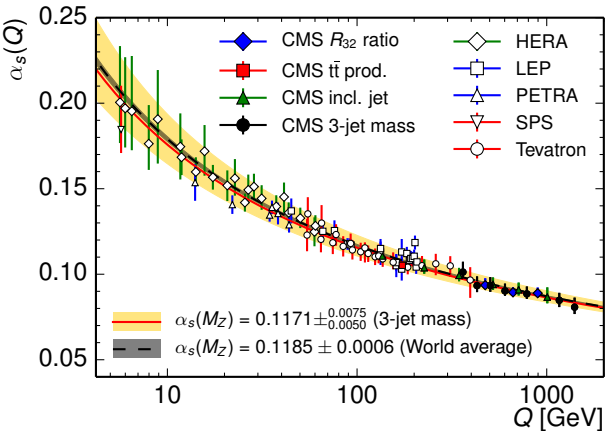

Figure 2.1: The picture shows the running of the strong coupling $\alpha_s = \frac{g^2}{4\pi}$ in the perturbative regime. Here Q corresponds to the $\overline{\text{MS}}$ scale. This figure has been taken from ref. [49].

Pure QCD has seven free parameters that have to be specified and are determined from experiment: the 6 quark masses and the coupling constant given in table 2.1 and figure 2.1, respectively. One immediately notices the strong hierarchy in the quark masses

$$m_u \lesssim m_d \ll m_s < \Lambda_{\text{QCD}} \ll \Lambda_{\text{had.}} < m_c < m_b \ll m_t \ , \tag{2.6}$$

where $\Lambda_{\text{QCD}} \approx 200$ MeV is the typical scale of nonperturbative effects in QCD (to be more specific: it corresponds to the scale where the perturbatively calculated running of the coupling shown in figure 2.1 would diverge) and $\Lambda_{\text{had.}} \approx 1$ GeV is the scale of the lowest-lying nonpseudoscalar hadrons. Since m_u, m_d and m_s have values below the relevant scales of QCD, we may consider them as approximately massless (i.e., we start without masses and introduce them as a small perturbation later on). A reexamination of the fermionic term in the QCD Lagrangian density,

$$\sum_a \bar{q}^a \left(i\not{D} - m_a\right) q^a = \sum_a \left(\bar{q}^a_L i\not{D} q^a_L + \bar{q}^a_R i\not{D} q^a_R - m^a \bar{q}^a_R q^a_L - m^a \bar{q}^a_L q^a_R\right) \ , \tag{2.7}$$

shows that quarks of different chiralities, $q_{L/R} = \gamma_{L/R} q = \frac{1}{2}(\mathbb{1} \mp \gamma_5) q$, are coupled by the mass term only. This enables us to perform symmetry transformations individually on left- and right-handed quarks, such that the QCD Lagrangian is approximately symmetric under global

$$\text{SU}(n_f)_L \otimes \text{SU}(n_f)_R \otimes \text{U}(1)_L \otimes \text{U}(1)_R \ , \tag{2.8}$$

transformations, where n_f is the number of light quarks equal to three or two, depending on whether one treats the strange quark as light or not.[4] On a classical level, these symmetries correspond to the conservation of the currents

$$j^i_{L/R,\mu} = \bar{q}\gamma_\mu\gamma_{L/R}\sigma^i q \ , \qquad j_{L/R,\mu} = \bar{q}\gamma_\mu\gamma_{L/R}\mathbb{1} q \ , \qquad q = \begin{pmatrix} q^u \\ q^d \end{pmatrix} \ , \qquad \text{for } n_f = 2 \ , \tag{2.9a}$$

$$j^i_{L/R,\mu} = \bar{q}\gamma_\mu\gamma_{L/R}\lambda^i q \ , \qquad j_{L/R,\mu} = \bar{q}\gamma_\mu\gamma_{L/R}\mathbb{1} q \ , \qquad q = \begin{pmatrix} q^u \\ q^d \\ q^s \end{pmatrix} \ , \qquad \text{for } n_f = 3 \ , \tag{2.9b}$$

by virtue of the Noether theorem [51]. σ^i and λ^i are Pauli and Gell-Mann matrices acting on flavor space, and the superscript i can take values between 1 and $n_f^2 - 1$. These currents can be combined to the usual vector and axialvector currents:

$$V^i_\mu = j^i_{R,\mu} + j^i_{L,\mu} \ , \qquad A^i_\mu = j^i_{R,\mu} - j^i_{L,\mu} \ , \tag{2.10a}$$

$$V_\mu = j_{R,\mu} + j_{L,\mu} \ , \qquad A_\mu = j_{R,\mu} - j_{L,\mu} \ . \tag{2.10b}$$

It is already clear that, apart from the $\mathrm{U}(1)_V$ case, these currents can only be partially conserved: in the presence of degenerate light quark masses the Lagrangian (2.7) is only invariant under vectorial symmetry transformations. If the masses of the light quarks differ from each other also the $\mathrm{SU}(n_f)_V$ symmetry is broken explicitly. However, the predominant reason for the breaking of the axial symmetries lies elsewhere. $\mathrm{U}(1)_A$ is broken due to the axial anomaly [52], which gives rise to the coupling of η^0 (the physical states η and η' are mixtures of η^0 and η^8) to two gluons and yields a nonvanishing mass of η^0 in the chiral limit (i.e., the limit of vanishing quark masses). In pure QCD without other standard model interactions the currents A^i_μ do not exhibit an anomaly. But, as is well known, the continuity equations for A_μ, A^3_μ and A^8_μ are broken anomalously due to QED effects which opens the electromagnetic decay channels $\pi^0, \eta, \eta' \to \gamma\gamma$. Historically, the $\pi^0 \to \gamma\gamma$ decay was the first measurement of the axial anomaly. It has a branching fraction of $> 98\%$ leading to a rapid decay of the π^0 (compare the mean lifetime $\tau(\pi^0) = 8.4 \times 10^{-17}$ s versus the mean lifetime of the charged pions $\tau(\pi^\pm) = 2.6 \times 10^{-8}$ s due to weak decays; cf. ref. [48]).

Neglecting the explicit breaking of the symmetries for a moment, we find conserved charges for the symmetries which are not broken anomalously in QCD: $\partial_\mu j^\mu = 0$, where j can be V^i, A^i and V from eq. (2.10). Using a simple quantum mechanical argument (see, e.g., ref. [53]) one can show that this leads to the occurrence of hadron multiplets with degenerate mass: being conserved, the currents commute with the QCD Hamiltonian, $[H_{\mathrm{QCD}}, Q] = 0$, such that one finds for any hadronic state $|h\rangle$ at zero three-momentum and with mass m_h

$$H_{\mathrm{QCD}}|h\rangle = m_h|h\rangle \qquad \Rightarrow \qquad H_{\mathrm{QCD}}(Q|h\rangle) = QH_{\mathrm{QCD}}|h\rangle = m_h Q|h\rangle \ , \tag{2.11}$$

i.e., $|h'\rangle = Q|h\rangle$ has the same mass as $|h\rangle$. For the vectorial currents h' has the same parity and lies in the same isospin/flavor multiplet as h. In particular for the $n_f = 2$ case the mass

[4] Yet another symmetry of a massless QCD Lagrangian is conformal symmetry. It is broken by quantum effects and we will not discuss it in detail here. See, e.g., ref. [50] for a review.

degeneracy is realized almost exactly for the isospin multiplets in the hadron spectrum. Recalling the mass differences within the baryon octet (up to $m_\Xi - m_N \approx 377$ MeV; cf. [48]) one immediately sees that this is not the case for $n_f = 3$. This can be attributed to the rather large explicit symmetry breaking due to the strange quark mass. For the axialvector currents h' has inverse parity compared to h, which means that each hadron should have a parity partner of similar mass. This is not the case at all. Even for $n_f = 2$ the mass difference between a nucleon and its (lowest-lying) parity partner is $m_{N^*} - m_N \approx 597$ MeV (cf. [48]). The way out of this dilemma is the interpretation of $|h'\rangle$ as a threshold state $|h\pi\rangle$ with a massless pseudoscalar hadron π. The necessary massless bosons are provided by a well-known mechanism: according to the Nambu–Goldstone theorem [54, 55], N massless bosons (so-called Goldstone bosons (GBs)) occur when a global symmetry created from N generators (in our case $N = n_f^2 - 1$) is broken spontaneously, which means that the Lagrangian is invariant under symmetry transformations, while the ground state is not (a detailed description is given in section 2.1.2). In QCD the symmetry is, in addition, broken explicitly due to nonzero quark masses which provides also the GBs with a mass, and allows us to identify them with the three pions (in case of $n_f = 2$) or the pseudoscalar meson octet (if $n_f = 3$) in the experimentally measured hadron spectrum.

We can summarize that symmetries in QCD are broken in manifold ways: $\mathrm{U}(1)_A$ is broken anomalously and explicitly, $\mathrm{SU}(n_f)_L \otimes \mathrm{SU}(n_f)_R$ is broken spontaneously to $\mathrm{SU}(n_f)_V$,[5] which in turn is broken explicitly. The only global symmetry of those stated above that stays completely intact is $\mathrm{U}(1)_V$, which guarantees exact baryon number conservation.

2.1.2 Spontaneous breaking of the chiral symmetry

Spontaneous symmetry breaking (SSB) is by no means a phenomenon limited to quantum field theories. It can be encountered in nearly every branch of physics. A simple example from classical mechanics is a particle of mass m sliding (without friction) along a ring (with radius R) that rotates around its vertical axis in a gravitational field with angular velocity ω (cf. refs. [57, 58] and figure 2.2(a)). After implementing the constraints the Lagrangian function of such a system reads

$$L = \frac{1}{2} m R^2 \big(\dot{\theta}^2 + \omega^2 \sin^2(\theta)\big) + mgR\cos(\theta) \ , \tag{2.12}$$

where the symmetry under the parity transformation of the angle $\theta \to -\theta$ is evident. Using the Euler–Lagrange equations of motion one finds static solutions if

$$0 = \sin(\theta)\Big(\cos(\theta) - \frac{g}{R\omega^2}\Big) \ . \tag{2.13}$$

For $\omega^2 < \frac{g}{R}$ there is only one stable equilibrium position at $\theta = 0$. However, for larger angular velocities ($\omega^2 > \frac{g}{R}$) the solution at $\theta = 0$ becomes unstable and two ground-state solutions at $\theta = \pm \arccos\big(\frac{g}{R\omega^2}\big)$ occur. In contrast to the Lagrangian, the latter ground states are not symmetric under the parity transformation mentioned above, which means that the symmetry is broken spontaneously.

[5] In ref. [56] it is shown, that a spontaneous breaking of the vectorlike global symmetries is not possible in QCD.

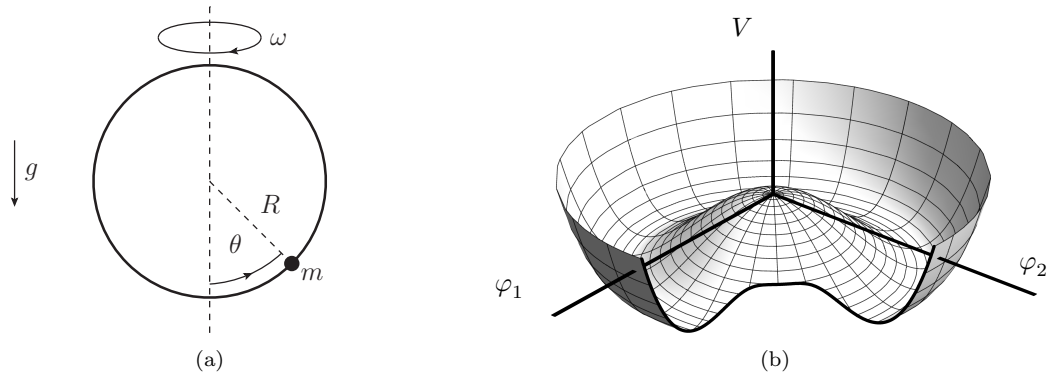

Figure 2.2: Subfigure (a) shows the setup for a massive particle that slides frictionlessly along a hoop rotating around its vertical axis in a gravitational field. This is a simple example from mechanics of a system that exhibits SSB of a discrete symmetry. Subfigure (b) is a plot of the so-called Mexican hat potential V used in eq. (2.14), which is the prime example for a potential that leads to SSB.

The situation described in the last paragraph is an example for the breaking of a discrete symmetry. In the continuous case one has to differentiate between global symmetries and local gauge symmetries. As already mentioned in the last section in the context of chiral symmetry breaking, the spontaneous breaking of a global symmetry leads to the occurrence of a massless boson for each broken generator. Another typical example for SSB of a global symmetry are ferromagnets (below the Curie temperature), where the alignment of the spins in the ground state breaks rotational invariance.[6] As pointed out by Higgs [60, 61], the spontaneous breaking of a gauge symmetry does not necessarily lead to massless bosons. Instead, the affected gauge bosons acquire a mass and a longitudinal degree of freedom.

Let us illustrate the spontaneous breaking of a continuous global symmetry using a complex boson field (this example dates back to Goldstone himself [54]). Consider the Lagrangian density

$$\mathcal{L} = \frac{1}{2}(\partial_\mu \varphi^*)\partial^\mu \varphi - V(\varphi^*\varphi) = \frac{1}{2}(\partial_\mu \varphi^*)\partial^\mu \varphi + \frac{\mu_0^2}{2}\varphi^*\varphi - \frac{\lambda_0}{4}(\varphi^*\varphi)^2 \ , \tag{2.14}$$

where $\varphi = \varphi_1 + i\varphi_2$, with real-valued fields φ_1 and φ_2. Obviously, $\mathcal{L}$ is invariant under phase transformations $\varphi \to e^{i\alpha}\varphi$. The parameter λ_0 has to be positive in order to have a lower bound for the potential. If $\mu_0^2 < 0$ the potential has a unique minimum at $|\varphi| = 0$. For $\mu_0^2 > 0$, however, the potential has a minimum at χ, where $|\chi| = \mu_0/\sqrt{\lambda}$, while the phase is undetermined, which yields an infinite set of possible vacua as illustrated in figure 2.2(b). The choice of a specific phase for the vacuum destroys (or hides) the symmetry. We can expand the Lagrangian (2.14) around the vacuum using the new variable $\varphi' = \varphi - \chi$. For real and positive χ the result reads

$$\mathcal{L} = \frac{1}{2}\big((\partial_\mu \varphi_1')\partial^\mu \varphi_1' - 2\mu_0^2 \varphi_1'^2\big) + \frac{1}{2}(\partial_\mu \varphi_2')\partial^\mu \varphi_2' - \lambda_0 \chi \varphi_1' \varphi'^* \varphi' - \frac{\lambda_0}{4}\big((\varphi'^*\varphi')^2 - \chi^4\big) \ , \tag{2.15}$$

[6] Actually, in the ferromagnet only one Goldstone boson occurs, instead of the two one would expect naively. Such a reduction of GBs in the spectrum can happen in Lorentz-noninvariant systems, if two Goldstone boson modes occur as canonically conjugate pair that corresponds to one joint degree of freedom (see ref. [59]).

where the absence of the mass term for φ_2' identifies it as the Goldstone boson.

Finding the correct low-energy description of QCD is a much less trivial task: since the SSB occurs dynamically on the level of the hadrons, it is an entirely nonperturbative effect, which means that (in contrast to the example above) we do not have direct access to the potential that governs the symmetry breakdown. However, already the knowledge of the underlying group theoretical structure, i.e., $\mathrm{SU}(n_f)_R \otimes \mathrm{SU}(n_f)_L \to \mathrm{SU}(n_f)_V$ in case of QCD, enables us to derive the transformation properties of the Goldstone bosons by group theoretical means. Our description of this procedure follows the derivations given in refs. [62–64] (cf. also [35]). For fundamental group theory definitions the reader may consult ref. [65].

Let $\Phi \in P$ be a field containing the Goldstone bosons, where P is the set of all possible field configurations. We omit the dependence on the spacetime position, since it is not relevant for our discussion (see ref. [64] for details). The operation of the group G on P is given by the mapping

$$f \ : \ G \times P \to P \ , \quad (g, \Phi) \mapsto \Phi' \ , \tag{2.16}$$

where the identity $\mathbb{1} \in G$ has to map each field configuration onto itself, and consecutive action of group elements has to fulfill the group homomorphism property (2.17b). Additionally, we require that all field configurations are connected by symmetry transformations. Hence, we have

$$f(\mathbb{1}, \Phi) = \Phi \ , \tag{2.17a}$$

$$f(g_1, f(g_2, \Phi)) = f(g_1 \circ g_2, \Phi) \ , \tag{2.17b}$$

$$\forall \Phi, \Phi' \in P \ , \ \exists g \in G \ : \ f(g, \Phi) = \Phi' \ . \tag{2.17c}$$

The goal of this paragraph is the determination of f. Using the properties of the mapping f one can check explicitly that the set H of group elements under whose action the ground state (i.e., the orgin of P at $\Phi = 0$) remains unaffected,

$$H = \big\{ g \in G \ \big| \ f(g, 0) = 0 \big\} \ , \tag{2.18}$$

forms a subgroup of G, which is sometimes called the stability group of the origin [66]. Looking at the definition of H, it is clear that it corresponds to the (largest possible) subgroup of G which is not broken spontaneously. Next, we define

$$G\!\diagup_{\!H} = \big\{ gH \ \big| \ g \in G \big\} \ , \tag{2.19}$$

which is the set of all left cosets $gH = \{g \circ h \mid h \in H\}$. For all elements of a left coset f maps the origin onto the same field configuration, which can be easily verified using eq. (2.17b). Hence, f induces a mapping $\tilde{f}$ of the set of left cosets onto the space of Goldstone boson fields:

$$\tilde{f} \ : \ G\!\diagup_{\!H} \to P \ , \quad \tilde{f}(gH) \mapsto f(g, 0) \ . \tag{2.20}$$

This mapping is isomorphic: its surjectivity follows directly from eq. (2.17c), while its injectivity can be proven by showing that for all $g, g' \in G$ it holds $f(g, 0) = f(g', 0) \Rightarrow g' \in gH$:

$$\begin{aligned} 0 = f(\mathbb{1}, 0) = f(g^{-1} \circ g, 0) = f(g^{-1}, f(g, 0)) = f(g^{-1}, f(g', 0)) = f(g^{-1} \circ g', 0) \ , \\ \Rightarrow g^{-1} \circ g' \in H \quad \Rightarrow g' \in gH \ . \end{aligned} \tag{2.21}$$

Therefore, each field configuration $\Phi = f(r_\Phi, 0)$ corresponds to a left coset $r_\Phi H$, where one may choose a convenient representative r_Φ for each left coset. The inherent beauty of this relation is that it allows us to determine the operation of the symmetry group on the Goldstone boson fields (described by f) from the action of the corresponding group elements g on the left coset $r_\Phi H$, which is simply $g \circ r_\Phi H$. The situation can be visualized by the commutative diagram [64]

$$\begin{array}{ccc} \Phi & \xrightarrow{\quad f \quad} & \Phi' \\ \tilde{f}\,\big\uparrow\wr & & \tilde{f}\,\big\uparrow\wr \\ r_\Phi H & \xrightarrow{\quad g \quad} & r'_\Phi H = g \circ r_\Phi H \ . \end{array} \tag{2.22}$$

Thus, the transformation properties of the Goldstone bosons are uniquely determined by the geometry up to reparametrizations of G/H.

After the discussion of the underlying group theory, we may now move on to its practical application in (massless) QCD, where the chiral symmetry group is broken spontaneously to its vectorial subgroup:

$$G = \mathrm{SU}(n_f)_L \otimes \mathrm{SU}(n_f)_R = \big\{(L,R) \;\big|\; L,R \in \mathrm{SU}(n_f)\big\} \ , \tag{2.23a}$$

$$H = \mathrm{SU}(n_f)_V = \big\{(V,V) \;\big|\; V \in \mathrm{SU}(n_f)\big\} \ . \tag{2.23b}$$

We can now choose a representative r_Φ for $g_\Phi H$, with $g_\Phi = (L_\Phi, R_\Phi) \in G$, that is characterized by a unique matrix $U_\Phi \in \mathrm{SU}(n_f)$ [64]:

$$\begin{aligned} g_\Phi H &= (L_\Phi, R_\Phi)H = (L_\Phi, R_\Phi L_\Phi^\dagger L_\Phi)H = (\mathbb{1}, R_\Phi L_\Phi^\dagger) \circ (L_\Phi, L_\Phi)H \\ &= (\mathbb{1}, R_\Phi L_\Phi^\dagger)H \equiv (\mathbb{1}, U_\Phi)H \ , \end{aligned} \tag{2.24}$$

i.e., we choose the representative always in such a way that the first component is the identity. This choice is particularly convenient, since it leads to a simple transformation behavior of the representative matrix:[7]

$$\begin{aligned} \Phi' &\cong r_{\Phi'} H = (\mathbb{1}, U_{\Phi'})H \\ &\overset{!}{=} g \circ r_\Phi H = (L,R) \circ (\mathbb{1}, U_\Phi)H = (L, RU_\Phi L^\dagger L)H = (\mathbb{1}, RU_\Phi L^\dagger)H \ , \\ &\Rightarrow U_{\Phi'} = RU_\Phi L^\dagger \ . \end{aligned} \tag{2.25}$$

Hence, we can represent the Goldstone pseudoscalars by a $\mathrm{SU}(n_f)$ matrix U (we will drop the index from now on) with simple transformation properties and the remaining freedom amounts to the choice of a parametrization for $\mathrm{SU}(n_f)$ matrices. A widespread and (for most purposes) convenient choice are canonical coordinates

$$U = e^{i\frac{\Phi}{F_0}} \ , \text{ with } \begin{cases} \Phi = \sum_{i=1}^{3} \phi^i \sigma^i \ , \text{ for } n_f = 2 \ , \\ \Phi = \sum_{i=1}^{8} \phi^i \lambda^i \ , \text{ for } n_f = 3 \ , \end{cases} \tag{2.26}$$

[7] Fixing the second component to be the identity and using the first one as the representative would be similarly convenient, and would lead to the transformation $U_{\Phi'} = LU_\Phi R^\dagger$, which is also found in the literature.

where σ^i and λ^i correspond to Pauli and Gell-Mann matrices, respectively, and F_0 is the pion decay constant in the chiral limit [67]. The ϕ^i are real-valued such that Φ is Hermitian ($\Phi^\dagger = \Phi$). The components of Φ can be identified with the pseudoscalar mesons:[8]

$$\Phi = \sqrt{2} \begin{pmatrix} \frac{1}{\sqrt{2}}\pi^0 & \pi^+ \\ \pi^- & -\frac{1}{\sqrt{2}}\pi^0 \end{pmatrix} \text{ , for } n_f = 2 \text{ ,} \tag{2.27a}$$

$$\Phi = \sqrt{2} \begin{pmatrix} \frac{1}{\sqrt{2}}\pi^0 + \frac{1}{\sqrt{6}}\eta & \pi^+ & K^+ \\ \pi^- & -\frac{1}{\sqrt{2}}\pi^0 + \frac{1}{\sqrt{6}}\eta & K^0 \\ K^- & \bar{K}^0 & -\frac{2}{\sqrt{6}}\eta \end{pmatrix} \text{ , for } n_f = 3 \text{ ,} \tag{2.27b}$$

which corresponds to the convention where $F_\pi = F_0 + \mathcal{O}(m_\pi^2, m_K^2, m_\eta^2) \approx 92\,\text{MeV}$. After the choice of a parametrization, eq. (2.25) fixes the transformation properties of the Goldstone bosons. For all parametrizations that map the origin ($\Phi = 0$) onto the identity one finds that the pseudoscalar fields transform particularly simple under chiral rotations along the unbroken vectorial subgroup: $\Phi' = V\Phi V^\dagger$. For general chiral rotations the transformation law is nonlinear (one therefore speaks of a nonlinear realization of chiral symmetry, cf. refs. [66, 68]) and depends on the explicit choice of parametrization. Note that the seeming ambiguity due to the free choice of a parametrization is not a problem, since all possible realizations of the symmetry are equivalent [68].

2.1.3 Meson chiral perturbation theory

In the last section we have derived the general form of the Goldstone boson fields occurring in an effective theory of QCD. They can be represented by a unique SU(n_f) matrix U, which has a definite transformation behavior under chiral rotations (see eq. (2.25)). At low energies $E \ll \Lambda_{\text{had.}}$ the heavier particles in the hadron spectrum decouple from the theory, i.e., they can be integrated out, see, e.g., ref. [69]. Hence, an effective Lagrangian for massless QCD can only consist of combinations of the field U and derivatives, that are invariant under both Lorentz transformations and chiral rotations. Unfortunately, there are infinitely many possible contributions and an arbitrary choice of terms would automatically lead to a model dependence. The solution to this problem is chiral perturbation theory, which is based on the observation that every occurrence of a derivative in a vertex leads to a suppression by a factor $p \propto E/\Lambda_{\text{had.}}$. Therefore, we can arrange the terms in the effective Lagrangian according to their order in p denoted by the superscript in parentheses:

$$\mathcal{L}_M = \mathcal{L}_M^{(2)} + \mathcal{L}_M^{(4)} + \mathcal{L}_M^{(6)} + \dots \ . \tag{2.28}$$

The series contains only even powers of p due to Lorentz invariance, and starts at 2, since the only zeroth order term $\text{tr}\left\{U^\dagger U\right\} = n_f$ is an irrelevant constant. However, this approach would be pointless if one would have to evaluate an infinite number of Feynman loop diagrams in order to obtain a result to a desired accuracy, say p^D. That this is not the case is guaranteed by the

[8] One should note that this identification fixes the phase conventions.

Weinberg power counting theorem [38], which provides the order D of a Feynman diagram in terms of the number of loops N_L and the number of vertices $N_M^{(n)}$ from $\mathcal{L}_M^{(n)}$:

$$D = (d-2)N_L + 2 + \sum_n (n-2)N_M^{(n)} \ , \tag{2.29}$$

where we are usually interested in the case with spacetime dimension $d = 4$. Using dimensional regularization the respective diagram is suppressed by a factor p^D. Thus, for any given order p^D the number of loops in the contributing Feynman diagrams is limited to $N_L \leq \frac{D}{2} - 1$. The lowest order part of the effective Lagrangian is rather simple. In the massless case it consists of one term only:

$$\mathcal{L}_M^{(2)}\Big|_{m_q=0} = \frac{F_0^2}{4} \operatorname{tr}\left\{(\partial_\mu U^\dagger)\partial^\mu U\right\} \ , \tag{2.30}$$

where the coefficient is (by convention) chosen in such a way that (after expanding the exponential U) the prefactor of the kinetic term for the mesons is independent of the decay constant. As argued in ref. [70], $4\pi F_0 \simeq 1\,\text{GeV}$ plays the role of the chiral symmetry breaking scale $\Lambda_{\text{had.}}$. One can show that all other possible contributions of lowest order are either equivalent or vanish by using the identities

$$0 = (\partial_\mu U)U^\dagger + U(\partial_\mu U^\dagger) = (\partial_\mu U^\dagger)U + U^\dagger(\partial_\mu U) \ , \tag{2.31a}$$

$$0 = \operatorname{tr}\left\{(\partial_\mu U)U^\dagger\right\} = \operatorname{tr}\left\{(\partial_\mu U^\dagger)U\right\} \ . \tag{2.31b}$$

As expected, $\mathcal{L}_M^{(2)}\big|_{m_q=0}$ does not contain a mass term for the pseudoscalar fields.

So far we have only considered the chiral limit, where the quarks are massless. However, in the real world, chiral symmetry is broken explicitly due to finite quark masses. In order to implement the explicit breaking systematically into the low-energy theory, we apply the source field formalism developed in refs. [67, 71]: in this formalism one implements the coupling of massless QCD to external (color-singlet) vector, axialvector, scalar and pseudoscalar background fields by adding the appropriate source term

$$\begin{aligned} \mathcal{L}_S[v_\mu, a_\mu, s, p] &= \bar{q}(\gamma^\mu v_\mu + \gamma^\mu\gamma_5 a_\mu)q - \bar{q}(s - i\gamma_5 p)q \\ &= \bar{q}_R\gamma^\mu(v_\mu + a_\mu)q_R + \bar{q}_L\gamma^\mu(v_\mu - a_\mu)q_L - \bar{q}_R(s+ip)q_L - \bar{q}_L(s-ip)q_R \ . \end{aligned} \tag{2.32}$$

to the Lagrangian of massless QCD. The external fields are Hermitian matrices in flavor space. Disregarding the anomalous breaking described in section 2.1.1, which would yield corrections starting from $\mathcal{O}(p^4)$ [71], the full theory is invariant under *local* chiral rotations

$$q_R(x) \to R(x)q_R(x) \ , \quad q_L(x) \to L(x)q_L(x) \ , \quad \text{where } R(x), L(x) \in \mathrm{U}(n_f) \ , \tag{2.33}$$

if the external fields transform as follows:

$$(v_\mu + a_\mu) \to R(v_\mu + a_\mu)R^\dagger + iR\partial_\mu R^\dagger \ , \tag{2.34a}$$

$$(v_\mu - a_\mu) \to L(v_\mu - a_\mu)L^\dagger + iL\partial_\mu L^\dagger \ , \tag{2.34b}$$

$$(s + ip) \to R(s+ip)L^\dagger \ . \tag{2.34c}$$

The last term in the transformation law for the right- and left-handed vector fields ($r_\mu = v_\mu + a_\mu$ and $l_\mu = v_\mu - a_\mu$) allows us to interpret the vectorial part of the source term as the second half of a covariant derivative, and is therefore responsible for the upgrade of the global symmetry (in pure QCD) to a local gauge symmetry (in the full theory). Obviously, one can restore massless QCD by setting all external fields to zero. However, the beauty of the formalism lies in the fact that one can evaluate nontrivial background field configurations. In particular, we obtain the case we are interested in (massive QCD), by setting v_μ, a_μ and p to zero, and the scalar field to its nonvanishing vacuum expectation value $s = \mathcal{M}$, where $\mathcal{M}$ is the diagonal quark mass matrix. Actually, $\mathcal{M}$ is diagonal, because we define the quark fields to be the mass eigenstates of the theory.

To introduce the explicit chiral symmetry breaking also in the low-energy theory, we simply have to add all possible scalar source terms to the theory. By setting them to the correct vacuum expectation value the quark masses are taken into account systematically. The two possible structures of lowest order including scalar and pseudoscalar source terms are

$$\mathrm{tr}\left\{(s+ip)U^\dagger \pm (s+ip)^\dagger U\right\} \ . \tag{2.35}$$

They have positive/negative parity (under parity transformation $s \to s$, $p \to -p$ and $U \leftrightarrow U^\dagger$ together with an inversion of the position in space; see also section 2.2) and, therefore, only the "+" combination is relevant for the leading Lagrangian density. In the limit $s = \mathcal{M}$ and $p = 0$ the latter reads

$$\mathcal{L}_M^{(2)} = \frac{F_0^2}{4}\,\mathrm{tr}\left\{\partial_\mu U^\dagger \partial^\mu U\right\} + \frac{F_0^2 B_0}{2}\,\mathrm{tr}\left\{\mathcal{M}\big(U + U^\dagger\big)\right\} \ , \tag{2.36}$$

where B_0 is the so-called condensate parameter in the chiral limit. The additional term provides the pseudoscalar Goldstone bosons with a mass, thereby promoting them to pseudo Goldstone bosons. Since the mass enters the propagator at the same level as the momentum, it turns out to be convenient to count the quark mass matrix (or rather scalar and pseudoscalar external fields) as order p^2 in the ChPT bookkeeping, which explains why we have added the lowest order source term to $\mathcal{L}_M^{(2)}$. With this choice also the hierarchical order in the EFT Lagrangian (2.28) and the power counting formula (2.29) hold unchanged. The higher order Lagrangians of the meson sector are not relevant for the projects presented in this work. We refer the reader to refs. [67, 71] for more details. A review of state of the art calculations in the mesonic sector at two-loop order (i.e., $\mathcal{O}(p^6)$) can be found in ref. [72].

To conclude this section, let us emphasize that the effective field theory we have constructed is Lorentz-covariant. Hence, the requirement for low energies of the external particles only has to be fulfilled in one freely choosable frame, and one can boost the result to any frame of interest, which means that ChPT is actually applicable to a much larger set of problems than one might think at first sight.

2.1.4 Baryon chiral perturbation theory

So far we have only considered a low-energy theory of QCD that was limited to the dynamics of the pseudo Goldstone bosons. This section is dedicated to the inclusion of $J^P = \frac{1}{2}^+$ ground-

state baryons. We restrict ourselves to the cases where one baryon occurs in the initial and one in the final state. The main obstacle connected to the description of baryons within the low-energy theory is their nonzero mass in the chiral limit, which introduces an additional large scale $m_0 \sim \Lambda_{\text{had.}}$ into the theory. Therefore, only the baryon three-momentum can be required to be small (of order p^1 in the ChPT counting scheme), while its energy is large (order p^0). In particular in loop diagrams containing both baryonic and mesonic propagators, the additional scale leads to problems with the usual power counting, whose solution will be addressed in section 2.1.5. One usually works in a quenched approximation, i.e., closed baryonic loops are neglected,[9] anticipating that they can be integrated out, and that their effect is parametrized by low-energy constants (LECs) without loss of generality.

The baryons are built from three valence quarks and should, therefore, be classified into flavor multiplets that transform under the following irreducible representations of the vectorial subgroup

$$2 \otimes 2 \otimes 2 = 2 \oplus 2 \oplus 4 \ , \qquad \text{for } n_f = 2 \ , \tag{2.37a}$$

$$3 \otimes 3 \otimes 3 = 1 \oplus 8 \oplus 8 \oplus 10 \ , \ \text{for } n_f = 3 \ . \tag{2.37b}$$

Since the vectorial subgroup is only broken explicitly due to quark mass differences, the baryons within one multiplet are mass-degenerate, as long as the masses of the light quarks are equal. The totally antisymmetric flavor structure (corresponding to 1) cannot occur in ground-state baryons (i.e., baryons with a symmetric spatial wave function), since this would require a totally antisymmetric spin wave function. The latter is simply impossible for the same reason for which no singlet flavor structure occurs in the two-flavor case: one cannot form a structure that is totally antisymmetric in three indices, if one has only two possible values for the indices to choose from. The four- and ten-dimensional representations lead to totally symmetric flavor multiplets corresponding to the Delta baryons and the full baryon decuplet, respectively, which have spin $\frac{3}{2}$. Of the two remaining two-dimensional (eight-dimensional) multiplets one has a mixed-symmetric and one a mixed-antisymmetric flavor structure, i.e., they are symmetric/antisymmetric under exchange of the flavors of the first and the second quark. However, under exchange of the third quark with one of the others, the two multiplets do mix with each other, such that only one doublet (octet) occurs in the hadron spectrum. In ChPT, the spin $\frac{1}{2}$ baryons are usually represented by the nucleon doublet (in case of $n_f = 2$) or by a traceless 3×3 matrix which contains the octet (in case of $n_f = 3$) [74]:

$$n_f = 2: \quad \Psi = \begin{pmatrix} p \\ n \end{pmatrix} \ , \tag{2.38a}$$

$$n_f = 3: \quad B = \begin{pmatrix} \frac{1}{\sqrt{2}}\Sigma^0 + \frac{1}{\sqrt{6}}\Lambda & \Sigma^+ & p \\ \Sigma^- & -\frac{1}{\sqrt{2}}\Sigma^0 + \frac{1}{\sqrt{6}}\Lambda & n \\ \Xi^- & \Xi^0 & -\frac{2}{\sqrt{6}}\Lambda \end{pmatrix} \equiv \kappa_p p + \kappa_n n + \dots \ , \tag{2.38b}$$

[9] Note, that this does not at all mean that the resulting theory is a description of quenched QCD (for such a variety of ChPT see, e.g., ref. [73]). We simply refer to the methodical similarity of neglecting closed fermionic loops.

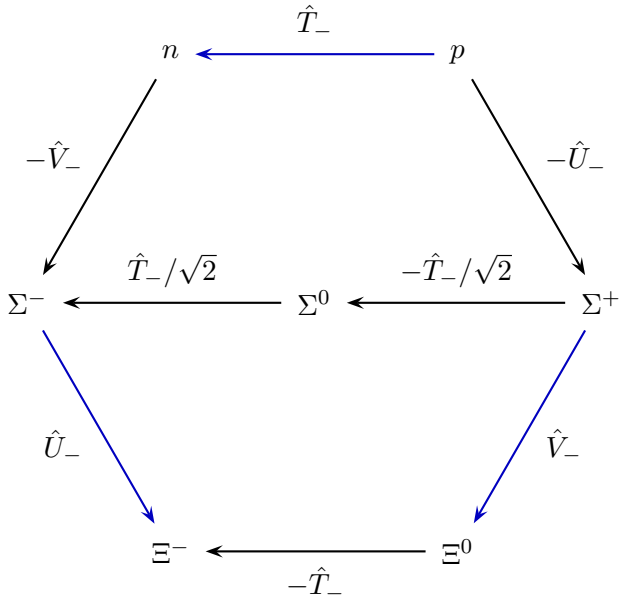

Figure 2.3: Illustration of our phase conventions. The Λ baryon is not shown since one needs a linear combination for the construction of its wave function, cf. eq. (2.41c). The blue arrows will be relevant in chapter 4. They indicate the cases where one has to apply a Fierz transformation (see ref. [76]) to relate the distribution amplitudes at the symmetric point. An explicit calculation shows that this always yields an additional minus sign that has to be taken into account in order to reproduce eq. (4.73) and eq. (4.74). This figure is taken from our work [75] and was created by M. Gruber.

where the second line defines the matrices κ_B. The choice of phases (or rather the absence of them) in these definitions fixes our phase conventions to a large extent (cf. also our article [75]). To see this, consider the isospin ($\hat{T}_-$), u-spin ($\hat{U}_-$) and v-spin ($\hat{V}_-$) lowering operators, which are defined via their action on specific quark flavors: $\hat{T}_- u = d$, $\hat{U}_- d = s$, $\hat{V}_- u = s$ and zero otherwise. If one identifies the flavors u, d and s with the first, second and third unit vector in a three-dimensional space, respectively, the matrix representations of the lowering operators read

$$T_- = \begin{pmatrix} 0 & 0 & 0 \\ 1 & 0 & 0 \\ 0 & 0 & 0 \end{pmatrix} , \qquad U_- = \begin{pmatrix} 0 & 0 & 0 \\ 0 & 0 & 0 \\ 0 & 1 & 0 \end{pmatrix} , \qquad V_- = \begin{pmatrix} 0 & 0 & 0 \\ 0 & 0 & 0 \\ 1 & 0 & 0 \end{pmatrix} . \tag{2.39}$$

We now identify each baryon B with the associated 3×3 matrix κ_B and we further define the action of the lowering operators $\hat{T}_-$, $\hat{U}_-$ and $\hat{V}_-$ on the octet by the usual expressions for the adjoint representation without any additional phase factors:

$$\hat{T}_- \kappa_B = [T_-, \kappa_B] , \qquad \hat{U}_- \kappa_B = [U_-, \kappa_B] , \qquad \hat{V}_- \kappa_B = [V_-, \kappa_B] . \tag{2.40}$$

The above choices specify our phase conventions. Starting from the proton state, the complete

octet can be constructed by applying the following transformations as illustrated in figure 2.3:[10]

$$\hat{T}_-|p\rangle = |n\rangle \ , \qquad -\hat{V}_-\hat{U}_-|p\rangle = |\Xi^0\rangle \ , \qquad \hat{T}_-\hat{V}_-\hat{U}_-|p\rangle = |\Xi^-\rangle \ , \tag{2.41a}$$

$$-\hat{U}_-|p\rangle = |\Sigma^+\rangle \ , \qquad \tfrac{1}{\sqrt{2}}\hat{T}_-\hat{U}_-|p\rangle = |\Sigma^0\rangle \ , \qquad \tfrac{1}{2}\hat{T}_-\hat{T}_-\hat{U}_-|p\rangle = |\Sigma^-\rangle \ , \tag{2.41b}$$

$$\tfrac{-1}{\sqrt{6}}\big(\hat{V}_- + \hat{U}_-\hat{T}_-\big)|p\rangle = |\Lambda\rangle \, . \tag{2.41c}$$

Starting from the mixed-symmetric and mixed-antisymmetric flavor wave functions for the proton defined as

$$|\mathrm{MS}, p\rangle = \frac{1}{\sqrt{6}}(2|uud\rangle - |udu\rangle - |duu\rangle) \ , \qquad |\mathrm{MA}, p\rangle = \frac{1}{\sqrt{2}}(|udu\rangle - |duu\rangle) \ , \tag{2.42}$$

the wave functions of the octet can now be constructed by applying the transformations in (2.41); cf. tables 4.5 and 4.6 on page 85.

As explained above, the behavior of the spin $\frac{1}{2}$ baryon fields under vectorial transformations is fixed. However, the transformation law for nonvectorial chiral rotations can be chosen freely, and one may even choose different transformation properties for the baryons of opposed handedness. For an arbitrary chiral rotation $g = (L, R)$ the most general transformation law reads

$$\left.\begin{aligned} &\Psi_L \to K_l(g)\Psi_L \ , \ K_l(g) \in \mathrm{SU}(2) \\ &\Psi_R \to K_r(g)\Psi_R \ , \ K_r(g) \in \mathrm{SU}(2) \end{aligned}\right\} \begin{aligned} &K_l(g) = K_r(g) = V \ , \\ &\text{for } g = (V, V) \ , \ V \in \mathrm{SU}(2) \ , \end{aligned} \tag{2.43}$$

for two light flavors, and

$$\left.\begin{aligned} &B_L \to K_{1l}(g) B_L K_{2l}^\dagger(g) \ , \ K_{il}(g) \in \mathrm{SU}(3) \\ &B_R \to K_{1r}(g) B_R K_{2r}^\dagger(g) \ , \ K_{ir}(g) \in \mathrm{SU}(3) \end{aligned}\right\} \begin{aligned} &K_{1l}(g) = K_{2l}(g) = K_{1r}(g) = K_{2r}(g) = V \ , \\ &\text{for } g = (V, V) \ , \ V \in \mathrm{SU}(3) \ , \end{aligned} \tag{2.44}$$

in the three-flavor case. I.e., there are many possible realizations of chiral symmetry for baryonic fields. However, all of them are equivalent to each other, since one can switch from one to another by field redefinitions (see refs. [74, 77] for detailed explanations). Obviously, one will make use of this freedom and select the most convenient one. We choose the realization which is commonly used in contemporary BChPT applications, since it combines two advantageous properties: its definition is parity invariant and only derivative couplings to Goldstone boson fields occur. To this end, let us define a new matrix-valued field $u = \exp\{i\Phi/(2F_0)\}$, which contains the GBs and fulfills $u^2 = U$. This fixes the transformation properties under chiral rotations to

$$u \to u' = RuK^\dagger = KuL^\dagger \ , \tag{2.45}$$

in order to reproduce the transformation properties of the original field U. That the compensator field $K = (u')^{-1}Ru = (Ru^2L^\dagger)^{-\frac{1}{2}}Ru$ is slightly unhandy does not have to bother us, since its explicit form will not be needed. However, one immediately notices that K is a local transformation and, accordingly, we will have to define a suitable covariant derivative (see below). One can convince oneself that K meets the conditions stated above (see eqs. (2.43) and (2.44)) for the case $g = (L, R) = (V, V)$:

$$U = u^2 \to KuL^\dagger RuK^\dagger = KuV^\dagger VuK^\dagger = KUK^\dagger \stackrel{!}{=} VUV^\dagger \ . \tag{2.46}$$

[10] These phase conventions have been worked out in collaboration with M. Gruber.

Hence, we can choose the baryon fields to transform as $\Psi \to K\Psi$ and $B \to KBK^\dagger$, where we do not make use of the possibility to discriminate transformation properties for left- and right-handed fields. Suitable chiral building blocks for the mesonic and source fields (transforming as $X \to KXK^\dagger$) read

$$u_\mu = i\big(u^\dagger \partial_\mu u - u \partial_\mu u^\dagger\big) \ , \tag{2.47}$$

$$\chi^\pm = u^\dagger \chi u^\dagger \pm u \chi^\dagger u \ , \tag{2.48}$$

where $\chi = s + ip \to 2B_0\mathcal{M}$ implements explicit chiral symmetry breaking without additional external fields (cf. explanation in section 2.1.3). Sometimes u_μ is called the chiral vielbein. The covariant derivative is defined as

$$D_\mu \Psi = (\partial_\mu + \Gamma_\mu)\Psi \ , \tag{2.49a}$$

$$D_\mu X = \partial_\mu X + [\Gamma_\mu, X] \ , \text{ with } X \in \{B, \bar{B}, u_\nu, \chi^\pm\} \ , \tag{2.49b}$$

where the chiral connection Γ_μ has to transform under chiral rotations as

$$\Gamma_\mu \to K\Gamma_\mu K^\dagger + K(\partial_\mu K^\dagger) \ , \tag{2.50}$$

in order to obtain a similar behavior for the covariant derivatives as for the fields themselves. Having introduced the local transformation behavior by hand, it is clear that the chiral connection does not correspond to a new gauge field. Instead, it is composed of Goldstone boson fields[11]

$$\Gamma_\mu = \frac{1}{2}\big(u^\dagger \partial_\mu u + u \partial_\mu u^\dagger\big) \ . \tag{2.51}$$

As already discussed at the beginning of this section, the baryon mass has to be counted as zeroth order in the chiral counting scheme and, correspondingly, four-derivatives acting on baryonic fields are not suppressed. However, the free equation of motion is fulfilled exactly in the chiral limit and the interaction terms are of first chiral order. Hence, the combination $i\not{D} - m_0$ has to be counted as $\mathcal{O}(p^1)$ and the expansion of the meson-baryon Lagrangian in ChPT starts at first order:

$$\mathcal{L}_{MB} = \mathcal{L}_{MB}^{(1)} + \mathcal{L}_{MB}^{(2)} + \mathcal{L}_{MB}^{(3)} + \dots \ . \tag{2.52}$$

In contrast to the mesonic sector the chiral order is not restricted to even values, since the occurrence of a four-vector does not automatically lead to a suppression by one order in p. Allowing only for terms that are separately invariant under charge conjugation, parity transformation and time reversal[12] the lowest order two-flavor meson-baryon Lagrangian reads [77, 78]

$$\mathcal{L}_{MB}^{(1)}\Big|_{n_f=2} = \bar{\Psi}\Big(i\not{D} - m_0 + \frac{g_A}{2}\gamma_\mu\gamma_5 u^\mu\Big)\Psi \ , \tag{2.53}$$

[11] In the presence of external fields one would need additional terms, see, e.g., ref. [77].

[12] I.e., one ignores contributions due to a theoretically possible (but experimentally unsupported) theta term.

where g_A is the axial coupling constant in the chiral limit. The first order meson-baryon Lagrangian for three light quark flavors taken from ref. [79] reads:

$$\mathcal{L}_{MB}^{(1)}\Big|_{n_f=3} = \mathrm{tr}\left\{\bar{B}i\not{D}B\right\} - m_0\,\mathrm{tr}\left\{\bar{B}B\right\} + \frac{D}{2}\,\mathrm{tr}\left\{\bar{B}\gamma_\mu\gamma_5\{u^\mu, B\}\right\} + \frac{F}{2}\,\mathrm{tr}\left\{\bar{B}\gamma_\mu\gamma_5[u^\mu, B]\right\} \ . \tag{2.54}$$

This version differs from that of refs. [77, 80] by a minus sign in the terms containing the low-energy constants D and F in order to be consistent with the standard sign convention $g_A \approx D + F > 0$. For our calculation in chapter 3 we also need a term from the second order two-flavor Lagrangian

$$\mathcal{L}_{MB}^{(2)}\Big|_{n_f=2} = c_1\,\mathrm{tr}\left\{\chi^+\right\}\bar{\Psi}\Psi + \dots \ . \tag{2.55}$$

For a full list of terms up to fourth order in two-flavor ChPT we refer the reader to ref. [81]. The three-flavor Lagrangian up to third order is presented in ref. [82]. Since the Feynman diagrams in BChPT also contain fermion propagators, one has to adjust the power counting formula, which then reads [83]

$$D = (d-2)N_L + 1 + \sum_n (n-2)N_M^{(n)} + \sum_n (n-1)N_{MB}^{(n)} \ , \tag{2.56}$$

where $N_M^{(n)}$ and $N_{MB}^{(n)}$ are the number of vertices from the meson and meson-baryon Lagrangian of n-th order, respectively, and d is the spacetime dimension. As in the meson case, for each order D the number of possible loops N_L is limited. The problem is, that in loop diagrams containing baryon propagators not all occurring scales are small such that a diagram of order D is actually only suppressed by a factor $m_0^k p^l \propto p^l$ with $k + l = D$. It is absolutely crucial that one finds a way to eliminate the contributions which violate the power counting (those with chiral order $l < D$), since, otherwise, one would have to calculate an infinite number of Feynman diagrams to reach an accuracy of p^D. Possible solutions to this problem will be discussed in the next section.

2.1.5 Regularization and renormalization

As almost all relativistic quantum field theories chiral perturbation theory contains ultraviolet divergences in loop contributions that have to be taken care of. After making the results well-defined by employing a suitable regulator (in perturbation theory, e.g., a fractional dimension or a momentum cutoff), the divergences are canceled by fine-tuned counterterms that have to be added to the Lagrangian in order to make the theory meaningful. As outlined in section 2.1.1, QCD relies only on a finite number of counterterms which can be obtained by rescaling the field variables and the parameters of the Lagrangian. Theories that require an infinite set of counterterms are called nonrenormalizable, which has the negative connotation of being nonpredictive due to the unlimited number of free parameters. While this is a major problem for fundamental field theories, the situation is different for effective field theories, where the cutoff has a physical

meaning and marks the mass scale of the particles which have been integrated out: at any given order in the power counting the effective theory can be renormalized with a finite number of counterterms such that its predictive power persists. Actually, one does not have to add a single structure to the ChPT Lagrangians, since they contain all possible terms from the beginning. Still, the increasing number of parameters at higher orders is a generic feature of effective field theories and, in practice (due to the limited amount of data), one has to restrict oneself to a certain accuracy (in the perturbative series) to get a meaningful result. The terminological problems which arise if one tries to apply the concept of renormalizablity to EFTs is apparent: on one hand, ChPT is not renormalizable in the usual sense to all orders (i.e., one needs an infinite number of counterterms), but, on the other hand, it is perfectly renormalizable order by order in the chiral counting, which is all one needs.

Let us now get back to the power counting violation in BChPT stated at the end of section 2.1.4. Historically, the first solution to this problem was obtained by treating the baryons as heavy, nonrelativistic particles. This approach is called heavy baryon ChPT (HBChPT) and detailed discussions can be found, e.g., in refs. [84, 85]. However, as explained in ref. [86], this approach has the deficiency that the corresponding perturbative series does not converge in the whole low-energy region. In particular production thresholds in triangle diagrams are problematic (cf. discussion in chapter 3). Another, slightly more elegant approach, which keeps Lorentz invariance intact throughout the calculation, is based on the idea to treat the power counting violating terms in a similar way as ultraviolet divergences: cancel them by the introduction of suitable counterterms. While such a renormalization procedure is automatically well-defined for the terms which violate the power counting, it leaves an ambiguity in the treatment of analytic higher order contributions which forces us to choose a specific scheme. The most trivial ansatz is a scheme which performs a minimal subtraction, known as modified infrared regularization ($\overline{\text{IR}}$, see ref. [87]), where one only removes the terms which violate the power counting and leaves the remaining terms untouched. Another popular scheme on the market is the extended on mass shell (EOMS) renormalization, see, e.g., refs. [88, 89]. The scheme we will use is infrared regularization[13] (IR, proposed in ref. [86]), where one removes all terms from loop integrals of fractional dimension that occur with integer chiral order. The advantage of the latter choice is that it can be implemented directly in the loop integrals via a particularly simple prescription (see below). Furthermore, it is defined in such a way that the power counting formula (2.56) also holds for noninteger spacetime dimensions d: i.e., a Feynman diagram that has (fractional) order D according to eq. (2.56) will only contain terms that are suppressed by p^{D+k}, where $k = 0, 1, 2, \ldots$, but no integer powers of p. While the latter property is not a necessity, it is still a nice feature.

[13] Infrared regularization is sometimes also called infrared renormalization in the literature, which actually describes the situation even better than the original name.

In order to clarify which parts of the Feynman diagrams are subtracted in the IR scheme, we will analyze arbitrary one-loop graphs following ref. [86]. Their general form reads

$$\frac{1}{i}\int \frac{d^dq}{(2\pi)^d}\frac{q^{\mu_1}\cdots q^{\mu_r}}{a_1\cdots a_k b_1\cdots b_l}\ , \tag{2.57}$$

where the a_i and b_i are the denominators of meson and nucleon propagators, respectively, and are defined as

$$a_i = m_\pi^2 - (q-K_i)^2 - i\epsilon\ , \qquad\qquad b_i = m_0^2 - (q-P_i)^2 - i\epsilon\ , \tag{2.58}$$

the K_i and P_i being external momenta. Using Feynman parametrization (see, e.g., ref. [39])

$$\frac{1}{x_1^{\alpha_1}\cdots x_k^{\alpha_k}} = \frac{\Gamma(\alpha_1+\cdots+\alpha_k)}{\Gamma(\alpha_1)\cdots\Gamma(\alpha_k)}\int_0^1 du_1\cdots du_k \frac{\delta\big(1-\sum_i u_i\big)u_1^{\alpha_1-1}\cdots u_l^{\alpha_k-1}}{(u_1x_1+\cdots+u_kx_k)^{\alpha_1+\cdots+\alpha_k}}\ , \tag{2.59}$$

we can combine all mesonic and all baryonic propagators such that, after a shift in the integration variable, the result can be written as a sum over integrals of the form

$$\int dUdV \frac{1}{i}\int \frac{d^dq}{(2\pi)^d}\frac{q^{\mu_1}\cdots q^{\mu_s}}{a^k b^l}\ , \tag{2.60}$$

where $s\leq r$. The integration over Feynman parameters is indicated by dU (and dV), which represents the integration measure, the prefactor and the numerator stemming from the application of eq. (2.59) to the meson (baryon) propagators. The denominator is given by

$$a = m^2 - q^2 - i\epsilon\ , \qquad\qquad b = M^2 - (p-q)^2 - i\epsilon\ , \tag{2.61}$$

where $m=m(u)$, $M=M(v)$ and $p=p(u,v)$ are functions of the Feynman parameters, external momenta and masses, with m being $\mathcal{O}(p^1)$, while M and p are $\mathcal{O}(p^0)$ in the chiral counting. For the case $k=l=1$ one simply has $m=m_\pi$ and $M=m_0$. For the explicit calculation of the nontrivial cases with three propagators, which will be needed in chapter 3 on generalized parton distributions, see appendix A.4.2. The Feynman parameter integrals $\int dUdV$ are not relevant for the power counting discussion, and, therefore, we will ignore them for the rest of this section. In an actual calculation one would perform them at the very end. Note, however, that already in the seemingly simple cases involving three propagators (i.e., the triangle diagrams occurring in chapter 3) one has to evaluate these integrals numerically, since an analytic integration over these Feynman parameters is not possible. Next, making use of Lorentz invariance, we can perform a tensor decomposition such that every integral can be expressed in terms of scalar integrals

$$H_{k,l} = \frac{1}{i}\int \frac{d^dq}{(2\pi)^d}\frac{1}{a^k b^l}\ . \tag{2.62}$$

For an explicit tensor decomposition up to four open Lorentz indices see appendix A.4.3. For the calculation of $H_{k,l}$ we, again, use Feynman parametrization to combine the meson and baryon parts of the denominator

$$H_{k,l} = \frac{\Gamma(k+l)}{\Gamma(k)\Gamma(l)}\int_0^1 dz\ \bar{z}^{k-1}z^{l-1}\ \frac{1}{i}\int\frac{d^dq}{(2\pi)^d}\frac{1}{(\bar{z}a+zb)^{k+l}}\ , \tag{2.63}$$

where $\bar{z} = 1 - z$. This integral can be split into the so-called infrared singular part $I_{k,l}$ and the regular part $R_{k,l}$, where $H_{k,l} = I_{k,l} + R_{k,l}$. The infrared singular and regular parts are defined as

$$I_{k,l} = \frac{\Gamma(k+l)}{\Gamma(k)\Gamma(l)} \int_0^\infty dz\ \bar{z}^{k-1} z^{l-1}\ \frac{1}{i} \int \frac{d^d q}{(2\pi)^d} \frac{1}{(\bar{z}a + zb)^{k+l}}\ , \tag{2.64a}$$

$$R_{k,l} = \frac{\Gamma(k+l)}{\Gamma(k)\Gamma(l)} \int_\infty^1 dz\ \bar{z}^{k-1} z^{l-1}\ \frac{1}{i} \int \frac{d^d q}{(2\pi)^d} \frac{1}{(\bar{z}a + zb)^{k+l}}\ , \tag{2.64b}$$

which corresponds to the unique decomposition of the integral in parts of fractional and integer chiral order for fractional spacetime dimension d (see ref. [86]). All terms that violate the power counting are contained in R, which is real and analytic in the low-energy region. Note that also the tensor decomposition mentioned above holds for both parts separately. To obtain the result in the IR scheme one replaces $H_{k,l}$ by $I_{k,l}$ everywhere, which is equivalent to the cancelation of $R_{k,l}$ by appropriate counterterms. Purely mesonic integrals already fulfill the power counting exactly such that $I_{k,0} = H_{k,0}$, which implies that $R_{k,0} = 0$. For integrals that contain baryonic propagators exclusively the opposite is the case: $I_{0,l} = 0$ and $R_{0,l} = H_{0,l}$, which is consistent with the absence of baryonic loops (for more details see ref. [86]). In fact, one can obtain all integrals from three basic integrals by using

$$H_{k+1,l} = -\frac{1}{k} \frac{\partial}{\partial m^2} H_{k,l} = -\frac{1}{2mk} \frac{\partial}{\partial m} H_{k,l}\ , \tag{2.65a}$$

$$H_{k,l+1} = -\frac{1}{l} \frac{\partial}{\partial M^2} H_{k,l} = -\frac{1}{2Ml} \frac{\partial}{\partial M} H_{k,l}\ , \tag{2.65b}$$

which holds similarly for $I_{k,l}$ and $R_{k,l}$. The infrared singular parts of these basic integrals are given explicitly in appendix A.4.1. One should note, that the integrals over the Feynman parameter z in (2.64) diverge for $d > 3$. Therefore, one *defines* their value in the limit $d \to 4$ as the analytic continuation from $d < 3$. After a shift in the integration variable ($q \to q + zp$) one finds for the basic integral

$$I_{1,1} = \int_0^\infty dz\ \frac{1}{i} \int \frac{d^d q}{(2\pi)^d} (\Delta - q^2)^{-2} = \frac{1}{(4\pi)^{\frac{d}{2}}} \frac{\Gamma(2 - \frac{d}{2})}{\Gamma(2)} \int_0^\infty dz\ \Delta^{\frac{d}{2}-2}\ , \tag{2.66}$$

where $\Delta = \bar{z}m^2 + zM^2 - z\bar{z}p^2 - i\epsilon$. The latter equality follows from the master formula of d-dimensional integration (see, e.g., ref. [39]):[14]

$$\frac{1}{i} \int \frac{d^d q}{(2\pi)^d} \frac{1}{(\Delta - q^2)^n} = \frac{1}{(4\pi)^{\frac{d}{2}}} \frac{\Gamma(n - \frac{d}{2})}{\Gamma(n)} \Delta^{\frac{d}{2}-n}\ . \tag{2.67}$$

In order to find the analytic continuation to $d \to 4$, we follow ref. [86] and rewrite

$$\Delta = d_0 + d_1 (z - z_0)^2 = d_0 + \frac{1}{2}(z - z_0) \frac{\partial \Delta}{\partial z}\ , \tag{2.68a}$$

$$d_0 = m^2 - i\epsilon - d_1 z_0^2\ , \qquad d_1 = p^2\ , \qquad z_0 = \frac{m^2 - M^2 + p^2}{2p^2}\ , \tag{2.68b}$$

[14] One obtains $I_{1,0}$ from this formula directly by setting $\Delta = m^2 - i\epsilon$ and $n = 1$. Cf. eq. (A.27a).

such that

$$\Delta^k = d_0 \Delta^{k-1} + \frac{1}{2k}(z - z_0)\frac{\partial \Delta^k}{\partial z} \ , \tag{2.69}$$

where in our case $k = \frac{d}{2} - 2$. Integration by parts leads to

$$\int_0^\infty dz\ \Delta^k = d_0 \int_0^\infty dz\ \Delta^{k-1} + \left[\frac{1}{2k}(z - z_0)\Delta^k\right]_0^\infty - \frac{1}{2k}\int_0^\infty dz\ \Delta^k \ , \tag{2.70}$$

$$\Rightarrow \int_0^\infty dz\ \Delta^k = \left[\frac{1}{2k+1}(z - z_0)\Delta^k\right]_0^\infty + \frac{2kd_0}{2k+1}\int_0^\infty dz\ \Delta^{k-1} \ . \tag{2.71}$$

The upper boundary of the surface term diverges for $d > 3$ but vanishes for $d < 3$. Hence, the unique analytic continuation is given by the remaining parts (the lower boundary of the surface term and the integral), since they yield the same result at $d < 3$ but, apart from the usual singularities at integer values of d, converge for $d < 5$. Therefore,

$$I_{1,1} = \frac{1}{(4\pi)^{\frac{d}{2}}}\frac{\Gamma(2 - \frac{d}{2})}{\Gamma(2)}\left(\frac{1}{d-3} z_0 (m^2 - i\epsilon)^{\frac{d}{2}-2} + d_0 \frac{d-4}{d-3}\int_0^\infty dz\ \Delta^{\frac{d}{2}-3}\right) \ . \tag{2.72}$$

The explicit result is given in eq. (A.27c).

2.2 Symmetry properties of fields

In order to correctly model a microscopic operator, expressed in terms of quark and gluon fields, within ChPT (in terms of hadrons), one has to make use of its symmetry properties. In addition to the symmetry properties under chiral rotations, which were discussed in the previous sections, also the transformation under discrete symmetries (parity, charge conjugation and time reversal) have to be reproduced. For convenient reference, this section reviews the properties under discrete symmetry transformations of both quark and hadron fields, which is for the most part textbook knowledge (see, e.g., refs. [39, 90, 91]). Other relevant, but operator specific symmetry properties, like the scaling property or behavior under quark exchange, will be discussed directly in the respective sections on operator construction.

2.2.1 Microscopic fields

In this section we will discuss the transformation of quark fields under discrete symmetry transformations. Since current construction within chiral perturbation can be performed most conveniently for operators with simple behavior under chiral rotations, we give the symmetry properties also for the left- and right-handed parts of the fields, $q_L(x)$ and $q_R(x)$, as defined below eq. (2.7). As a convenient notation we use X as placeholder for R and L. Furthermore, we define $\bar{L} = R$, $\bar{R} = L$, $(-1)_R = +1$ and $(-1)_L = -1$.

Parity transformation ($\mathcal{P}$) is defined as an inversion of the space with respect to an arbitrary point. It reverses the three-momentum of a particle, but does not flip its spin. Quark fields are fermionic spin $\frac{1}{2}$ fields and transform as

$$\mathcal{P}q(x)\mathcal{P}^\dagger = \eta_q^P \gamma^0 q(\tilde{x}) \ , \tag{2.73a}$$

$$\mathcal{P}\bar{q}(x)\mathcal{P}^\dagger = \eta_q^{P^*} \bar{q}(\tilde{x})\gamma^0 \ , \tag{2.73b}$$

where $\tilde{x} = (x_0, -\mathbf{x})$, and η_q^P is an additional, fermion species dependent phase called intrinsic parity. For spin $\frac{1}{2}$ fields one can redefine the parity transformation always in such a way that $\eta_q^P = \pm 1$.[15] For quark fields one usually chooses $\eta_q^P = +1$. Parity interchanges the chiralities

$$\mathcal{P}q_X(x)\mathcal{P}^\dagger = \eta_q^P \gamma^0 q_{\bar{X}}(\tilde{x}) \ , \tag{2.74a}$$

$$\mathcal{P}\bar{q}_X(x)\mathcal{P}^\dagger = \eta_q^{P^*} \bar{q}_{\bar{X}}(\tilde{x})\gamma^0 \ , \tag{2.74b}$$

since γ_5 anticommutes with γ^0.

Charge conjugation ($\mathcal{C}$) interchanges particles and antiparticles. For the quark fields this means

$$\mathcal{C}q(x)\mathcal{C}^\dagger = \eta_q^C \bar{q}(x)C \ , \tag{2.75a}$$

$$\mathcal{C}\bar{q}(x)\mathcal{C}^\dagger = \eta_q^{C^*} Cq(x) \ , \tag{2.75b}$$

where $C = i\gamma^2\gamma^0$ is called charge conjugation matrix and η_q^C is the intrinsic charge conjugation parity. One can define the charge conjugation always in such a way that $\eta_q^C = \pm 1$ (for discussion see ref. [90]. The usual choice for quark fields is $\eta_q^C = +1$. For the chirally projected fields one finds

$$\mathcal{C}q_X(x)\mathcal{C}^\dagger = \eta_q^C \bar{q}_{\bar{X}}(x)C \ , \tag{2.76a}$$

$$\mathcal{C}\bar{q}_X(x)\mathcal{C}^\dagger = \eta_q^{C^*} Cq_{\bar{X}}(x) \ . \tag{2.76b}$$

Time reversal ($\mathcal{T}$) literally reverses the time direction. Time reversal has to be defined as a antilinear and antiunitary operation (see refs. [39, 90]), and, thus, acts as a complex conjugation on prefactors. For the quark fields one has

$$\mathcal{T}q(x)\mathcal{T}^\dagger = \eta_q^T C\gamma_5 q(-\tilde{x}) \ , \tag{2.77a}$$

$$\mathcal{T}\bar{q}(x)\mathcal{T}^\dagger = -\eta_q^{T^*} \bar{q}(-\tilde{x})C\gamma_5 \ , \tag{2.77b}$$

where $\eta_q^T = +1$ is the usual choice for quark fields. For left- and right-handed fields one obtains

$$\mathcal{T}q_X(x)\mathcal{T}^\dagger = \eta_q^T C\gamma_5 q_X(-\tilde{x}) = \eta_q^T (-1)_X C q_X(-\tilde{x}) \ , \tag{2.78a}$$

$$\mathcal{T}\bar{q}_X(x)\mathcal{T}^\dagger = \eta_q^{T^*} (-1)_X \bar{q}_X(-\tilde{x})C \ . \tag{2.78b}$$

[15] Except for Majorana fermions, for which one can achieve $\eta_q^P = \pm i$; compare refs. [90, 91]

Hermitian conjugation can also be used to obtain information about the transformation properties of the operators. However, this does not yield additional information, since

$$\begin{aligned}\mathcal{CPT}q(x)\mathcal{T}^\dagger\mathcal{P}^\dagger\mathcal{C}^\dagger &= \eta_q^T\mathcal{CP}(C\gamma_5 q(-\tilde{x}))\mathcal{P}^\dagger\mathcal{C}^\dagger = \eta_q^P\eta_q^T\mathcal{C}(C\gamma_5\gamma^0 q(-x))\mathcal{C}^\dagger \\ &= \eta_q^C\eta_q^P\eta_q^T\bar{q}(-x)C(C\gamma_5\gamma^0)^T = -\eta_q^C\eta_q^P\eta_q^T q^\dagger(-x)\gamma_5 \ ,\end{aligned} \tag{2.79}$$

and

$$\mathcal{CPT}q_X(x)\mathcal{T}^\dagger\mathcal{P}^\dagger\mathcal{C}^\dagger = -(-1)_X\eta_q^C\eta_q^P\eta_q^T q_X^\dagger(-x) \ . \tag{2.80}$$

Phase conventions: A violation of $\mathcal{CPT}$ symmetry, i.e., invariance under consecutive time reversal, parity transformation and charge conjugation, has never been measured experimentally. To incorporate $\mathcal{CPT}$ symmetry into the theory one uses the famous $\mathcal{CPT}$ theorem. It states that every Lorentz-invariant theory is invariant under $\mathcal{CPT}$ transformation if the inversion phases are chosen appropriately for each particle. One possible choice (consistent with $\mathcal{CPT}$ symmetry) is $\eta^C\eta^P\eta^T = +1$ for all particles (compare refs. [90, 92, 93]). Note that for spin $\frac{1}{2}$ fermions the actual condition to have a $\mathcal{CPT}$ conserving theory is much weaker, since they occur in bilinears only. Therefore it would be sufficient to have $\eta^C\eta^P\eta^T$ equal for all spin $\frac{1}{2}$ particles and $|\eta^C\eta^P\eta^T| = 1$.

2.2.2 Hadronic building blocks

For baryon fields the transformation properties look similar as for the quark fields, since they are also spin $\frac{1}{2}$ fermions

$$\mathcal{P}\Psi(x)\mathcal{P}^\dagger = \eta_b^P\gamma^0\Psi(\tilde{x}) \ , \qquad \mathcal{P}B(x)\mathcal{P}^\dagger = \eta_b^P\gamma^0 B(\tilde{x}) \ , \tag{2.81}$$

$$\mathcal{C}\Psi(x)\mathcal{C}^\dagger = \eta_b^C\bar{\Psi}(x)C \ , \qquad \mathcal{C}B_{ab}(x)\mathcal{C}^\dagger = \eta_b^C\bar{B}_{ba}(x)C \ , \tag{2.82}$$

$$\mathcal{T}\Psi(x)\mathcal{T}^\dagger = \eta_b^T C\gamma_5\Psi(-\tilde{x}) \ , \qquad \mathcal{T}B(x)\mathcal{T}^\dagger = \eta_b^T C\gamma_5 B(-\tilde{x}) \ , \tag{2.83}$$

where we have written out the flavor indices a and b explicitly for the charge conjugation of the baryon octet to avoid confusion. For the ground-state baryons it holds $\eta_b^P = \eta_b^C\eta_b^T = +1$. While the choice of the phases for the unobservable quark fields is highly arbitrary, the phase conventions for hadrons are meaningful. E.g., changing η_b^P and $\eta_b^C\eta_b^T$ to -1 for the octet (while keeping it fixed for the quark fields) would correspond to a description of the parity partners of the octet.

For the pseudoscalar fields, which are collected in $u = \exp\big(i\Phi/(2F_0)\big)$, where the definition of Φ is given in eq. (2.27), one has

$$\mathcal{P}\Phi(x)\mathcal{P}^\dagger = -\Phi(\tilde{x}) \ , \qquad \mathcal{P}u(x)\mathcal{P}^\dagger = u^\dagger(\tilde{x}) \ , \qquad \mathcal{P}u_X(x)\mathcal{P}^\dagger = u_{\bar{X}}(\tilde{x}) \ , \tag{2.84a}$$

$$\mathcal{T}\Phi(x)\mathcal{T}^\dagger = -\Phi(-\tilde{x}) \ , \qquad \mathcal{T}u(x)\mathcal{T}^\dagger = u(-\tilde{x}) \ , \qquad \mathcal{T}u_X(x)\mathcal{T}^\dagger = u_X(-\tilde{x}) \ , \tag{2.84b}$$

$$\mathcal{C}\Phi(x)\mathcal{C}^\dagger = \Phi^*(x) = \Phi^T(x) \ , \qquad \mathcal{C}u(x)\mathcal{C}^\dagger = u^T(x) \ , \qquad \mathcal{C}u_X(x)\mathcal{C}^\dagger = u_X^T(x) \ , \tag{2.84c}$$

where we have used the convenient definition $u_R = u$ and $u_L = u^\dagger$ in the last column. For the mesonic building blocks u_μ and $\chi^\pm$ used in BChPT, which have been defined in eqs. (2.47)

and (2.48), this leads to the following properties under discrete symmetry transformations and Hermitian conjugation:

$$\mathcal{P}u_\mu(x)\mathcal{P}^\dagger = -(-1)_\mu u_\mu(\tilde{x}) \ , \qquad \mathcal{P}\chi^\pm(x)\mathcal{P}^\dagger = \pm\chi^\pm(\tilde{x}) \ , \tag{2.85a}$$

$$\mathcal{C}u_\mu(x)\mathcal{C}^\dagger = u_\mu^T(x) \ , \qquad \mathcal{C}\chi^\pm(x)\mathcal{C}^\dagger = \big(\chi^\pm(x)\big)^T \ , \tag{2.85b}$$

$$\mathcal{T}u_\mu(x)\mathcal{T}^\dagger = (-1)_\mu u_\mu(-\tilde{x}) \ , \qquad \mathcal{T}\chi^\pm(x)\mathcal{T}^\dagger = \chi^\pm(-\tilde{x}) \ , \tag{2.85c}$$

$$u_\mu^\dagger(x) = u_\mu(x) \ , \qquad \big(\chi^\pm(x)\big)^\dagger = \pm\chi^\pm(x) \ . \tag{2.85d}$$

where $(-1)_\mu$ is 1 for $\mu = 0$ and -1 for $\mu = 1, 2, 3$. In order to allow for a general construction independent of the used building block one can define $\eta_u^P = -1$, $\eta_u^C = +1$, $\eta_u^T = +1$, $\eta_u^H = +1$ and $\eta_{\chi^\pm}^P = \pm 1$, $\eta_{\chi^\pm}^C = +1$, $\eta_{\chi^\pm}^T = +1$, $\eta_{\chi^\pm}^H = \pm 1$ such that

$$\mathcal{P}A(x)\mathcal{P}^\dagger = \eta_A^P A(\tilde{x}) \ , \tag{2.86a}$$

$$\mathcal{C}A(x)\mathcal{C}^\dagger = \eta_A^C A^T(x) \ , \tag{2.86b}$$

$$\mathcal{T}A(x)\mathcal{T}^\dagger = \eta_A^T A(-\tilde{x}) \ , \tag{2.86c}$$

$$A^\dagger(x) = \eta_A^H A(x) \ , \tag{2.86d}$$

holds for $A \in \{u_0, \chi^+, \chi^-\}$. Additional covariant derivatives acting on the mesonic building blocks do (apart from the typical $(-1)_\mu$ and $-(-1)_\mu$ factors occurring in parity transformation and time reversal due to open Lorentz indices) not affect the symmetry properties.

Often nucleon bilinears of the form $\bar{\Psi}(x)A\Gamma\Psi(x)$ occur as fundamental structures, where A and Γ are placeholders for chiral building blocks and gamma structures. Ψ here is the isospinor containing the proton and the neutron field. For the three-flavor version the flavor structure would look slightly different, since the baryon octet is contained in the matrix-valued field B. For the operator construction in chapter 3 it is convenient to define covariant left-right derivatives that only act on the baryon fields

$$\bar{\Psi}A\Gamma D_\mu^\pm\Psi = \bar{\Psi}\big(A\Gamma\overrightarrow{D}_\mu \pm \overleftarrow{D}_\mu A\Gamma\big)\Psi \ , \tag{2.87}$$

such that they do not interact with the mesonic building blocks. Note that D_μ^+ has to be counted as small (first order) since the nucleon mass term drops out in the momentum difference. To see how such a derivative affects the symmetry properties we compare bilinears with and without derivatives. Let us neglect A in the following discussion for simplicity. One finds

$$\mathcal{P}\bar{\Psi}(x)\Gamma\Psi(x)\mathcal{P}^\dagger = \bar{\Psi}(\tilde{x})\gamma_0\Gamma\gamma_0\Psi(\tilde{x}) \ , \tag{2.88a}$$

$$\mathcal{C}\bar{\Psi}(x)\Gamma\Psi(x)\mathcal{C}^\dagger = -\bar{\Psi}(x)C\Gamma^T C\Psi(x) \ , \tag{2.88b}$$

$$\mathcal{T}\bar{\Psi}(x)\Gamma\Psi(x)\mathcal{T}^\dagger = -\bar{\Psi}(-\tilde{x})C\gamma_5\Gamma^* C\gamma_5\Psi(-\tilde{x}) \ , \tag{2.88c}$$

$$\big(\bar{\Psi}(x)\Gamma\Psi(x)\big)^\dagger = \bar{\Psi}(x)\gamma_0\Gamma^\dagger\gamma_0\Psi(x) \ , \tag{2.88d}$$

versus

$$\mathcal{P}\bar{\Psi}(x)\Gamma D_\mu^\pm \Psi(x)\mathcal{P}^\dagger = (-1)_\mu \bar{\Psi}(\tilde{x})\gamma_0\Gamma\gamma_0 D_\mu^\pm \Psi(\tilde{x}) \ , \tag{2.89a}$$

$$\mathcal{C}\bar{\Psi}(x)\Gamma D_\mu^\pm \Psi(x)\mathcal{C}^\dagger = -(\pm 1)\bar{\Psi}(x)C\Gamma^T C D_\mu^\pm \Psi(x) \ , \tag{2.89b}$$

$$\mathcal{T}\bar{\Psi}(x)\Gamma D_\mu^\pm \Psi(x)\mathcal{T}^\dagger = (-1)_\mu \bar{\Psi}(-\tilde{x})C\gamma_5\Gamma^* C\gamma_5 D_\mu^\pm \Psi(-\tilde{x}) \ , \tag{2.89c}$$

$$\left(\bar{\Psi}(x)\Gamma D_\mu^\pm \Psi(x)\right)^\dagger = \pm\bar{\Psi}(x)\gamma_0\Gamma^\dagger\gamma_0 D_\mu^\pm \Psi(x) \ , \tag{2.89d}$$

which means that one gets an additional factor $(-1)_\mu$ in a parity transformation, (± 1) in charge conjugation, $-(-1)_\mu$ in time reversal and ± 1 in Hermitian conjugation. In a case where we have more than one covariant derivative we define a string of plus and minus derivatives as

$$\begin{aligned} D_{\mu_1}^{\pm_1}\cdots D_{\mu_n}^{\pm_n} = \sum_{k=0}^{n}\sum_{\sigma\in S_n} & \frac{(\pm_{\sigma(1)}1)\cdots(\pm_{\sigma(k)}1)}{k!(n-k)!} \\ & \times \overleftarrow{D}_{\mu_{\sigma(1)}}\cdots\overleftarrow{D}_{\mu_{\sigma(k)}}\overrightarrow{D}_{\mu_{\sigma(k+1)}}\cdots\overrightarrow{D}_{\mu_{\sigma(n)}} \ , \end{aligned} \tag{2.90}$$

where S_n is the symmetric group of degree n. Again, the derivatives are meant to act on the nucleon fields only. The symmetrization within the covariant derivatives acting to the left/right is possible due to the curvature relation

$$[D_\mu, D_\nu] = \frac{1}{4}[u_\mu, u_\nu] \ , \tag{2.91}$$

where the right-hand side is of second chiral order. It also holds for derivatives acting to the left. If such a multiple derivative occurs in a bilinear, it yields for each derivative the same additional factor in the transformation properties as described above for the single derivative.

2.3 Primer to Fierz transformation

In this brief section we provide a derivation of Fierz identities [94]. We will make extensive use of them in chapter 4 to construct operators with correct symmetry properties under quark exchange. However, the original form of Fierz transformations, which is found in many textbooks (see, e.g., ref. [95]), is restricted to the case where all Lorentz indices are contracted (e.g., $\gamma_\mu\otimes\gamma^\mu$). We will need a slightly more general form, that allows for open indices. Our derivation of these generalized identities will follow ref. [96] and was already presented in [35]. We use the standard Dirac basis that spans the space of complex 4×4 matrices:

$$\left\{\Gamma^A\right\} = \{\mathbb{1}, \gamma_5, \gamma^\mu, \gamma_5\gamma^\mu, \sigma^{\mu\nu}\} \ , \quad \mu < \nu \ . \tag{2.92}$$

We define the dual basis as $\left\{\Gamma_A\right\} = \{\mathbb{1}, \gamma_5, \gamma_\mu, \gamma_\mu\gamma_5, \sigma_{\mu\nu}\}$ $(\mu < \nu)$, where γ_μ and γ_5 are interchanged in the axialvector part. The latter is important in order to have an orthogonality relation of the form

$$\mathrm{tr}\left\{\Gamma^A\Gamma_B\right\} = 4\delta_B^A \ , \tag{2.93}$$

which can be verified by a straightforward calculation. Obviously, every 4×4 matrix X can be written as a linear combination of elements of the Dirac basis $X = X_A\Gamma^A$, where here and below

a sum over indices occurring twice is implied. Utilizing the orthogonality relation (2.93), the coefficients can be obtained from $\mathrm{tr}\left\{X\Gamma_B\right\} = X_A \,\mathrm{tr}\left\{\Gamma^A\Gamma_B\right\} = 4X_B$. Hence, we can derive the completeness relation as follows:

$$\begin{aligned} X_{ij} &= \frac{1}{4}\,\mathrm{tr}\left\{X\Gamma_A\right\}\left(\Gamma^A\right)_{ij} = X_{kl}\frac{1}{4}\left(\Gamma_A\right)_{lk}\left(\Gamma^A\right)_{ij} \\ &\Rightarrow \delta_{ik}\delta_{jl} = \frac{1}{4}\left(\Gamma_A\right)_{lk}\left(\Gamma^A\right)_{ij} \,. \end{aligned} \tag{2.94}$$

Using the completeness relation twice, we obtain Fierz-like identities for general 4×4 matrices X and Y:

$$\begin{aligned} X_{ij}Y_{kl} &= X_{im}Y_{nl}\delta_{mj}\delta_{nk} = \frac{1}{4}X_{im}Y_{nl}\left(\Gamma^A\right)_{kj}\left(\Gamma_A\right)_{mn} = \frac{1}{4}\left(X\Gamma_A Y\right)_{il}\left(\Gamma^A\right)_{kj} \\ &= \frac{1}{4}\left(X\Gamma_A Y\right)_{mn}\left(\Gamma^A\right)_{kj}\delta_{im}\delta_{ln} = \frac{1}{16}\left(X\Gamma_A Y\right)_{mn}\left(\Gamma^A\right)_{kj}\left(\Gamma_B\right)_{nm}\left(\Gamma^B\right)_{il} \\ &= \frac{1}{16}\,\mathrm{tr}\left\{X\Gamma_A Y\Gamma_B\right\}\left(\Gamma^B\right)_{il}\left(\Gamma^A\right)_{kj} \,. \end{aligned} \tag{2.95}$$

Due to the definition of the basis elements in eq. (2.92), the summation only runs over indices $\mu < \nu$ if $\Gamma^A = \sigma^{\mu\nu}$. In order to restore the usual summation convention one has to use that the expression summed over is symmetric ($f(\mu,\nu) = f(\nu,\mu)$) and traceless ($f(\mu,\mu) = 0$) with respect to the summation indices. Therefore, one acquires an extra factor $\frac{1}{2}$:

$$\sum_{\mu<\nu} f(\mu,\nu) = \frac{1}{2}\left(\sum_{\mu<\nu} + \sum_{\mu>\nu} + \sum_{\mu=\nu}\right) f(\mu,\nu) = \frac{1}{2}\sum_{\mu,\nu} f(\mu,\nu) \,. \tag{2.96}$$

If $\Gamma^A = \sigma^{\alpha\beta}$ and $\Gamma^B = \sigma^{\mu\nu}$ one obtains a factor $\frac{1}{4}$, accordingly. Choosing $X = \Gamma^C$ and $Y = \Gamma^D$ in particular, eq. (2.95) leads to the Fierz identities:

$$\left(\Gamma^C\right)_{ij}\left(\Gamma^D\right)_{kl} = \frac{1}{16}\,\mathrm{tr}\left\{\Gamma^C\Gamma_A\Gamma^D\Gamma_B\right\}\left(\Gamma^B\right)_{il}\left(\Gamma^A\right)_{kj} \,, \tag{2.97}$$

which reproduces the textbook type Fierz transformations (see, e.g., ref. [95]), if one chooses $\Gamma^C \otimes \Gamma^D \in \{\mathbb{1}\otimes\mathbb{1}, \gamma_5\otimes\gamma_5, \gamma^\mu\otimes\gamma_\mu, \gamma_5\gamma^\mu\otimes\gamma_5\gamma_\mu, \sigma^{\mu\nu}\otimes\sigma_{\mu\nu}\}$.

CHAPTER 3

Generalized parton distributions

In this chapter we discuss generalized (or off-forward) parton distributions, which unify the seemingly unrelated concepts of elastic form factors (relevant for elastic scattering processes) and parton distribution functions (relevant for deep inelastic scattering). The main part of this chapter has been published in ref. [97] and is dedicated to the derivation of the quark mass dependence of the first moments of nucleon GPDs using chiral perturbation theory at full one-loop accuracy.

3.1 Overview

By the end of the last century generalized parton distributions have been identified as a suitable tool to parametrize exclusive processes and to extract the contained information on hadron structure [15–17, 98] (for a detailed description we refer to the reviews [18, 99, 100]), which has triggered large activities in both experimental and theoretical communities. The contemporary experimental data mainly comes from the measurement of deeply virtual compton scattering (DVCS) and deeply virtual meson production (DVMP) in electron-proton and positron-proton collisions (at JLab and DESY) and is complemented by data from muon-proton collisions (from the COMPASS experiment at CERN). Additional information may come from neutrino-induced DVMP measured at neutrino beam experiments (see ref. [101]).

On the experimental side one faces the difficulty that (hard) exclusive processes are power-suppressed. Hence, precision measurements are challenging and require high luminosities. In addition, GPDs enter the cross section not directly, but via a convolution with a hard scattering kernel, which complicates their extraction from experimental data (for a recent review of the current status of phenomenological fits see, e.g., refs. [102] (DVCS) and [103] (DVMP)). Complementary information from the theoretical side which constrains the functional form of GPDs (e.g., by providing bounds for their moments) is therefore most valuable. One framework capable of providing such information on nonperturbative quantities is lattice QCD. Unfortunately

simulations suffer typically from systematic errors associated with discretization, finite volume and unphysical quark masses. Therefore, having a better control over some of the various extrapolations and the associated systematic errors is very helpful to obtain reliable quantitative results. As argued in chapter 1, the most rigorous way to gain such control is given by chiral perturbation theory (see chapter 2 and references therein) as opposed to ad hoc or model-based extrapolation formulas.

In this chapter we focus on the first x-moments of chiral-even GPDs. In the positive parity sector those encode information on the momentum distribution of the considered parton species, since the corresponding local operators coincide with the off-diagonal elements of the energy-momentum tensor. In the forward limit one has simple relations to the momentum fraction and the total angular momentum carried by a specific parton species (as pointed out by Ji [15]). The first moment of the parity-odd quark GPD has been linked to the quark spin-orbit correlation (see ref. [104]). We use the framework of two-flavor BChPT described in section 2.1.4, applying infrared regularization [86] (see section 2.1.5) to obtain analytic formulas describing the pion mass dependence of the first moments at full one-loop order ($\simeq \mathcal{O}(p^3)$, where p represents both the scale of the pion mass and the momentum transfer, which are considered to be small in the low-energy regime). There already exist various heavy baryon calculations on the topic (see, e.g., refs. [105–111]) as well as covariant leading one-loop calculations [34, 112], where third order effects are only partially included. The work presented in this chapter is an extension of ref. [34].

This chapter is organized as follows: we will start our analysis with a short review of the matrix element decompositions that define the generalized form factors (see section 3.2). Advancing to third chiral order, the number of possible low-energy structures rises significantly. Eliminating some of them using the equations of motion (EOM) will therefore be an important topic in section 3.3, which contains the construction of the operators in terms of hadronic fields. It turns out that the full one-loop calculation (see section 3.4) contains numerous new low-energy constants (LECs). In section 3.5 we therefore discuss two possibilities to reduce the number of free parameters, since the currently available lattice data is not sufficient to pin down all LECs. The reduction of the results to the heavy BChPT version is presented in section 3.5.2. Section 3.6 contains a first application of our results to two-flavor lattice QCD data. We summarize in section 3.7.

3.2 Matrix element decomposition

There are in total four different kinds of chiral-even GPDs: two quark distributions F^q, $\tilde{F}^q$, which are defined for each quark flavor separately, and two gluon distributions F^g, $\tilde{F}^g$, where $\tilde{F}^q$ and $\tilde{F}^g$ are (parton-) spin dependent. The n-th x-moments of these quantities are defined as the integral over x from -1 to 1, with the weight factor x^n for quark and x^{n-1} for gluon distributions.[1] Mirroring the fact that gluons are their own antiparticles, F^g is an even and

[1] Note that there is no standard naming convention in the literature: sometimes the n-th moment is related to weight factors x^{n-1} and x^{n-2} for quark and gluon distributions, respectively.

$\tilde{F}^g$ an odd function of x and all odd moments of $\tilde{F}^g$ vanish accordingly. The three GPDs with nonvanishing first moments are defined as [18]

$$\begin{aligned} F^q &= \frac{1}{2}\int\limits_{-\infty}^{\infty}\frac{dz^-}{2\pi}e^{ix\bar{p}^+z^-}\langle p',s'|\bar{q}(-z/2)\gamma^+q(z/2)|p,s\rangle \\ &= \frac{1}{2\bar{p}^+}\bar{u}(p',s')\left[H^q(x,\xi,t)\gamma^+ + E^q(x,\xi,t)\frac{i\sigma^{+\alpha}\Delta_\alpha}{2m_N}\right]u(p,s)\ , \end{aligned} \tag{3.1a}$$

$$\begin{aligned} \tilde{F}^q &= \frac{1}{2}\int\limits_{-\infty}^{\infty}\frac{dz^-}{2\pi}e^{ix\bar{p}^+z^-}\langle p',s'|\bar{q}(-z/2)\gamma^+\gamma_5q(z/2)|p,s\rangle \\ &= \frac{1}{2\bar{p}^+}\bar{u}(p',s')\left[\tilde{H}^q(x,\xi,t)\gamma^+\gamma_5 + \tilde{E}^q(x,\xi,t)\frac{\gamma_5\Delta^+}{2m_N}\right]u(p,s)\ , \end{aligned} \tag{3.1b}$$

$$\begin{aligned} F^g &= \frac{1}{\bar{p}^+}\int\limits_{-\infty}^{\infty}\frac{dz^-}{2\pi}e^{ix\bar{p}^+z^-}\langle p',s'|G^{+\mu}(-z/2)G_\mu{}^+(z/2)|p,s\rangle \\ &= \frac{1}{2\bar{p}^+}\bar{u}(p',s')\left[H^g(x,\xi,t)\gamma^+ + E^g(x,\xi,t)\frac{i\sigma^{+\alpha}\Delta_\alpha}{2m_N}\right]u(p,s)\ , \end{aligned} \tag{3.1c}$$

where z is a lightlike vector with vanishing plus component (for the definition of plus and minus components see ref. [18]; compare also [16]). To assure gauge invariance the fields in the nonlocal operators are connected by Wilson lines which we do not write out explicitly. The kinematic variables are defined as

$$\begin{aligned} \bar{p} &= \frac{1}{2}(p'+p)\ , & \Delta &= p'-p\ , \\ \xi &= -\frac{\Delta^+}{2\bar{p}^+}\ , & t &= \Delta^2\ . \end{aligned} \tag{3.2}$$

The first moments of the GPDs are related to the matrix elements of the local twist-two operators

$$\mathcal{O}^q_{\mu\nu} = \frac{1}{2}\,\mathbf{S}\,\bar{q}\gamma_\mu iD^-_\nu q\ , \tag{3.3a}$$

$$\tilde{\mathcal{O}}^q_{\mu\nu} = \frac{1}{2}\,\mathbf{S}\,\bar{q}\gamma_\mu\gamma_5 iD^-_\nu q\ , \tag{3.3b}$$

$$\mathcal{O}^g_{\mu\nu} = \mathbf{S}\,G_{\mu\alpha}G^\alpha{}_\nu\ , \tag{3.3c}$$

where $D^-_\mu = \overrightarrow{D}_\mu - \overleftarrow{D}_\mu$ with

$$\overrightarrow{D}_\mu \equiv \overrightarrow{\partial}_\mu + igA_\mu\ , \qquad \overleftarrow{D}_\mu \equiv \overleftarrow{\partial}_\mu - igA_\mu\ , \tag{3.4}$$

and the operator $\mathbf{S}$ projects onto leading twist by symmetrizing in Lorentz indices and subtracting traces. When acting on an object with two open indices $\mathbf{S}$ has the explicit form

$$\mathbf{S}\,\mathcal{O}^{\mu\nu} \equiv \mathbf{S}^{\mu\nu}_{\alpha\beta}\,\mathcal{O}^{\alpha\beta} = \frac{1}{2}\Big(g^\mu_\alpha g^\nu_\beta + g^\mu_\beta g^\nu_\alpha - \frac{2}{d}g^{\mu\nu}g_{\alpha\beta}\Big)\mathcal{O}^{\alpha\beta}\ . \tag{3.5}$$

In contrast to the matrix elements of the nonlocal operators with quarks at lightlike separations the nucleon-to-nucleon matrix elements of these local currents are directly accessible by lattice

simulations. Taking into account symmetry properties under discrete symmetry transformation a covariant form factor decomposition of these matrix elements reads [18]

$$\langle p',s'|\mathcal{O}^q_{\mu\nu}|p,s\rangle = \mathbf{S}\,\bar u(p',s')\left[\gamma_\mu\bar p_\nu A^q_{2,0}(t) + \frac{i\sigma_{\mu\alpha}\Delta^\alpha}{2m_N}\bar p_\nu B^q_{2,0}(t) + \frac{\Delta_\mu\Delta_\nu}{m_N}C^q_2(t)\right]u(p,s)\ , \tag{3.6a}$$

$$\langle p',s'|\tilde{\mathcal{O}}^q_{\mu\nu}|p,s\rangle = \mathbf{S}\,\bar u(p',s')\left[\gamma_\mu\gamma_5\bar p_\nu \tilde A^q_{2,0}(t) + \frac{\gamma_5\Delta_\mu}{2m_N}\bar p_\nu \tilde B^q_{2,0}(t)\right]u(p,s)\ , \tag{3.6b}$$

$$\langle p',s'|\mathcal{O}^g_{\mu\nu}|p,s\rangle = \mathbf{S}\,\bar u(p',s')\left[\gamma_\mu\bar p_\nu A^g_{2,0}(t) + \frac{i\sigma_{\mu\alpha}\Delta^\alpha}{2m_N}\bar p_\nu B^g_{2,0}(t) + \frac{\Delta_\mu\Delta_\nu}{m_N}C^g_2(t)\right]u(p,s)\ . \tag{3.6c}$$

All symmetry arguments used to derive the matrix element decomposition are also taken into account in the construction of effective low-energy operators (see below). It is therefore guaranteed that the results of the effective theory calculation can be cast into a similar form. The occurring generalized form factors (GFFs) are related to the GPD moments via

$$\int\limits_{-1}^{1} dx\, x\, H^q(x,\xi,t) = A^q_{2,0}(t) + 4\xi^2 C^q_2(t)\ , \qquad \int\limits_{-1}^{1} dx\, x\, E^q(x,\xi,t) = B^q_{2,0}(t) - 4\xi^2 C^q_2(t)\ , \tag{3.7a}$$

$$\int\limits_{-1}^{1} dx\, x\, \tilde H^q(x,\xi,t) = \tilde A^q_{2,0}(t)\ , \qquad \int\limits_{-1}^{1} dx\, x\, \tilde E^q(x,\xi,t) = \tilde B^q_{2,0}(t)\ , \tag{3.7b}$$

$$\int\limits_{0}^{1} dx\, H^g(x,\xi,t) = A^g_{2,0}(t) + 4\xi^2 C^g_2(t)\ , \qquad \int\limits_{0}^{1} dx\, E^g(x,\xi,t) = B^g_{2,0}(t) - 4\xi^2 C^g_2(t)\ . \tag{3.7c}$$

The generalized form factors, which are introduced to parametrize the matrix elements of the local operators, carry manifold information on hadron structure. Their physical interpretation is given by the operator they describe. For instance the form factors connected to the zeroth moments of the spin independent generalized quark distribution coincide with the Pauli and Dirac form factors, because the examined operator is the standard vector current. In the spin dependent case the corresponding operator is the axialvector current described by the pseudoscalar and axialvector form factor (cf., e.g., ref. [18]). The interpretation of the form factors connected to the first moments of the spin independent GPDs is given by the observation that the examined operators defined in eq. (3.3) are equal to the off-diagonal elements of the energy-momentum tensor linked to the considered parton species (cf. refs. [15, 113], where it is shown that the decomposition of the energy-momentum tensor in quark and gluon parts is gauge-invariant). They therefore allow a resolution of the spatial distribution of parton momenta within a hadron by calculating the following spatial moments

$$\begin{aligned}
&\int d^3x\ x_{j_1}\cdots x_{j_n}\langle \mathbf{p}',\mathbf{s}|\mathcal{O}^{q,g}_{0i}(\mathbf{x})|\mathbf{p},\mathbf{s}\rangle = \\
&\quad = i^n\int d^3x\left(\frac{\partial}{\partial\Delta_{j_1}}\cdots\frac{\partial}{\partial\Delta_{j_n}}e^{-i\boldsymbol{\Delta}\mathbf{x}}\right)\langle\bar{\mathbf{p}}+\boldsymbol{\Delta}/2,\mathbf{s}|\mathcal{O}^{q,g}_{0i}(\mathbf{0})|\bar{\mathbf{p}}-\boldsymbol{\Delta}/2,\mathbf{s}\rangle \\
&\quad = (2\pi)^3\delta^{(3)}(\boldsymbol{\Delta})\ (-i)^n\ \frac{\partial}{\partial\Delta_{j_1}}\cdots\frac{\partial}{\partial\Delta_{j_n}}\langle\bar{\mathbf{p}}+\boldsymbol{\Delta}/2,\mathbf{s}|\mathcal{O}^{q,g}_{0i}(\mathbf{0})|\bar{\mathbf{p}}-\boldsymbol{\Delta}/2,\mathbf{s}\rangle\ ,
\end{aligned} \tag{3.8}$$

where $\mathbf{s}$ is the polarization direction (with unit length). These moments must not be confused with the aforementioned x-moments of the GPDs. The zeroth moment (corresponding to the momentum), and the first moments (which yield the angular momentum) are certainly the most important ones. Taking into account the normalization factor from $\langle \mathbf{p}', \mathbf{s} | \mathbf{p}, \mathbf{s} \rangle = 2E_{\mathbf{p}}(2\pi)^3 \delta^{(3)}(\mathbf{p}' - \mathbf{p})$ one obtains

$$P_i^{q,g}(\bar{\mathbf{p}}, \mathbf{s}) = \frac{1}{2\bar{p}^0} \langle \bar{\mathbf{p}} + \boldsymbol{\Delta}/2, \mathbf{s} | \mathcal{O}_{0i}^{q,g}(\mathbf{0}) | \bar{\mathbf{p}} - \boldsymbol{\Delta}/2, \mathbf{s} \rangle \Big|_{\boldsymbol{\Delta}=\mathbf{0}} , \tag{3.9a}$$

$$J_i^{q,g}(\bar{\mathbf{p}}, \mathbf{s}) = \frac{1}{2\bar{p}^0} (-i)\varepsilon_{ijk} \frac{\partial}{\partial \Delta_j} \langle \bar{\mathbf{p}} + \boldsymbol{\Delta}/2, \mathbf{s} | \mathcal{O}_{0k}^{q,g}(\mathbf{0}) | \bar{\mathbf{p}} - \boldsymbol{\Delta}/2, \mathbf{s} \rangle \Big|_{\boldsymbol{\Delta}=\mathbf{0}} . \tag{3.9b}$$

On the right-hand side of the equations, one now inserts the matrix element decompositions given in (3.6) to arrive at

$$\mathbf{P}^{q,g}(\mathbf{p}, \mathbf{s}) = \mathbf{p} A_{2,0}^{q,g}(0) , \tag{3.10a}$$

$$\begin{aligned} \mathbf{J}^{q,g}(\mathbf{p}, \mathbf{s}) &= \mathbf{s} \frac{1}{2} \big(A_{2,0}^{q,g}(0) + B_{2,0}^{q,g}(0) \big) + \frac{1}{2m(m+p_0)} \big(\mathbf{p}^2 \mathbf{s} - (\mathbf{p} \cdot \mathbf{s}) \mathbf{p} \big) B_{2,0}^{q,g}(0) \\ &= \mathbf{s} \times \begin{cases} \frac{1}{2} \big(A_{2,0}^{q,g}(0) + B_{2,0}^{q,g}(0) \big) , & \text{if } \mathbf{s} \parallel \mathbf{p} , \\ \frac{1}{2} \big(A_{2,0}^{q,g}(0) + \frac{p_0}{m} B_{2,0}^{q,g}(0) \big) , & \text{if } \mathbf{s} \perp \mathbf{p} . \end{cases} \end{aligned} \tag{3.10b}$$

Here it becomes clear that the forward limit of the form factor $A_{2,0}^{q,g}$ corresponds to the mean momentum fraction carried by a parton species, while the combination $(A_{2,0}^{q,g} + B_{2,0}^{q,g})/2$ yields its total angular momentum in a longitudinally polarized nucleon. From the fact that all parton species together have to carry the (total angular) momentum of the nucleon one directly deduces sum rules for the generalized form factors [15]:

$$A_{2,0}^{g}(0) + \sum_q A_{2,0}^{q}(0) = 1 , \qquad B_{2,0}^{g}(0) + \sum_q B_{2,0}^{q}(0) = 0 . \tag{3.11}$$

If we consider the form factors connected to the first moments of the (quark-) spin dependent GPDs we have to analyze the matrix elements of the operator $\tilde{\mathcal{O}}_{\mu\nu}^{q}$. In contrast to the situation in the spin independent case, quarks of different helicities occur with different signs. Therefore, we can interpret the corresponding matrix elements as the spatial distribution of the momentum-asymmetry between helicity plus and minus quarks. Defining everything analogously to the spin independent case one obtains

$$\tilde{\mathbf{P}}^{q}(\mathbf{p}, \mathbf{s}) = \left(\frac{m}{2} \mathbf{s} + \frac{2p_0 + m}{2p_0(m+p_0)} (\mathbf{p} \cdot \mathbf{s}) \mathbf{p} \right) \tilde{A}_{2,0}^{q}(0) = \mathbf{s} \times \begin{cases} p_0 \big(1 - \frac{m^2}{2p_0^2} \big) \tilde{A}_{2,0}^{q}(0) , & \text{if } \mathbf{s} \parallel \mathbf{p} , \\ \frac{m}{2} \tilde{A}_{2,0}^{q}(0) , & \text{if } \mathbf{s} \perp \mathbf{p} , \end{cases} \tag{3.12a}$$

$$\tilde{\mathbf{J}}^{q}(\mathbf{p}, \mathbf{s}) = \frac{1}{2(m+p_0)} \mathbf{p} \tilde{A}_{2,0}^{q}(0) . \tag{3.12b}$$

Putting everything together we can calculate the separate contribution of helicity plus ($\uparrow$) and minus ($\downarrow$) quarks to the nucleon momentum and total angular momentum. For the momentum we find

$$\begin{aligned}\mathbf{P}^{q\uparrow/q\downarrow}(\mathbf{p},\mathbf{s}) &= \frac{1}{2}\big(\mathbf{P}^q(\mathbf{p},\mathbf{s}) \pm \tilde{\mathbf{P}}^q(\mathbf{p},\mathbf{s})\big) = \begin{cases} \mathbf{p}\big(\frac{1}{2}A^q_{2,0}(0) \pm \frac{\lambda p_0}{2|\mathbf{p}|}\big(1-\frac{m^2}{2p_0^2}\big)\tilde{A}^q_{2,0}(0)\big)\ , & \text{if } \mathbf{s} = \lambda\frac{\mathbf{p}}{|\mathbf{p}|}\ , \\ \mathbf{p}\frac{1}{2}A^q_{2,0}(0) \pm \mathbf{s}\frac{m}{4}\tilde{A}^q_{2,0}(0)\ , & \text{if } \mathbf{s}\perp\mathbf{p}\ , \end{cases} \\ &\overset{p_0\gg m}{\approx} \mathbf{p}\times\begin{cases} \frac{1}{2}\big(A^q_{2,0}(0) \pm \lambda\tilde{A}^q_{2,0}(0)\big)\ , & \text{if } \mathbf{s} = \lambda\frac{\mathbf{p}}{|\mathbf{p}|}\ , \\ \frac{1}{2}A^q_{2,0}(0)\ , & \text{if } \mathbf{s}\perp\mathbf{p}\ , \end{cases}\end{aligned} \tag{3.13}$$

i.e., at high energies a momentum asymmetry between quarks of different helicities can only occur in longitudinally polarized nucleons. A similar picture arises for the total angular momentum

$$\begin{aligned}\mathbf{J}^{q\uparrow/q\downarrow}(\mathbf{p},\mathbf{s}) &= \frac{1}{2}\big(\mathbf{J}^q(\mathbf{p},\mathbf{s}) \pm \tilde{\mathbf{J}}^q(\mathbf{p},\mathbf{s})\big) \\ &= \begin{cases} \mathbf{s}\frac{1}{4}\big(A^q_{2,0}(0)+B^q_{2,0}(0) \pm \frac{\lambda|\mathbf{p}|}{m+p_0}\tilde{A}^q_{2,0}(0)\big)\ , & \text{if } \mathbf{s} = \lambda\frac{\mathbf{p}}{|\mathbf{p}|}\ , \\ \mathbf{s}\frac{1}{4}\big(A^q_{2,0}(0)+\frac{p_0}{m}B^q_{2,0}(0)\big) \pm \mathbf{p}\frac{1}{4(m+p_0)}\tilde{A}^q_{2,0}(0)\ , & \text{if } \mathbf{s}\perp\mathbf{p}\ , \end{cases} \\ &\overset{p_0\gg m}{\approx} \mathbf{s}\times\begin{cases} \frac{1}{4}\big(A^q_{2,0}(0)+B^q_{2,0}(0) \pm \lambda\tilde{A}^q_{2,0}(0)\big)\ , & \text{if } \mathbf{s} = \lambda\frac{\mathbf{p}}{|\mathbf{p}|}\ , \\ \frac{p_0}{4m}B^q_{2,0}(0)\ , & \text{if } \mathbf{s}\perp\mathbf{p}\ , \end{cases}\end{aligned} \tag{3.14}$$

i.e., quarks of opposite helicity in a longitudinally polarized nucleon can carry different fractions of the total angular momentum. Note that a consideration of higher moments of the momentum densities is straightforward. However, the expressions get a bit lengthy (including the C-type form factors and derivatives of the form factors in the forward limit) and their physical significance, apart from encoding information about the momentum distribution, is not as clear as for the zeroth and first moment.

3.3 Operator construction

In this section we construct the low-energy version of the local operators given in eq. (3.3). We do this by taking into account all possible Lorentz-covariant combinations of chiral building blocks that have the desired properties under chiral rotations ($\hat{\chi}$), parity transformation ($\mathcal{P}$), charge ($\mathcal{C}$) and Hermitian conjugation. As explained in section 2.2.1 one can use time reversal instead of Hermitian conjugation at will, because of the famous $\mathcal{CPT}$ theorem. Note that the derivation of the matrix element decomposition given in eq. (3.6) relies, aside from chiral behavior, on the same symmetry principles. This automatically ensures, that the results we obtain for the matrix elements are compatible with the form factor decomposition.

3.3.1 Symmetry properties

For the following construction it is convenient to define operators with arbitrary quark flavors by

$$\mathcal{O}^Q_{\mu\nu}(x) = \frac{1}{2}\,\mathbf{S}\,\bar{q}^a(x)\gamma_\mu i D^-_\nu Q^{ab} q^b(x)\ , \tag{3.15a}$$

$$\tilde{\mathcal{O}}^Q_{\mu\nu}(x) = \frac{1}{2}\,\mathbf{S}\,\bar{q}^a(x)\gamma_\mu\gamma_5 i D^-_\nu Q^{ab} q^b(x)\ , \tag{3.15b}$$

where Q is a 2×2 matrix and a, b are flavor indices. Since the operator is local the quark and the antiquark field are at the same spacetime position x. Being chiral-even, the operators can be split into parts that contain left- or right-handed quarks ($q_X = \gamma_X q_X$, $\gamma_{R/L} = (\mathbb{1} \pm \gamma_5)/2$) exclusively:

$$\mathcal{O}^Q_{\mu\nu}(x) = Q^{ab}\big(\mathcal{O}^{ab}_{R,\mu\nu}(x) + \mathcal{O}^{ab}_{L,\mu\nu}(x)\big)\ , \tag{3.16a}$$

$$\tilde{\mathcal{O}}^Q_{\mu\nu}(x) = Q^{ab}\big(\mathcal{O}^{ab}_{R,\mu\nu}(x) - \mathcal{O}^{ab}_{L,\mu\nu}(x)\big)\ , \tag{3.16b}$$

where the operators $\mathcal{O}_X$, $X \in \{R, L\}$ are given by

$$\mathcal{O}^{ab}_{X,\mu\nu}(x) = \frac{1}{2}\mathbf{S}\,\bar{q}^a_X(x)\gamma_\mu i D^-_\nu q^b_X(x)\ . \tag{3.17}$$

Under chiral rotations these operators transform either only left- or right-handedly:

$$\mathcal{O}^{ab}_{X,\mu\nu}(x) \xrightarrow{\hat{\chi}} X_{bb'}\mathcal{O}^{a'b'}_{X,\mu\nu}(x)\big(X^\dagger\big)_{a'a}\ . \tag{3.18}$$

Using the transformation properties of the quark fields under discrete symmetry transformations and Hermitian conjugation described in section 2.2.1 yields the following symmetry properties for the composite operators:

$$\mathcal{P}\mathcal{O}^{ab}_{X,\mu\nu}(x)\mathcal{P}^\dagger = (-1)_\mu(-1)_\nu\mathcal{O}^{ab}_{\bar{X},\mu\nu}(\tilde{x})\ , \tag{3.19a}$$

$$\mathcal{C}\mathcal{O}^{ab}_{X,\mu\nu}(x)\mathcal{C}^\dagger = \mathcal{O}^{ba}_{\bar{X},\mu\nu}(x)\ , \tag{3.19b}$$

$$\mathcal{T}\mathcal{O}^{ab}_{X,\mu\nu}(x)\mathcal{T}^\dagger = (-1)_\mu(-1)_\nu\mathcal{O}^{ab}_{X,\mu\nu}(-\tilde{x})\ , \tag{3.19c}$$

$$\big(\mathcal{O}^{ab}_{X,\mu\nu}(x)\big)^\dagger = \mathcal{O}^{ba}_{X,\mu\nu}(x)\ , \tag{3.19d}$$

where $(-1)_\mu$ is 1 for $\mu = 0$ and -1 for $\mu = 1, 2, 3$. These transformation properties have to be reproduced by the low-energy version of the currents and will guide the construction performed in the following sections.

3.3.2 Pion sector

In the mesonic sector we can easily write down the operator in terms of chiral fields which have the correct properties under chiral rotations

$$\mathcal{O}^{ab}_{X,\mu\nu} = \mathbf{S}\sum_A L_{X,A}\big(u_X A_{\mu\nu} u_{\bar{X}}\big)^{ab} + \mathbb{1}^{ab}\,\mathbf{S}\sum_A L^s_{X,A}\,\mathrm{tr}\left\{u_X A_{\mu\nu} u_{\bar{X}}\right\}\ , \tag{3.20}$$

where the As have to be combinations of chiral building blocks. To comply with the remaining symmetry properties given in eq. (3.19) we have to demand that the LECs fulfill the following constraints

$$L_{\bar{X},A} = L_{X,A}\eta_A^P \in \begin{cases} \{0\} \ , & \text{if } \eta_A^C\eta_A^P = -1 \ , \\ \mathbb{R} \ , & \text{if } \eta_A^H = 1 \ , \\ \mathbb{I} \ , & \text{if } \eta_A^H = -1 \ , \end{cases} \tag{3.21}$$

and similar for $L^s_{X,A}$. Up to second (chiral) order there is only one possible structure for A, which is $u_\mu u_\nu$. The other possible candidate which immediately comes to ones mind, $D_\mu u_\nu$, does not occur, since it has $\eta_A^C\eta_A^P = -1$, i.e., it has wrong transformation properties under $\mathcal{CP}$ transformations. Defining the LECs such that isosinglet and -triplet are neatly separated ($l = L_{R,A}$ and $l^s = L^s_{R,A} + L_{R,A}/2$), we find for the mesonic parts of the complete operators

$$\mathcal{O}^Q_{\mu\nu}\Big|_{\pi,2} = \mathbf{S}\,\mathrm{tr}\left\{\left(l\tilde{Q} + l^s\,\mathrm{tr}\,\{Q\}\right)\left(uu_\mu u_\nu u^\dagger + u^\dagger u_\mu u_\nu u\right)\right\} \ , \tag{3.22a}$$

$$\tilde{\mathcal{O}}^Q_{\mu\nu}\Big|_{\pi,2} = \mathbf{S}\,\mathrm{tr}\left\{l\tilde{Q}\left(uu_\mu u_\nu u^\dagger - u^\dagger u_\mu u_\nu u\right)\right\} \ , \tag{3.22b}$$

where

$$\tilde{Q} \equiv Q - \frac{1}{2}\,\mathrm{tr}\,\{Q\} \ . \tag{3.23}$$

These structures are of second chiral order. We will not discuss structures of higher order since they do not contribute to our calculation.

3.3.3 Nucleon sector

A power counting analysis of all possible Feynman diagrams (compare figure 3.1 on page 46) yields that only zeroth and first order $N\pi\pi N$- and $N\pi N$-operator insertions contribute to graphs (b), (d) and (e) at full one-loop level. Thus, in the nucleon sector, we only have to construct second and third order operator structures without additional pions. Working in the limit of exact isospin symmetry this leaves us, aside from covariant derivatives acting on the nucleon fields, with only three possible chiral building blocks, $\mathbb{1}$, $\mathrm{tr}\,\{\chi^+\}\,\mathbb{1}$ and u_μ, where the chiral vielbein only occurs at most once in operators of first chiral order. As a first step we write down all structures with correct behavior under chiral transformations,

$$\begin{aligned} \mathcal{O}^{ab}_{X,\mu\nu} = {} & \mathbf{S}\sum_{(\mathbf{A})_{\mu\nu},\pm} L^{\pm}_{X,\mathbf{A}}\Big(\left(\bar{\Psi}A_1u_{\bar{X}}\right)^a A_\Gamma\left(u_X A_2\Psi\right)^b \pm \left(\bar{\Psi}A_2u_{\bar{X}}\right)^a A_\Gamma\left(u_X A_1\Psi\right)^b\Big) \\ & + \mathbf{S}\sum_{(\mathbf{A})_{\mu\nu}} L^s_{X,\mathbf{A}}\left(u_X A_1 u_{\bar{X}}\right)^{ba}\left(\bar{\Psi}A_2A_\Gamma\Psi\right) \ , \end{aligned} \tag{3.24}$$

with $\mathbf{A} \equiv A_1 \otimes A_2 \otimes A_\Gamma$, where A_1 and A_2 are chiral building blocks while A_Γ contains elements of the Clifford algebra and derivatives acting on the nucleon fields. Obviously, the antisymmetric contribution in the first line can only occur if A_1 and A_2 are not equal. In order to have correct

properties under parity transformation, charge and Hermitian conjugation the LECs have to fulfill the following relations

$$L^{\pm}_{\bar{X},\mathbf{A}} = L^{\pm}_{X,\mathbf{A}}\eta^P_{\mathbf{A}} \in \begin{cases} \{0\}\,, & \text{if } \eta^C_{\mathbf{A}}\eta^P_{\mathbf{A}} = \pm 1\,, \\ \mathbb{R}\,, & \text{if } \eta^H_{\mathbf{A}} = \pm 1\,, \\ \mathbb{I}\,, & \text{if } \eta^H_{\mathbf{A}} = \mp 1\,, \end{cases} \tag{3.25a}$$

$$L^{s}_{\bar{X},\mathbf{A}} = L^{s}_{X,\mathbf{A}}\eta^P_{\mathbf{A}} \in \begin{cases} \{0\}\,, & \text{if } \eta^C_{\mathbf{A}}\eta^P_{\mathbf{A}} = +1\,, \\ \mathbb{R}\,, & \text{if } \eta^H_{\mathbf{A}} = +1\,, \\ \mathbb{I}\,, & \text{if } \eta^H_{\mathbf{A}} = -1\,, \end{cases} \tag{3.25b}$$

where $\eta^P_{\mathbf{A}} \equiv \eta^P_{A_1}\eta^P_{A_2}\eta^P_{A_\Gamma}$, $\eta^C_{\mathbf{A}} \equiv \eta^C_{A_1}\eta^C_{A_2}\eta^C_{A_\Gamma}$ and $\eta^H_{\mathbf{A}} \equiv \eta^H_{A_1}\eta^H_{A_2}\eta^H_{A_\Gamma}$. As expected, the constraint obtained by time reversal is compatible with the ones given above and does not yield any further restrictions on the operator. For the actual construction the general form of the operator is quite unhandy. It is more convenient to treat the parts of the operator containing different chiral building blocks separately. The simplest case ($A_1 = A_2 = \mathbb{1}$) reads

$$\mathcal{O}^{ab,\mathbb{1},(n)}_{X,\mu\nu} = \mathbf{S}\sum_{A_{\mu\nu}}\Big(L^{\mathbb{1}}_{X,A}\big(\bar{\Psi}u_{\bar{X}}\big)^a A_{\mu\nu}\big(u_X\Psi\big)^b + L^{\mathbb{1},s}_{X,A}\,\mathbb{1}^{ba}\,\big(\bar{\Psi}A_{\mu\nu}\Psi\big)\Big)\,, \tag{3.26}$$

where the sum runs over $A_{\mu\nu} \in \mathcal{D}^{(n)}_{\{\mu\nu\}}$, see table 3.1, and the number in parentheses denotes the chiral order. The low-energy constants have to fulfill the following constraints

$$L^{\mathbb{1}(,s)}_{\bar{X},A} = L^{\mathbb{1}(,s)}_{X,A}\eta^P_A \in \begin{cases} \{0\}\,, & \text{if } \eta^C_A\eta^P_A = +1\,, \\ \mathbb{R}\,, & \text{if } \eta^H_A = +1\,, \\ \mathbb{I}\,, & \text{if } \eta^H_A = -1\,, \end{cases} \tag{3.27}$$

where η^C_A, η^P_A and η^H_A are given in table 3.1. The operators containing the quark mass insertions start at second chiral order. They have the form

$$\mathcal{O}^{ab,\chi^+,(n\geq 2)}_{X,\mu\nu} = \mathrm{tr}\left\{\chi^+\right\}\mathbf{S}\sum_{A_{\mu\nu}}\Big(L^{\chi^+}_{X,A}\big(\bar{\Psi}u_{\bar{X}}\big)^a A_{\mu\nu}\big(u_X\Psi\big)^b + L^{\chi^+,s}_{X,A}\,\mathbb{1}^{ba}\,\big(\bar{\Psi}A_{\mu\nu}\Psi\big)\Big)\,, \tag{3.28}$$

where $A_{\mu\nu}$ can be chosen from $\mathcal{D}^{(n-2)}_{\{\mu\nu\}}$. The LECs are constrained by

$$L^{\chi^+(,s)}_{\bar{X},A} = L^{\chi^+(,s)}_{X,A}\eta^P_A \in \begin{cases} \{0\}\,, & \text{if } \eta^C_A\eta^P_A = +1\,, \\ \mathbb{R}\,, & \text{if } \eta^H_A = +1\,, \\ \mathbb{I}\,, & \text{if } \eta^H_A = -1\,. \end{cases} \tag{3.29}$$

Finally, we have to take into account terms which contain u_μ. These operators are of first chiral order and occur in Feynman diagrams containing at least one pion.

$$\begin{aligned}\mathcal{O}^{ab,u,(1)}_{X,\mu\nu} = \mathbf{S}\sum_{A_{\mu\nu\alpha}}\Big(& L^{u}_{X,A}\Big(\big(\bar{\Psi}u^\alpha u_{\bar{X}}\big)^a A_{\mu\nu\alpha}\big(u_X\Psi\big)^b + \eta^C_A\eta^P_A\big(\bar{\Psi}u_{\bar{X}}\big)^a A_{\mu\nu\alpha}\big(u_X u^\alpha\Psi\big)^b\Big) \\ & + L^{u,s1}_{X,A}\,\mathbb{1}^{ba}\,\big(\bar{\Psi}u^\alpha A_{\mu\nu\alpha}\Psi\big) + L^{u,s2}_{X,A}\,\big(u_X u^\alpha u_{\bar{X}}\big)^{ba}\big(\bar{\Psi}A_{\mu\nu\alpha}\Psi\big)\Big)\,,\end{aligned} \tag{3.30}$$

Table 3.1: Elements of $\mathcal{D}^{(0)}_{\mu}$, $\mathcal{D}^{(0)}_{\{\mu\nu\}}$, $\mathcal{D}^{(1)}_{\{\mu\nu\}}$, $\mathcal{D}^{(2)}_{\{\mu\nu\}}$, $\mathcal{D}^{(3)}_{\{\mu\nu\}}$ and $\mathcal{D}^{(0)}_{\{\mu\nu\}\alpha}$ and their symmetry properties. The braces indicate, that we only take into account terms that survive the symmetrization by **S**.

	A	η_A^P	η_A^C	η_A^H	
$A \in \mathcal{D}^{(0)}_{\mu}$	$\gamma_5 D^-_\mu$	-1	$+1$	$+1$	
	γ_μ	$+1$	$+1$	$+1$	
	$\gamma_\mu\gamma_5$	-1	-1	$+1$	
$A \in \mathcal{D}^{(0)}_{\{\mu\nu\}}$	$\gamma_5 D^-_\mu D^-_\nu$	-1	-1	-1	
	$\gamma_\mu D^-_\nu$	$+1$	-1	-1	
	$\gamma_\mu\gamma_5 D^-_\nu$	-1	$+1$	-1	
$A \in \mathcal{D}^{(1)}_{\{\mu\nu\}}$	$\gamma_5 D^+_\mu D^-_\nu$	-1	$+1$	$+1$	
	$\gamma_\mu D^+_\nu$	$+1$	$+1$	$+1$	
	$\gamma_\mu\gamma_5 D^+_\nu$	-1	-1	$+1$	
	$\sigma_{\mu\beta} D^{+\beta} D^-_\nu$	$+1$	-1	-1	
$A \in \mathcal{D}^{(2)}_{\{\mu\nu\}}$	$D^+_\mu D^+_\nu$	$+1$	-1	$+1$	
	$\gamma_5 D^+_\mu D^+_\nu$	-1	-1	-1	
	$\sigma_{\mu\beta} D^{+\beta} D^+_\nu$	$+1$	$+1$	$+1$	
	$\gamma_5 D^-_\mu D^-_\nu \; D^+\!\cdot D^+$	-1	-1	-1	$\hat{=} \mathcal{D}^{(0)}_{\{\mu\nu\}} \; D^+\!\cdot D^+$
	$\gamma_\mu D^-_\nu \; D^+\!\cdot D^+$	$+1$	-1	-1	
	$\gamma_\mu\gamma_5 D^-_\nu \; D^+\!\cdot D^+$	-1	$+1$	-1	
$A \in \mathcal{D}^{(3)}_{\{\mu\nu\}}$	$\gamma_5 D^+_\mu D^-_\nu \; D^+\!\cdot D^+$	-1	$+1$	$+1$	$\hat{=} \mathcal{D}^{(1)}_{\{\mu\nu\}} \; D^+\!\cdot D^+$
	$\gamma_\mu D^+_\nu \; D^+\!\cdot D^+$	$+1$	$+1$	$+1$	
	$\gamma_\mu\gamma_5 D^+_\nu \; D^+\!\cdot D^+$	-1	-1	$+1$	
	$\sigma_{\mu\beta} D^{+\beta} D^-_\nu \; D^+\!\cdot D^+$	$+1$	-1	-1	
$A \in \mathcal{D}^{(0)}_{\{\mu\nu\}\alpha}$	$\gamma_5 D^-_\mu D^-_\nu D^-_\alpha$	-1	$+1$	$+1$	
	$\gamma_\mu D^-_\nu D^-_\alpha$	$+1$	$+1$	$+1$	
	$\gamma_\alpha D^-_\mu D^-_\nu$	$+1$	$+1$	$+1$	
	$\gamma_\mu\gamma_5 D^-_\nu D^-_\alpha$	-1	-1	$+1$	
	$\gamma_\alpha\gamma_5 D^-_\mu D^-_\nu$	-1	-1	$+1$	
	$\sigma_{\mu\alpha} D^-_\nu$	$+1$	-1	-1	
	$\epsilon_{\mu\alpha\rho\sigma}\sigma^{\rho\sigma} D^-_\nu$	-1	-1	-1	

where the $A_{\mu\nu\alpha}$ have to be taken from $\mathcal{D}^{(0)}_{\{\mu\nu\}\alpha}$ and $g_{\alpha\{\mu}\mathcal{D}^{(0)}_{\nu\}}$, which can be found in table 3.1. For the LECs one finds the constraints

$$L^u_{\bar{X},A} = -L^u_{X,A}\eta^P_A \in \begin{cases} \mathbb{R}\,, & \text{if } \eta^H_A = +\eta^C_A\eta^P_A\,, \\ \mathbb{I}\,, & \text{if } \eta^H_A = -\eta^C_A\eta^P_A\,, \end{cases} \tag{3.31a}$$

$$L^{u,s1/s2}_{\bar{X},A} = -L^{u,s1/s2}_{X,A}\eta^P_A \in \begin{cases} \{0\}\,, & \text{if } \eta^C_A\eta^P_A = -1\,, \\ \mathbb{R}\,, & \text{if } \eta^H_A = +1\,, \\ \mathbb{I}\,, & \text{if } \eta^H_A = -1\,. \end{cases} \tag{3.31b}$$

The number of possible terms can be reduced significantly by using the (free) equations of motion

$$i\vec{\not{D}}\Psi \doteq m\Psi \ , \qquad\qquad \bar{\Psi}i\overleftarrow{\not{D}} \doteq -\bar{\Psi}m \ , \tag{3.32}$$

where the dot over the equal sign means up to higher order in the chiral counting. Using eq. (3.32) one finds two identities

$$\bar{\Psi}\Gamma\gamma^\beta\vec{D}_\beta\Psi = \bar{\Psi}\left(\frac{1}{2}\{\Gamma,\gamma^\beta\}+\frac{1}{2}[\Gamma,\gamma^\beta]\right)\vec{D}_\beta\Psi \doteq -im\bar{\Psi}\Gamma\Psi \ , \tag{3.33a}$$

$$\bar{\Psi}\gamma^\beta\Gamma\overleftarrow{D}_\beta\Psi = \bar{\Psi}\left(\frac{1}{2}\{\Gamma,\gamma^\beta\}-\frac{1}{2}[\Gamma,\gamma^\beta]\right)\overleftarrow{D}_\beta\Psi \doteq im\bar{\Psi}\Gamma\Psi \ , \tag{3.33b}$$

which can be rewritten as

$$\bar{\Psi}\left(\frac{1}{2}\{\Gamma,\gamma^\beta\}D^+_\beta+\frac{1}{2}[\Gamma,\gamma^\beta]D^-_\beta\right)\Psi \doteq 0 \ , \tag{3.34a}$$

$$\bar{\Psi}\left(\frac{1}{2}\{\Gamma,\gamma^\beta\}D^-_\beta+\frac{1}{2}[\Gamma,\gamma^\beta]D^+_\beta\right)\Psi \doteq -2im\bar{\Psi}\Gamma\Psi \ , \tag{3.34b}$$

where $\Gamma \in \{\mathbb{1},\gamma_5,\gamma_\mu,\gamma_\mu\gamma_5,\sigma_{\mu\nu},\sigma_{\mu\nu}\gamma_5\}$. These relations also hold if we insert additional chiral building blocks or an arbitrary number of derivatives. They are similar to those given in refs. [81, 114]. For the different possible Clifford matrices we find explicitly

$\underline{\mathbb{1}}$

$$\bar{\Psi}\gamma^\beta D^+_\beta\Psi \doteq 0 \ , \tag{3.35a}$$

$$\bar{\Psi}\gamma^\beta D^-_\beta\Psi \doteq -2im\bar{\Psi}\Psi \ , \tag{3.35b}$$

$\underline{\gamma_5}$

$$\bar{\Psi}\gamma^\beta\gamma_5 D^-_\beta\Psi \doteq 0 \ , \tag{3.35c}$$

$$\bar{\Psi}\gamma^\beta\gamma_5 D^+_\beta\Psi \doteq -2im\bar{\Psi}\gamma_5\Psi \ , \tag{3.35d}$$

$\underline{\gamma^\mu}$

$$\bar{\Psi}i\sigma^{\mu\beta}D^-_\beta\Psi \doteq \bar{\Psi}D^{+\mu}\Psi \ , \tag{3.35e}$$

$$\bar{\Psi}i\sigma^{\mu\beta}D^+_\beta\Psi \doteq \bar{\Psi}D^{-\mu}\Psi + 2im\bar{\Psi}\gamma^\mu\Psi \ , \tag{3.35f}$$

$\underline{\gamma^\mu\gamma_5}$

$$\bar{\Psi}\frac{1}{2}\epsilon^{\mu\beta\rho\sigma}\sigma_{\rho\sigma}D^+_\beta\Psi \doteq \bar{\Psi}\gamma_5 D^{-\mu}\Psi \ , \tag{3.35g}$$

$$\bar{\Psi}\frac{1}{2}\epsilon^{\mu\beta\rho\sigma}\sigma_{\rho\sigma}D^-_\beta\Psi \doteq \bar{\Psi}\gamma_5 D^{+\mu}\Psi - 2im\bar{\Psi}\gamma^\mu\gamma_5\Psi \ , \tag{3.35h}$$

$\underline{\sigma^{\mu\nu}}$

$$\bar{\Psi}\epsilon^{\mu\nu\beta\delta}\gamma_\delta\gamma_5 D^+_\beta\Psi \doteq -i\bar{\Psi}\big(\gamma^\mu D^{-\nu}-\gamma^\nu D^{-\mu}\big)\Psi \ , \tag{3.35i}$$

$$\bar{\Psi}\epsilon^{\mu\nu\beta\delta}\gamma_\delta\gamma_5 D^-_\beta\Psi \doteq -i\bar{\Psi}\big(\gamma^\mu D^{+\nu}-\gamma^\nu D^{+\mu}\big)\Psi - 2im\bar{\Psi}\sigma^{\mu\nu}\Psi \ , \tag{3.35j}$$

$\underline{\sigma^{\mu\nu}\gamma_5}$

$$\bar{\Psi}\epsilon^{\mu\nu\beta\delta}\gamma_\delta D^-_\beta\Psi \doteq -i\bar{\Psi}\big(\gamma^\mu\gamma_5 D^{+\nu}-\gamma^\nu\gamma_5 D^{+\mu}\big)\Psi \ , \tag{3.35k}$$

$$\bar{\Psi}\epsilon^{\mu\nu\beta\delta}\gamma_\delta D^+_\beta\Psi \doteq -i\bar{\Psi}\big(\gamma^\mu\gamma_5 D^{-\nu}-\gamma^\nu\gamma_5 D^{-\mu}\big)\Psi + m\bar{\Psi}\epsilon^{\mu\nu\rho\sigma}\sigma_{\rho\sigma}\Psi \ . \tag{3.35l}$$

Note that, owing to the identity $\sigma^{\mu\nu}\gamma_5 = \frac{i}{2}\epsilon^{\mu\nu\rho\sigma}\sigma_{\rho\sigma}$, eqs. (3.35k) and (3.35l) are actually only useful reformulations of eqs. (3.35i) and (3.35j). We use eqs. (3.35a)-(3.35e) to eliminate all terms where a derivative is contracted with an element of the Clifford algebra apart from $\sigma^{\mu\beta}D^+_\beta$. We

Table 3.2: Structures contributing to the full one-loop calculation. We only write down terms that survive the EOM eliminations discussed in the text and the symmetrization by **S** later on.

n	i	$\mathcal{O}^{n,i}_{\mu\nu}$	$\tilde{\mathcal{O}}^{n,i}_{\mu\nu}$
0	1	$u^{Q,+s}_{0,1}\gamma_\mu iD^-_\nu$	$u^{Q,-}_{0,1}\gamma_\mu iD^-_\nu$
	2	$u^{Q,-}_{0,2}\gamma_\mu\gamma_5 iD^-_\nu$	$u^{Q,+s}_{0,2}\gamma_\mu\gamma_5 iD^-_\nu$
1	1	$u^{Q,-}_{1,1}\gamma_5 D^+_\mu D^-_\nu$	$u^{Q,+s}_{1,1}\gamma_5 D^+_\mu D^-_\nu$
	2	$u^{Q,+s}_{1,2}\sigma_\mu{}^\alpha D^+_\alpha iD^-_\nu$	$u^{Q,-}_{1,2}\sigma_\mu{}^\alpha D^+_\alpha iD^-_\nu$
	3	$\big[u_\mu, u^{Q,+}_{1,3}\big]\gamma_5 iD^-_\nu$	$\big[u_\mu, u^{Q,-}_{1,3}\big]\gamma_5 iD^-_\nu$
	4	$\big\{u_\mu, u^{Q,-}_{1,4}\big\}\gamma_\nu$	$\big\{u_\mu, u^{Q,+s}_{1,4}\big\}\gamma_\nu$
	5	$\mathrm{tr}\big\{u_\mu u^{Q,-}_{1,5}\big\}\gamma_\nu$	$\mathrm{tr}\big\{u_\mu u^{Q,+}_{1,5}\big\}\gamma_\nu$
	6	$\big\{u_\mu, u^{Q,+s}_{1,6}\big\}\gamma_\nu\gamma_5$	$\big\{u_\mu, u^{Q,-}_{1,6}\big\}\gamma_\nu\gamma_5$
	7	$\mathrm{tr}\big\{u_\mu u^{Q,+}_{1,7}\big\}\gamma_\nu\gamma_5$	$\mathrm{tr}\big\{u^\mu u^{Q,-}_{1,7}\big\}\gamma_\nu\gamma_5$
	8	$\big[u^\alpha, u^{Q,+}_{1,8}\big]\gamma_5 iD^-_\mu D^-_\nu D^-_\alpha$	$\big[u^\alpha, u^{Q,-}_{1,8}\big]\gamma_5 iD^-_\mu D^-_\nu D^-_\alpha$
	9	$\big\{u^\alpha, u^{Q,-}_{1,9}\big\}\gamma_\mu D^-_\nu D^-_\alpha$	$\big\{u^\alpha, u^{Q,+s}_{1,9}\big\}\gamma_\mu D^-_\nu D^-_\alpha$
	10	$\mathrm{tr}\big\{u^\alpha u^{Q,-}_{1,10}\big\}\gamma_\mu D^-_\nu D^-_\alpha$	$\mathrm{tr}\big\{u^\alpha u^{Q,+}_{1,10}\big\}\gamma_\mu D^-_\nu D^-_\alpha$
	11	$\big\{u^\alpha, u^{Q,-}_{1,11}\big\}\gamma_\alpha D^-_\mu D^-_\nu$	$\big\{u^\alpha, u^{Q,+s}_{1,11}\big\}\gamma_\alpha D^-_\mu D^-_\nu$
	12	$\mathrm{tr}\big\{u^\alpha u^{Q,-}_{1,12}\big\}\gamma_\alpha D^-_\mu D^-_\nu$	$\mathrm{tr}\big\{u^\alpha u^{Q,+}_{1,12}\big\}\gamma_\alpha D^-_\mu D^-_\nu$
	13	$\big\{u^\alpha, u^{Q,+s}_{1,13}\big\}\gamma_\mu\gamma_5 D^-_\nu D^-_\alpha$	$\big\{u^\alpha, u^{Q,-}_{1,13}\big\}\gamma_\mu\gamma_5 D^-_\nu D^-_\alpha$
	14	$\mathrm{tr}\big\{u^\alpha u^{Q,+}_{1,14}\big\}\gamma_\mu\gamma_5 D^-_\nu D^-_\alpha$	$\mathrm{tr}\big\{u^\alpha u^{Q,-}_{1,14}\big\}\gamma_\mu\gamma_5 D^-_\nu D^-_\alpha$
	15	$\big\{u^\alpha, u^{Q,+s}_{1,15}\big\}\gamma_\alpha\gamma_5 D^-_\mu D^-_\nu$	$\big\{u^\alpha, u^{Q,-}_{1,15}\big\}\gamma_\alpha\gamma_5 D^-_\mu D^-_\nu$
	16	$\mathrm{tr}\big\{u^\alpha u^{Q,+}_{1,16}\big\}\gamma_\alpha\gamma_5 D^-_\mu D^-_\nu$	$\mathrm{tr}\big\{u^\alpha u^{Q,-}_{1,16}\big\}\gamma_\alpha\gamma_5 D^-_\mu D^-_\nu$
	17	$\big[u^\alpha, u^{Q,-}_{1,17}\big]\sigma_{\mu\alpha} D^-_\nu$	$\big[u^\alpha, u^{Q,+}_{1,17}\big]\sigma_{\mu\alpha} D^-_\nu$
	18	$\big\{u^\alpha, u^{Q,+s}_{1,18}\big\}\epsilon_{\mu\alpha\rho\sigma}\sigma^{\rho\sigma} iD^-_\nu$	$\big\{u^\alpha, u^{Q,-}_{1,18}\big\}\epsilon_{\mu\alpha\rho\sigma}\sigma^{\rho\sigma} iD^-_\nu$
	19	$\mathrm{tr}\big\{u^\alpha u^{Q,+}_{1,19}\big\}\epsilon_{\mu\alpha\rho\sigma}\sigma^{\rho\sigma} iD^-_\nu$	$\mathrm{tr}\big\{u^\alpha u^{Q,-}_{1,19}\big\}\epsilon_{\mu\alpha\rho\sigma}\sigma^{\rho\sigma} iD^-_\nu$
2	1	$u^{Q,+s}_{2,1} D^+_\mu D^+_\nu$	$u^{Q,-}_{2,1} D^+_\mu D^+_\nu$
	2	$u^{Q,+s}_{2,2}\gamma_\mu iD^-_\nu\ \mathrm{tr}\{\chi^+\}$	$u^{Q,-}_{2,2}\gamma_\mu iD^-_\nu\ \mathrm{tr}\{\chi^+\}$
	3	$u^{Q,+s}_{2,3}\gamma_\mu iD^-_\nu D^+{\cdot}D^+$	$u^{Q,-}_{2,3}\gamma_\mu iD^-_\nu D^+{\cdot}D^+$
	4	$u^{Q,-}_{2,4}\gamma_\mu\gamma_5 iD^-_\nu\ \mathrm{tr}\{\chi^+\}$	$u^{Q,+s}_{2,4}\gamma_\mu\gamma_5 iD^-_\nu\ \mathrm{tr}\{\chi^+\}$
	5	$u^{Q,-}_{2,5}\gamma_\mu\gamma_5 iD^-_\nu D^+{\cdot}D^+$	$u^{Q,+s}_{2,5}\gamma_\mu\gamma_5 iD^-_\nu D^+{\cdot}D^+$
3	1	$u^{Q,-}_{3,1}\gamma_5 D^+_\mu D^-_\nu\ \mathrm{tr}\{\chi^+\}$	$u^{Q,+s}_{3,1}\gamma_5 D^+_\mu D^-_\nu\ \mathrm{tr}\{\chi^+\}$
	2	$u^{Q,-}_{3,2}\gamma_5 D^+_\mu D^-_\nu D^+{\cdot}D^+$	$u^{Q,+s}_{3,2}\gamma_5 D^+_\mu D^-_\nu D^+{\cdot}D^+$
	3	$u^{Q,+s}_{3,3}\sigma_\mu{}^\alpha D^+_\alpha iD^-_\nu\ \mathrm{tr}\{\chi^+\}$	$u^{Q,-}_{3,3}\sigma_\mu{}^\alpha D^+_\alpha iD^-_\nu\ \mathrm{tr}\{\chi^+\}$
	4	$u^{Q,+s}_{3,4}\sigma_\mu{}^\alpha D^+_\alpha iD^-_\nu D^+{\cdot}D^+$	$u^{Q,-}_{3,4}\sigma_\mu{}^\alpha D^+_\alpha iD^-_\nu D^+{\cdot}D^+$

use eq. (3.35f), which is the Gordon identity, to replace all terms that simultaneously have the identity matrix as Dirac structure and contain a minus derivative. The remaining eqs. (3.35g)-(3.35l) are used to dispose of as many structures containing the ϵ-tensor as possible. Another useful identity is the curvature relation

$$[D_\mu, D_\nu] = \frac{1}{4}[u_\mu, u_\nu] \ , \tag{3.36}$$

which also holds for derivatives acting to the left and allows us to consider only symmetric combinations of derivatives. The EOM yields three additional relations:

$$\bar{\Psi}\Gamma D^+ \cdot D^- \Psi = \bar{\Psi}\big(\Gamma \overrightarrow{\not{D}}\overrightarrow{\not{D}} - \overleftarrow{\not{D}}\overleftarrow{\not{D}}\Gamma\big)\Psi \doteq 0 \ , \tag{3.37a}$$

$$\begin{aligned}\bar{\Psi}\Gamma D^\pm \cdot D^\pm \Psi &= \bar{\Psi}\big(\Gamma \overrightarrow{\not{D}}\overrightarrow{\not{D}} + \overleftarrow{\not{D}}\overleftarrow{\not{D}}\Gamma \pm 2\overleftarrow{D}^\alpha \Gamma \overrightarrow{D}_\alpha\big)\Psi \\ &\doteq \bar{\Psi}\big(-2m^2\Gamma \pm 2\overleftarrow{D}^\alpha \Gamma \overrightarrow{D}_\alpha\big)\Psi \ ,\end{aligned} \tag{3.37b}$$

which we use to eliminate all contractions of derivatives (acting on nucleon fields) apart from $D^+ \cdot D^+$.

Rewriting the flavor matrix Q as a sum of a traceless matrix $\tilde{Q}$ (see eq. (3.23)) and a trace term one finds that the trace part either vanishes or can (by a redefinition of LECs) be absorbed into a singlet contribution. We write down the low-energy form of the complete operators $\mathcal{O}^Q_{\mu\nu}$ and $\tilde{\mathcal{O}}^Q_{\mu\nu}$ as

$$\mathcal{O}^Q_{\mu\nu}\Big|_{N\pi,n} = \mathbf{S}\sum_i \bar{\Psi}\mathcal{O}^{n,i}_{\mu\nu}\Psi \ , \qquad \tilde{\mathcal{O}}^Q_{\mu\nu}\Big|_{N\pi,n} = \mathbf{S}\sum_i \bar{\Psi}\tilde{\mathcal{O}}^{n,i}_{\mu\nu}\Psi \ , \tag{3.38}$$

where n indicates the chiral order. The $\mathcal{O}^{n,i}_{\mu\nu}$ and $\tilde{\mathcal{O}}^{n,i}_{\mu\nu}$, given in table 3.2, are expressed economically using the following abbreviations for recurring structures

$$u^{Q,\pm}_{n,i} = l_{n,i}\big(u^\dagger \tilde{Q} u \pm u \tilde{Q} u^\dagger\big) \ , \tag{3.39a}$$

$$u^{Q,s}_{n,i} = 2l^s_{n,i}\,\mathrm{tr}\,\{Q\} \ , \tag{3.39b}$$

$$u^{Q,+s}_{n,i} = u^{Q,+}_{n,i} + u^{Q,s}_{n,i} \ , \tag{3.39c}$$

where the $l_{n,i}$ and $l^s_{n,i}$ are real-valued low-energy constants. The superscript s indicates the isoscalar contributions.

3.4 Details on the calculation

The different types of Feynman diagrams needed for the full one-loop calculation in BChPT of the first moments of the quark GPDs are shown in figure 3.1. Full one-loop in this context means that we take into account all orders of ChPT that do not contain two-loop contributions (i.e., up to and including third order). Diagram type (a) starts to contribute at zeroth, (b)-(e) at second and (f) at third order. Additional diagrams with quark mass insertions from the second order pion-nucleon Lagrangian are not depicted in figure 3.1. We take them into account via replacing m_0 by $m_N = m_0 - 4c_1 m_\pi^2$ everywhere. Due to this procedure our results sporadically contain higher order diagrams.

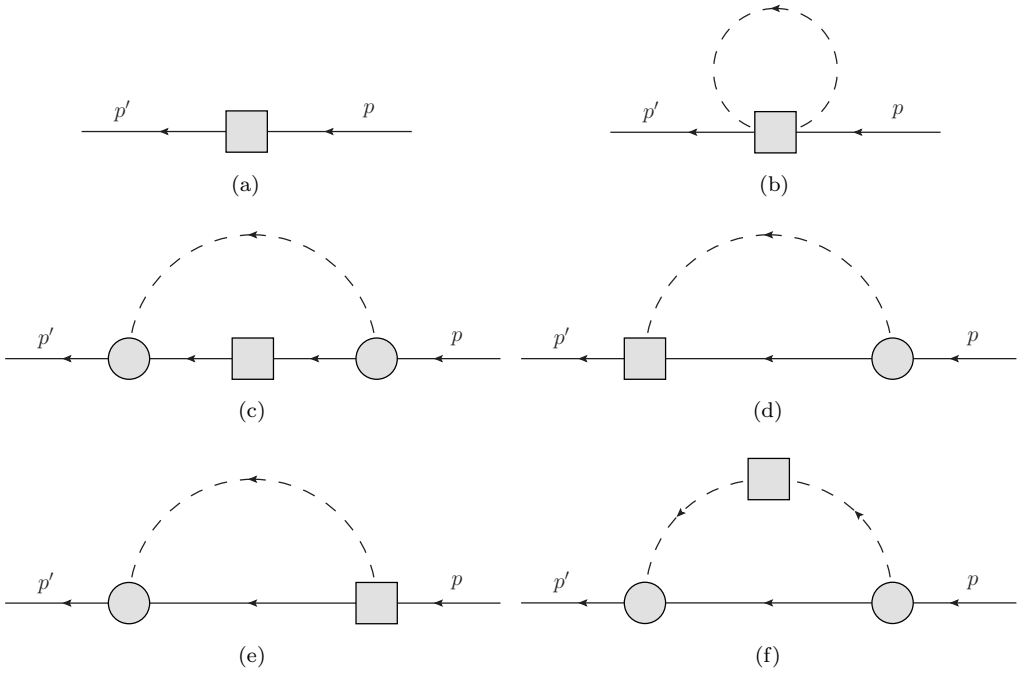

Figure 3.1: Feynman diagrams needed for the full one-loop calculation. Solid/dashed lines depict nucleon/meson propagators. The circles stand for vertices from the chiral Lagrangian, while the squares indicate the operator insertion. Diagram (f) only contributes to the (isosinglet) vector current. Diagram (a) has to be multiplied with a Z-factor if the operator insertion is of zeroth or first order. Additional Feynman diagrams containing quark mass insertions from the second order pion-nucleon Lagrangian are not shown explicitly.

In order to present the results in the most convenient way we match the expressions obtained for the full matrix elements to the form factor decomposition given in eq. (3.6). Special care has to be taken of diagrams (d) and (e), since they cannot be matched individually. Only their sum is compatible with the form factor decomposition. For the remaining contributions the matching works diagram by diagram. The final results are given for the isoscalar and isovector combinations of the generalized form factors, which are defined as

$$A_{2,0}^{s,v} = \big(A_{2,0}^{u} \pm A_{2,0}^{d}\big)^{p} = \pm\big(A_{2,0}^{u} \pm A_{2,0}^{d}\big)^{n} \,, \tag{3.40a}$$

$$B_{2,0}^{s,v} = \big(B_{2,0}^{u} \pm B_{2,0}^{d}\big)^{p} = \pm\big(B_{2,0}^{u} \pm B_{2,0}^{d}\big)^{n} \,, \tag{3.40b}$$

$$C_{2}^{s,v} = \big(C_{2}^{u} \pm C_{2}^{d}\big)^{p} = \pm\big(C_{2}^{u} \pm C_{2}^{d}\big)^{n} \,, \tag{3.40c}$$

$$\tilde{A}_{2,0}^{s,v} = \big(\tilde{A}_{2,0}^{u} \pm \tilde{A}_{2,0}^{d}\big)^{p} = \pm\big(\tilde{A}_{2,0}^{u} \pm \tilde{A}_{2,0}^{d}\big)^{n} \,, \tag{3.40d}$$

$$\tilde{B}_{2,0}^{s,v} = \big(\tilde{B}_{2,0}^{u} \pm \tilde{B}_{2,0}^{d}\big)^{p} = \pm\big(\tilde{B}_{2,0}^{u} \pm \tilde{B}_{2,0}^{d}\big)^{n} \,, \tag{3.40e}$$

where the superscripts p and n are introduced to differentiate between proton and neutron form factors. For these form factors we obtain expressions in terms of standard integrals and a remaining integration over a Feynman parameter (originating from the three-point functions

contained in diagrams of type (c) and (f)). The full one-loop result obtained by a manifestly covariant calculation in the infrared regularization scheme [86] is presented in section 3.5.1.

In general, nucleon four-momenta have to be counted as large (zeroth order) in BChPT. However, $\Delta = p' - p$ has to be counted as small (first order) since the nucleon mass drops out in the momentum difference. This is also true for the Δs in the decomposition of the matrix elements (see eq. (3.6)) and, accordingly, our results for $A_{2,0}^{s,v}$, $\tilde{A}_{2,0}^{s,v}$ are exact to third, those for $B_{2,0}^{s,v}$, $\tilde{B}_{2,0}^{s,v}$ to second and the one for $C_2^{s,v}$ to first chiral order.

The low-energy versions of the gluon operator $\mathcal{O}_{\mu\nu}^g$ and the singlet combination of the quark operator $\mathcal{O}_{\mu\nu}^{\mathbb{1}}$ are equal up to the numerical value of the LECs since they behave similar under chiral rotations, charge conjugation and parity transformation. We therefore define the operator by a mere replacement of LECs:

$$\mathcal{O}_{\mu\nu}^g \equiv \mathcal{O}_{\mu\nu}^{\mathbb{1}} \quad (l^s \to l^g, l_{i,j}^s \to l_{i,j}^g) \ . \tag{3.41}$$

The generalized form factors inherit this property and are obtained via replacing all superscripts s by g.

3.5 Results

3.5.1 Full one-loop result

In the following we will present the full one-loop results for the generalized form factors. We split the result for each form factor X into parts orginating from the different Feynman diagrams shown in figure 3.1:

$$X^{s/v} = X_{(a)}^{s/v} + X_{(b)}^{s/v} + X_{(de)}^{s/v} + \int_{-\frac{1}{2}}^{\frac{1}{2}} du \, \left(X_{(c)}^{s/v} + X_{(f)}^{s/v} \right) \ , \tag{3.42}$$

where the triangle diagrams still have to be integrated over the Feynman parameter u. As explained above, the contributions from diagrams (d) and (e) cannot be matched to the form factors individually and are therefore treated together. Note that diagrams (b) and (f) do not contribute to all form factors. (b) only occurs in the isovector case, while (f) is only relevant for the isoscalar form factors of the vector current, i.e., $A_{2,0}^s$, $B_{2,0}^s$ and C_2^s. The rather lengthy explicit expressions for the contributions of the different diagrams are given in appendix B.2 in terms of the standard integrals given in appendix A.4. The result in terms of elementary functions can be found in our work [97].

The expressions given in appendix B.2 still contain divergences. Up to the order to which our results are exact the occurring divergences can be absorbed in LECs by the use of eq. (B.1). The higher order divergences have to be canceled by hand which introduces the unphysical scale dependence in higher order terms typical for manifestly covariant calculations. In order to obtain a meaningful result one has to set this scale to a hadronic value around 1 GeV, as argued in ref. [86]. A variation of this scale within reasonable bounds, say 0.8 GeV-1.2 GeV, can be used

to estimate the systematic error due to higher order effects (cf. [115], where the ρ (Ξ) mass has been chosen as lower (upper) bound).

Taking a closer look at the results one finds that many new LECs occur. They mainly originate from first order operator insertions in diagrams of type (d) and (e). While at least in principle one would prefer to keep all these structures, the reality of a finite amount of available lattice data forces us to reduce the number of free parameters in the end, cf. section 3.6. One possibility to achieve such a reduction would be a strict truncation of the results at the order to which they are exact, which leads to the same extrapolation formulas as an equivalent calculation within the framework of heavy baryon ChPT (cf. section 3.5.2). Doing so one would, however, lose all benefits of the covariant result, like the correct behavior near the two-pion threshold at $t = 4m_\pi^2$ and the improved convergence that is often ascribed to the untruncated results. A reasonable compromise could look as follows: truncate diagrams (d) and (e), which yield the main share of the new LECs, but keep the triangle diagrams (c) and (f), which do not introduce new LECs, to all orders. This tradeoff is particularly appealing since diagram (f) is responsible for the threshold behavior that is not described correctly by the truncated version.

3.5.2 Heavy baryon reduction

To obtain the heavy baryon reduced result one has to truncate the simultaneous expansion in the pion mass m_π and the momentum transfer $t = \Delta^2$ at full one-loop order. To be consistent with the chiral counting scheme one has to count t as second order. This can be achieved most easily by keeping the ratio t/m_π^2, which is counted as $\mathcal{O}(1)$, fixed. After the truncation the remaining integral over the Feynman parameter u in diagrams (c) and (f) can be carried out analytically, which allows us to give the heavy baryon reduced result in closed form.

Generalized form factors

The heavy baryon reduced version of our result has the advantage that it can be written in a compact and lucid way. Writing all functions in such a way that only real quantities occur in the spacelike region, we obtain for the isoscalar form factors

$$\begin{aligned} A^s_{2,0} &= A^{s,(0)}_{2,0} + A^{s,(m2)}_{2,0} m_\pi^2 + A^{s,(m3)}_{2,0} m_\pi^3 + A^{s,(t)}_{2,0} t - \frac{3\pi A^{\pi,s,(0)}_{2,0} g_A^2}{8m_0(4\pi F_\pi)^2} m_\pi t \\ &\quad + \frac{3\pi A^{\pi,s,(0)}_{2,0} g_A^2 \left(8m_\pi^4 - 6m_\pi^2 t + t^2\right)}{16m_0(4\pi F_\pi)^2\sqrt{-t}} \arcsin\left(\frac{1}{\sigma}\right) + \mathcal{O}(p^4) \ , \end{aligned} \tag{3.43a}$$

$$\begin{aligned} B^s_{2,0} &= B^{s,(0)}_{2,0} + B^{s,(m2)}_{2,0}(\mu) m_\pi^2 + B^{s,(t)}_{2,0}(\mu) t - \frac{A^{\pi,s,(0)}_{2,0} g_A^2}{(4\pi F_\pi)^2} t\sigma^3 \operatorname{arctanh}\left(\frac{1}{\sigma}\right) \\ &\quad - 3g_A^2 \frac{A^{s,(0)}_{2,0} + B^{s,(0)}_{2,0} - A^{\pi,s,(0)}_{2,0}}{(4\pi F_\pi)^2} m_\pi^2 \ln\frac{m_\pi^2}{\mu^2} - \frac{A^{\pi,s,(0)}_{2,0} g_A^2}{2(4\pi F_\pi)^2} t \ln\frac{m_\pi^2}{\mu^2} + \mathcal{O}(p^3) \ , \end{aligned} \tag{3.43b}$$

$$C_2^s = C_2^{s,(0)} + \frac{3\pi A_{2,0}^{\pi,s,(0)} g_A^2 m_0 m_\pi \left(-2m_\pi^2 + t\right)}{8(4\pi F_\pi)^2 t} + \frac{3\pi A_{2,0}^{\pi,s,(0)} g_A^2 m_0 \left(-8m_\pi^4 + 2m_\pi^2 t + t^2\right)}{16(4\pi F_\pi)^2 (-t)^{3/2}} \arcsin\left(\frac{1}{\sigma}\right) + \mathcal{O}(p^2) \ , \tag{3.43c}$$

$$\tilde{A}_{2,0}^s = \tilde{A}_{2,0}^{s,(0)} + \tilde{A}_{2,0}^{s,(m2)}(\mu) m_\pi^2 + \tilde{A}_{2,0}^{s,(m3)} m_\pi^3 + \tilde{A}_{2,0}^{s,(t)} t - \frac{3\tilde{A}_{2,0}^{s,(0)} g_A^2}{(4\pi F_\pi)^2} m_\pi^2 \ln\frac{m_\pi^2}{\mu^2} + \mathcal{O}(p^4) \ , \tag{3.43d}$$

$$\tilde{B}_{2,0}^s = \tilde{B}_{2,0}^{s,(0)} + \tilde{B}_{2,0}^{s,(m2)}(\mu) m_\pi^2 + \tilde{B}_{2,0}^{s,(t)} t - \frac{(\tilde{A}_{2,0}^{s,(0)} + 3\tilde{B}_{2,0}^{s,(0)}) g_A^2}{(4\pi F_\pi)^2} m_\pi^2 \ln\frac{m_\pi^2}{\mu^2} + \mathcal{O}(p^3) \ , \tag{3.43e}$$

where

$$\sigma = \sqrt{1 - \frac{4m_\pi^2}{t}} \ . \tag{3.44}$$

For the isovector generalized form factors one obtains

$$A_{2,0}^v = A_{2,0}^{v,(0)} + A_{2,0}^{v,(m2)}(\mu) m_\pi^2 + A_{2,0}^{v,(m3)} m_\pi^3 + A_{2,0}^{v,(t)} t - \frac{A_{2,0}^{v,(0)} \left(1 + 3g_A^2\right)}{(4\pi F_\pi)^2} m_\pi^2 \ln\frac{m_\pi^2}{\mu^2} + \mathcal{O}(p^4) \ , \tag{3.45}$$

$$B_{2,0}^v = B_{2,0}^{v,(0)} + B_{2,0}^{v,(m2)}(\mu) m_\pi^2 + B_{2,0}^{v,(t)} t - \frac{B_{2,0}^{v,(0)} - (A_{2,0}^{v,(0)} - 2B_{2,0}^{v,(0)}) g_A^2}{(4\pi F_\pi)^2} m_\pi^2 \ln\frac{m_\pi^2}{\mu^2} + \mathcal{O}(p^3) \ , \tag{3.46}$$

$$C_2^v = C_2^{v,(0)} + \mathcal{O}(p^2) \ , \tag{3.47}$$

$$\tilde{A}_{2,0}^v = \tilde{A}_{2,0}^{v,(0)} + \tilde{A}_{2,0}^{v,(m2)}(\mu) m_\pi^2 + \tilde{A}_{2,0}^{v,(m3)} m_\pi^3 + \tilde{A}_{2,0}^{v,(t)} t - \frac{\tilde{A}_{2,0}^{v,(0)} \left(1 + 2g_A^2\right)}{(4\pi F_\pi)^2} m_\pi^2 \ln\frac{m_\pi^2}{\mu^2} + \mathcal{O}(p^4) \ , \tag{3.48}$$

$$\tilde{B}_{2,0}^v = \tilde{B}_{2,0}^{v,(0)} + \tilde{B}_{2,0}^{v,(m2)}(\mu) m_\pi^2 + \tilde{B}_{2,0}^{v,(t)} t + \frac{(\tilde{A}_{2,0}^{v,(0)} - 6\tilde{B}_{2,0}^{v,(0)}) g_A^2 - 3\tilde{B}_{2,0}^{v,(0)}}{3(4\pi F_\pi)^2} m_\pi^2 \ln\frac{m_\pi^2}{\mu^2} + \mathcal{O}(p^3) \ . \tag{3.49}$$

The fit parameters are related to the original LECs defined in section 3.3 by eqs. (B.4) and (B.5). The parameter $A_{2,0}^{\pi,s,(0)}$ which occurs in the isoscalar generalized form factors of the vector current and originates from diagram (f), where the operator couples to two pions, should not be treated as a free parameter. Instead one should obtain it from a fit to the pion GPD, where it fixes

the chiral limit value in the forward case. For consistency we propose to use the one-loop result derived in ref. [116] (see also refs. [69, 117]), which reads

$$A_{2,0}^{\pi,s} = A_{2,0}^{\pi,s,(0)} + A_{2,0}^{\pi,s,(m2)} m_\pi^2 + A_{2,0}^{\pi,s,(t)} t + \mathcal{O}(p^4) \ , \tag{3.50a}$$

$$\begin{aligned} A_{2,2}^{\pi,s} = &-\frac{1}{4} A_{2,0}^{\pi,s,(0)} + A_{2,2}^{\pi,s,(m2)}(\mu) m_\pi^2 + A_{2,2}^{\pi,s,(t)}(\mu) t \\ &- \frac{1}{4} A_{2,0}^{\pi,s,(0)} \frac{m_\pi^2 - 2t}{3(4\pi F_\pi)^2} \left(\ln \frac{m_\pi^2}{\mu^2} + \frac{4}{3} - \frac{t+2m_\pi^2}{t} J \right) + \mathcal{O}(p^4) \ , \end{aligned} \tag{3.50b}$$

where

$$J = 2 + \sigma \ln \frac{\sigma - 1}{\sigma + 1} \ . \tag{3.51}$$

In ref. [116] all moments of GPDs have been treated simultaneously by the use of nonlocal operators, which is obviously a very elegant method. For the specific case of the first moments, connected to the form factors shown above, we were able to confirm this result by a straightforward calculation with local operators.

Value and slope in the forward limit

For small values of the momentum transfer $|t| \ll 4m_\pi^2$ the form factors are often represented by a Taylor expansion in t. We use the notation of ref. [34]

$$X^{s,v}(t) = X^{s,v}(0) + \rho_X^{s,v} t + \mathcal{O}(t^2) \ , \tag{3.52}$$

where X can stand for arbitrary form factors. For the nontrivial cases one obtains

$$A_{2,0}^{s}(0) = A_{2,0}^{s,(0)} + A_{2,0}^{s,(m2)} m_\pi^2 + \left(A_{2,0}^{s,(m3)} + \frac{3\pi A_{2,0}^{\pi,s,(0)} g_A^2}{4 m_0 (4\pi F_\pi)^2} \right) m_\pi^3 + \mathcal{O}(p^4) \ , \tag{3.53a}$$

$$\begin{aligned} B_{2,0}^{s}(0) = &B_{2,0}^{s,(0)} + \left(B_{2,0}^{s,(m2)}(\mu) + \frac{4 A_{2,0}^{\pi,s,(0)} g_A^2}{(4\pi F_\pi)^2} \right) m_\pi^2 \\ &- 3 g_A^2 \frac{A_{2,0}^{s,(0)} + B_{2,0}^{s,(0)} - A_{2,0}^{\pi,s,(0)}}{(4\pi F_\pi)^2} m_\pi^2 \ln \frac{m_\pi^2}{\mu^2} + \mathcal{O}(p^3) \ , \end{aligned} \tag{3.53b}$$

$$C_2^{s}(0) = C_2^{s,(0)} + \frac{\pi A_{2,0}^{\pi,s,(0)} g_A^2 m_0}{4(4\pi F_\pi)^2} m_\pi + \mathcal{O}(p^2) \ , \tag{3.53c}$$

$$\begin{aligned} A_{2,2}^{\pi,s}(0) = &-\frac{1}{4} A_{2,0}^{\pi,s,(0)} + \left(A_{2,2}^{\pi,s,(m2)}(\mu) - \frac{A_{2,0}^{\pi,s,(0)}}{12(4\pi F_\pi)^2} \right) m_\pi^2 \\ &- \frac{A_{2,0}^{\pi,s,(0)}}{12(4\pi F_\pi)^2} m_\pi^2 \ln \frac{m_\pi^2}{\mu^2} + \mathcal{O}(p^4) \ , \end{aligned} \tag{3.53d}$$

and

$$\rho^s_{A_{2,0}} = A^{s,(t)}_{2,0} - \frac{7\pi A^{\pi,s,(0)}_{2,0} g_A^2}{8m_0(4\pi F_\pi)^2} m_\pi + \mathcal{O}(p^2) \ , \tag{3.54a}$$

$$\rho^s_{B_{2,0}} = B^{s,(t)}_{2,0}(\mu) - \frac{4A^{\pi,s,(0)}_{2,0} g_A^2}{3(4\pi F_\pi)^2} - \frac{A^{\pi,s,(0)}_{2,0} g_A^2}{2(4\pi F_\pi)^2} \ln\frac{m_\pi^2}{\mu^2} + \mathcal{O}(p^1) \ , \tag{3.54b}$$

$$\rho^s_{C_2} = -\frac{\pi A^{\pi,s,(0)}_{2,0} g_A^2 m_0}{10(4\pi F_\pi)^2} m_\pi^{-1} + \mathcal{O}(p^0) \ , \tag{3.54c}$$

$$\rho^s_{A^\pi_{2,2}} = A^{\pi,s,(t)}_{2,2}(\mu) + \frac{11A^{\pi,s,(0)}_{2,0}}{60(4\pi F_\pi)^2} + \frac{A^{\pi,s,(0)}_{2,0}}{6(4\pi F_\pi)^2} \ln\frac{m_\pi^2}{\mu^2} + \mathcal{O}(p^2) \ . \tag{3.54d}$$

The formula for the slope is always two orders less accurate than the one for the corresponding form factor since one has to take a derivative with respect to t to obtain it. The forward limit values and slopes of the form factors not given here can easily be obtained from eqs. (3.43), (3.45) and (3.50).

Our result is consistent with the heavy baryon result provided in refs. [107, 108]. In particular the chiral logarithms in the B-type form factors are reproduced, which was not yet the case for the leading one-loop calculation presented in ref. [34]. Note that the truncated version of our result has the same accuracy as the above cited heavy baryon calculations for B-type form factors, but is one order more/less precise for the A/C-type ones. This is because in refs. [107, 108] contributions going beyond the one-loop level are taken into account for the C-type form factor. Note however, that our untruncated covariant result already contains these contributions up to higher order tree-level insertions, which could be added by hand if necessary.

3.6 Analysis of lattice QCD data

In this section we will present numerical results for generalized form factors obtained from lattice QCD simulations with two dynamical quark flavors provided by QCDSF and RQCD. The main lattice analysis and the ChPT fits have been performed by R. H. Rödl.

3.6.1 Correlation functions

To extract information on (generalized) form factors from lattice QCD one has to consider three-point functions, where one uses interpolating currents at the source/sink (at t_i and t_f) to create/annihilate states with the desired quantum numbers. The currents in whose matrix element one is interested in (in our case the ones given in eq. (3.3)) are inserted in between, at the insertion time t_ins, with $t_\mathrm{f} > t_\mathrm{ins} > t_\mathrm{i}$. We fix the three-momentum at the sink to $\mathbf{p}'$ and the three-momentum transfer at the insertion to (incoming) $\mathbf{\Delta} = \mathbf{p}' - \mathbf{p}$:

$$\langle 0|\mathcal{N}_\tau(t_\mathrm{f})_{\mathbf{p}'}\ \mathcal{O}(t_\mathrm{ins})_{\mathbf{\Delta}}\ \bar{\mathcal{N}}_{\tau'}(t_\mathrm{i},\mathbf{0})|0\rangle = a^6 \sum_{\mathbf{x},\mathbf{y}} e^{i\mathbf{p}'\mathbf{x}} e^{-i\mathbf{\Delta}\mathbf{y}} \langle 0|\mathcal{N}_\tau(t_\mathrm{f},\mathbf{x})\mathcal{O}_\tau(t_\mathrm{ins},\mathbf{y})\ \bar{\mathcal{N}}_{\tau'}(t_\mathrm{i},\mathbf{0})|0\rangle \ . \tag{3.55}$$

The incoming momentum at the source is fixed to $\mathbf{p}$ automatically due to momentum conservation. As interpolating current for the nucleon one uses

$$\big(u^T C\gamma_5 d\big)u \ , \tag{3.56}$$

which (using Fierz identities) can be rewritten as a linear combination of the Ioffe and Dosch currents (see, e.g., ref. [118]) and is known to have a large ground-state overlap. To further enhance the coupling Wuppertal smearing [119] with spatially APE smoothed [120] links has been applied. The smearing leads to a momentum dependent ground-state overlap

$$\langle 0|\mathcal{N}_\tau(0,\mathbf{0})|N(p,s)\rangle = \sqrt{Z(\mathbf{p})}u^N_\tau(p,s) \ , \tag{3.57}$$

which can be extracted from the two-point functions

$$\begin{aligned}(\gamma_+)_{\tau'\tau}\langle 0|\mathcal{N}_\tau(t)_{\mathbf{p}}\ \bar{\mathcal{N}}_{\tau'}(0,\mathbf{0})|0\rangle &\approx \sum_s \frac{Z(\mathbf{p})}{2E(\mathbf{p})}e^{-E(\mathbf{p})t}\frac{(\mathbb{1}+\gamma_0)_{\tau'\tau}}{2}u^N_\tau(p,s)\bar{u}^N_{\tau'}(p,s)\\ &= \frac{Z(\mathbf{p})}{4E(\mathbf{p})}e^{-E(\mathbf{p})t}\,\mathrm{tr}\left\{(\mathbb{1}+\gamma_0)(\not{p}+m_N)\right\} = Z(\mathbf{p})\frac{E(\mathbf{p})+m_N}{E(\mathbf{p})}e^{-E(\mathbf{p})t} \ ,\end{aligned} \tag{3.58}$$

where we have omitted exponentially suppressed excited state contributions. For the case $\mathbf{p}=\mathbf{0}$ the parity projector $\gamma_+ = (\mathbb{1}+\gamma_0)/2$ removes the leading negative parity contribution from the two-point function. For the three-point function introduced above one obtains (we, again, only show the ground-state contribution)

$$\begin{aligned}&\langle 0|\mathcal{N}_\tau(t_\mathrm{f})_{\mathbf{p}'}\ \mathcal{O}(t_\mathrm{ins})_{\mathbf{\Delta}}\ \bar{\mathcal{N}}^B_{\tau'}(t_\mathrm{i},\mathbf{0})|0\rangle \approx\\ &\quad\approx \sum_{s',s}\langle 0|\mathcal{N}_\tau(0,\mathbf{0})|N(p',s')\rangle\ \langle N(p',s')|\mathcal{O}(0,\mathbf{0})|N(p,s)\rangle\ \langle N(p,s)|\mathcal{N}_{\tau'}(0,\mathbf{0})|0\rangle\\ &\qquad\times \frac{e^{-E(\mathbf{p}')(t_\mathrm{f}-t_\mathrm{ins})}}{2E(\mathbf{p}')}\frac{e^{-E(\mathbf{p})(t_\mathrm{ins}-t_\mathrm{i})}}{2E(\mathbf{p})}\\ &\quad= \sum_{s',s}\frac{\sqrt{Z(\mathbf{p}')}\sqrt{Z(\mathbf{p})}}{4E(\mathbf{p}')E(\mathbf{p})}e^{-E(\mathbf{p}')(t_\mathrm{f}-t_\mathrm{ins})}e^{-E(\mathbf{p})(t_\mathrm{ins}-t_\mathrm{i})}\\ &\qquad\times u^N_\tau(p',s')\ \langle N(p',s')|\mathcal{O}(0,\mathbf{0})|N(p,s)\rangle\ \bar{u}^N_{\tau'}(p,s) \ .\end{aligned} \tag{3.59}$$

Up to this point the derivation is general, and one could, e.g., insert a standard vector current for $\mathcal{O}$ to obtain the electromagnetic form factors. Using the matrix element decompositions (3.6) and $\sum_s u^N_\tau(p,s)\bar{u}^N_{\tau'}(p,s) = (\not{p}+m_N)_{\tau\tau'}$ one obtains for the operators we are interested in (cf. eq. (3.3))

$$\begin{aligned}\langle 0|\mathcal{N}_\tau(t_\mathrm{f})_{\mathbf{p}'}\ \mathcal{O}^q_{\mu\nu}(t_\mathrm{ins})_{\mathbf{\Delta}}\ \bar{\mathcal{N}}^B_{\tau'}(t_\mathrm{i},\mathbf{0})|0\rangle &\approx \sum_{s',s}\frac{\sqrt{Z(\mathbf{p}')}\sqrt{Z(\mathbf{p})}}{4E(\mathbf{p}')E(\mathbf{p})}e^{-E(\mathbf{p}')(t_\mathrm{f}-t_\mathrm{ins})}e^{-E(\mathbf{p})(t_\mathrm{ins}-t_\mathrm{i})}\\ &\times\left[(\not{p}'+m_N)\mathbf{S}\left[\gamma_\mu\bar{p}_\nu A^q_{2,0}(t)+\frac{i\sigma_{\mu\alpha}\Delta^\alpha}{2m_N}\bar{p}_\nu B^q_{2,0}(t)+\frac{\Delta_\mu\Delta_\nu}{m_N}C^q_2(t)\right](\not{p}+m_N)\right]_{\tau\tau'} \ ,\end{aligned} \tag{3.60a}$$

$$\begin{aligned}\langle 0|\mathcal{N}_\tau(t_\mathrm{f})_{\mathbf{p}'}\ \tilde{\mathcal{O}}^q_{\mu\nu}(t_\mathrm{ins})_{\mathbf{\Delta}}\ \bar{\mathcal{N}}^B_{\tau'}(t_\mathrm{i},\mathbf{0})|0\rangle &\approx \sum_{s',s}\frac{\sqrt{Z(\mathbf{p}')}\sqrt{Z(\mathbf{p})}}{4E(\mathbf{p}')E(\mathbf{p})}e^{-E(\mathbf{p}')(t_\mathrm{f}-t_\mathrm{ins})}e^{-E(\mathbf{p})(t_\mathrm{ins}-t_\mathrm{i})}\\ &\times\left[(\not{p}'+m_N)\mathbf{S}\left[\gamma_\mu\gamma_5\bar{p}_\nu \tilde{A}^q_{2,0}(t)+\frac{\gamma_5\Delta_\mu}{2m_N}\bar{p}_\nu \tilde{B}^q_{2,0}(t)\right](\not{p}+m_N)\right]_{\tau\tau'} \ .\end{aligned} \tag{3.60b}$$

By evaluating traces of these expressions with different parity projection and polarization matrices at various momentum configurations one obtains an overdetermined system of equations, which can be solved for the generalized form factors (see refs. [121, 122]).

In the preceding presentation we have only taken into account the ground-state contribution. However, in three-point functions excited state contributions are enhanced (compared to two-point functions), since the relevant time scale for their suppression is not the sink-source "distance" $t_\mathrm{f} - t_\mathrm{i}$ (as in two-point functions), but the time differences between source and insertion, $t_\mathrm{ins} - t_\mathrm{i}$, and between insertion and sink, $t_\mathrm{f} - t_\mathrm{ins}$, which are smaller. It turns out that the smearing techniques (applied to the interpolating currents) alone are not sufficient to overcome the problem. Therefore, one (additionally) takes into account the first excited states in the correlation function and performs a multi-exponential fit. To be more specific, the data points used in the following sections are obtained from a three-exponential fit to the lattice data as described in ref. [122].

3.6.2 Details on the lattice simulation

The analysis is based on gauge configurations generated by QCDSF and RQCD using a Wilson gauge action [31]. The two mass-degenerate dynamical quark flavors ($N_f = 2$) have been simulated using a first order Symanzik improved Wilson fermion action [123], also known as Sheikholeslami–Wohlert or clover action. Table 3.3 shows a list of the analyzed ensembles. The lattice spacings have been determined from the quark static potential using the Sommer parameter $r_0 = 0.5$ fm obtained in ref. [124] (a description of the method can be found in ref. [125]). More details on the lattice setup can be found in ref. [126]. Note that ensemble VII has to be treated with care, since $m_\pi L < 3$ can give rise to significant finite volume effects due to pions traveling around the spacetime torus. Ensemble IX has a pion mass close to 500 MeV and presumably lies beyond the range of applicability of BChPT.

The bare lattice results are nonperturbatively renormalized using a regularization independent renormalization scheme. In a second step they are converted to the widely used $\overline{\mathrm{MS}}$ scheme using continuum perturbation theory. The method is described in ref. [127]. All results will be given at the $\overline{\mathrm{MS}}$ renormalization scale $\mu = 2$ GeV.

At the moment, reliable lattice data is only available for the isovector generalized form factors. The calculation of the isoscalar GFFs is very demanding and costly, since it requires the inclusion of disconnected contributions. Therefore, we will not be able to make statements about the individual contribution of up and down quarks to the (total angular) momentum. Instead, we will only provide information about the asymmetry between the contributions of the different quark flavors.

The analysis of C_2^{u-d}, $\tilde{A}_{2,0}^{u-d}$ and $\tilde{B}_{2,0}^{u-d}$ has not been finished up to now, which is why we will focus on the generalized form factors $A_{2,0}^{u-d}$ and $B_{2,0}^{u-d}$ in the following. (Nevertheless, we will share some qualitative insights that can already be gained from the pure lattice data on $\tilde{A}_{2,0}^{u-d}$ below.) Furthermore, we are in the unfortunate situation that we can only show the result of the BChPT fits but not the lattice data itself, since the data obtained from the improved analysis

Table 3.3: $N_f = 2$ lattice gauge configurations used in this chapter. The column labeled $(t_\mathrm{f} - t_\mathrm{i})/a$ lists the sink-source distances for which measurements have been carried out on the respective ensemble. This table has been taken from ref. [122]. For more information consider also ref. [126].

Ensemble	β	a[fm]	κ	N_s	N_t	m_π[GeV]	$m_\pi L$	#conf.	$(t_\mathrm{f} - t_\mathrm{i})/a$
I	5.20	0.081	0.13596	32	64	0.2795(18)	3.69	1986	13
II	5.29	0.071	0.13620	24	48	0.4264(20)	3.71	1999	15
III			0.13620	32	64	0.4222(13)	4.90	1998	15,17
IV			0.13632	32	64	0.2946(14)	3.42	2023	7,9,11,13,15,17
V				40	64	0.2888(11)	4.19	2025	15
VI				64	64	0.2895(07)	6.71	1232	15
VII			0.13640	48	64	0.1597(15)	2.78	3442	15
VIII				64	64	0.1497(13)	3.47	1593	9,12,15
IX	5.40	0.060	0.13640	32	64	0.4897(17)	4.81	1123	17
X			0.13647	32	64	0.4262(20)	4.18	1999	17
XI			0.13660	48	64	0.2595(09)	3.82	2177	17

method that takes into account the excited states in the correlation functions (cf. ref. [122]) are still unpublished for $A_{2,0}^{u-d}$, $B_{2,0}^{u-d}$ and C_2^{u-d} (with exception of the forward limit of $A_{2,0}^{u-d}$, cf. refs. [33, 128]). One can conceive an idea of such lattice data from figure 3.5, which shows the published results for $\tilde{A}_{2,0}^{u-d}$ and $\tilde{B}_{2,0}^{u-d}$. The lattice data (for ensembles II, IV, V, VIII, IX and XI) obtained from the standard analysis method, which takes into account only the ground-state contribution to the correlation functions and does not consider systematics due to the choice of the fit window, can be found in ref. [129].

3.6.3 Chiral extrapolation and numerical results

For the chiral extrapolation and the parametrization of the t dependence we apply the formulas presented in section 3.5. In particular we compare the HBChPT-reduced and the tradeoff version, where only the triangle diagrams are taken into account to all orders. We did not use the original full one-loop formula since it contains a large number of parameters that only affect higher order terms in our observables. Taking all these parameters into account would therefore very likely result in overfitting. To pin down these LECs reliably one would have to consider additional observables such as, e.g., nucleon-to-nucleon-pion transition GPDs.

For the standard low-energy constants we have used input values: the pion decay constant was set to $F_\pi = F_0 + \mathcal{O}(p^2) = 92.4$ MeV, the nucleon mass in the chiral limit $m_0 = 0.893$ GeV and $c_1 = -0.784$ GeV^{-1} (m_0 and c_1 have been taken from the fit labeled Sop1 in ref. [124], where already most of the ensembles listed in table 3.3 have been taken into account). In the tradeoff version of the fits the (unphysical) chiral renormalization scale was fixed to 1 GeV, which is a standard choice.

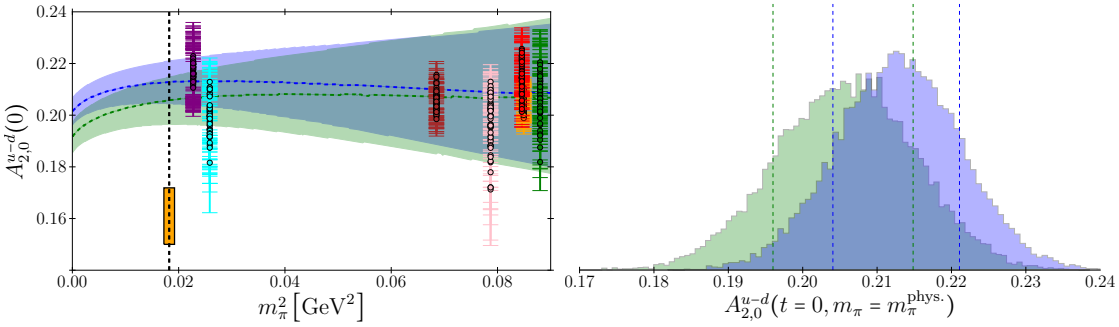

Figure 3.2: Result obtained for $\langle x \rangle^{u-d}$, which is defined as the forward limit of $A_{2,0}^{u-d}$, from a combined fit to the data (including data at $t = 0$ and $t < 0$, but excluding ensembles VII (cyan-colored; second from left) and IX for reasons explained in the main text) using both the HBChPT-reduced (green) and the tradeoff (purple) fit ansatz. The color coding for the data points is given in table 3.3. The histogram plot shows that the given one-sigma errors are reasonable. The orange band contains the values obtained from phenomenological fits (taken from ref. [128]) of ordinary parton distribution functions to global experimental data [130–133]. It is only given for comparison and has not been used in the fit. The plots have been created in collaboration with R. H. Rödl.

The result for the generalized form factors $A_{2,0}^{u-d}$ and $B_{2,0}^{u-d}$ in the forward limit as a function of m_π^2 is shown on the left-hand sides of figures 3.2 and 3.3. They have been obtained by a combined fit to lattice data for both form factors using the ensembles listed in table 3.3 (excluding ensembles VII and IX, see explanation in section 3.6.2) at various momentum transfers $0 \leq -t < 0.6\ \mathrm{GeV}^2$. Actually, the plot in figure 3.3 shows the result of an extrapolation to the forward limit, since $B_{2,0}^{u-d}$ can only be measured at $t \neq 0$ due to its prefactor in the form factor decomposition (3.6). Our first observation is that the HBChPT-reduced fit ansatz (plotted in green) leads to a slightly smaller (larger) forward limit value of $A_{2,0}^{u-d}$ ($B_{2,0}^{u-d}$) at the physical point than the tradeoff fit ansatz (plotted in purple). However, both results agree within the error. This agreement is expected, since the triangle diagram containing two pion propagators (cf. figure 3.1(f)) which is known to be problematic in the heavy baryon expansion (cf. ref. [86]) does not contribute to the isovector form factors. To have a real benchmark for the difference between the manifestly covariant and the heavy baryon ChPT formulas one has to consider isoscalar (generalized) form factors. The histogram plots on the right-hand side of the figures show a Gaussian distribution, which demonstrates that the plotted one-sigma error bands are meaningful despite the fact that they include the systematic error due to the variation of the fit ranges (compare ref. [122]).

The generalized form factor $A_{2,0}^{u-d}$ at vanishing momentum transfer (given in figure 3.2) corresponds to the difference between the momentum fractions carried by up and down quarks, $\langle x \rangle^{u-d}$. The experimental bounds on this observable are relatively strict, since it can be obtained in the forward limit, where generalized parton distributions reduce to conventional parton distribution functions that are measurable in (inclusive) deep inelastic scattering processes. Therefore it is an important benchmark quantity for the reliability of all lattice QCD computations in the baryon sector that exceed the ordinary determination of the mass spectrum. Qualitatively both

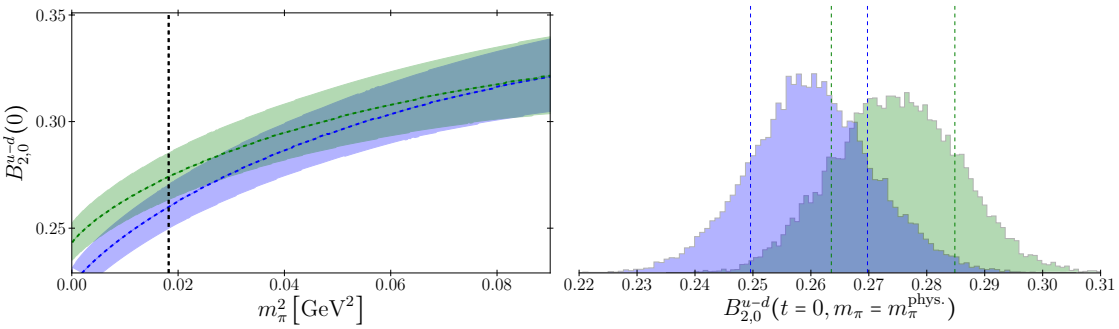

Figure 3.3: Result obtained from a combined fit to the data (excluding ensembles VII and IX) for the forward limit of the generalized form factor $B^{u-d}_{2,0}$, using both the HBChPT-reduced (green) and the tradeoff (purple) fit ansatz. The plot does not contain any lattice data points, since $B^{u-d}_{2,0}$ can only be measured at $t \neq 0$ and has to be extrapolated to the forward limit. The histogram plot shows that the given one-sigma errors are reasonable. The plots have been created in collaboration with R. H. Rödl.

the lattice QCD and the experimental value agree on the fact that, within a proton, up quarks carry a larger fraction of the momentum than down quarks (and vice versa for the neutron). Numerically, however, there is a long-standing discrepancy between lattice simulations and the experiment (see, e.g., the comparison in ref. [128]), which is also true for our result. The disagreement is caused by the large numerical value measured at nearly physical pion mass and can obviously not be cured by any kind of chiral extrapolation. It is also unlikely that excited state contaminations are responsible, since great care has been bestowed on their removal using advanced smearing techniques and excited state fits to the correlation functions. In ref. [134] we have calculated the finite volume effects due to pions traveling around the box in the forward limit.[2] This work was based on the one-loop formulas presented in section 3.5 (see also ref. [97]) and its results have been used in ref. [33] to demonstrate that finite volume effects do not explain the discrepancy found for $\langle x \rangle^{u-d}$. Actually, one finds that finite volume effects abate with decreasing pion masses as long as $m_\pi L$ is kept fixed, which is a consequence of the fact that the leading finite volume effects occur at one-loop order and are therefore suppressed with a factor $\propto m_\pi^2 e^{-m_\pi L}$.[3] The remaining candidate for an explanation of the observed discrepancy are discretization effects. Having data points at three different lattice spacings (cf. table 3.3) should enable us to take the continuum limit. However, it was already mentioned in ref. [128] that the rather narrow range of available lattice spacings $0.06\ \mathrm{fm} \leq a \leq 0.08\ \mathrm{fm}$ (combined with the fact that data at nearly physical quark masses is only available at one lattice spacing) does not allow for a conclusive continuum extrapolation. In summary, one can state that discretization effects are the most likely explanation for the observed disagreement between lattice QCD and experiment, and providing data that allows for a reliable continuum extrapolation has to be a prime goal of future simulation programs.

[2] This project was mainly carried out by L. Greil.

[3] Note that this argument does not hold for matrix elements of operators that can couple to single pions as, e.g., pseudoscalar or axialvector currents without derivatives.

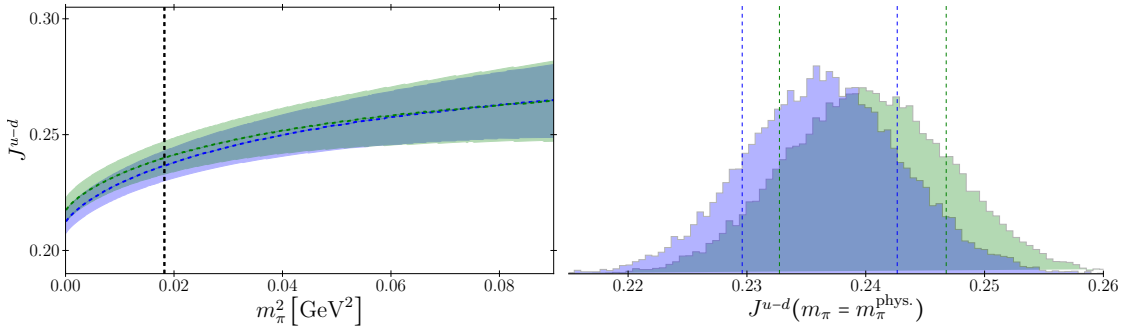

Figure 3.4: Result for the isovector total angular momentum $J^{u-d} = (A_{2,0}^{u-d}(0) + B_{2,0}^{u-d}(0))/2$ as a function of m_π^2 using both the HBChPT-reduced (green) and the tradeoff (purple) fit ansatz. The histogram plot shows that the given one-sigma errors are reasonable. The plots have been created in collaboration with R. H. Rödl.

In figure 3.4 we show the difference between the total angular momentum carried by up and by down quarks, J^{u-d}. The obtained numerical value has to be treated with caution, since the error does not include discretization effects which might be $\sim 20\%$, as we know from the discussion above. Qualitatively, however, the result clearly shows that up quarks carry a larger share of the proton spin than down quarks (and vice versa for the neutron). We can conclude (in the nucleon sector) that the quark flavor which contributes the larger number of valence quarks also carries a larger part of both the momentum and the spin of the respective nucleon. One can draw a more detailed picture if one takes into account the quark helicity dependent generalized form factor $\tilde{A}_{2,0}^{u-d}$. According to eqs. (3.13) and (3.14) it allows us to differentiate between quarks with helicities parallel and antiparallel to the polarization direction of a longitudinally polarized nucleon. At high energies one has

$$\langle x \rangle^{u^\uparrow - d^\uparrow} = \frac{1}{2}\big(A_{2,0}^{u-d}(0) + \tilde{A}_{2,0}^{u-d}(0)\big)\ , \tag{3.61a}$$

$$\langle x \rangle^{u^\downarrow - d^\downarrow} = \frac{1}{2}\big(A_{2,0}^{u-d}(0) - \tilde{A}_{2,0}^{u-d}(0)\big)\ , \tag{3.61b}$$

$$J^{u^\uparrow - d^\uparrow} = \frac{1}{4}\big(A_{2,0}^{u-d}(0) + B_{2,0}^{u-d}(0) + \tilde{A}_{2,0}^{u-d}(0)\big)\ , \tag{3.61c}$$

$$J^{u^\downarrow - d^\downarrow} = \frac{1}{4}\big(A_{2,0}^{u-d}(0) + B_{2,0}^{u-d}(0) - \tilde{A}_{2,0}^{u-d}(0)\big)\ , \tag{3.61d}$$

where, obviously, the special case of vanishing $\tilde{A}_{2,0}^{u-d}(0)$ would correspond to a helicity independent behavior. However, already a short look at the lattice data plotted in figure 3.5 reveals that the latter is not the case. Instead, as a very rough first approximation one can read off $\tilde{A}_{2,0}^{u-d}(0) \approx A_{2,0}^{u-d}(0)$, which means that in large part the flavor asymmetry of the momentum distribution (measured with $\langle x \rangle^{u-d}$) originates from quarks with positive helicity, while up and down quarks with negative helicity carry (approximately) the same amount of momentum. Also in case of the total angular momentum this value of $\tilde{A}_{2,0}^{u-d}(0)$ corresponds to a larger flavor asymmetry for quarks of positive helicity.

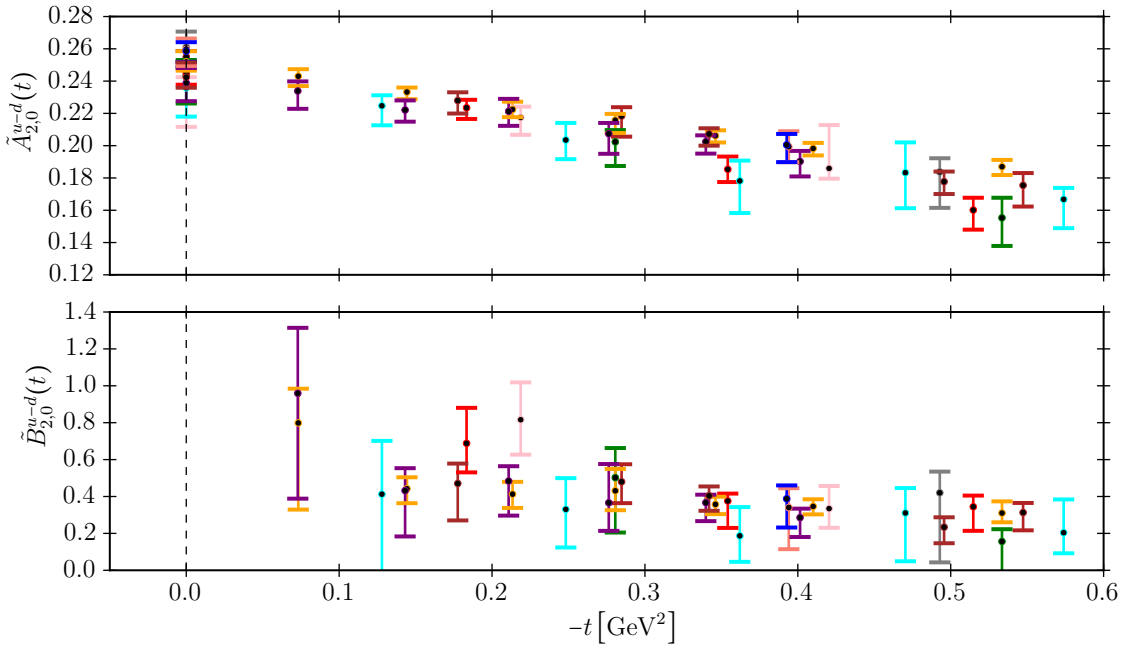

Figure 3.5: Renormalized lattice data as a function of the momentum transfer for the isovector generalized form factors $\tilde{A}^{u-d}_{2,0}$ and $\tilde{B}^{u-d}_{2,0}$ published in ref. [122]. The color coding for the data points is specified in table 3.3. We cannot show the corresponding data for $A^{u-d}_{2,0}$, $B^{u-d}_{2,0}$ and C^{u-d}_{2} (which was used to obtain the BChPT fit results shown in figures 3.2, 3.3 and 3.4) since it has not been published yet.

3.7 Summary

In this chapter we have extended the results of ref. [34] to full one-loop accuracy and have provided chiral extrapolation formulas for the first moments of chiral-even nucleon GPDs. Due to the overlap in LECs some of the form factors should be fitted to lattice data simultaneously. If one uses the heavy baryon reduced fit formulas, those are the two pairs $(A^v_{2,0}, B^v_{2,0})$ and $(\tilde{A}^v_{2,0}, \tilde{B}^v_{2,0})$ in the isotriplet sector. In the isosinglet sector the situation is more entangled and calls for simultaneous fits of $(A^s_{2,0}, B^s_{2,0}, C^s_2, A^{\pi,s}_{2,0}, A^{\pi,s}_{2,2})$ and $(\tilde{A}^s_{2,0}, \tilde{B}^s_{2,0})$. If the reader is more ambitious and wants to apply the untruncated formulas given in appendix B.2 he has to treat all form factors from the isosinglet/isotriplet sector simultaneously. Since reliable lattice data on the isoscalar generalized form factors is not available we have focused on the isovector case in our analysis (see sect. 3.6.3). In the ideal case one also has data for the matrix elements of the gluonic and the isoscalar operators: in a first step one would fit the two sectors separately and check whether the sum rules given in eq. (3.11) are fulfilled to a satisfactory degree. Afterwards one can invoke the sum rules to restrict the LECs in order to find the most precise result.

It is reasonable to expect the range of applicability of covariant BChPT to extend up to values of the pion mass around $m_{\pi,\mathrm{max}} \approx 300$ MeV - 400 MeV (see, e.g., refs. [135, 136]). Therefore we had to exclude ensemble IX (cf. table 3.3), which has a pion mass close ot 500 MeV from the

analysis. One can a priori not say for sure in which range of t our formulas are applicable. A careful estimate based on the argument that the chiral counting scheme ranks t as a quantity of second order leads to $|t_{\max}| \sim m^2_{\pi,\max} \approx 0.1\ \text{GeV}^2$ - $0.2\ \text{GeV}^2$. At least for the isovector generalized form factors, which we have analyzed in section 3.6.3, this estimate seems to be overcautious, since the lattice data exhibits a quite linear behavior in the momentum transfer that can be described by our formulas up to $|t| \approx 0.6\ \text{GeV}^2$ in the spacelike region.

We have found that the results for the isovector generalized form factors the HBChPT-reduced and the tradeoff fit ansatz, which are explained in section 3.5, are compatible. This is hardly surprising, since the triangle diagram (see figure 3.1(f)) which, as explained in ref. [86], is not described correctly in HBChPT, does not contribute to these form factors. We therefore have a plausible explanation why HBChPT formulas yield compatible results in these cases. However, at the same time, it disqualifies our finding as a benchmark for the isoscalar observables, where the situation can be totally different since the respective diagram occurs.

Our numerical result for $\langle x \rangle^{u-d}$ at the physical point is slightly larger than the value extracted from experiments and does not agree with it within errors. We have discussed the origin of this discrepancy in some detail with the conclusion that discretization effects are the most likely explanation for the found deviation. Until this issue is resolved one has to assume discretization effects $\sim 20\%$ also in the other observables like J^{u-d}. Qualitatively the results show that up quarks carry a larger fraction of both the momentum and the spin of the proton than down quarks. In both cases the flavor asymmetry is much larger for the quarks with positive helicity.

One can think of numerous extensions of this work. For instance one could investigate (possibly relevant) decuplet contributions and isospin breaking. Another interesting and related subject to study are chiral-odd GPDs (also known as helicity-flip or transversity GPDs), which shed light on the correlation between quark (total) angular momentum and transverse quark spin (see, e.g., refs. [104, 137, 138]). Furthermore, one could extend our calculation of finite volume effects (see ref. [134]) to nonforward quantities. Another challenging topic would be the (simultaneous) calculation of all x-moments by the use of nonlocal operators. In ref. [112] it has been shown that such an approach is only applicable in a covariant framework and that particular care has to be taken of the regularization procedure. In particular in the face of upcoming CLS lattice data of three-point functions with 2+1 dynamical quark flavors it would be very appealing to perform such a calculation within three-flavor BChPT, extending the work done in ref. [79]. The latter would provide (similar to our analysis of baryon distribution amplitudes presented in chapter 4) a valuable insight into the behavior of (transition) GPDs in the limit of exact flavor symmetry and its breaking.

CHAPTER 4

Baryon distribution amplitudes

In this chapter we will study baryon distribution amplitudes which are relevant for the description of exclusive processes at high momentum transfer and can be construed as light-cone wave functions integrated over transverse quark momenta. They are nonperturbative functions encoding the distribution of the longitudinal momentum on the constituent partons within a specific Fock state. In this respect DAs are complementary to ordinary parton distribution functions, which are relevant in inclusive reactions (like deep inelastic scattering) and yield the probability to find a parton (carrying some momentum fraction) within the hadron as a whole, without discriminating between single Fock states. The one-loop BChPT calculation and the lattice analysis presented in this chapter have been published in ref. [139] and ref. [75], respectively.

4.1 Overview

Due to the unstable nature of the weakly decaying hyperons scattering experiments with hyperons in the initial state are both challenging and scarce. An example is the WA89 experiment at CERN, where inclusive Ξ^- production was studied [140] using a high-intensity Σ^- beam [141] on copper and carbon targets. More naturally, hyperons occur in the final state, for instance in baryon-antibaryon pair production via electron-positron annihilation $e^+e^- \to \bar{B}B$, in deeply virtual exclusive meson electroproduction $\gamma^* p \to K^+\Lambda,\ K^+\Sigma^0,\ K^0\Sigma^+$, and in decays of heavy quarkonia to baryon-antibaryon pairs like $J/\Psi,\ \Upsilon \to \bar{B}B$. The standard way to parametrize the nonperturbative information contained in such exclusive processes are (transition) GPDs or ordinary form factors. At (very) high momentum transfer the contributions from Fock states containing more than the minimal number of partons are power-suppressed and the process can be approximated by a convolution of the involved distribution amplitudes with the process-dependent hard scattering kernel (see, e.g., ref. [9]). At intermediate momentum transfer soft contributions that are not factorizable into DAs play an important role, which means that the expansion in Fock states mentioned above is not feasible. In this kinematic regime the connection

of DAs to the experiment can be established by using light-cone sum rules, which allow an approximate determination of (generalized) form factors from DAs including soft contributions, see, e.g, ref. [25]. The requirement of large momentum transfer, the instability of the final state hadrons and the fact that distribution amplitudes only occur in convolutions, make high luminosity and high granularity detectors necessary to extract information on the hyperon DAs from experiment.

Another type of process where hyperon DAs are involved are the exclusive rare decays of b-baryons, like Ξ_b, Λ_b, Σ_b and Ω_b, into octet baryons (plus γ, l^+l^-, ...). Due to the large mass difference one can hope that higher order Fock states are sufficiently suppressed to allow for a description by three-quark DAs. Since the bottom baryons are produced with increasing rates at LHC and at B-factories worldwide, we have to expect that ever more precise experimental results will be available in future, even for rare decays containing flavor-changing neutral currents, which are sensitive to new physics. Notwithstanding the fact that b-baryons are produced at much lower rates than b-mesons, they are not less interesting since they allow for an examination of the helicity structure of the $b \to s$ transition and thus complement the measurements in the meson sector [142]. As shown in refs. [143, 144] there are possible scenarios where deviations from the standard model are not seen in the branching ratio of $\Lambda_b \to \Lambda l^+l^-$ but only in the Λ baryon polarization (see also refs. [145, 146] and references therein). In particular the decay $\Lambda_b \to \Lambda\mu^+\mu^-$ has received a lot of attention lately, since it has been measured by both the CDF [147] and the LHCb [148] collaboration. It is therefore mandatory to establish a theoretical basis for the description of such decays, and the knowledge of hyperon DAs is one important ingredient. Even the higher twist components can yield relevant contributions [149]. Note that constraining the shape of wave functions by calculating the moments of the DAs with lattice QCD plays an even more important role for hyperons than for nucleons, since experimental bounds are less strict than in the nucleon sector.

A first parametrization of the leading twist contributions in hyperon wave functions was already presented in ref. [150]. A complete parametrization (including all contributions from higher twist) of baryon-to-vacuum matrix elements was first performed for the case of the nucleon in ref. [76], where it turned out that higher twist contributions can yield substantial effects in the baryon sector, since the corresponding normalization constants λ_1^N and λ_2^N are large compared to the leading twist wave function normalization constant f^N. The same procedure has later on been reused in refs. [151, 152] to give similar parametrizations for matrix elements of the hyperons in the baryon octet, namely $\Sigma^\pm$, Σ^0, Ξ^-, Ξ^0 and Λ. Our work unifies these different approaches and we find relations between the distribution amplitudes for different baryons even if $\mathrm{SU}(3)_f$ symmetry is broken. The obtained relations are exact including terms up to first order in the quark masses. In this sense we call our results model-independent. However, one should keep in mind that higher order contributions which lie beyond the accuracy of our analysis are model-dependent indeed, since they are affected by the neglection of higher order terms during operator construction and by the choice of the regularization scheme.

As shown in refs. [151, 152] one has to introduce six additional DAs if one extends the formalism from the nucleon doublet to the complete baryon octet. Our results show that these

additional DAs are (at leading one-loop accuracy in BChPT) determined by the eight independent DAs already known from the nucleon sector. I.e., if one knows the eight standard DAs (and their dependence on the mass splitting between light and strange quarks) for the Λ and for at least two types of octet baryons with nonzero isospin, one can predict all the rest. Using the parametrization given in refs. [153–155], where contributions of Wandzura–Wilczek type [156] are taken into account, and applying the approximation advocated in ref. [153], where contributions that can mix with four-particle operators are systematically neglected, we need only 43 parameters to describe the complete set of baryon octet DAs, including their dependence on the splitting between light and strange quark mass. For details see section 4.5.4. This amounts to a significant reduction of the number of parameters compared to an ad hoc linear extrapolation without the knowledge of $\mathrm{SU}(3)_f$ symmetry breaking, which would require 72 parameters for the given setup. Therefore our results are useful for the extrapolation of lattice data. Note that the parameters occurring in the approximation described above are determined by the zeroth, first and second moments of the leading twist DAs and by the zeroth and first moments of twist-four DAs, which are, apart from the first moments of the higher twist amplitudes, within reach of state of the art lattice simulations (see ref. [37] for the nucleon case). However, in our first lattice QCD analysis of the full baryon octet (see section 4.6 and ref. [75]) we have restricted ourselves to the leading twist zeroth and first moments and to the higher twist normalization constants.

In hyperon decays the observed pattern of SU(3) flavor symmetry breaking is known to be nontrivial. In particular the weak radiative decay $\Sigma^+ \to p\gamma$ shows an unexpected large negative asymmetry that remains poorly understood at the parton level (see, e.g., ref. [157]). In this context it is interesting that our numerical results (cf. section 4.6.4) exhibit significant flavor symmetry breaking for the octet baryon normalization constants (up to $\sim 50\%$), and even larger effects for the shape parameters describing the deviations from the asymptotic shape.

At this point we want to highlight a conclusion that can be drawn from our results, which is of conceptual importance and also affects the nucleon sector: we find that the nonanalytic chiral behavior of moments of DAs does not depend on the twist of the amplitude. Instead, the leading chiral logarithms in the chiral-odd sector are determined by the type of amplitude to which the corresponding moment contributes. The ones occurring in $\Phi^B_{+,i}$ ($\Phi^B_{-,i}$) amplitudes, which will be defined in eq. (4.70), have the same chiral logarithms as f^B (λ_1^B). The odd moments of the leading twist DA therefore behave like λ_1^B instead of f^B, which is quite contrary to intuition-based expectation. The shape parameters occurring in ref. [153] can all be assigned uniquely to one of the two classes, which means that the distinction between moments described above is to some extent already present in currently used parametrizations.

This chapter is organized as follows: in section 4.2 we briefly review the matrix element decomposition given in ref. [76] for convenient reference. The parametrization of the nonlocal three-quark operators in terms of baryon and meson fields is performed in section 4.3. A sketch of the leading one-loop baryon chiral perturbation theory calculation is given in section 4.4, where we also explain how we have matched our results to the standard DAs given in ref. [76]. In section 4.5 we present our main results. We provide a definition for DAs that do not mix under chiral extrapolation and naturally embed the Λ baryon. The result section is to the most part

self-contained such that the reader can skip the details of the derivation at will. In section 4.6 we present an analysis of lattice QCD data. We summarize the chapter in section 4.7.

4.2 Matrix element decomposition

We start our analysis with a brief review of the decomposition of baryon-to-vacuum matrix elements of light-cone three-quark operators. The complete decomposition (including higher-twist contributions) has originally been performed for the nucleon in ref. [76], but it works in a similar way for hyperons (see, e.g., refs. [151, 152]). The light-cone three-quark operator reads

$$q^a_\alpha(a_1 n) q^b_\beta(a_2 n) q^c_\gamma(a_3 n) \;, \tag{4.1}$$

where n is a lightlike four-vector. The antisymmetrization in color indices (which makes the operator a color singlet) and the Wilson lines connecting the quark fields (providing gauge invariance) are not written out explicitly. a, b, c are flavor and α, β, γ Dirac indices. Already the number of open Dirac indices adumbrates that the general matrix element decomposition contains a large amount of independent structures. The explicit Lorentz-covariant parametrization taking into account parity and spin of the nucleon (given in ref. [76]) uses 24 different functions $\mathcal{S}^B_{1\text{-}2}$, $\mathcal{P}^B_{1\text{-}2}$, $\mathcal{V}^B_{1\text{-}6}$, $\mathcal{A}^B_{1\text{-}6}$ and $\mathcal{T}^B_{1\text{-}8}$ for each baryon:

$$\begin{aligned}
&\langle 0|q^a_\alpha(a_1 n) q^b_\beta(a_2 n) q^c_\gamma(a_3 n)|B(p,s)\rangle = \\
&\quad = \frac{1}{4}\Big[\mathcal{S}^B_1 m_B C_{\alpha\beta} (\gamma_5)_{\gamma\delta} + \mathcal{S}^B_2 m_B^2 C_{\alpha\beta} (\not{n}\gamma_5)_{\gamma\delta} \\
&\qquad + \mathcal{P}^B_1 m_B (\gamma_5 C)_{\alpha\beta} \mathbb{1}_{\gamma\delta} + \mathcal{P}^B_2 m_B^2 (\gamma_5 C)_{\alpha\beta} (\not{n})_{\gamma\delta} \\
&\qquad + \mathcal{V}^B_1 (\not{p} C)_{\alpha\beta} (\gamma_5)_{\gamma\delta} + \mathcal{V}^B_2 m_B (\not{p} C)_{\alpha\beta} (\not{n}\gamma_5)_{\gamma\delta} \\
&\qquad + \mathcal{V}^B_3 m_B (\gamma_\mu C)_{\alpha\beta} (\gamma^\mu\gamma_5)_{\gamma\delta} + \mathcal{V}^B_4 m_B^2 (\not{n} C)_{\alpha\beta} (\gamma_5)_{\gamma\delta} \\
&\qquad + \mathcal{V}^B_5 m_B^2 (\gamma_\mu C)_{\alpha\beta} (i\sigma^{\mu\nu} n_\nu \gamma_5)_{\gamma\delta} + \mathcal{V}^B_6 m_B^3 (\not{n} C)_{\alpha\beta} (\not{n}\gamma_5)_{\gamma\delta} \\
&\qquad + \mathcal{A}^B_1 (\not{p}\gamma_5 C)_{\alpha\beta} \mathbb{1}_{\gamma\delta} + \mathcal{A}^B_2 m_B (\not{p}\gamma_5 C)_{\alpha\beta} (\not{n})_{\gamma\delta} \\
&\qquad + \mathcal{A}^B_3 m_B (\gamma_\mu\gamma_5 C)_{\alpha\beta} (\gamma^\mu)_{\gamma\delta} + \mathcal{A}^B_4 m_B^2 (\not{n}\gamma_5 C)_{\alpha\beta} \mathbb{1}_{\gamma\delta} \\
&\qquad + \mathcal{A}^B_5 m_B^2 (\gamma_\mu\gamma_5 C)_{\alpha\beta} (i\sigma^{\mu\nu} n_\nu)_{\gamma\delta} + \mathcal{A}^B_6 m_B^3 (\not{n}\gamma_5 C)_{\alpha\beta} (\not{n})_{\gamma\delta} \\
&\qquad + \mathcal{T}^B_1 (p^\nu i\sigma_{\mu\nu} C)_{\alpha\beta} (\gamma^\mu\gamma_5)_{\gamma\delta} + \mathcal{T}^B_2 m_B (n^\mu p^\nu i\sigma_{\mu\nu} C)_{\alpha\beta} (\gamma_5)_{\gamma\delta} \\
&\qquad + \mathcal{T}^B_3 m_B (\sigma_{\mu\nu} C)_{\alpha\beta} (\sigma^{\mu\nu}\gamma_5)_{\gamma\delta} + \mathcal{T}^B_4 m_B (p^\nu \sigma_{\mu\nu} C)_{\alpha\beta} (\sigma^{\mu\rho} n_\rho \gamma_5)_{\gamma\delta} \\
&\qquad + \mathcal{T}^B_5 m_B^2 (n^\nu i\sigma_{\mu\nu} C)_{\alpha\beta} (\gamma^\mu\gamma_5)_{\gamma\delta} + \mathcal{T}^B_6 m_B^2 (n^\mu p^\nu i\sigma_{\mu\nu} C)_{\alpha\beta} (\not{n}\gamma_5)_{\gamma\delta} \\
&\qquad + \mathcal{T}^B_7 m_B^2 (\sigma_{\mu\nu} C)_{\alpha\beta} (\sigma^{\mu\nu}\not{n}\gamma_5)_{\gamma\delta} + \mathcal{T}^B_8 m_B^3 (n^\nu \sigma_{\mu\nu} C)_{\alpha\beta} (\sigma^{\mu\rho} n_\rho \gamma_5)_{\gamma\delta} \Big] u^B_\delta(p,s) \;,
\end{aligned} \tag{4.2}$$

where m_B is the baryon mass and $u^B(p,s)$ is the baryon spinor such that the Dirac equation $\not{p} u^B(p,s) = m_B u^B(p,s)$ holds. The 24 functions denoted by calligraphic letters depend on a_1, a_2, a_3 and the scalar product $n \cdot p$. This dependence is fixed to some extent by the constraint that the three-quark operator is invariant if one simultaneously rescales $a_i \longrightarrow \lambda a_i$ and $n_\mu \longrightarrow n_\mu/\lambda$, which we will call scaling property. It directly yields that the product of such a function with

$(n\cdot p)^{\#n}$, where $\#n$ is the number of the four-vectors n occurring in the corresponding Dirac structure, can only depend on $a_1 n\cdot p$, $a_2 n\cdot p$ and $a_3 n\cdot p$. Additionally the functions depend on the choice of the flavor structure on the l.h.s. of eq. (4.2). It is convenient to use a specific choice of flavors for each baryon that will be described below.

Being confronted with a large amount of structures one naturally tries to sort them according to relevance. In hard exclusive processes contributions of lowest twist typically play the key role, such that an ordering with respect to twist is most promising. There are two differing notions of twist: *collinear* or *dynamical* twist versus *geometric* twist (see, e.g., ref. [50]). *Collinear* twist counts the suppression with powers of k_+, which is the plus component of a specific light-cone projection of the nucleon momentum $k_\mu = p_\mu - n_\mu m_B^2/(2n\cdot p)$, where $k^2 = 0$ and $n\cdot p = n\cdot k$. Choosing the hadron to fly with large momentum in positive 3-direction on has $p_\pm = p_0 \pm p_3$, where p_+ is large while p_- is small. For an appropriate choice of n (in this case $n^T \propto (1,0,0,-1)$)[1] one has $k_+ = p_+$ such that leading collinear twist yields the most important contribution at high momentum. This direct connection to power counting is a major advantage of collinear twist, that has to be paid for: already the definition of collinear twist explicitly depends on the external hadron momentum p and it turns out that only the operators which project onto leading collinear twist can be defined without the knowledge of the external momentum (they only depend on n; for details see ref. [76]). Therefore (apart from the leading contribution) collinear twist is not a property of the operator itself. This is different in the case of *geometric* twist, which is defined directly for the operator as its mass dimension minus its (Lorentz-)spin. For geometric twist one lacks the simple power counting interpretation. However, distribution amplitudes of a certain collinear twist can be decomposed into parts of different geometric twist, where, applying the Wandzura–Wilczek approximation [156], it is often assumed that the contributions of leading geometric twist dominate. The decomposition of nonlocal operators in parts of definite geometric twist is a highly nontrivial task (see, e.g., ref. [154]). In order to take into account the expansions in both *collinear* and *geometric* twist in the best possible way we will proceed as follows: in a first step we will introduce distributions of definite collinear twist by using the twist-projection given in ref. [76]. The decomposition with respect to geometric twist will be taken into account directly via the parametrization of the DAs in section 4.5.4.

The projection onto parts of definite collinear twist is performed with great care in ref. [76]. The 24 functions used in eq. (4.2) can be replaced by 24 twist-projected functions $S^B_{1\text{-}2}$, $P^B_{1\text{-}2}$, $V^B_{1\text{-}6}$, $A^B_{1\text{-}6}$ and $T^B_{1\text{-}8}$ (their twist is specified in table 4.1) as follows [76]:

$$\underline{\text{scalar distributions:}} \tag{4.3}$$
$$\mathcal{S}_1^B = S_1^B, \qquad 2n\cdot p\mathcal{S}_2^B = S_1^B - S_2^B,$$

$$\underline{\text{pseudoscalar distributions:}} \tag{4.4}$$
$$\mathcal{P}_1^B = P_1^B, \qquad 2n\cdot p\mathcal{P}_2^B = P_2^B - P_1^B,$$

[1] The argumentation relies on the specific choice of n relative to p. For the opposite choice ($n^T \propto (1,0,0,1)$) one even finds $k_+ = 0$. Note, however, that both the matrix element decomposition and the (collinear) twist projected DAs are independent of the choice – only their meaning in terms of power counting is affected.

	twist-3	twist-4	twist-5	twist-6
scalar		S_1^B	S_2^B	
pseudoscalar		P_1^B	P_2^B	
vector	V_1^B	V_2^B, V_3^B	V_4^B, V_5^B	V_6^B
axialvector	A_1^B	A_2^B, A_3^B	A_4^B, A_5^B	A_6^B
tensor	T_1^B	T_2^B, T_3^B, T_7^B	T_4^B, T_5^B, T_8^B	T_6^B

Table 4.1: Classification of distribution amplitudes with respect to collinear twist. This table is taken from ref. [76].

vector distributions: (4.5)

$$\mathcal{V}_1^B = V_1^B, \qquad 2n\cdot p\mathcal{V}_2^B = V_1^B - V_2^B - V_3^B,$$
$$2\mathcal{V}_3^B = V_3^B, \qquad 4n\cdot p\mathcal{V}_4^B = -2V_1^B + V_3^B + V_4^B + 2V_5^B,$$
$$4n\cdot p\mathcal{V}_5^B = V_4^B - V_3^B, \qquad 4(n\cdot p)^2\mathcal{V}_6^B = -V_1^B + V_2^B + V_3^B + V_4^B + V_5^B - V_6^B,$$

axialvector distributions: (4.6)

$$\mathcal{A}_1^B = A_1^B, \qquad 2n\cdot p\mathcal{A}_2^B = -A_1^B + A_2^B - A_3^B,$$
$$2\mathcal{A}_3^B = A_3^B, \qquad 4n\cdot p\mathcal{A}_4^B = -2A_1^B - A_3^B - A_4^B + 2A_5^B,$$
$$4n\cdot p\mathcal{A}_5^B = A_3^B - A_4^B, \qquad 4(n\cdot p)^2\mathcal{A}_6^B = A_1^B - A_2^B + A_3^B + A_4^B - A_5^B + A_6^B,$$

tensor distributions: (4.7)

$$\mathcal{T}_1^B = T_1^B, \qquad 2n\cdot p\mathcal{T}_2^B = T_1^B + T_2^B - 2T_3^B,$$
$$2\mathcal{T}_3^B = T_7^B, \qquad 2n\cdot p\mathcal{T}_4^B = T_1^B - T_2^B - 2T_7^B,$$
$$2n\cdot p\mathcal{T}_5^B = -T_1^B + T_5^B + 2T_8^B, \qquad 2(n\cdot p)^2\mathcal{T}_6^B = T_2^B - T_3^B - T_4^B + T_5^B + T_7^B + T_8^B,$$
$$4n\cdot p\mathcal{T}_7^B = T_7^B - T_8^B, \qquad 4(n\cdot p)^2\mathcal{T}_8^B = -T_1^B + T_2^B + T_5^B - T_6^B + 2T_7^B + 2T_8^B.$$

From the discussion under eq. (4.2) it follows directly, that the functions which are projected onto definite collinear twist depend (aside from the factorization scale) on $a_1 n\cdot p$, $a_2 n\cdot p$ and $a_3 n\cdot p$ only. Together with the behavior under infinitesimal translations along the light-cone vector n this yields that the twist-projected functions can be written in terms of distribution amplitudes. For $F \in \{S_{1\text{-}2}^B, P_{1\text{-}2}^B, V_{1\text{-}6}^B, A_{1\text{-}6}^B, T_{1\text{-}8}^B\}$ one has

$$F(a_i n\cdot p) = \int [dx]\, e^{-in\cdot p\sum x_i a_i}\, F(x_i)\ , \tag{4.8}$$

where the integration measure $[dx]$ is defined as

$$\int [dx] = \int dx_1 dx_2 dx_3\, \delta\big(1 - \sum x_i\big)\ , \tag{4.9}$$

with all integrations running from 0 to 1. The x_i can usually be interpreted as baryon momentum fractions carried by the respective quark fields. The delta distribution within the integration measure therefore represents momentum conservation. Note that the term distribution amplitude can be used for both $F(a_i n\cdot p)$ and $F(x_i)$. However, when we call something a DA, we always

mean the latter. The amplitudes have the following symmetry properties under exchange of the first and the second variable

$$\begin{aligned} S_i^B(x_1,x_2,x_3) &= -(-1)_B S_i^B(x_2,x_1,x_3)\ , \qquad & P_i^B(x_1,x_2,x_3) &= -(-1)_B P_i^B(x_2,x_1,x_3)\ , \\ V_i^B(x_1,x_2,x_3) &= +(-1)_B V_i^B(x_2,x_1,x_3)\ , \qquad & A_i^B(x_1,x_2,x_3) &= -(-1)_B A_i^B(x_2,x_1,x_3)\ , \\ T_i^B(x_1,x_2,x_3) &= +(-1)_B T_i^B(x_2,x_1,x_3)\ , \end{aligned} \tag{4.10}$$

where we use

$$(-1)_B \equiv \begin{cases} +1\ , & \text{for } B \neq \Lambda\ , \\ -1\ , & \text{for } B = \Lambda\ , \end{cases} \tag{4.11}$$

in order to implement the different sign for the Λ originating from the antisymmetry of the isospin-singlet state. To obtain these nice symmetry properties one has to choose the flavor content in the operator in eq. (4.2) according to

$$\begin{aligned} p &\mathrel{\hat{=}} uud\ , & n &\mathrel{\hat{=}} ddu\ , & \Sigma^+ &\mathrel{\hat{=}} uus\ , & \Sigma^0 &\mathrel{\hat{=}} uds\ , \\ \Sigma^- &\mathrel{\hat{=}} dds\ , & \Xi^0 &\mathrel{\hat{=}} ssu\ , & \Xi^- &\mathrel{\hat{=}} ssd\ , & \Lambda &\mathrel{\hat{=}} uds\ , \end{aligned} \tag{4.12}$$

where the order of the flavors is relevant.

4.3 Operator construction

In this section we will construct the light-cone three-quark operator given in eq. (4.1) in terms of baryon octet and meson octet fields. Note that there are many possible parametrizations due to the freedom of choice one has by neglecting higher order effects. The task is therefore not only to find a parametrization, but to find one that is most convenient for the loop calculation to be performed and can be easily matched to the standard decomposition given in eq. (4.2). For the parametrization of the nonlocal operator one needs functions, where the moments of the functions play the role of low-energy constants. For the parametrization presented below these functions can be easily matched to standard distribution amplitudes.

4.3.1 Symmetry properties

To perform the construction of an operator within the effective theory we have to know its symmetry properties. To make use of chiral symmetry it is convenient to split the quark fields into left- and right-handed parts

$$\begin{aligned} q_\alpha^a(a_1 n) q_\beta^b(a_2 n) q_\gamma^c(a_3 n) = {} & \mathcal{O}^{abc}_{RR,\alpha\beta\gamma}(a_1,a_2,a_3) + \mathcal{O}^{abc}_{LL,\alpha\beta\gamma}(a_1,a_2,a_3) \\ & + \mathcal{O}^{abc}_{RL,\alpha\beta\gamma}(a_1,a_2,a_3) + \mathcal{O}^{abc}_{LR,\alpha\beta\gamma}(a_1,a_2,a_3) \\ & + \mathcal{O}^{cab}_{RL,\gamma\alpha\beta}(a_3,a_1,a_2) + \mathcal{O}^{cab}_{LR,\gamma\alpha\beta}(a_3,a_1,a_2) \\ & + \mathcal{O}^{bca}_{RL,\beta\gamma\alpha}(a_2,a_3,a_1) + \mathcal{O}^{bca}_{LR,\beta\gamma\alpha}(a_2,a_3,a_1)\ , \end{aligned} \tag{4.13}$$

where the operators $\mathcal{O}_{XY}$ for $X,\, Y \in \{L, R\}$ are given by

$$\mathcal{O}^{abc}_{XY,\alpha\beta\gamma}(a_1, a_2, a_3) = q^a_{X,\alpha}(a_1 n) q^b_{X,\beta}(a_2 n) q^c_{Y,\gamma}(a_3 n) \;, \tag{4.14}$$

where the left-/right-handed quark fields are $q_{L/R} = \gamma_{L/R} q = \frac{1}{2}(\mathbb{1} \mp \gamma_5) q$, as defined on page 10. These operators can be characterized by their transformation properties under parity transformation ($\mathcal{P}$), time reversal ($\mathcal{T}$), charge conjugation ($\mathcal{C}$), Hermitian conjugation and chiral rotations ($\hat{\chi}$). For chiral symmetry transformations one obtains

$$\mathcal{O}^{abc}_{XY,\alpha\beta\gamma}(a_1, a_2, a_3) \xrightarrow{\hat{\chi}} X_{aa'} X_{bb'} Y_{cc'} \mathcal{O}^{a'b'c'}_{XY,\alpha\beta\gamma}(a_1, a_2, a_3) \;. \tag{4.15}$$

Using the transformation properties of the quark fields that have been detailed in section 2.2.1 one finds the following behavior under the discrete symmetry transformations:

$$\mathcal{P}\mathcal{O}^{abc}_{XY,\alpha\beta\gamma}(a_1, a_2, a_3)\mathcal{P}^\dagger = (\eta_q^P)^3 (\gamma_0)_{\alpha\alpha'} (\gamma_0)_{\beta\beta'} (\gamma_0)_{\gamma\gamma'} \mathcal{O}^{abc}_{\bar{X}\bar{Y},\alpha'\beta'\gamma'}(a_1, a_2, a_3)\big|_{\mathbf{n}\to-\mathbf{n}} \;, \tag{4.16a}$$

$$\mathcal{C}\mathcal{P}\mathcal{O}^{abc}_{XY,\alpha\beta\gamma}(a_1, a_2, a_3)\mathcal{P}^\dagger\mathcal{C}^\dagger = (\eta_q^C \eta_q^P)^3 C_{\alpha\alpha'} C_{\beta\beta'} C_{\gamma\gamma'} \big(\mathcal{O}^{abc}_{XY,\alpha'\beta'\gamma'}(a_1, a_2, a_3)\big|_{\mathbf{n}\to-\mathbf{n}}\big)^\dagger \;, \tag{4.16b}$$

$$\mathcal{T}\mathcal{O}^{abc}_{XY,\alpha\beta\gamma}(a_1, a_2, a_3)\mathcal{T}^\dagger = (\eta_q^T)^3 (-1)_Y C_{\alpha\alpha'} C_{\beta\beta'} C_{\gamma\gamma'} \mathcal{O}^{abc}_{XY,\alpha'\beta'\gamma'}(a_1, a_2, a_3)\big|_{n_0\to-n_0} \;. \tag{4.16c}$$

It would also be possible to use charge conjugation alone, but the combined $\mathcal{CP}$ is more convenient, since it has the advantage that it leaves the quark chiralities unchanged. We will find that the constraints obtained from $\mathcal{CP}$ and $\mathcal{T}$ are compatible as long as the inversion phases for the baryon fields are chosen appropriately, cf. section 2.2.1. Additionally we know that each operator transforms under a translation in n-direction as

$$\mathcal{O}^{abc}_{XY,\alpha\beta\gamma}(a_1 + \delta a, a_2 + \delta a, a_3 + \delta a) = \exp\big\{i\,\delta a\, n\cdot\hat{P}\big\} \mathcal{O}^{abc}_{XY,\alpha\beta\gamma}(a_1, a_2, a_3) \exp\big\{-i\,\delta a\, n\cdot\hat{P}\big\} \;, \tag{4.17}$$

where $\hat{P}$ is the momentum operator which acts as a generator of translations. Another symmetry of the three-quark operators defined in eq. (4.14) is the invariance under the exchange of the quark in the first and the second position or even an invariance under exchange of all three quarks in case of the operators containing right-handed or left-handed fields exclusively. On top of this the operator fulfills the scaling property explained below eq. (4.2) on page 64.

4.3.2 Low-energy operators

Using the previously defined fields u_R and u_L we can write down the operators, which contribute to baryon-to-vacuum matrix elements of three-quark currents at leading one-loop level and have correct transformation properties under chiral rotations, in the following compact form:

$$\mathcal{O}^{abc}_{XY,\alpha\beta\gamma}(a_1, a_2, a_3) = \int [dx] \sum_{i,j} \sum_{k=1}^{k_j} \mathcal{F}^{i,j,k}_{XY}(x_1, x_2, x_3)\, \Gamma^{i,XXY}_{\alpha\beta\gamma\delta}\, B^{j,k,XXY}_{\delta,abc}(z) \;, \tag{4.18}$$

where the correct transformation behavior under translations in n-direction is ensured by $z_\mu = n_\mu \sum x_i a_i$ and the constraint that $x_1 + x_2 + x_3 = 1$ in the integration measure $[dx]$, which has

Table 4.2: List of $\Gamma^i_A \otimes \Gamma^i_B$. $\eta^P_{\Gamma,i} = 1$ by choice (see comment in the text; for the definition of $\eta^P_{\Gamma,i}$, $\eta^C_{\Gamma,i}$, $\eta^H_{\Gamma,i}$ see appendix C.4). We have multiplied structures 1 and 6 with a factor of i such that $\eta^H_{\Gamma,i} = \eta^C_{\Gamma,i}$ for all structures and, thus, $\eta^P_{\Gamma,i}\eta^C_{\Gamma,i}\eta^H_{\Gamma,i} = 1$. In cases where four-vectors are used in the place of Lorentz indices the notation means that the corresponding Lorentz index is contracted with the index of the vector; e.g., $\sigma^{\partial n} = \sigma^{\mu\nu}\partial_\mu n_\nu$.

i	$\Gamma^i_A \otimes \Gamma^i_B$	$\eta^H_{\Gamma,i} = \eta^C_{\Gamma,i}$	$\eta^C_{\Gamma^A,i}$	$\eta^5_{\Gamma^B,i}$	d^m_i	d^n_i
1	$i\mathbb{1} \otimes \not{n}$	-1	-1	-1	2	-1
2	$\mathbb{1} \otimes \mathbb{1}$	1	-1	1	1	0
3	$\sigma^{\partial n} \otimes \not{n}$	1	1	-1	2	-2
4	$\sigma^{\mu n} \otimes \gamma_\mu$	1	1	-1	2	-1
5	$\sigma^{\mu\nu} \otimes \sigma_{\mu\nu}$	1	1	1	1	0
6	$i\sigma^{\partial n} \otimes \mathbb{1}$	-1	1	1	1	-1
7	$\sigma^{\mu\partial} \otimes \sigma_{\mu n}$	1	1	1	1	-1
8	$\sigma^{\mu\partial} \otimes \gamma_\mu$	1	1	-1	0	0
9	$\sigma^{\mu n} \otimes \sigma_{\mu n}$	1	1	1	3	-2

been defined in eq. (4.9). The $\mathcal{F}$s are functions of x_1, x_2, x_3 only and k_j is given in table 4.3. The Γs are defined as

$$\Gamma^{i,XYZ}_{\alpha\beta\gamma\delta} = (\gamma_X \Gamma^i_A \gamma_Y C)_{\alpha\beta} (\gamma_Z \Gamma^i_B (i\not{\partial})^{d^m_i})_{\gamma\delta} (n\cdot\partial)^{d^n_i} \ , \tag{4.19}$$

where Γ^i_A, Γ^i_B, d^m_i and d^n_i can be taken from table 4.2. The occurring derivatives act on the Bs. We have introduced adequate powers of $i\not{\partial}$ to have functions $\mathcal{F}$ of mass dimension 2, which is compatible with the standard mass dimension of distribution amplitudes. Using $i\not{\partial}$ (which leads to a factor m_B in the final result) instead of the baryon mass in the chiral limit m_0 (which would be the standard choice) has the advantage that it allows for a straightforward matching of our parametrization to the general decomposition given in ref. [76] and to refs. [151, 152] (see also section 4.4.3). The power of $(n\cdot\partial)$ is chosen such that the scaling property is fulfilled. Note that in the chiral-odd sector one can actually write down more structures, which have the form $\Gamma^{i,XYX}_{\beta\gamma\alpha\delta}$ or $\Gamma^{i,YXX}_{\gamma\alpha\beta\delta}$. However, these structures are not independent. They can be rewritten in terms of $\Gamma^{i,XXY}_{\alpha\beta\gamma\delta}$ using Fierz transformations. In order to reduce the Γs to the minimal set given in table 4.2 one has to use the identity $\sigma^{\mu\nu}\gamma_5 = \frac{i}{2}\varepsilon^{\mu\nu\rho\sigma}\sigma_{\rho\sigma}$ and the fact that it is sufficient to construct structures of positive parity. The negative parity structures, which one can obtain by multiplying all Γ_B with a γ_5, would only lead to a relative minus sign between operators $\mathcal{O}_{XY}$ and $\mathcal{O}_{\bar{X}\bar{Y}}$ which is automatically compensated by an extra minus sign in the parity constraint given in eq. (4.24a) (see also explanation below eq. (4.24)). Additionally one has to use that multiplying both structures Γ^i_A and Γ^i_B with a γ_5 does not lead to a new, independent structure owing to the projection with $\gamma_{L/R}$ in eq. (4.19).

The Bs in eq. (4.18) are defined as

$$B^{j,k,XYZ}_{\delta,abc} = (u_X)_{aa'}(u_Y)_{bb'}(u_Z)_{cc'} B^{j,k}_{\delta,a'b'c'} \ , \tag{4.20}$$

where we take into account all possible permutations

Table 4.3: In this table we list only terms which contribute to the one-loop calculation of baryon-to-vacuum matrix elements of the operator. $\tilde{\chi}_+$ is defined as $\chi_+ - \mathrm{tr}\{\chi_+\}/3$. This is a convenient choice since this combination (in a leading one-loop calculation) vanishes along the symmetric line, where $m_u = m_d = m_s$. The octet baryon field B_δ has been defined in eq. (2.38b).

j	$B^j_{1,\delta}$	B^j_2	B^j_3	trace^j	k_j
1	B_δ	$\mathbb{1}$	$\mathbb{1}$	1	3
2	B_δ	$\mathbb{1}$	$\mathbb{1}$	$\mathrm{tr}\{\chi_+\}\, m_0^{-2}$	3
3	B_δ	$\tilde{\chi}_+ m_0^{-2}$	$\mathbb{1}$	1	6

$$B^{j,1}_{\delta,abc} = (B^j_{1,\delta})_{aa'}(B^j_2)_{bb'}(B^j_3)_{cc'}\varepsilon_{a'b'c'} \times \mathrm{trace}^j \ , \tag{4.21a}$$

$$B^{j,2}_{\delta,abc} = (B^j_3)_{aa'}(B^j_{1,\delta})_{bb'}(B^j_2)_{cc'}\varepsilon_{a'b'c'} \times \mathrm{trace}^j \ , \tag{4.21b}$$

$$B^{j,3}_{\delta,abc} = (B^j_2)_{aa'}(B^j_3)_{bb'}(B^j_{1,\delta})_{cc'}\varepsilon_{a'b'c'} \times \mathrm{trace}^j \ , \tag{4.21c}$$

$$B^{j,4}_{\delta,abc} = (B^j_2)_{aa'}(B^j_{1,\delta})_{bb'}(B^j_3)_{cc'}\varepsilon_{a'b'c'} \times \mathrm{trace}^j \ , \tag{4.21d}$$

$$B^{j,5}_{\delta,abc} = (B^j_{1,\delta})_{aa'}(B^j_3)_{bb'}(B^j_2)_{cc'}\varepsilon_{a'b'c'} \times \mathrm{trace}^j \ , \tag{4.21e}$$

$$B^{j,6}_{\delta,abc} = (B^j_3)_{aa'}(B^j_2)_{bb'}(B^j_{1,\delta})_{cc'}\varepsilon_{a'b'c'} \times \mathrm{trace}^j \ . \tag{4.21f}$$

For cases where $B^j_2 = B^j_3$ we only use $B^{j,1}_{\delta,abc}$, $B^{j,2}_{\delta,abc}$ and $B^{j,3}_{\delta,abc}$ and thus $k_j = 3$. The different possible combinations of Bs can be taken from table 4.3. All baryon and meson fields which are connected to each other (by a summation over a shared flavor index) have to be at the same spacetime position, owing to the fact that the compensator field K is a local transformation. However, chiral symmetry actually also allows for the possibility that the trace term in B is situated at a different spacetime position as the rest of the operator. We consider this possibility in appendix C.4 and show that such a parametrization only differs in higher order terms. Note that no structures of the form $[B_\delta, \tilde{\chi}_+]$, $\{B_\delta, \tilde{\chi}_+\}$, or $\mathrm{tr}\{B_\delta\tilde{\chi}_+\}$ occur in table 4.3, since they can be expressed in terms of the third structure, which means that we have only one second order structure ($j = 3$) that is responsible for SU(3)$_f$ breaking. Also the operators which describe the behavior along the SU(3)$_f$ symmetric line ($j = 1, 2$) are not linearly independent, but the situation is more complicated in this case: since operators of the same class (i.e., same j but different k) are related to each other (see eq. (4.41)) one has to take care that the symmetry properties of the operator under quark exchange are respected. Therefore, we postpone this discussion to section 4.3.4.

There are no covariant derivatives acting on the baryon field within the Bs. In appendix C.4 we show that they can always be traded for derivatives acting on the whole structure plus higher order contributions, which can be neglected. This fact will turn out to be very convenient for calculating loop contributions, since the derivatives acting on the complete structure do not lead to additional loop momenta in the integrals.

The effective operator given in eq. (4.18) already transforms correctly under chiral rotations and translations along the light-cone vector n. It also fulfills the scaling property. The remaining

symmetry properties given in section 4.3.1 will now be implemented by constraining the functions $\mathcal{F}$. We consider

$$\mathcal{P} B^{j,k,XYZ}_{\delta,abc} \mathcal{P}^\dagger = \eta_b^P (\gamma_0)_{\delta\delta'} B^{j,k,\bar{X}\bar{Y}\bar{Z}}_{\delta',abc}\big|_{\mathbf{n}\to-\mathbf{n}} \,, \tag{4.22a}$$

$$\mathcal{C}\mathcal{P} B^{j,k,XYZ}_{\delta,abc} \mathcal{P}^\dagger\mathcal{C}^\dagger = \eta_b^C \eta_b^P C_{\delta\delta'} \big(B^{j,k,XYZ}_{\delta',abc}|_{\mathbf{n}\to-\mathbf{n}}\big)^\dagger \,, \tag{4.22b}$$

$$\mathcal{T} B^{j,k,XYZ}_{\delta,abc} \mathcal{T}^\dagger = \eta_b^T (C\gamma_5)_{\delta\delta'} B^{j,k,XYZ}_{\delta',abc}\big|_{n_0\to-n_0} \,, \tag{4.22c}$$

and

$$\mathcal{P} \Gamma^{i,XYZ}_{\alpha\beta\gamma\delta} \mathcal{P}^\dagger = -\eta^P_{\Gamma,i}\ (\gamma_0)_{\alpha\alpha'}(\gamma_0)_{\beta\beta'}(\gamma_0)_{\gamma\gamma'}\ \Gamma^{i,\bar{X}\bar{Y}\bar{Z}}_{\alpha'\beta'\gamma'\delta'}\big|_{\mathbf{n}\to-\mathbf{n}}\ (\gamma_0)_{\delta'\delta} \,, \tag{4.23a}$$

$$\mathcal{C}\mathcal{P} \Gamma^{i,XYZ}_{\alpha\beta\gamma\delta} \mathcal{P}^\dagger\mathcal{C}^\dagger = -\eta^C_{\Gamma,i}\eta^P_{\Gamma,i}\eta^H_{\Gamma,i}\ C_{\alpha\alpha'}C_{\beta\beta'}C_{\gamma\gamma'}\ \big(\Gamma^{i,XYZ}_{\alpha'\beta'\gamma'\delta'}\big|_{\mathbf{n}\to-\mathbf{n}}\big)^*\ C_{\delta'\delta} \,, \tag{4.23b}$$

$$\mathcal{T} \Gamma^{i,XYZ}_{\alpha\beta\gamma\delta} \mathcal{T}^\dagger = -\eta^C_{\Gamma,i}\eta^P_{\Gamma,i}\eta^H_{\Gamma,i}\ (-1)_X(-1)_Y(-1)_Z C_{\alpha\alpha'}C_{\beta\beta'}C_{\gamma\gamma'}\ \Gamma^{i,\bar{X}\bar{Y}\bar{Z}}_{\alpha'\beta'\gamma'\delta'}\big|_{n_0\to-n_0}\ C_{\delta'\delta} \,. \tag{4.23c}$$

We have defined the structures given in table 4.2 in such a way that $\eta^P_{\Gamma,i} = +1$ and $\eta^H_{\Gamma,i}\eta^C_{\Gamma,i} = +1$, where the latter one can be achieved by multiplying appropriate structures with a factor of i. By using the relations (4.22) and (4.23) one can easily apply $\mathcal{P}$, $\mathcal{C}\mathcal{P}$ and $\mathcal{T}$ transformations to the effective operator defined in eq. (4.18). From the comparison of the result with the symmetry constraints for the three-quark operator given in eq. (4.16) one obtains the following three constraints

$$-\eta_b^P\ \mathcal{F}^{i,j,k}_{XY} = (\eta_q^P)^3\ \mathcal{F}^{i,j,k}_{\bar{X}\bar{Y}} \,, \qquad \text{obtained from } \mathcal{P} \,, \tag{4.24a}$$

$$\eta_b^P\eta_b^C\mathcal{F}^{i,j,k}_{XY} = (\eta_q^C\eta_q^P)^3\big(\mathcal{F}^{i,j,k}_{XY}\big)^* \,, \qquad \text{obtained from } \mathcal{C}\mathcal{P} \,, \tag{4.24b}$$

$$\eta_b^T\big(\mathcal{F}^{i,j,k}_{XY}\big)^* = (\eta_q^T)^3\mathcal{F}^{i,j,k}_{XY} \,, \qquad \text{obtained from } \mathcal{T} \,. \tag{4.24c}$$

For the alternative choice of Γ structures with $\eta^P_{\Gamma,i} = -1$ the parity constraint would yield an extra minus sign, which would automatically cancel the relative sign in the definition. For each choice of parity inversion phases that follows the rule that the intrinsic parity of the ground state of a composite particle (the octet baryons in our case) is given by the product of the intrinsic parities of its constituents (i.e., $\eta_b^P = (\eta_q^P)^3$) one obtains $\mathcal{F}_{XY} = -\mathcal{F}_{\bar{X}\bar{Y}}$ from eq. (4.24a). Therefore we only have to differentiate between chiral-even $\mathcal{F}_{RR} = -\mathcal{F}_{LL} \equiv \mathcal{F}_{\text{even}}$ and chiral-odd $\mathcal{F}_{LR} = -\mathcal{F}_{RL} \equiv \mathcal{F}_{\text{odd}}$ distribution amplitudes. The constraints obtained from eqs. (4.24b) and (4.24c) are consistent with each other as long as the $\mathcal{C}\mathcal{P}\mathcal{T}$ phases fulfill the constraint $\eta_b^C\eta_b^P\eta_b^T = (\eta_q^C\eta_q^P\eta_q^T)^3$, which obviously agrees with the standard phase conventions, where all the inversion phases are defined to be $+1$. The result is a so-called reality condition

$$e^{-i\phi}\mathcal{F}^{i,j,k}_{XY} = \big(e^{-i\phi}\mathcal{F}^{i,j,k}_{XY}\big)^* \,, \tag{4.25}$$

where

$$e^{2i\phi} = \frac{(\eta_q^C\eta_q^P)^3}{\eta_b^C\eta_b^P} = \frac{\eta_b^T}{(\eta_q^T)^3} \,, \tag{4.26}$$

which means that the $\mathcal{F}$s are real for the standard choice of inversion phases. However, as known from quantum mechanics, two states are equivalent if they lie within the same ray in

Hilbert space, i.e., if they only differ by a phase. Hence, the overall phase in eq. (4.25) has no physical significance. The inversion phases are part of the definition of the effective baryon field. Two differing baryon field definitions which lead to a different phase in eq. (4.25) can therefore be interpreted as fields that create different (physically equivalent) representatives of the same physical state. The main information contained in the reality condition is, therefore, not the phase and how it is obtained from the inversion phases. The important information is, that there are no relative phases between different distribution amplitudes. E.g., for the wave function normalization constants f^B, λ_1^B and λ_2^B eq. (4.25) guarantees that the products $f^B(\lambda_1^B)^*$, $f^B(\lambda_2^B)^*$ and $\lambda_1^B(\lambda_2^B)^*$ are real.

4.3.3 Symmetry under exchange of quark fields

In this section we use the symmetry of the original three-quark operators under exchange of quark fields with the same handedness to reduce the number of amplitudes. Using the constraint that the operators have to be equal under exchange of the first and the second quark yields

$$\underline{j=1,2:} \qquad \mathcal{F}_{XY}^{i,j,1}(x_1,x_2,x_3) = -\eta^C_{\Gamma^A,i}\mathcal{F}_{XY}^{i,j,2}(x_2,x_1,x_3)\ , \tag{4.27a}$$

$$\mathcal{F}_{XY}^{i,j,3}(x_1,x_2,x_3) = -\eta^C_{\Gamma^A,i}\mathcal{F}_{XY}^{i,j,3}(x_2,x_1,x_3)\ , \tag{4.27b}$$

$$\underline{j=3:} \qquad \mathcal{F}_{XY}^{i,3,1}(x_1,x_2,x_3) = -\eta^C_{\Gamma^A,i}\mathcal{F}_{XY}^{i,3,4}(x_2,x_1,x_3)\ , \tag{4.27c}$$

$$\mathcal{F}_{XY}^{i,3,2}(x_1,x_2,x_3) = -\eta^C_{\Gamma^A,i}\mathcal{F}_{XY}^{i,3,5}(x_2,x_1,x_3)\ , \tag{4.27d}$$

$$\mathcal{F}_{XY}^{i,3,3}(x_1,x_2,x_3) = -\eta^C_{\Gamma^A,i}\mathcal{F}_{XY}^{i,3,6}(x_2,x_1,x_3)\ . \tag{4.27e}$$

In the chiral-odd sector one now uses these relations to eliminate $\mathcal{F}_{XY}^{i,j,2}$ (if $j=1,2$) and $\mathcal{F}_{XY}^{i,3,4/5/6}$. Additionally we can use that

$$(\gamma_Y\Gamma_A\gamma_X C)_{\gamma\beta}(\gamma_X\Gamma_B)_{\alpha\delta} = 0\ , \quad \text{if } X\neq Y \text{ and } \Gamma_A\in\{\mathbb{1},\gamma_5,\sigma_{\mu\nu}\}\ . \tag{4.28}$$

Using Fierz transformation this leads to

$$\Gamma^{3,XXY}_{\alpha\beta\gamma\delta} = \Gamma^{4,XXY}_{\alpha\beta\gamma\delta} + \frac{1}{2}\Gamma^{9,XXY}_{\alpha\beta\gamma\delta}\ , \tag{4.29a}$$

$$\Gamma^{5,XXY}_{\alpha\beta\gamma\delta} = 0\ , \tag{4.29b}$$

$$\Gamma^{6,XXY}_{\alpha\beta\gamma\delta} = \Gamma^{4,XXY}_{\alpha\beta\gamma\delta} - \Gamma^{7,XXY}_{\alpha\beta\gamma\delta}\ , \tag{4.29c}$$

if $X\neq Y$. Therefore we have the freedom to choose

$$\mathcal{F}^{3,j,k}_{\text{odd}}(x_1,x_2,x_3) = \mathcal{F}^{5,j,k}_{\text{odd}}(x_1,x_2,x_3) = \mathcal{F}^{6,j,k}_{\text{odd}}(x_1,x_2,x_3) = 0\ . \tag{4.30}$$

In the chiral-even sector the projection with $\gamma_{L/R}$ leads to similar constraints. The counterpart of eq. (4.28) reads

$$(\gamma_X\Gamma_A\gamma_X C)_{\gamma\beta}(\gamma_X\Gamma_B)_{\alpha\delta} = 0\ , \quad \text{if } \Gamma_A\in\{\gamma_\mu,\gamma_\mu\gamma_5\}\ . \tag{4.31}$$

With a Fierz transformation one obtains

$$\Gamma^{7,XXX}_{\alpha\beta\gamma\delta} = -\Gamma^{4,XXX}_{\alpha\beta\gamma\delta} + \frac{1}{2}\Gamma^{5,XXX}_{\alpha\beta\gamma\delta} + \Gamma^{6,XXX}_{\alpha\beta\gamma\delta} \ , \tag{4.32a}$$

$$\Gamma^{8,XXX}_{\alpha\beta\gamma\delta} = -\frac{1}{4}\Gamma^{5,XXX}_{\alpha\beta\gamma\delta} \ , \tag{4.32b}$$

$$\Gamma^{9,XXX}_{\alpha\beta\gamma\delta} = 0 \ . \tag{4.32c}$$

Therefore, we can choose

$$\mathcal{F}^{7,j,k}_{\text{even}}(x_1,x_2,x_3) = \mathcal{F}^{8,j,k}_{\text{even}}(x_1,x_2,x_3) = \mathcal{F}^{9,j,k}_{\text{even}}(x_1,x_2,x_3) = 0 \ . \tag{4.33}$$

The operators containing left-/right-handed quarks exclusively also have to be invariant under an exchange of the first and the last quark. Performing a Fierz transformation and using the identities given above we find

$$\Gamma^{i,XXX}_{\gamma\beta\alpha\delta} = \sum_{i'=1}^{6} \Gamma^{i',XXX}_{\alpha\beta\gamma\delta} c^{i'i} \ . \tag{4.34}$$

The matrix c is given by

$$c = \begin{pmatrix} \frac{1}{2} & 0 & -\frac{1}{2} & -\frac{3}{2} & 0 & -\frac{1}{2} \\ 0 & \frac{1}{2} & 0 & 0 & 6 & -\frac{1}{2} \\ 0 & 0 & 1 & 0 & 0 & 0 \\ -\frac{1}{2} & 0 & -\frac{1}{2} & -\frac{1}{2} & 0 & -\frac{1}{2} \\ 0 & \frac{1}{8} & 0 & 0 & -\frac{1}{2} & \frac{1}{8} \\ 0 & 0 & 0 & 0 & 0 & 1 \end{pmatrix} . \tag{4.35}$$

By the use of this relation the symmetry property of the operator under exchange of the first and the last quark translates to the following constraints on the amplitudes:

$\underline{j = 1,2:}$

$$\mathcal{F}^{i,j,1}_{XX}(x_1,x_2,x_3) = -\sum_{i'=1}^{6} c^{ii'} \mathcal{F}^{i',j,3}_{XX}(x_3,x_2,x_1) \ , \tag{4.36a}$$

$$\mathcal{F}^{i,j,2}_{XX}(x_1,x_2,x_3) = -\sum_{i'=1}^{6} c^{ii'} \mathcal{F}^{i',j,2}_{XX}(x_3,x_2,x_1) \ , \tag{4.36b}$$

$$\mathcal{F}^{i,j,3}_{XX}(x_1,x_2,x_3) = -\sum_{i'=1}^{6} c^{ii'} \mathcal{F}^{i',j,1}_{XX}(x_3,x_2,x_1) \ , \tag{4.36c}$$

$\underline{j=3}$:

$$\mathcal{F}_{XX}^{i,3,1}(x_1,x_2,x_3) = -\sum_{i'=1}^{6} c^{ii'}\,\mathcal{F}_{XX}^{i',3,6}(x_3,x_2,x_1)\ , \tag{4.36d}$$

$$\mathcal{F}_{XX}^{i,3,2}(x_1,x_2,x_3) = -\sum_{i'=1}^{6} c^{ii'}\,\mathcal{F}_{XX}^{i',3,4}(x_3,x_2,x_1)\ , \tag{4.36e}$$

$$\mathcal{F}_{XX}^{i,3,3}(x_1,x_2,x_3) = -\sum_{i'=1}^{6} c^{ii'}\,\mathcal{F}_{XX}^{i',3,5}(x_3,x_2,x_1)\ , \tag{4.36f}$$

$$\mathcal{F}_{XX}^{i,3,4}(x_1,x_2,x_3) = -\sum_{i'=1}^{6} c^{ii'}\,\mathcal{F}_{XX}^{i',3,2}(x_3,x_2,x_1)\ , \tag{4.36g}$$

$$\mathcal{F}_{XX}^{i,3,5}(x_1,x_2,x_3) = -\sum_{i'=1}^{6} c^{ii'}\,\mathcal{F}_{XX}^{i',3,3}(x_3,x_2,x_1)\ , \tag{4.36h}$$

$$\mathcal{F}_{XX}^{i,3,6}(x_1,x_2,x_3) = -\sum_{i'=1}^{6} c^{ii'}\,\mathcal{F}_{XX}^{i',3,1}(x_3,x_2,x_1)\ . \tag{4.36i}$$

Using these equations one finds for the operator with $j=3$ that one can eliminate all amplitudes apart from $\mathcal{F}_{XX}^{i,3,1}$, by using the following relations recursively:

$$\mathcal{F}_{XX}^{i,3,2}(x_1,x_2,x_3) = \eta_{\Gamma^A,i}^{C}\sum_{i'=1}^{6} c^{ii'}\,\mathcal{F}_{XX}^{i',3,3}(x_3,x_1,x_2)\ , \tag{4.37a}$$

$$\mathcal{F}_{XX}^{i,3,3}(x_1,x_2,x_3) = \eta_{\Gamma^A,i}^{C}\sum_{i'=1}^{6} c^{ii'}\,\mathcal{F}_{XX}^{i',3,1}(x_3,x_1,x_2)\ , \tag{4.37b}$$

$$\mathcal{F}_{XX}^{i,3,4}(x_1,x_2,x_3) = -\eta_{\Gamma^A,i}^{C}\mathcal{F}_{XX}^{i,3,1}(x_2,x_1,x_3)\ , \tag{4.37c}$$

$$\mathcal{F}_{XX}^{i,3,5}(x_1,x_2,x_3) = -\eta_{\Gamma^A,i}^{C}\mathcal{F}_{XX}^{i,3,2}(x_2,x_1,x_3)\ , \tag{4.37d}$$

$$\mathcal{F}_{XX}^{i,3,6}(x_1,x_2,x_3) = -\eta_{\Gamma^A,i}^{C}\mathcal{F}_{XX}^{i,3,3}(x_2,x_1,x_3)\ . \tag{4.37e}$$

For the operators with $j=1,2$ we can eliminate

$$\mathcal{F}_{XX}^{i,j,2}(x_1,x_2,x_3) = -\eta_{\Gamma^A,i}^{C}\mathcal{F}_{XX}^{i,j,1}(x_2,x_1,x_3)\ , \tag{4.38a}$$

$$\mathcal{F}_{XX}^{i,j,3}(x_1,x_2,x_3) = -\sum_{i'=1}^{6} c^{ii'}\,\mathcal{F}_{XX}^{i',j,1}(x_3,x_2,x_1)\ , \tag{4.38b}$$

and additionally

$$\begin{aligned}\mathcal{F}_{XX}^{1,j,1}(x_1,x_2,x_3) = {}& \mathcal{F}_{XX}^{3,j,1}(x_1,x_2,x_3) + \mathcal{F}_{XX}^{4,j,1}(x_1,x_2,x_3) - 2\mathcal{F}_{XX}^{4,j,1}(x_1,x_3,x_2)\\ & + \mathcal{F}_{XX}^{6,j,1}(x_1,x_2,x_3)\ ,\end{aligned} \tag{4.39a}$$

$$\mathcal{F}_{XX}^{2,j,1}(x_1,x_2,x_3) = -4\mathcal{F}_{XX}^{5,j,1}(x_1,x_2,x_3) + 8\mathcal{F}_{XX}^{5,j,1}(x_1,x_3,x_2) + \mathcal{F}_{XX}^{6,j,1}(x_1,x_2,x_3)\ , \tag{4.39b}$$

$$\mathcal{F}_{XX}^{3,j,1}(x_1,x_2,x_3) = -\mathcal{F}_{XX}^{3,j,1}(x_1,x_3,x_2)\ , \tag{4.39c}$$

$$\mathcal{F}_{XX}^{6,j,1}(x_1,x_2,x_3) = -\mathcal{F}_{XX}^{6,j,1}(x_1,x_3,x_2)\ . \tag{4.39d}$$

From the fact that the local operator at the origin, where $a_1 = a_2 = a_3 = 0$, is independent of the light-cone vector n one can deduce constraints for the zeroth moments of the distribution amplitudes

$$\int [dx] \mathcal{F}_{XY}^{i,j,k}(x_1, x_2, x_3) = 0 \ , \quad \text{for } i = 1, 3, 4, 6, 7, 9 \ . \tag{4.40}$$

4.3.4 Elimination of linearly dependent structures

To avoid overparametrization we will now annihilate linearly dependent structures of those given in table 4.3. Considering all possible three-quark operators and all baryons from the octet, one finds (for $j = 1, 2$) that only two out of the three structures $B_{\delta,abc}^{j,1}$, $B_{\delta,abc}^{j,2}$ and $B_{\delta,abc}^{j,3}$ are linearly independent, since one has

$$0 = B_{\delta,abc}^{j,1} + B_{\delta,abc}^{j,2} + B_{\delta,abc}^{j,3} \ . \tag{4.41}$$

In the chiral-odd sector we can use this relation to replace $B_{\delta,abc}^{j,3} = -B_{\delta,abc}^{j,1} - B_{\delta,abc}^{j,2}$, which is equivalent to the replacement

$$\mathcal{F}_{\text{odd}}^{i,j,1}(x_1, x_2, x_3) \longrightarrow \tilde{\mathcal{F}}_{\text{odd}}^{i,j,1}(x_1, x_2, x_3) \equiv \mathcal{F}_{\text{odd}}^{i,j,1}(x_1, x_2, x_3) - \mathcal{F}_{\text{odd}}^{i,j,3}(x_1, x_2, x_3) \ , \tag{4.42a}$$

$$\mathcal{F}_{\text{odd}}^{i,j,2}(x_1, x_2, x_3) \longrightarrow \tilde{\mathcal{F}}_{\text{odd}}^{i,j,2}(x_1, x_2, x_3) \equiv \mathcal{F}_{\text{odd}}^{i,j,2}(x_1, x_2, x_3) - \mathcal{F}_{\text{odd}}^{i,j,3}(x_1, x_2, x_3) \ , \tag{4.42b}$$

$$\mathcal{F}_{\text{odd}}^{i,j,3}(x_1, x_2, x_3) \longrightarrow \tilde{\mathcal{F}}_{\text{odd}}^{i,j,3}(x_1, x_2, x_3) \equiv 0 \ . \tag{4.42c}$$

Using eqs. (4.27a) and (4.27b) one finds that the new functions have the same symmetry properties as the old ones. Therefore we can choose

$$\mathcal{F}_{\text{odd}}^{i,j,3}(x_1, x_2, x_3) = 0 \ , \quad j = 1, 2 \ , \tag{4.43}$$

in accordance with symmetry properties and without loss of generality. In the chiral-even sector the situation is different since the amplitudes are already constrained by the symmetry under exchange of the first and the third quark. An elimination of one structure in favor of the two others would therefore not lead to a simplification. Instead one just obtains a reparametrization of the problem for which it would be hard to implement the symmetry properties under exchange of the first and the last quark.

4.4 Details on the calculation

In this section we describe the leading one-loop calculation. In section 4.4.3 we explain how we have matched to the standard DAs defined in ref. [76].

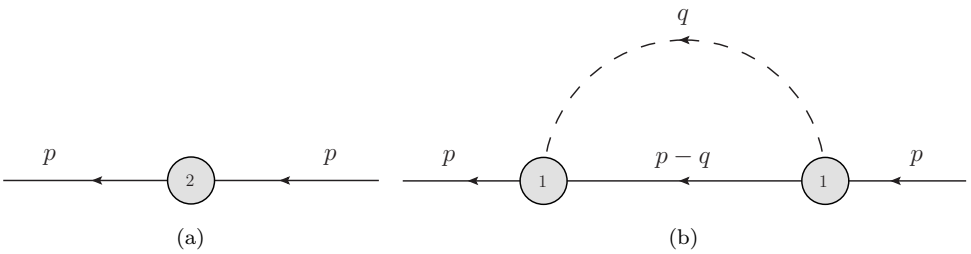

Figure 4.1: Feynman diagrams needed for the calculation of the self-energy. The circles indicate vertices from the meson-baryon Lagrangian (the number inside denotes the chiral order), while the dashed and solid lines represent meson and baryon propagators, respectively.

4.4.1 Meson masses and the Z-factor

We work in the limit of exact isospin symmetry, where $m_u = m_d \equiv m_l$. Using the standard leading order meson Lagrangian (2.36) one finds for the meson masses the standard Gell-Mann–Oakes–Renner relations

$$m_\pi^2 = 2B_0 m_l = m_{i=1,2,3}^2 = 2B_0(\bar{m}_q - \delta m_l) \ , \tag{4.44a}$$

$$m_K^2 = B_0(m_l + m_s) = m_{i=4,\dots,7}^2 = B_0(2\bar{m}_q + \delta m_l) \ , \tag{4.44b}$$

$$m_\eta^2 = \frac{B_0}{3}(2m_l + 4m_s) = m_{i=8}^2 = 2B_0(\bar{m}_q + \delta m_l) \ , \tag{4.44c}$$

where

$$\bar{m}_q = \frac{1}{3}(2m_l + m_s) \ , \tag{4.45a}$$

$$\delta m_l = \bar{m}_q - m_l \ , \tag{4.45b}$$

and B_0 is the LEC proportional to the quark condensate in the chiral limit. As additional ingredient we need the first order meson-baryon Lagrangian given in eq. (2.54). From the latter one deduces the baryon-meson-baryon vertex for an incoming baryon B, an outgoing baryon B' and an incoming meson (the k-th one in the Cartesian basis) with momentum q, which is relevant in our calculation:

$$\frac{-1}{2F_0}\not{q}\gamma_5 \operatorname{tr}\left\{\kappa_{B'}^T(D\{\lambda^k, \kappa_B\} + F[\lambda^k, \kappa_B])\right\} \ . \tag{4.46}$$

The self-energy to third chiral order is given by the sum of the irreducible diagrams shown in figure 4.1 (where external legs are to be amputated) multiplied with an i. The contribution of diagram (b), which is relevant for the calculation of the Z-factor is given by

$$i \times (\mathrm{b}) = 3g_{B,\pi} f(m_\pi, m_0, \not{p}) + 4g_{B,K} f(m_K, m_0, \not{p}) + g_{B,\eta} f(m_\eta, m_0, \not{p}) \ , \tag{4.47}$$

where

$$f(m, m_0, \not{p}) = \frac{-1}{4F_0^2}\big((p^2 - m_0^2)\not{p} I_{1,1}^{(1)}(m, m_0, \not{p}) + (\not{p} + m_0)\big(I_{0,1}(m_0, \not{p}) - m^2 I_{1,1}(m, m_0, \not{p})\big)\big) \ . \tag{4.48}$$

The loop functions $I_{k,l}$ and $I^{(1)}_{k,l}$ are defined in appendix A.4 and the coefficients are given by

$$\begin{aligned}
g_{N,\pi} &= (D+F)^2 \ , & g_{N,K} &= \frac{5}{6}D^2 - DF + \frac{3}{2}F^2 \ , & g_{N,\eta} &= \frac{1}{3}(D-3F)^2 \ , \\
g_{\Sigma,\pi} &= \frac{4}{9}(D^2+6F^2) \ , & g_{\Sigma,K} &= D^2 + F^2 \ , & g_{\Sigma,\eta} &= \frac{4}{3}D^2 \ , \\
g_{\Xi,\pi} &= (D-F)^2 \ , & g_{\Xi,K} &= \frac{5}{6}D^2 + DF + \frac{3}{2}F^2 \ , & g_{\Xi,\eta} &= \frac{1}{3}(D+3F)^2 \ , \\
g_{\Lambda,\pi} &= \frac{4}{3}D^2 \ , & g_{\Lambda,K} &= \frac{1}{3}(D^2+9F^2) \ , & g_{\Lambda,\eta} &= \frac{4}{3}D^2 \ .
\end{aligned} \tag{4.49}$$

These constants fulfill the constraints that the sums

$$3g_{B,\pi} + 4g_{B,K} + g_{B,\eta} = \frac{4}{3}(5D^2+9F^2) \ , \tag{4.50a}$$

$$2g_{N,M} + 3g_{\Sigma,M} + 2g_{\Xi,M} + g_{\Lambda,M} = \frac{4}{3}(5D^2+9F^2) \ , \tag{4.50b}$$

are independent of the baryon/meson species. This yields similar baryon masses and Z-factors along the line of equal quark masses and is a consequence of $\mathrm{SU}(3)_f$ symmetry. For a detailed study of baryon masses under symmetry breaking see ref. [135]. The square root of the Z-factor needed in our calculation is given by

$$\sqrt{Z_B} \doteq 1 + \frac{1}{2}\Sigma'_B \ , \tag{4.51}$$

where the prime indicates taking a derivative with respect to $\not{p}$ and substituting $\not{p} \to m_B$. The dotted equal sign $\doteq$ means equal up to terms which are of higher order than our level of accuracy (which is second order in chiral power counting). The derivative of the self-energy

$$\begin{aligned}
\Sigma'_B(\bar{m}_q, \delta m_l) &= 3g_{B,\pi} f'(m_\pi, m_0, m_B) + 4g_{B,K} f'(m_K, m_0, m_B) + g_{B,\eta} f'(m_\eta, m_0, m_B) \\
&\equiv \Sigma'^{\star}(\bar{m}_q) + \Delta\Sigma'_B(\bar{m}_q, \delta m_l) \ ,
\end{aligned} \tag{4.52}$$

can be split into a flavor-symmetric and a flavor symmetry breaking part

$$\begin{aligned}
\Sigma'^{\star}(\bar{m}_q) &= \Sigma'_B(\bar{m}_q, 0) = (3g_{B,\pi} + 4g_{B,K} + g_{B,\eta}) f'(m^\star_m, m_0, m_B) \\
&= \frac{4}{3}(5D^2+9F^2) f'(m^\star_m, m_0, m_B) \\
&\doteq \frac{4}{3}(5D^2+9F^2) f'(m^\star_m, m^\star_b, m^\star_b) \ ,
\end{aligned} \tag{4.53a}$$

$$\begin{aligned}
\Delta\Sigma'_B(\bar{m}_q, \delta m_l) &= \Sigma'_B(\bar{m}_q, \delta m_l) - \Sigma'_B(\bar{m}_q, 0) \\
&= 3g_{B,\pi} f'(m_\pi, m_0, m_B) + 4g_{B,K} f'(m_K, m_0, m_B) \\
&\quad + g_{B,\eta} f'(m_\eta, m_0, m_B) - \frac{4}{3}(5D^2+9F^2) f'(m^\star_m, m_0, m_B) \\
&\doteq 3g_{B,\pi} f'(m_\pi, m^\star_b, m^\star_b) + 4g_{B,K} f'(m_K, m^\star_b, m^\star_b) \\
&\quad + g_{B,\eta} f'(m_\eta, m^\star_b, m^\star_b) - \frac{4}{3}(5D^2+9F^2) f'(m^\star_m, m^\star_b, m^\star_b) \ ,
\end{aligned} \tag{4.53b}$$

where $m^\star_{m/b} = m^\star_{m/b}(\bar{m}_q)$ is the meson/baryon mass along the symmetric line ($\delta m_l = 0$). For explicit results see appendix C.1.

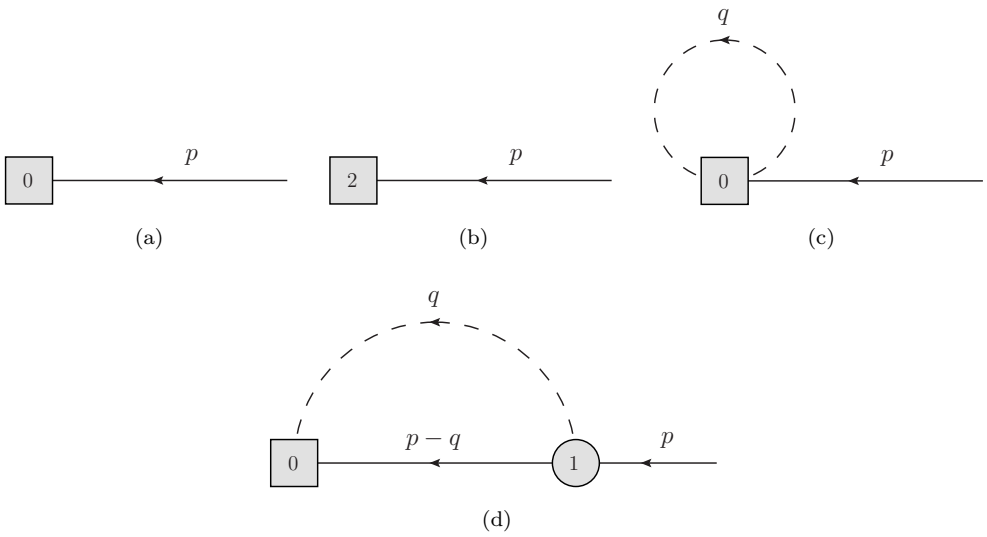

Figure 4.2: Feynman diagrams needed for the calculation of the baryon-to-vacuum matrix elements. The squares depict the operator insertions given in eqs. (4.56), the circle stands for the vertex from the meson-baryon Lagrangian given in eq. (4.46) and the dashed/solid lines represent mesons/baryons. The numbers inside the vertices and operator insertions denote their chiral order. Diagram (a) has to be multiplied with $\sqrt{Z}$. However, one knows that at higher orders all of the diagrams will receive a $\sqrt{Z}$ contribution, which can be used as an argument in favor of the factorized version of our results (see eq. (4.85) in section 4.5).

4.4.2 Baryon-to-vacuum matrix elements

In this section we describe the actual loop calculation for the baryon-to-vacuum matrix elements of the three-quark operators. From a simple power counting argument one finds that at leading one-loop level the only contributing graphs are the ones shown in figure 4.2. One easily observes that the second order operator insertions only occur without additional mesons. Therefore we only have to compute the higher order vertices where a single baryon couples to the operator. Contributions with additional mesons only occur for the leading order operator insertion ($j = 1$). For the BChPT calculation mainly the structure $B^{j,k,XYZ}_{\delta,abc}$ is relevant. Graph (d) of figure 4.2 is an exception because the extra γ_5 from the baryon-meson-baryon vertex has to be canceled with a γ_5 from the Dirac structure of the operator. The calculation gets simplified considerably if one uses the fact that (by construction) the $B^{j,k,XYZ}_{\delta,abc}$ with $k \neq 1$ can be obtained from the case $k = 1$ by a permutation of indices:

$$\begin{aligned} B^{j,2,XYZ}_{\delta,abc} &= B^{j,1,YZX}_{\delta,bca} , & B^{j,3,XYZ}_{\delta,abc} &= B^{j,1,ZXY}_{\delta,cab} , & B^{j,4,XYZ}_{\delta,abc} &= -B^{j,1,YXZ}_{\delta,bac} , \\ B^{j,5,XYZ}_{\delta,abc} &= -B^{j,1,XZY}_{\delta,acb} , & B^{j,6,XYZ}_{\delta,abc} &= -B^{j,1,ZYX}_{\delta,cba} , \end{aligned} \tag{4.54}$$

which means that we actually only have to calculate the case $k = 1$. Using the definition

$$(-1)_X \equiv \begin{cases} +1 , & \text{for } X = R , \\ -1 , & \text{for } X = L , \end{cases} \tag{4.55}$$

from section 2.2.1, we can write down the relevant operator insertions in a quite economic way:

$$B^{1,1,XYZ}_{\delta,abc}(z)\Big|_{B_\epsilon(p)} = (\kappa_B)^{aa'}\varepsilon^{a'bc}e^{-ip\cdot z}\mathbb{1}_{\delta\epsilon}\ , \tag{4.56a}$$

$$\begin{aligned} B^{1,1,XYZ}_{\delta,abc}(z)\Big|_{B_\epsilon(p-q)\phi^k(q)} = \frac{i}{2F_0}\Big[&(-1)_X(\lambda^k\kappa_B)^{aa'}\delta^{bb'}\delta^{cc'} + (-1)_Y(\kappa_B)^{aa'}(\lambda^k)^{bb'}\delta^{cc'} \\ &+ (-1)_Z(\kappa_B)^{aa'}\delta^{bb'}(\lambda^k)^{cc'}\Big]\varepsilon^{a'b'c'}e^{-ip\cdot z}\mathbb{1}_{\delta\epsilon}\ , \end{aligned} \tag{4.56b}$$

$$\begin{aligned} &B^{1,1,XYZ}_{\delta,abc}(z)\Big|_{B_\epsilon(p-q_1-q_2)\phi^k(q_1)\phi^l(q_2)} = \\ &= \frac{-1}{16F_0^2}\Big[(\lambda^k\lambda^l\kappa_B)^{aa'}\delta^{bb'}\delta^{cc'} + (\kappa_B)^{aa'}\big((\lambda^k\lambda^l)^{bb'}\delta^{cc'} + \delta^{bb'}(\lambda^k\lambda^l)^{cc'}\big) \\ &\quad + 2(-1)_X(-1)_Y(\lambda^k\kappa_B)^{aa'}(\lambda^l)^{bb'}\delta^{cc'} + 2(-1)_X(-1)_Z(\lambda^k\kappa_B)^{aa'}\delta^{bb'}(\lambda^l)^{cc'} \\ &\quad + 2(-1)_Y(-1)_Z(\kappa_B)^{aa'}(\lambda^k)^{bb'}(\lambda^l)^{cc'}\Big]\varepsilon^{a'b'c'}e^{-ip\cdot z}\mathbb{1}_{\delta\epsilon} \\ &\quad + (k\leftrightarrow l)\ . \end{aligned} \tag{4.56c}$$

The second order tree-level operator insertions read

$$B^{2,1,XYZ}_{\delta,abc}(z)\Big|_{B_\epsilon(p)} = 4B_0m_0^{-2}\,\mathrm{tr}\,\{\mathcal{M}\}\,(\kappa_B)^{aa'}\varepsilon^{a'bc}e^{-ip\cdot z}\mathbb{1}_{\delta\epsilon}\ , \tag{4.56d}$$

$$B^{3,1,XYZ}_{\delta,abc}(z)\Big|_{B_\epsilon(p)} = 4B_0m_0^{-2}(\kappa_B)^{aa'}\tilde{\mathcal{M}}^{bb'}\varepsilon^{a'b'c}e^{-ip\cdot z}\mathbb{1}_{\delta\epsilon}\ , \tag{4.56e}$$

where $\tilde{\mathcal{M}} = \mathcal{M} - \mathrm{tr}\,\{\mathcal{M}\}/3$ and $\mathcal{M}$ is the diagonal quark mass matrix, cf. section 2.1.3. After performing the loop calculation one finds that the results can be expressed as

$$\begin{aligned} &\langle 0|\mathcal{O}^{abc}_{RR,\alpha\beta\gamma}(a_1,a_2,a_3) + \mathcal{O}^{abc}_{LL,\alpha\beta\gamma}(a_1,a_2,a_3)|B(p,s)\rangle = \\ &\quad = \int[dx]e^{-i\,n\cdot p\sum_k x_ka_k}\sum_i \Gamma^{i,\mathrm{even}}_{\alpha\beta\gamma\delta}u^B_\delta(p,s)h^{i,abc}_{B,\mathrm{even}}(x_1,x_2,x_3)\ , \end{aligned} \tag{4.57a}$$

$$\begin{aligned} &\langle 0|\mathcal{O}^{abc}_{RL,\alpha\beta\gamma}(a_1,a_2,a_3) + \mathcal{O}^{abc}_{LR,\alpha\beta\gamma}(a_1,a_2,a_3)|B(p,s)\rangle = \\ &\quad = \int[dx]e^{-i\,n\cdot p\sum_k x_ka_k}\sum_i \Gamma^{i,\mathrm{odd}}_{\alpha\beta\gamma\delta}u^B_\delta(p,s)h^{i,abc}_{B,\mathrm{odd}}(x_1,x_2,x_3)\ , \end{aligned} \tag{4.57b}$$

where $u^B_\delta(p,s)$ is the baryon spinor,

$$\Gamma^{i,\mathrm{even}}_{\alpha\beta\gamma\delta} = \Gamma^{i,RRR}_{\alpha\beta\gamma\delta} - \Gamma^{i,LLL}_{\alpha\beta\gamma\delta}\ , \tag{4.58a}$$

$$\Gamma^{i,\mathrm{odd}}_{\alpha\beta\gamma\delta} = \Gamma^{i,LLR}_{\alpha\beta\gamma\delta} - \Gamma^{i,RRL}_{\alpha\beta\gamma\delta}\ , \tag{4.58b}$$

and

$$h^{i,abc}_{B,\mathrm{even}}(x_1,x_2,x_3) = \sum_{j,k} c^{j,k,abc}_{B,RRR}\mathcal{F}^{i,j,k}_{\mathrm{even}}(x_1,x_2,x_3)\ , \tag{4.59a}$$

$$h^{i,abc}_{B,\mathrm{odd}}(x_1,x_2,x_3) = \sum_{j,k} c^{j,k,abc}_{B,LLR}\mathcal{F}^{i,j,k}_{\mathrm{odd}}(x_1,x_2,x_3)\ . \tag{4.59b}$$

The coefficients $c^{j,k,abc}_{B,XYZ}$ inherit the property that the ones with $k \neq 1$ can be obtained from the case $k = 1$ by a permutation of indices:

$$\begin{aligned} c^{j,2,abc}_{B,XYZ} &= c^{j,1,bca}_{B,YZX} \ , & c^{j,3,abc}_{B,XYZ} &= c^{j,1,cab}_{B,ZXY} \ , & c^{j,4,abc}_{B,XYZ} &= -c^{j,1,bac}_{B,YXZ} \ , \\ c^{j,5,abc}_{B,XYZ} &= -c^{j,1,acb}_{B,XZY} \ , & c^{j,6,abc}_{B,XYZ} &= -c^{j,1,cba}_{B,ZYX} \ . \end{aligned} \tag{4.60}$$

For those with $k = 1$ we find

$$c^{1,1,abc}_{B,XYZ} = c^{1,1,abc}_{B,XYZ}\Big|_{(a)} + c^{1,1,abc}_{B,XYZ}\Big|_{(c)} + c^{1,1,abc}_{B,XYZ}\Big|_{(d)} \ , \tag{4.61a}$$

$$c^{1,1,abc}_{B,XYZ}\Big|_{(a)} = \sqrt{Z_B}(\kappa_B)^{aa'}\varepsilon^{a'bc} \ , \tag{4.61b}$$

$$\begin{aligned} c^{1,1,abc}_{B,XYZ}\Big|_{(c)} = \frac{-1}{8F_0^2}\sum_k \Big[& (\lambda^{k^2}\kappa_B)^{aa'}\delta^{bb'}\delta^{cc'} + (\kappa_B)^{aa'}\big((\lambda^{k^2})^{bb'}\delta^{cc'} + \delta^{bb'}(\lambda^{k^2})^{cc'}\big) \\ & + 2(-1)_X(-1)_Y(\lambda^k\kappa_B)^{aa'}(\lambda^k)^{bb'}\delta^{cc'} + 2(-1)_X(-1)_Z(\lambda^k\kappa_B)^{aa'}\delta^{bb'}(\lambda^k)^{cc'} \\ & + 2(-1)_Y(-1)_Z(\kappa_B)^{aa'}(\lambda^k)^{bb'}(\lambda^k)^{cc'}\Big]\varepsilon^{a'b'c'} I_{1,0}(m_l) \ , \end{aligned} \tag{4.61c}$$

$$\begin{aligned} c^{1,1,abc}_{B,XYZ}\Big|_{(d)} = \frac{-1}{4F_0^2}\sum_{k,\tilde{B}} \Big[& (-1)_X(\lambda^k\kappa_{\tilde{B}})^{aa'}\delta^{bb'}\delta^{cc'} + (-1)_Y(\kappa_{\tilde{B}})^{aa'}(\lambda^k)^{bb'}\delta^{cc'} \\ & + (-1)_Z(\kappa_{\tilde{B}})^{aa'}\delta^{bb'}(\lambda^k)^{cc'}\Big] \operatorname{tr}\left\{\kappa^T_{\tilde{B}}(D\{\lambda^k,\kappa_B\} + F[\lambda^k,\kappa_B])\right\} \\ \times \Big(I_{1,0}(m_k) + (m_B^2 - m_0^2)I_{1,1}(m_k,m_0,m_B) & - m_B(m_B+m_0)I^{(1)}_{1,1}(m_k,m_0,m_B)\Big) \ . \end{aligned} \tag{4.61d}$$

In the contribution from graph (d) commuting γ_5 from the vertex with the Dirac structure in the operator yields $\eta^5_{\Gamma^B,i}(-1)^{d^m_i} = -1$ (compare table 4.2). In operators of type $\mathcal{O}_{XR}$ the γ_5 has no effect owing to $\gamma_R\gamma_5 = \gamma_R$. The relative sign in the vertex in operators of type $\mathcal{O}_{\bar{X}L}$ is compensated by $\gamma_L\gamma_5 = -\gamma_L$. Therefore the result only contains structures of the form given in eq. (4.58). This is no coincidence but rather has to happen in order to obtain a result that behaves correctly under parity transformation. For the second order tree-level contributions we find

$$c^{2,1,abc}_{B,XYZ} = 4B_0 m_0^{-2}\operatorname{tr}\{\mathcal{M}\}(\kappa_B)^{aa'}\varepsilon^{a'bc} \ , \tag{4.61e}$$

$$c^{3,1,abc}_{B,XYZ} = 4B_0 m_0^{-2}(\kappa_B)^{aa'}\tilde{\mathcal{M}}^{bb'}\varepsilon^{a'b'c} \ . \tag{4.61f}$$

Using eq. (4.13) the matrix element of the complete three-quark operator reads

$$\begin{aligned} \langle 0|q^a_\alpha(a_1 n)q^b_\beta(a_2 n)q^c_\gamma(a_3 n)|B(p,s)\rangle = & \int [dx] e^{-i\,n\cdot p\sum_k x_k a_k} \\ \times \sum_i \Big(& \Gamma^{i,\mathrm{even}}_{\alpha\beta\gamma\delta} h^{i,abc}_{B,\mathrm{even}}(x_1,x_2,x_3) + \Gamma^{i,\mathrm{odd}}_{\alpha\beta\gamma\delta} h^{i,abc}_{B,\mathrm{odd}}(x_1,x_2,x_3) \\ & + \Gamma^{i,\mathrm{odd}}_{\gamma\alpha\beta\delta} h^{i,cab}_{B,\mathrm{odd}}(x_3,x_1,x_2) + \Gamma^{i,\mathrm{odd}}_{\beta\gamma\alpha\delta} h^{i,bca}_{B,\mathrm{odd}}(x_2,x_3,x_1)\Big) u^B_\delta(p,s) \ . \end{aligned} \tag{4.62}$$

4.4.3 Projection onto standard DAs

In this section we relate our parametrization of the baryon-to-vacuum matrix element, which was guided by the behavior under chiral rotations, to the general decomposition given in eq. (4.2), which is more convenient for daily use. To do so we have contracted both our result (eq. (4.62))

and eq. (4.2) with Dirac structures of the form $\Gamma^A_{\alpha\beta} \otimes \Gamma^B_{\gamma'\gamma}$. It is sufficient to use structures where Lorentz indices are either contracted between Γ^A and Γ^B or with the light-cone vector n or the momentum p. Afterwards we have used the identity $\not{p} u^B(p) = m_B u^B(p)$ and have matched the prefactors of the remaining Dirac structures (γ_5 and $\not{n}\gamma_5$). Using the twist-projection described in section 4.2, we obtain the results for the distribution amplitudes S_i^B, P_i^B, A_i^B, V_i^B and T_i^B. We have collected these lengthy matching relations in appendix C.5.

4.5 Results

In the following we present the results of the one-loop calculation. In section 4.5.1 we define a convenient set of distribution amplitudes, that optimally mirrors the constraints obtained for the limit of exact flavor symmetry. Furthermore, it allows us to present the flavor symmetry breaking and the dependence on the mean quark mass in a very compact and lucid form in sections 4.5.2 and 4.5.3. In section 4.5.4 we will delineate how one can parametrize baryon octet DAs in terms of shape parameters in order to make full use of $\mathrm{SU}(3)_f$ constraints and to allow for simple description of flavor symmetry breaking.

4.5.1 General strategy and choice of distribution amplitudes

We will split up every distribution amplitude in the following way:

$$\begin{aligned} \mathrm{DA}(\bar{m}_q, \delta m_l) &= \mathrm{DA}(\bar{m}_q, 0) + \big(\mathrm{DA}(\bar{m}_q, \delta m_l) - \mathrm{DA}(\bar{m}_q, 0)\big) \\ &\equiv \mathrm{DA}^\star(\bar{m}_q) + \Delta\mathrm{DA}(\bar{m}_q, \delta m_l) \ , \end{aligned} \tag{4.63a}$$

$$\begin{aligned} \mathrm{DA}^\star(\bar{m}_q) &= \mathrm{DA}^\star(0) + \big(\mathrm{DA}^\star(\bar{m}_q) - \mathrm{DA}^\star(0)\big) \\ &\equiv \mathrm{DA}^\circ + \Delta\mathrm{DA}^\star(\bar{m}_q) \ , \end{aligned} \tag{4.63b}$$

where the main idea is to use the second formula to parametrize everything in terms of the DAs at the symmetric point, which are measurable on the lattice as opposed to the amplitudes in the chiral limit. Lattice simulations where the mean quark mass is fixed at its physical value while δm_l is varied are already available for hadron masses and some form factors [158–160]. Corresponding simulations for the baryon octet DAs are presented in section 4.6 (cf. also our article [75]). This strategy has the additional advantage that one gets rid of the parameters that describe the behavior under variation of the mean quark mass. For the presentation of the results it turns out to be convenient to write down the second order tree-level and the loop contribution separately. We define for all baryons

$$\Delta\mathrm{DA} = \Delta\mathrm{DA}^{\mathrm{loop}} + \delta m \ \Delta\mathrm{DA}^{\mathrm{tree}} \ , \tag{4.64}$$

using the dimensionless parameter

$$\delta m = \frac{4 B_0 \delta m_l}{m_b^{\star\,2}} \doteq \frac{4(m_K^2 - m_\pi^2)}{3 X_b^2} \ , \tag{4.65}$$

where the average octet baryon mass X_b is defined by

$$X_b = \frac{1}{8}\big(2m_N + 3m_\Sigma + 2m_\Xi + m_\Lambda\big) \ . \tag{4.66}$$

Then we use the fact that we can rewrite ΔDA in terms of $m_b^\star$ and DA* using the corresponding expansions in $\bar{m}_q$. For a specific set of DAs, which do not mix under chiral extrapolation (see below), this allows us to rewrite the loop contribution as the DA along the symmetric line multiplied with a loop function f such that the results have the form

$$\mathrm{DA}(\bar{m}_q, \delta m_l) = \mathrm{DA}^\star(\bar{m}_q)(1+f) + \delta m \ \Delta\mathrm{DA}^{\mathrm{tree}} \ . \tag{4.67}$$

By virtue of SU(3)$_f$ symmetry we find the following relations between DAs along the line of symmetric quark masses $m_u = m_d = m_s$:

$$2T_{1/6}^{B\star}(x_1,x_2,x_3) = (-1)_B\big[V_{1/6}^{B\star} - A_{1/6}^{B\star}\big](x_1,x_3,x_2) + \big[V_{1/6}^{B\star} - A_{1/6}^{B\star}\big](x_2,x_3,x_1) \ , \tag{4.68a}$$

$$\begin{aligned} 2T_{2/5}^{B\star}(x_1,x_2,x_3) = {}& \big[T_{3/4}^{B\star} - T_{7/8}^{B\star} + S_{1/2}^{B\star} + P_{1/2}^{B\star}\big](x_3,x_1,x_2) \\ & + \big[T_{3/4}^{B\star} - T_{7/8}^{B\star} + S_{1/2}^{B\star} + P_{1/2}^{B\star}\big](x_3,x_2,x_1) \ , \end{aligned} \tag{4.68b}$$

$$\big[T_{3/4}^{B\star} + T_{7/8}^{B\star} + S_{1/2}^{B\star} - P_{1/2}^{B\star}\big](x_1,x_2,x_3) = \big[V_{2/5}^{B\star} - A_{2/5}^{B\star}\big](x_2,x_3,x_1) + \big[V_{3/4}^{B\star} - A_{3/4}^{B\star}\big](x_3,x_1,x_2) \ . \tag{4.68c}$$

Note that we do not impose these relations. They are automatically fulfilled by our calculation (loop contributions included). For the nucleon case these relations are known as isospin constraints, since they are fulfilled exactly also for $\delta m_l \neq 0$ owing to isospin symmetry (again this is also true for the loop contributions), which was already shown in ref. [76]. If we were only interested in the SU(3)$_f$ symmetric case (or in nucleons only), it would therefore be enough to define the independent amplitudes as

$$\Phi_{3/6}^B(x_1,x_2,x_3) = \big[V_{1/6}^B - A_{1/6}^B\big](x_1,x_2,x_3) \ , \tag{4.69a}$$

$$\Phi_{4/5}^B(x_1,x_2,x_3) = \big[V_{2/5}^B - A_{2/5}^B\big](x_1,x_2,x_3) \ , \tag{4.69b}$$

$$\Psi_{4/5}^B(x_1,x_2,x_3) = \big[V_{3/4}^B - A_{3/4}^B\big](x_1,x_2,x_3) \ , \tag{4.69c}$$

$$\Xi_{4/5}^B(x_1,x_2,x_3) = \big[T_{3/4}^B - T_{7/8}^B + S_{1/2}^B + P_{1/2}^B\big](x_1,x_2,x_3) \ , \tag{4.69d}$$

where the Φ_i^B and Ψ_i^B describe the coupling to chiral-odd operators, while the Ξ_i^B describe the chiral-even sector. The subscript indicates the twist. As it turns out the amplitudes Φ_i^B, Ψ_i^B and Ξ_i^B are not yet the optimal choice for a description of the complete baryon octet, since they mix under chiral extrapolation. Additionally one finds that it is very convenient to use differing definitions for the Λ, which we choose in such a way that the DAs of the Λ coincide with the DAs of the other octet baryons in the limit of equal quark masses. Therefore we define

$$\Phi_{\pm,3/6}^B(x_1,x_2,x_3) = \frac{c_B^\pm}{2}\big(\big[V_{1/6}^B - A_{1/6}^B\big](x_1,x_2,x_3) \pm \big[V_{1/6}^B - A_{1/6}^B\big](x_3,x_2,x_1)\big) \ , \tag{4.70a}$$

$$\Phi_{\pm,4/5}^B(x_1,x_2,x_3) = c_B^\pm\big(\big[V_{2/5}^B - A_{2/5}^B\big](x_1,x_2,x_3) \pm (-1)_B\big[V_{3/4}^B - A_{3/4}^B\big](x_2,x_3,x_1)\big) \ , \tag{4.70b}$$

$$\begin{aligned} \Xi_{\pm,4/5}^B(x_1,x_2,x_3) = 3(-1)_B c_B^\pm\big(& \big[T_{3/4}^B - T_{7/8}^B + S_{1/2}^B + P_{1/2}^B\big](x_1,x_2,x_3) \\ & \pm \big[T_{3/4}^B - T_{7/8}^B + S_{1/2}^B + P_{1/2}^B\big](x_1,x_3,x_2)\big) \ , \end{aligned} \tag{4.70c}$$

where

$$c_B^+ = \begin{cases} 1\,, & \text{for } B \neq \Lambda\,, \\ \sqrt{\frac{2}{3}}\,, & \text{for } B = \Lambda\,, \end{cases} \qquad c_B^- = \begin{cases} 1\,, & \text{for } B \neq \Lambda\,, \\ -\sqrt{6}\,, & \text{for } B = \Lambda\,. \end{cases} \tag{4.71}$$

Being interested in $\mathrm{SU}(3)_f$ violation one cannot use the constraints given in eq. (4.68) and therefore one needs six additional DAs. Our choices are (up to differing prefactors for the Λ and exchange of variables) the left-hand sides in eq. (4.68) since they coincide with the DAs in eq. (4.70) in the $\mathrm{SU}(3)_f$ symmetric limit. We define

$$\Pi^B_{3/6}(x_1,x_2,x_3) = c_B^-(-1)_B\; T^B_{1/6}(x_1,x_3,x_2)\;, \tag{4.72a}$$
$$\Pi^B_{4/5}(x_1,x_2,x_3) = c_B^-\big[T^B_{3/4} + T^B_{7/8} + S^B_{1/2} - P^B_{1/2}\big](x_3,x_1,x_2)\;, \tag{4.72b}$$
$$\Upsilon^B_{4/5}(x_1,x_2,x_3) = 6c_B^-\; T^B_{2/5}(x_3,x_2,x_1)\;, \tag{4.72c}$$

where the Π_i describe the chiral-odd sector, while the Υ_i describe the chiral-even part. For each octet baryon the standard DAs can be decomposed into the amplitudes defined in eqs. (4.70) and (4.72) (see appendix C.2). We find that the DAs for different nucleons, Σs and Ξs are related to each other exactly by isospin symmetry. Therefore we define

$$\mathrm{DA}^N \equiv \mathrm{DA}^p = -\mathrm{DA}^n\;, \tag{4.73a}$$
$$\mathrm{DA}^\Sigma \equiv \mathrm{DA}^{\Sigma^-} = -\mathrm{DA}^{\Sigma^+} = \sqrt{2}\mathrm{DA}^{\Sigma^0}\;, \tag{4.73b}$$
$$\mathrm{DA}^\Xi \equiv \mathrm{DA}^{\Xi^0} = -\mathrm{DA}^{\Xi^-}\;, \tag{4.73c}$$

and give all results only for DA^N, DA^Σ, DA^Ξ and DA^Λ. The relative signs between the different baryons depend on both the phase conventions shown in figure 2.3 (on page 20) and the choice of flavors within the definition of the DAs specified in eq. (4.12). In the $\mathrm{SU}(3)_f$ symmetric limit the DAs of all octet baryons can be related to each other:

$$\Phi^\star_{+,i} \equiv \Phi^{N\star}_{+,i} = \Phi^{\Sigma\star}_{+,i} = \Phi^{\Xi\star}_{+,i} = \Phi^{\Lambda\star}_{+,i} = \Pi_i^{N\star} = \Pi_i^{\Sigma\star} = \Pi_i^{\Xi\star}\;, \tag{4.74a}$$
$$\Phi^\star_{-,i} \equiv \Phi^{N\star}_{-,i} = \Phi^{\Sigma\star}_{-,i} = \Phi^{\Xi\star}_{-,i} = \Phi^{\Lambda\star}_{-,i} = \Pi_i^{\Lambda\star}\;, \tag{4.74b}$$
$$\Xi^\star_{+,i} \equiv \Xi^{N\star}_{+,i} = \Xi^{\Sigma\star}_{+,i} = \Xi^{\Xi\star}_{+,i} = \Xi^{\Lambda\star}_{+,i} = \Upsilon_i^{N\star} = \Upsilon_i^{\Sigma\star} = \Upsilon_i^{\Xi\star}\;, \tag{4.74c}$$
$$\Xi^\star_{-,i} \equiv \Xi^{N\star}_{-,i} = \Xi^{\Sigma\star}_{-,i} = \Xi^{\Xi\star}_{-,i} = \Xi^{\Lambda\star}_{-,i} = \Upsilon_i^{\Lambda\star}\;. \tag{4.74d}$$

In addition to the relation between different baryons, these equations contain all information included in the SU(3) constraints (4.68). Also the corresponding isospin constraints for the nucleon case

$$\Pi_i^N = \Phi^N_{+,i}\;, \qquad \Upsilon_i^N = \Xi^N_{+,i}\;, \tag{4.75}$$

have a very simple form.

To understand the physical meaning of these DAs it is instructive to work out their relation to light-front wave functions. For simplicity, we restrict ourselves to the leading twist approximation taking into account S-wave contributions only. In this case the helicities of the quarks sum up to

the helicity of the baryon (cf. refs. [100, 161]). Suppressing the transverse momentum dependence one finds, schematically,[2]

$$\begin{aligned}|(B\neq\Lambda)^{\uparrow}\rangle &= \int\frac{[dx]}{8\sqrt{6x_1x_2x_3}}|fgh\rangle\otimes\big\{[V_1+A_1]^B(x_1,x_2,x_3)|\downarrow\uparrow\uparrow\rangle+[V-A]^B(x_1,x_2,x_3)|\uparrow\downarrow\uparrow\rangle\\ &\qquad -2T_1^B(x_1,x_2,x_3)|\uparrow\uparrow\downarrow\rangle\big\}\\ &= \int\frac{[dx]}{8\sqrt{3x_1x_2x_3}}|\uparrow\uparrow\downarrow\rangle\otimes\big\{-\sqrt{3}\Phi^B_{+,3}(x_1,x_3,x_2)\big(|\mathrm{MS},B\rangle-\sqrt{2}|\mathrm{S},B\rangle\big)/3\\ &\qquad -\sqrt{3}\Pi_3^B(x_1,x_3,x_2)\big(2|\mathrm{MS},B\rangle+\sqrt{2}|\mathrm{S},B\rangle\big)/3\\ &\qquad +\Phi^B_{-,3}(x_1,x_3,x_2)|\mathrm{MA},B\rangle\big\}\,,\end{aligned}\tag{4.76}$$

and

$$\begin{aligned}|\Lambda^{\uparrow}\rangle &= \int\frac{[dx]}{4\sqrt{6x_1x_2x_3}}|uds\rangle\otimes\big\{[V_1+A_1]^\Lambda(x_1,x_2,x_3)|\downarrow\uparrow\uparrow\rangle+[V_1-A_1]^\Lambda(x_1,x_2,x_3)|\uparrow\downarrow\uparrow\rangle\\ &\qquad -2T_1^\Lambda(x_1,x_2,x_3)|\uparrow\uparrow\downarrow\rangle\big\}\\ &= \int\frac{[dx]}{8\sqrt{3x_1x_2x_3}}|\uparrow\uparrow\downarrow\rangle\otimes\big\{-\sqrt{3}\Phi^\Lambda_{+,3}(x_1,x_3,x_2)|\mathrm{MS},\Lambda\rangle\\ &\qquad +\Pi_3^\Lambda(x_1,x_3,x_2)\big(2|\mathrm{MA},\Lambda\rangle+\sqrt{2}|\mathrm{A},\Lambda\rangle\big)/3\\ &\qquad +\Phi^\Lambda_{-,3}(x_1,x_3,x_2)\big(|\mathrm{MA},\Lambda\rangle-\sqrt{2}|\mathrm{A},\Lambda\rangle\big)/3\big\}\,,\end{aligned}\tag{4.77}$$

where $|\uparrow\downarrow\uparrow\rangle$ etc. show quark helicities and $|fgh\rangle$ stands for the flavor ordering as specified in eq. (4.12). $|\mathrm{MS},B\rangle$ and $|\mathrm{MA},B\rangle$ are the usual mixed-symmetric and mixed-antisymmetric octet flavor wave functions, respectively (see tables 4.5 and 4.6). $|\mathrm{A},\Lambda\rangle$ and $|\mathrm{S},B\neq\Lambda\rangle$ are totally antisymmetric and symmetric flavor wave functions (see tables 4.4 and 4.7), which only occur in the octet if SU(3) symmetry is broken. From this representation it becomes obvious that V_1^B, A_1^B and T_1^B are convenient DAs if one sorts the quarks with respect to their flavor, while $\Phi^B_{+,3}$, $\Phi^B_{-,3}$ and Π_3^B correspond to three distinct flavor structures in a helicity-ordered wave function. Their meaning becomes even clearer if one analyzes the flavor symmetric point, where $\Phi^\star_{+,3}$ and $\Phi^\star_{-,3}$ isolate the mixed-symmetric and mixed-antisymmetric flavor wave functions:

$$|B^{\uparrow}\rangle^\star = \int\frac{[dx]}{8\sqrt{3x_1x_2x_3}}|\uparrow\uparrow\downarrow\rangle\otimes\big\{-\sqrt{3}\Phi^\star_{+,3}(x_1,x_3,x_2)|\mathrm{MS},B\rangle+\Phi^\star_{-,3}(x_1,x_3,x_2)|\mathrm{MA},B\rangle\big\}\,.\tag{4.78}$$

4.5.2 Flavor symmetry breaking

The DAs introduced in section 4.5.1 have been chosen such that one can make full use of SU(3) flavor symmetry. In this section we will provide a detailed description of SU(3) breaking based on our leading one-loop BChPT analysis in section 4.4, which allows us to understand the octet structure of the distribution amplitudes. For the time being we will keep the mean quark mass fixed in order to isolate the SU(3) breaking effects. The nontrivial dependence on the mean

[2] The formulas have been worked out in collaboration with M. Gruber; cf. also ref. [75].

Table 4.4: Totally antisymmetric (A) flavor wave functions.

B	$\lvert \mathrm{A}, B\rangle$
Λ	$(\lvert dus\rangle - \lvert uds\rangle + \lvert usd\rangle - \lvert dsu\rangle + \lvert sdu\rangle - \lvert sud\rangle)/\sqrt{6}$

Table 4.5: Mixed-symmetric (MS) flavor wave functions.

B	$\lvert \mathrm{MS}, B\rangle$
N	$(2\lvert uud\rangle - \lvert udu\rangle - \lvert duu\rangle)/\sqrt{6}$
Σ	$(2\lvert dds\rangle - \lvert dsd\rangle - \lvert sdd\rangle)/\sqrt{6}$
Ξ	$(2\lvert ssu\rangle - \lvert sus\rangle - \lvert uss\rangle)/\sqrt{6}$
Λ	$(\lvert dsu\rangle - \lvert usd\rangle + \lvert sdu\rangle - \lvert sud\rangle)/2$

Table 4.6: Mixed-antisymmetric (MA) flavor wave functions.

B	$\lvert \mathrm{MA}, B\rangle$
N	$(\lvert udu\rangle - \lvert duu\rangle)/\sqrt{2}$
Σ	$(\lvert dsd\rangle - \lvert sdd\rangle)/\sqrt{2}$
Ξ	$(\lvert sus\rangle - \lvert uss\rangle)/\sqrt{2}$
Λ	$(2\lvert dus\rangle - 2\lvert uds\rangle + \lvert dsu\rangle - \lvert usd\rangle + \lvert sud\rangle - \lvert sdu\rangle)/\sqrt{12}$

Table 4.7: Totally symmetric (S) flavor wave functions.

B	$\lvert \mathrm{S}, B\rangle$
N	$(\lvert uud\rangle + \lvert udu\rangle + \lvert duu\rangle)/\sqrt{3}$
Σ	$(\lvert dds\rangle + \lvert dsd\rangle + \lvert sdd\rangle)/\sqrt{3}$
Ξ	$(\lvert ssu\rangle + \lvert sus\rangle + \lvert uss\rangle)/\sqrt{3}$

quark mass will be presented in section 4.5.3. Based on our convenient choice of distribution amplitudes (see eqs. (4.70) and (4.72)), the result can be presented in a very compact form:

$$\Phi^B_{\pm,i} = \Phi^\star_{\pm,i}\Big(1 + \tfrac{1}{2}\Delta\Sigma'_B + \Delta g^B_{\Phi\pm}\Big) + \delta m\ \Delta\Phi^B_{\pm,i}\ , \tag{4.79a}$$

$$\Xi^B_{\pm,i} = \Xi^\star_{\pm,i}\Big(1 + \tfrac{1}{2}\Delta\Sigma'_B + \Delta g^B_{\Xi}\Big) + \delta m\ \Delta\Xi^B_{\pm,i}\ , \tag{4.79b}$$

$$\Pi^B_{i} = \Phi^\star_{\pm_B,i}\Big(1 + \tfrac{1}{2}\Delta\Sigma'_B + \Delta g^B_{\Pi}\Big) + \delta m\ \Delta\Pi^B_{i}\ , \tag{4.79c}$$

$$\Upsilon^B_{i} = \Xi^\star_{\pm_B,i}\Big(1 + \tfrac{1}{2}\Delta\Sigma'_B + \Delta g^B_{\Xi}\Big) + \delta m\ \Delta\Upsilon^B_{i}\ , \tag{4.79d}$$

where "$\pm_B$" stands for "+" if $B \neq \Lambda$ and for "−" if $B = \Lambda$. The second term in the equations above originates from quark mass insertions, while the first term (or, to be more precise, $\Delta\Sigma'_B$ and Δg^B_{DA}) is generated by meson loops and contains chiral logarithms. Owing to our choice of DAs the functions Δg^B_{DA}, which are listed in appendix C.1 together with $\Delta\Sigma'_B$, do not depend on the twist of the amplitude. Both Δg^B_{DA} and $\Delta\Sigma'_B$ vanish for equal quark masses ($\delta m = 0$) such that $\Phi^\star_{\pm,i}$ and $\Xi^\star_{\pm,i}$ are the amplitudes in the flavor symmetric limit. It is important

that the nonanalytic terms do not depend on the quark momentum fractions. The remaining quantities $\Phi^\star_{\pm,i}$, $\Xi^\star_{\pm,i}$, $\Delta\Phi^B_{\pm,i}$, $\Delta\Xi^B_{\pm,i}$, $\Delta\Pi^B_i$ and $\Delta\Upsilon^B_i$ play the role of low-energy constants, meaning that they are independent of δm.[3] However, note that they still depend on x_1, x_2, x_3 and their functional forms cannot be predicted by an effective low-energy theory. Our calculation imposes, however, certain relations between the DAs which originate from higher order tree-level contributions and parametrize the SU(3) breaking. It holds

$$\Delta\mathrm{DA}^\Xi = -\Delta\mathrm{DA}^N - \Delta\mathrm{DA}^\Sigma \ . \tag{4.80}$$

Furthermore, the amplitudes $\Delta\Pi^B_i$ and $\Delta\Upsilon^B_i$ can be expressed in terms of $\Delta\Phi^B_{\pm,i}$ and $\Delta\Xi^B_{\pm,i}$:

$$\Delta\Pi^N_i = \Delta\Phi^N_{+,i} \ , \qquad \Delta\Upsilon^N_i = \Delta\Xi^N_{+,i} \ , \tag{4.81a}$$

$$\Delta\Pi^\Sigma_i = -\frac{1}{2}\Delta\Phi^\Sigma_{+,i} - \frac{3}{2}\Delta\Phi^\Lambda_{+,i} \ , \qquad \Delta\Upsilon^\Sigma_i = -\frac{1}{2}\Delta\Xi^\Sigma_{+,i} - \frac{3}{2}\Delta\Xi^\Lambda_{+,i} \ , \tag{4.81b}$$

$$\Delta\Pi^\Lambda_i = -\frac{1}{2}\Delta\Phi^\Lambda_{-,i} - \frac{3}{2}\Delta\Phi^\Sigma_{-,i} \ , \qquad \Delta\Upsilon^\Lambda_i = -\frac{1}{2}\Delta\Xi^\Lambda_{-,i} - \frac{3}{2}\Delta\Xi^\Sigma_{-,i} \ , \tag{4.81c}$$

which means that the Π^B_i and Υ^B_i are completely fixed by the other amplitudes. The divergences of leading one-loop order contained in $\Delta\Sigma'_B$ and Δg^B_{DA} can be canceled by the introduction of counterterms

$$\Delta\Phi^B_{\pm,i} \longrightarrow \frac{m_b^{\star 2} c^B_{\Phi\pm}}{24F_\star^2}\Phi^\star_{\pm,i}L + \Delta\Phi^{B,\mathrm{ren.}}_{\pm,i}(\mu) \ , \tag{4.82a}$$

$$\Delta\Xi^B_{\pm,i} \longrightarrow \frac{m_b^{\star 2} c^B_{\Xi}}{24F_\star^2}\Xi^\star_{\pm,i}L + \Delta\Xi^{B,\mathrm{ren.}}_{\pm,i}(\mu) \ , \tag{4.82b}$$

where L contains the divergence and the typical constants of the modified minimal subtraction scheme (see eq. (A.28)). $F_\star$ is the meson decay constant in the $\mathrm{SU}(3)_f$ symmetric limit. The coefficients c^B_{DA} are given by

$$c^N_{\Phi\pm} = -9(D^2 + 10DF - 3F^2) - 23 \mp 24 \ , \tag{4.83a}$$

$$c^\Sigma_{\Phi\pm} = 18(D^2 - 3F^2) + 10 \pm 12 \ , \tag{4.83b}$$

$$c^\Lambda_{\Phi\pm} = -18(D^2 - 3F^2) - 26 \pm 12 \ , \tag{4.83c}$$

$$c^N_{\Xi} = -9(D^2 + 10DF - 3F^2) + 9 \ , \tag{4.83d}$$

$$c^\Sigma_{\Xi} = -c^\Lambda_{\Xi} = 18(D^2 - 3F^2) - 18 \ . \tag{4.83e}$$

Note that we give no values for $c^\Xi_{\Phi\pm}$ and c^Ξ_Ξ, since the renormalization of the corresponding amplitudes is already fixed via eq. (4.80). The renormalized amplitudes acquire a dependence on the chiral renormalization scale μ, which exactly cancels the scale dependence of the leading chiral logarithms:

$$\mu\frac{\partial}{\partial\mu}\Delta\Phi^{B,\mathrm{ren.}}_{\pm,i}(\mu) = \frac{-1}{(4\pi)^2}\frac{m_b^{\star 2} c^B_{\Phi\pm}}{24F_\star^2}\Phi^\star_{\pm,i} \ , \tag{4.84a}$$

$$\mu\frac{\partial}{\partial\mu}\Delta\Xi^{B,\mathrm{ren.}}_{\pm,i}(\mu) = \frac{-1}{(4\pi)^2}\frac{m_b^{\star 2} c^B_{\Xi}}{24F_\star^2}\Xi^\star_{\pm,i} \ . \tag{4.84b}$$

[3] The flavor symmetric amplitudes actually still depend on the mean quark mass (cf. section 4.5.3) and can therefore only be called constant as long as the mean quark mass is kept fixed.

The replacements given in eq. (4.82) also have to cancel the divergences in the distribution amplitudes for the Ξ baryon and the Π_i^B and Υ_i^B distribution amplitudes, which is the case and can be seen as a nontrivial check of our calculation. The higher order divergences, which are contained in our result as a consequence of using IR regularization [86], have to be set to zero by hand. This introduces an unphysical scale dependence in higher order terms, which is usually solved by fixing the scale at a typical hadronic value like 1 GeV. A variation of this scale within reasonable bounds, say between 0.8 GeV and 1.2 GeV, can be used to estimate higher order effects.

If we neglect higher order contributions, we can rewrite eqs. (4.79) in such a way that the complete nonanalytic behavior is encoded in an overall prefactor:

$$\Phi_{\pm,i}^B \doteq \sqrt{\frac{Z_B}{Z^\star}}\Big(1+\Delta g_{\Phi\pm}^B\Big)\Big(\Phi_{\pm,i}^\star + \delta m\ \Delta\Phi_{\pm,i}^B\Big)\ , \tag{4.85a}$$

$$\Xi_{\pm,i}^B \doteq \sqrt{\frac{Z_B}{Z^\star}}\Big(1+\Delta g_{\Xi}^B\Big)\Big(\Xi_{\pm,i}^\star + \delta m\ \Delta\Xi_{\pm,i}^B\Big)\ , \tag{4.85b}$$

$$\Pi_i^B \doteq \sqrt{\frac{Z_B}{Z^\star}}\Big(1+\Delta g_{\Pi}^B\Big)\Big(\Phi_{\pm_B,i}^\star + \delta m\ \Delta\Pi_i^B\Big)\ , \tag{4.85c}$$

$$\Upsilon_i^B \doteq \sqrt{\frac{Z_B}{Z^\star}}\Big(1+\Delta g_{\Xi}^B\Big)\Big(\Xi_{\pm_B,i}^\star + \delta m\ \Delta\Upsilon_i^B\Big)\ , \tag{4.85d}$$

where

$$\sqrt{\frac{Z_B}{Z^\star}} \doteq 1+\frac{1}{2}\Delta\Sigma_B'\ . \tag{4.86}$$

From eq. (4.85) it follows directly that at leading one-loop order the complete nonanalytic structure is contained in the normalization of the distribution amplitudes, while their shape only exhibits the simple dependence on δm shown in eq. (4.92). Therefore leading finite volume effects do only affect the normalization. We want to emphasize that this is only true by virtue of our specific choice of DAs. A similar behavior was found for the meson sector (see refs. [162, 163]).

The zeroth moments of the given DAs are not independent, due to eq. (4.40). In particular all DAs which correspond to operators of certain symmetry classes are normalized by the same wave function normalization constants independent of the twist of the corresponding amplitude. The zeroth moments of the distribution amplitudes define the following normalization constants:

$$f^B = \int [dx]\Phi_{+,i}^B(x_1,x_2,x_3) = \sqrt{\frac{Z_B}{Z^\star}}\Big(1+\Delta g_{\Phi+}^B\Big)\Big(f^\star + \delta m\ \Delta f^B\Big)\ , \tag{4.87a}$$

$$\lambda_1^B = \int [dx]\Phi_{-,4/5}^B(x_1,x_2,x_3) = \sqrt{\frac{Z_B}{Z^\star}}\Big(1+\Delta g_{\Phi-}^B\Big)\Big(\lambda_1^\star + \delta m\ \Delta\lambda_1^B\Big)\ , \tag{4.87b}$$

$$\lambda_2^B = \int [dx]\Xi_{+,4/5}^B(x_1,x_2,x_3) = \sqrt{\frac{Z_B}{Z^\star}}\Big(1+\Delta g_{\Xi}^B\Big)\Big(\lambda_2^\star + \delta m\ \Delta\lambda_2^B\Big)\ , \tag{4.87c}$$

and

$$f_T^{B\neq\Lambda} = \int [dx]\Pi_i^B(x_1,x_2,x_3) = \sqrt{\frac{Z_B}{Z^\star}}\Big(1+\Delta g_{\Pi}^B\Big)\Big(f^\star + \delta m\ \Delta f_T^B\Big)\ , \tag{4.87d}$$

$$\lambda_T^\Lambda = \int [dx]\Pi_{4/5}^\Lambda(x_1,x_2,x_3) = \sqrt{\frac{Z_\Lambda}{Z^\star}}\Big(1+\Delta g_{\Pi}^\Lambda\Big)\Big(\lambda_1^\star + \delta m\ \Delta\lambda_T^\Lambda\Big)\ , \tag{4.87e}$$

where $f_T^N = f^N$ due to isospin symmetry. For N, Σ and Ξ the chiral-even higher twist normalization constant λ_2 also normalizes Υ_i^B:

$$\lambda_2^{B\neq\Lambda} = \int [dx] \Upsilon_{4/5}^B(x_1, x_2, x_3) \ . \tag{4.87f}$$

The remaining zeroth moments vanish by construction

$$\begin{aligned} 0 &= \int [dx] \Phi_{-,3/6}^B(x_1, x_2, x_3) = \int [dx] \Xi_{-,4/5}^B(x_1, x_2, x_3) \\ &= \int [dx] \Pi_{3/6}^\Lambda(x_1, x_2, x_3) = \int [dx] \Upsilon_{4/5}^\Lambda(x_1, x_2, x_3) \ . \end{aligned} \tag{4.87g}$$

In the equations above we have introduced convenient new definitions of f^Λ, λ_1^Λ, λ_2^Λ, f_T^Σ, f_T^Ξ and λ_T^Λ such that, in the limit of exact SU(3) flavor symmetry,

$$f^\star = f^{N\star} = f^{\Sigma\star} = f^{\Xi\star} = f^{\Lambda\star} = f_T^{\Sigma\star} = f_T^{\Xi\star} \ , \tag{4.88a}$$

$$\lambda_1^\star = \lambda_1^{N\star} = \lambda_1^{\Sigma\star} = \lambda_1^{\Xi\star} = \lambda_1^{\Lambda\star} = \lambda_T^{\Lambda\star}, \tag{4.88b}$$

$$\lambda_2^\star = \lambda_2^{N\star} = \lambda_2^{\Sigma\star} = \lambda_2^{\Xi\star} = \lambda_2^{\Lambda\star} \ . \tag{4.88c}$$

If the reader favors a different definition he or she can easily read off the conversion factor from eq. (4.70), noting that additional signs can arise from eq. (4.73) if one uses different baryons for the definition of the distribution amplitudes, and that one has to take into account additional factors originating from differing definitions of S_i, P_i, V_i, A_i and T_i (we use the definitions given in section 4.2, which is equivalent to the definitions of ref. [76]). We have performed this matching procedure for the constants defined in refs. [76, 150] (see appendix C.3). In principle f_T^Σ, f_T^Ξ and λ_T^Λ given above are additional independent normalization constants. However, knowing about the structure of SU(3) breaking it is clear that they are (at leading one-loop accuracy) completely fixed by f^B and λ_1^B, since

$$\begin{aligned} \Delta f_T^\Sigma &= -\frac{3}{2}\Delta f^\Lambda - \frac{1}{2}\Delta f^\Sigma \ , & \Delta f_T^\Xi &= \frac{3}{2}\Delta f^\Lambda + \frac{1}{2}\Delta f^\Sigma - \Delta f^N \ , \\ \Delta \lambda_T^\Lambda &= -\frac{1}{2}\Delta \lambda_1^\Lambda - \frac{3}{2}\Delta \lambda_1^\Sigma \ , \end{aligned} \tag{4.89}$$

due to eq. (4.81). $f^\star$, Δf^B, $\lambda_i^\star$ and $\Delta\lambda_i^B$ are given by

$$f^\star = \int [dx] \Phi_{+,i}^\star(x_1, x_2, x_3) \ , \qquad \Delta f^B = \int [dx] \Delta\Phi_{+,i}^B(x_1, x_2, x_3) \ , \tag{4.90a}$$

$$\lambda_1^\star = \int [dx] \Phi_{-,4/5}^\star(x_1, x_2, x_3) \ , \qquad \Delta \lambda_1^B = \int [dx] \Delta\Phi_{-,4/5}^B(x_1, x_2, x_3) \ , \tag{4.90b}$$

$$\lambda_2^\star = \int [dx] \Xi_{+,4/5}^\star(x_1, x_2, x_3) \ , \qquad \Delta \lambda_2^B = \int [dx] \Delta\Xi_{+,4/5}^B(x_1, x_2, x_3) \ , \tag{4.90c}$$

where, as a consequence of eq. (4.80) (first line) and eq. (4.40) (second line) one has

$$\begin{aligned} &\Delta f^\Xi = -\Delta f^\Sigma - \Delta f^N \ , \qquad \Delta \lambda_1^\Xi = -\Delta \lambda_1^\Sigma - \Delta \lambda_1^N \ , \qquad \Delta \lambda_2^\Xi = -\Delta \lambda_2^\Sigma - \Delta \lambda_2^N \ , \\ &\Delta \lambda_2^\Lambda = -\Delta \lambda_2^\Sigma \ . \end{aligned} \tag{4.91}$$

As mentioned above, the zeroth moments of $\Phi^B_{-,3/6}$ and $\Pi^\Lambda_{3/6}$ ($\Xi^B_{-,4/5}$ and $\Upsilon^\Lambda_{4/5}$) vanish by construction, since they are antisymmetric under exchange of x_1 and x_3 (x_2 and x_3). One possible approach would be to normalize these amplitudes by their first moments. However, our main goal is to divide the DAs by normalization constants in such a way that the nonanalytic prefactor is canceled. This can be achieved without the definition of additional constants, since all prefactors present in eqs. (4.85) also occur in eqs. (4.87). Explicitly, one can consider the ratios

$$\frac{\Phi^B_{+,i}}{f^B} = \frac{\Phi^\star_{+,i} + \delta m\ \Delta\Phi^B_{+,i}}{f^\star + \delta m\ \Delta f^B}\ , \qquad \frac{\Phi^B_{-,i}}{\lambda^B_1} = \frac{\Phi^\star_{-,i} + \delta m\ \Delta\Phi^B_{-,i}}{\lambda^\star_1 + \delta m\ \Delta\lambda^B_1}\ , \tag{4.92a}$$

$$\frac{\Pi^{B\neq\Lambda}_i}{f^{B\neq\Lambda}_T} = \frac{\Phi^\star_{+,i} + \delta m\ \Delta\Pi^B_i}{f^\star + \delta m\ \Delta f^B_T}\ , \qquad \frac{\Pi^\Lambda_i}{\lambda^\Lambda_T} = \frac{\Phi^\star_{-,i} + \delta m\ \Delta\Pi^\Lambda_i}{\lambda^\star_1 + \delta m\ \Delta\lambda^\Lambda_T}\ , \tag{4.92b}$$

$$\frac{\Xi^B_{\pm,i}}{\lambda^B_2} = \frac{\Xi^\star_{\pm,i} + \delta m\ \Delta\Xi^B_{\pm,i}}{\lambda^\star_2 + \delta m\ \Delta\lambda^B_2}\ , \qquad \frac{\Upsilon^B_i}{\lambda^B_2} = \frac{\Xi^\star_{\pm_B,i} + \delta m\ \Delta\Upsilon^B_i}{\lambda^\star_2 + \delta m\ \Delta\lambda^B_2}\ . \tag{4.92c}$$

The idea behind the latter choice is to normalize all DAs with similar behavior under chiral extrapolation (including the ones with vanishing zeroth moment) with the same normalization constant containing the complete nonanalytic behavior. In this way one obtains a one-to-one correspondence between a normalization constant and a certain chiral behavior. Note that, following this argument, some of the moments of the leading twist DA Φ^B_3 should be normalized with λ^B_1 instead of f^B. Otherwise the chiral logarithms do not cancel.

Combining eqs. (4.80) and (4.81) with the explicit functional form of the nonanalytic prefactor in eq. (4.85) one can find specific linear combinations of DAs for which all terms linear in δm cancel so that the SU(3) breaking is minimized (cf. also our work [75]). Similar combinations exist for the baryon masses:

$$0 + \mathcal{O}(\delta m^2) = 2m_N - m_\Sigma + 2m_\Xi - 3m_\Lambda\ , \tag{4.93a}$$

$$8m^\star_b + \mathcal{O}(\delta m^2) = 2m_N + 3m_\Sigma + 2m_\Xi + m_\Lambda\ . \tag{4.93b}$$

The first relation is the famous Gell-Mann–Okubo (GMO) sum rule for baryon masses [164], whose almost exact realization in nature is widely known. The second one cannot be checked for the physical masses since it depends on $m^\star_b$, the baryon mass at the flavor symmetric point, which is inherently inaccessible in experiment. The analogous expressions for the distribution amplitudes in the chiral-odd sector read:

$$0 + \mathcal{O}(\delta m^2) = \Phi^\Sigma_{+,i} - \Pi^\Sigma_i + \Phi^\Xi_{+,i} - \Pi^\Xi_i\ , \tag{4.94a}$$

$$8\cdot 3\Phi^\star_{+,i} + \mathcal{O}(\delta m^2) = 2\cdot 3\Phi^N_{+,i} + 3\cdot(\Phi^\Sigma_{+,i} + 2\Pi^\Sigma_i) + 2\cdot(\Phi^\Xi_{+,i} + 2\Pi^\Xi_i) + 1\cdot 3\Phi^\Lambda_{+,i}\ , \tag{4.94b}$$

$$8\cdot 3\Phi^\star_{-,i} + \mathcal{O}(\delta m^2) = 2\cdot 3\Phi^N_{-,i} + 3\cdot 3\Phi^\Sigma_{-,i} + 2\cdot 3\Phi^\Xi_{-,i} + 1\cdot(\Phi^\Lambda_{-,i} + 2\Pi^\Lambda_i)\ . \tag{4.94c}$$

For the chiral-even distribution amplitudes the relations have the same form:

$$0 + \mathcal{O}(\delta m^2) = \Xi^\Sigma_{+,i} - \Upsilon^\Sigma_i + \Xi^\Xi_{+,i} - \Upsilon^\Xi_i\ , \tag{4.95a}$$

$$8\cdot 3\Xi^\star_{+,i} + \mathcal{O}(\delta m^2) = 2\cdot 3\Xi^N_{+,i} + 3\cdot(\Xi^\Sigma_{+,i} + 2\Upsilon^\Sigma_i) + 2\cdot(\Xi^\Xi_{+,i} + 2\Upsilon^\Xi_i) + 1\cdot 3\Xi^\Lambda_{+,i}\ , \tag{4.95b}$$

$$8\cdot 3\Xi^\star_{-,i} + \mathcal{O}(\delta m^2) = 2\cdot 3\Xi^N_{-,i} + 3\cdot 3\Xi^\Sigma_{-,i} + 2\cdot 3\Xi^\Xi_{-,i} + 1\cdot(\Xi^\Lambda_{-,i} + 2\Upsilon^\Lambda_i)\ . \tag{4.95c}$$

Eqs. (4.94a) and (4.95a) are similar to the GMO sum rule with respect to the property that they do not depend explicitly on the value in the flavor symmetric limit. This might explain why they are fulfilled to high accuracy by the lattice data, see section 4.6.

4.5.3 Dependence on the mean quark mass

The distribution amplitudes $\Phi^\star_{\pm,i}$ and $\Xi^\star_{\pm,i}$ have a nontrivial dependence on the mean quark mass $\bar{m}_q$. This is not really interesting from a phenomenological point of view, since the number of independent distribution amplitudes cannot be further reduced compared to eq. (4.85), even if one expands everything around the chiral limit. However, the dependence is of importance for the analysis of lattice data if one wants to include data points from simulations with unphysical mean quark mass. The mass dependence reads

$$\Phi^\star_{\pm,i} = \Phi^\circ_{\pm,i}\Big(1 + \tfrac{1}{2}\Sigma'^\star + g^\star_{\Phi\pm}\Big) + \bar{m}\Delta\Phi^\star_{\pm,i} \ , \tag{4.96a}$$

$$\Xi^\star_{\pm,i} = \Xi^\circ_{\pm,i}\Big(1 + \tfrac{1}{2}\Sigma'^\star + g^\star_{\Xi}\Big) + \bar{m}\Delta\Xi^\star_{\pm,i} \ , \tag{4.96b}$$

where

$$\bar{m} = \frac{12B_0\bar{m}_q}{m_b^{\star\,2}} \ . \tag{4.97}$$

$g^\star_{\Phi\pm}$, $g^\star_{\Xi}$ and $\Sigma'^\star$ are functions of the mean quark mass that can be taken from appendix C.1. The divergences occurring at linear order in the mean quark mass can be canceled via the following introduction of counterterms

$$\Delta\Phi^\star_{\pm,i} \longrightarrow \frac{m_b^{\star\,2}c^\star_{\Phi\pm}}{24F_\star^2}\Phi^\circ_{\pm,i}L + \Delta\Phi^{\star,\text{ren.}}_{\pm,i}(\mu) \ , \tag{4.98a}$$

$$\Delta\Xi^\star_{\pm,i} \longrightarrow \frac{m_b^{\star\,2}c^\star_{\Xi}}{24F_\star^2}\Xi^\circ_{\pm,i}L + \Delta\Xi^{\star,\text{ren.}}_{\pm,i}(\mu) \ , \tag{4.98b}$$

where L contains the divergence (see appendix C.1) and the coefficients are

$$c^\star_{\Phi\pm} = \frac{4}{3}\big(6(5D^2+9F^2) + 13 \pm 6\big) \ , \tag{4.99a}$$

$$c^\star_{\Xi} = \frac{4}{3}\big(6(5D^2+9F^2) + 9\big) \ . \tag{4.99b}$$

This leads to the following scale dependence in the renormalized amplitudes:

$$\mu\frac{\partial}{\partial\mu}\Delta\Phi^{\star,\text{ren.}}_{\pm,i}(\mu) = \frac{-1}{(4\pi)^2}\frac{m_b^{\star\,2}c^\star_{\Phi\pm}}{24F_\star^2}\Phi^\circ_{\pm,i} \ , \tag{4.100a}$$

$$\mu\frac{\partial}{\partial\mu}\Delta\Xi^{\star,\text{ren.}}_{\pm,i}(\mu) = \frac{-1}{(4\pi)^2}\frac{m_b^{\star\,2}c^\star_{\Xi}}{24F_\star^2}\Xi^\circ_{\pm,i} \ . \tag{4.100b}$$

The divergences occurring together with higher orders of the quark masses have to be canceled by hand as discussed in section 4.5.2.

If one wants to take into account the mean quark mass dependence one needs the complete leading one-loop BChPT result, that describes all possible values of light and strange quark

masses, instead of the simplified extrapolation formulas given in section 4.5.2, which describe only the SU(3) symmetry breaking. The full result reads

$$\Phi^B_{\pm,i} = \Phi^\circ_{\pm,i}\Big(1 + \tfrac{1}{2}\Sigma'^\star + \tfrac{1}{2}\Delta\Sigma'_B + g^\star_{\Phi\pm} + \Delta g^B_{\Phi\pm}\Big) + \bar{m}\ \Delta\Phi^\star_{\pm,i} + \delta m\ \Delta\Phi^B_{\pm,i}\ , \tag{4.101a}$$

$$\Xi^B_{\pm,i} = \Xi^\circ_{\pm,i}\Big(1 + \tfrac{1}{2}\Sigma'^\star + \tfrac{1}{2}\Delta\Sigma'_B + g^\star_{\Xi} + \Delta g^B_{\Xi}\Big) + \bar{m}\ \Delta\Xi^\star_{\pm,i} + \delta m\ \Delta\Xi^B_{\pm,i}\ , \tag{4.101b}$$

$$\Pi^B_{i} = \Phi^\circ_{\pm_B,i}\Big(1 + \tfrac{1}{2}\Sigma'^\star + \tfrac{1}{2}\Delta\Sigma'_B + g^\star_{\Phi\pm_B} + \Delta g^B_{\Pi}\Big) + \bar{m}\ \Delta\Phi^\star_{\pm_B,i} + \delta m\ \Delta\Pi^B_{i}\ , \tag{4.101c}$$

$$\Upsilon^B_{i} = \Xi^\circ_{\pm_B,i}\Big(1 + \tfrac{1}{2}\Sigma'^\star + \tfrac{1}{2}\Delta\Sigma'_B + g^\star_{\Xi} + \Delta g^B_{\Xi}\Big) + \bar{m}\ \Delta\Xi^\star_{\pm_B,i} + \delta m\ \Delta\Upsilon^B_{i}\ , \tag{4.101d}$$

where, as defined above, "$\pm_B$" stands for "+" if $B \neq \Lambda$ and for "−" if $B = \Lambda$. The Z-factor contributions $\Sigma'^\star$ and $\Delta\Sigma'_B$, as well as the other loop contributions $g^\star_{\mathrm{DA}}$ and Δg^B_{DA} can be found in appendix C.1. Note that all loop contributions are zero for vanishing quark masses, such that the chiral limit value of the chiral-odd and chiral-even DAs is given by $\Phi^\circ_{\pm,i}$ and $\Xi^\circ_{\pm,i}$. The DAs originating from the next-to-leading tree-level contributions in the BChPT calculation parametrize the dependence on the mean quark mass ($\Delta\Phi^\star_{\pm_B,i}$ and $\Delta\Xi^\star_{\pm_B,i}$) and the SU(3) symmetry breaking ($\Delta\Phi^B_{\pm,i}$, $\Delta\Pi^B_i$, $\Delta\Xi^B_{\pm,i}$ and $\Delta\Upsilon^B_i$). The latter obey the constraints given in eqs. (4.80) and (4.81). The distribution amplitudes in the chiral limit and the ones describing the quark mass dependence are low-energy constants, i.e., they do not depend on quark masses. However, they are functions of the momentum fractions x_1, x_2 and x_3. The parametrization of their functional form is (aside from the constraints in the flavor symmetric limit and the constraints on the symmetry breaking) orthogonal to the BChPT calculation and will be discussed in section 4.5.4.

Similar to the fixed mean quark mass case one can rewrite the result in a factorized form, if one ignores terms that lie beyond leading one-loop accuracy. The resulting extrapolation formulas, which are analogous to eq. (4.85), read

$$\Phi^B_{\pm,i} \doteq \sqrt{Z_B}\Big(1 + g^\star_{\Phi\pm} + \Delta g^B_{\Phi\pm}\Big)\Big(\Phi^\circ_{\pm,i} + \bar{m}\ \Delta\Phi^\star_{\pm,i} + \delta m\ \Delta\Phi^B_{\pm,i}\Big)\ , \tag{4.102a}$$

$$\Xi^B_{\pm,i} \doteq \sqrt{Z_B}\Big(1 + g^\star_{\Xi} + \Delta g^B_{\Xi}\Big)\Big(\Xi^\circ_{\pm,i} + \bar{m}\ \Delta\Xi^\star_{\pm,i} + \delta m\ \Delta\Xi^B_{\pm,i}\Big)\ , \tag{4.102b}$$

$$\Pi^B_{i} \doteq \sqrt{Z_B}\Big(1 + g^\star_{\Phi\pm_B} + \Delta g^B_{\Pi}\Big)\Big(\Phi^\circ_{\pm_B,i} + \bar{m}\ \Delta\Phi^\star_{\pm_B,i} + \delta m\ \Delta\Pi^B_{i}\Big)\ , \tag{4.102c}$$

$$\Upsilon^B_{i} \doteq \sqrt{Z_B}\Big(1 + g^\star_{\Xi} + \Delta g^B_{\Xi}\Big)\Big(\Xi^\circ_{\pm_B,i} + \bar{m}\ \Delta\Xi^\star_{\pm_B,i} + \delta m\ \Delta\Upsilon^B_{i}\Big)\ , \tag{4.102d}$$

where

$$\sqrt{Z_B} \doteq 1 + \frac{1}{2}\Sigma'^\star + \frac{1}{2}\Delta\Sigma'_B\ . \tag{4.103}$$

Starting from this point everything can be worked out analogously to the case of fixed mean quark mass.

4.5.4 Parametrization of baryon octet distribution amplitudes

In this section we will work out explicit expressions for the distribution amplitudes defined in eqs. (4.70) and (4.72) in terms of the shape parameters given in refs. [153–155], where contributions of Wandzura–Wilczek type [156] are taken into account explicitly. This corresponds to

the so-called conformal partial wave expansion, where the DAs are expanded in a set of orthogonal polynomials such that the coefficients (i.e., the shape parameters) have autonomous scale dependence at one-loop accuracy in QCD. For brevity we apply the approximation advocated in ref. [153], where contributions that can mix with four-particle operators are systematically neglected. Let us note in passing that our general result does not rely on the separation of Wandzura–Wilczek and genuine higher twist terms at all, since the calculation within chiral perturbation theory does not distinguish between these contributions. This allows us to generalize the results for the nucleon given in refs. [153–155] to the full baryon octet.[4] For the parametrization we use the definitions of said references and we define additionally

$$\mathcal{P}_{nk}(x_1,x_2,x_3) = p_{nk}\mathcal{P}_{nk}(x_3,x_2,x_1)\ , \tag{4.104}$$

where $p_{nk} = \pm 1$, depending on n and k. This definition is possible since the polynomials $\mathcal{P}_{nk}$ have definite parity under exchange of x_1 and x_3 [153]. We will call the polynomials with $p_{nk} = +1$ ($p_{nk} = -1$) even (odd). The polynomials up to $n = 2$ are given by

$$\begin{aligned}
&\mathcal{P}_{00} = 1\ , && \mathcal{P}_{20} = \frac{63}{10}[3(x_1-x_3)^2 - 3x_2(x_1+x_3) + 2x_2^2]\ ,\\
&\mathcal{P}_{10} = 21(x_1-x_3)\ , && \mathcal{P}_{21} = \frac{63}{2}(x_1-3x_2+x_3)(x_1-x_3)\ ,\\
&\mathcal{P}_{11} = 7(x_1-2x_2+x_3)\ , && \mathcal{P}_{22} = \frac{9}{5}[x_1^2 + 9x_2(x_1+x_3) - 12x_1x_3 - 6x_2^2 + x_3^2]\ ,
\end{aligned} \tag{4.105}$$

where we can read off $p_{00} = p_{11} = p_{20} = p_{22} = +1$ and $p_{10} = p_{21} = -1$. Distribution amplitudes of fixed collinear twist can be split into a part with similar geometric twist, called genuine (higher twist) contributions, and parts of lower geometric twist, which we have already refered to as Wandzura–Wilczek contributions above. The decomposition reads[5]

$$\begin{aligned}
&\Phi^B_{\pm,3} = \Phi^{B,t=3}_{\pm,3}\ ,\\
&\Phi^B_{\pm,4} = \Phi^{B,WW_3}_{\pm,4} + \Phi^{B,t=4}_{\pm,4}\ , && \Xi^B_{\pm,4} = \Xi^{B,t=4}_{\pm,4}\ ,\\
&\Phi^B_{\pm,5} = \Phi^{B,WW_3}_{\pm,5} + \Phi^{B,WW_4}_{\pm,5} + \Phi^{B,t=5}_{\pm,5}\ , && \Xi^B_{\pm,5} = \Xi^{B,WW_4}_{\pm,5} + \Xi^{B,t=5}_{\pm,5}\ .
\end{aligned} \tag{4.106}$$

Analogous expressions for the Π and Υ DAs will be given below in eq. (4.111). Genuine twist-five contributions ($\Phi^{B,t=5}_{\pm,5}$, $\Xi^{B,t=5}_{\pm,5}$) will be neglected in the following, since we apply the approximation of ref. [153] as mentioned above. Also twist-six DAs are neglected; one could in principle take into account Wandzura–Wilczek contributions to the twist-six DAs, but the correspond-

[4] A similar parametrization has been worked out recently in ref. [165], adopting our phase conventions, but choosing different basic DAs.

[5] Note that, in contrast to our work [139], we do not normalize the Wandzura–Wilczek and the genuine higher twist contributions with the corresponding normalization constants.

ing expressions are not known yet. The genuine twist-three and twist-four contributions are parametrized as (cf. refs. [153–155])

$$\Phi_{\pm,3}^{B,t=3} = 120 x_1 x_2 x_3 \sum_{\substack{n,k\leq n\\ p_{nk}=\pm 1}} \varphi_{nk}^B \mathcal{P}_{nk}(x_1,x_2,x_3) \;, \tag{4.107a}$$

$$\Phi_{+,4}^{B,t=4} = 24 x_1 x_2 \Big(\frac{10}{3}(2x_1 - x_2 - 2x_3)\tilde{\eta}_{11}^B + \dots\Big) \;, \tag{4.107b}$$

$$\Phi_{-,4}^{B,t=4} = 24 x_1 x_2 \Big(\eta_{00}^B + 2(2-5x_2)\eta_{10}^B + \dots\Big) \;, \tag{4.107c}$$

$$\Xi_{+,4}^{B,t=4} = 24 x_2 x_3 \Big(\xi_{00}^B - \frac{9}{4}(1-5x_1)\xi_{10}^B + \dots\Big) \;, \tag{4.107d}$$

$$\Xi_{-,4}^{B,t=4} = 24 x_2 x_3 \Big(-\frac{45}{4}(x_2 - x_3)\xi_{10}^B + \dots\Big) \;, \tag{4.107e}$$

where the summation over n starts from 0 and, generally, goes to infinity, but is truncated at $n = 2$ in the approximation of ref. [153]. The zeroth moments of the DAs are equivalent to the normalization constants $\varphi_{00}^B = f^B$, $\eta_{00}^B = \lambda_1^B$ and $\xi_{00}^B = \lambda_2^B$. The Wandzura–Wilczek contributions (see refs. [153–155]) are fixed by the same parameters as the corresponding genuine twist contribution; e.g., $\Phi_{+,4}^{B,WW_3}$ and $\Phi_{+,5}^{B,WW_3}$ are described by the same set of parameters as $\Phi_{+,3}^{B,t=3}$. The explicit functional form reads

$$\Phi_{\pm,4}^{B,WW_3} = -\sum_{\substack{n,k\leq n\\ p_{nk}=\pm 1}} \frac{240\varphi_{nk}^B}{(n+2)(n+3)} \left(n+2-\frac{\partial}{\partial x_3}\right) x_1 x_2 x_3 \mathcal{P}_{nk}(x_1,x_2,x_3) \;, \tag{4.108a}$$

$$\begin{aligned}\Phi_{\pm,5}^{B,WW_3} = \sum_{\substack{n,k\leq n\\ p_{nk}=\pm 1}} \frac{240\varphi_{nk}^B}{(n+2)(n+3)} \left[\left(n+2-\frac{\partial}{\partial x_1}\right)\left(n+1-\frac{\partial}{\partial x_2}\right) - (n+2)^2\right] \\ \times x_1 x_2 x_3 \mathcal{P}_{nk}(x_1,x_2,x_3) \;,\end{aligned} \tag{4.108b}$$

$$\Phi_{+,5}^{B,WW_4} = 4 x_3 \big(5(x_1^2 + 2x_2 x_3 - x_3^2)\eta_{11}^B + \dots\big) \;, \tag{4.108c}$$

$$\Phi_{-,5}^{B,WW_4} = 4 x_3 (1-x_2)\big(2\eta_{00}^B + 3(1-5x_2)\eta_{10}^B + \dots\big) \;, \tag{4.108d}$$

$$\Xi_{+,5}^{B,WW_4} = 4 x_1 (1+x_1)\xi_{00}^B - \frac{27}{2}(4 - 4x_1 + x_1^2 - 5x_1^3)\xi_{10}^B + \dots \;, \tag{4.108e}$$

$$\Xi_{-,5}^{B,WW_4} = -12 x_1 (x_2 - x_3)\xi_{00}^B + \frac{27}{2}(5 - x_1 + 5x_1^2)(x_2 - x_3)\xi_{10}^B + \dots \;. \tag{4.108f}$$

Note that one should not take into account explicit quark mass corrections to eq. (4.108) and eq. (4.116) below (compare, e.g., refs. [166, 167] where such computations have been performed for vector meson and pseudoscalar meson DAs), since they are (by definition) already included in the genuine higher twist terms in eqs. (4.106) and (4.111). For leading geometric twist our separation into "+" and "−" amplitudes corresponds to a separation of even ($p_{nk} = +1$) and odd ($p_{nk} = -1$) polynomials. We cannot make such a general statement for the higher twist DAs, since we have worked out only their explicit parametrization up to the first moments. However, one could guess from our result that the separation into "+" and "−" amplitudes corresponds to a separation of contributions with different symmetry properties also in the higher twist contributions.

The dependence of the shape parameters on the quark mass splitting can be determined from eq. (4.85). For the (trivial) extension to variable mean quark mass one would use eq. (4.102)

instead. In analogy to eq. (4.92) the nonanalytic prefactor drops out if one divides the moments by an appropriate normalization constant:

$$\frac{\varphi^B_{nk}}{f^B} = \frac{\varphi^\star_{nk} + \delta m\ \Delta\varphi^B_{nk}}{f^\star + \delta m\ \Delta f^B}\ ,\ p_{nk} = +1\ , \qquad \frac{\varphi^B_{nk}}{\lambda_1^B} = \frac{\varphi^\star_{nk} + \delta m\ \Delta\varphi^B_{nk}}{\lambda_1^\star + \delta m\ \Delta\lambda_1^B}\ ,\ p_{nk} = -1\ , \tag{4.109a}$$

$$\frac{\eta^B_{11}}{f^B} = \frac{\eta^\star_{11} + \delta m\ \Delta\eta^B_{11}}{f^\star + \delta m\ \Delta f^B}\ , \qquad \frac{\eta^B_{10}}{\lambda_1^B} = \frac{\eta^\star_{10} + \delta m\ \Delta\eta^B_{10}}{\lambda_1^\star + \delta m\ \Delta\lambda_1^B}\ , \tag{4.109b}$$

$$\frac{\xi^B_{10}}{\lambda_2^B} = \frac{\xi^\star_{10} + \delta m\ \Delta\xi^B_{10}}{\lambda_2^\star + \delta m\ \Delta\lambda_2^B}\ . \tag{4.109c}$$

In particular for the parameters describing the genuine higher twist contributions the simplicity of the result is a consequence of the twist independence of the chiral extrapolation formulas (4.85). The parameters describing $\mathrm{SU}(3)_f$ symmetry breaking are restricted by eq. (4.80) such that

$$\Delta x^\Xi_{nk} = -\Delta x^N_{nk} - \Delta x^\Sigma_{nk}\ , \quad \text{for } x \in \{\varphi, \tilde\varphi, \eta, \tilde\eta, \xi\}\ . \tag{4.110}$$

For a description of the complete baryon octet one also needs the Π and Υ DAs defined in eq. (4.72), which are relevant for the hyperons. These are (at leading one-loop accuracy in BChPT) completely fixed by the $\Phi_\pm$ and Ξ DAs. Consequently, the following equations do not contain any additional parameters:

$$\Pi^B_3 = \Pi^{B,t=3}_3\ , \tag{4.111a}$$

$$\Pi^B_4 = \Pi^{B,WW_3}_4 + \Pi^{B,t=4}_4\ , \qquad \Upsilon^B_4 = \Upsilon^{B,t=4}_4\ , \tag{4.111b}$$

$$\Pi^B_5 = \Pi^{B,WW_3}_5 + \Pi^{B,WW_4}_5 + \Pi^{B,t=5}_5\ , \qquad \Upsilon^B_5 = \Upsilon^{B,WW_4}_5 + \Upsilon^{B,t=5}_5\ , \tag{4.111c}$$

where

$$\Pi^N_i = \Phi^N_{+,i}\ , \qquad \Upsilon^N_i = \Xi^N_{+,i}\ , \tag{4.112}$$

due to isospin symmetry. As above, the genuine twist-five contributions $\Pi^{B,t=5}_5$ and $\Upsilon^{B,t=5}_5$ will be neglected in the following. The genuine twist-three and twist-four contributions are

$$\Pi^{B,t=3}_3 = 120 x_1 x_2 x_3 \sum_{\substack{n,k\le n\\ p_{nk}=(-1)_B}} \pi^B_{nk} \mathcal{P}_{nk}(x_1,x_2,x_3)\ , \tag{4.113a}$$

$$\Pi^{B\neq\Lambda,t=4}_4 = 24 x_1 x_2 \Big(\frac{10}{3}(2x_1 - x_2 - 2x_3)\zeta^B_{11} + \dots\Big)\ , \tag{4.113b}$$

$$\Pi^{\Lambda,t=4}_4 = 24 x_1 x_2 \Big(\zeta^\Lambda_{00} + 2(2-5x_2)\zeta^\Lambda_{10} + \dots\Big)\ , \tag{4.113c}$$

$$\Upsilon^{B\neq\Lambda,t=4}_4 = 24 x_2 x_3 \Big(v^B_{00} - \frac{9}{4}(1-5x_1)v^B_{10} + \dots\Big)\ , \tag{4.113d}$$

$$\Upsilon^{\Lambda,t=4}_4 = 24 x_2 x_3 \Big(-\frac{45}{4}(x_2 - x_3)v^\Lambda_{10} + \dots\Big)\ , \tag{4.113e}$$

where, as defined above, $(-1)_{B\neq\Lambda} = +1$ and $(-1)_\Lambda = -1$. The dependence of the shape parameters on the quark mass splitting reads

$$\frac{\pi_{nk}^{B\neq\Lambda}}{f_T^{B\neq\Lambda}} = \frac{\varphi_{nk}^\star + \delta m\ \Delta\pi_{nk}^B}{f^\star + \delta m\ \Delta f_T^B}\ , \qquad \frac{\pi_{nk}^\Lambda}{\lambda_T^\Lambda} = \frac{\varphi_{nk}^\star + \delta m\ \Delta\pi_{nk}^\Lambda}{\lambda_1^\star + \delta m\ \Delta\lambda_T^\Lambda}\ , \tag{4.114a}$$

$$\frac{\zeta_{11}^{B\neq\Lambda}}{f_T^{B\neq\Lambda}} = \frac{\eta_{11}^\star + \delta m\ \Delta\zeta_{11}^B}{f^\star + \delta m\ \Delta f_T^B}\ , \qquad \frac{\zeta_{10}^\Lambda}{\lambda_T^\Lambda} = \frac{\eta_{10}^\star + \delta m\ \Delta\zeta_{10}^\Lambda}{\lambda_1^\star + \delta m\ \Delta\lambda_T^\Lambda}\ , \tag{4.114b}$$

$$\frac{\upsilon_{10}^B}{\lambda_2^B} = \frac{\xi_{10}^\star + \delta m\ \Delta\upsilon_{10}^B}{\lambda_2^\star + \delta m\ \Delta\lambda_2^B}\ , \tag{4.114c}$$

where $\Delta f_T^{B\neq\Lambda}$ and $\Delta\lambda_T^\Lambda$ are defined in eq. (4.89). The parameters describing $\mathrm{SU}(3)_f$ symmetry breaking can be determined by eqs. (4.80) and (4.81):

$$\Delta\pi_{nk}^N = \Delta\varphi_{nk}^N\ , \qquad \Delta\pi_{nk}^\Sigma = -\frac{1}{2}\Delta\varphi_{nk}^\Sigma - \frac{3}{2}\Delta\varphi_{nk}^\Lambda\ , \tag{4.115a}$$

$$\Delta\pi_{nk}^\Xi = \frac{3}{2}\Delta\varphi_{nk}^\Lambda + \frac{1}{2}\Delta\varphi_{nk}^\Sigma - \Delta\varphi_{nk}^N\ , \qquad \Delta\pi_{nk}^\Lambda = -\frac{1}{2}\Delta\varphi_{nk}^\Lambda - \frac{3}{2}\Delta\varphi_{nk}^\Sigma\ , \tag{4.115b}$$

$$\Delta\zeta_{11}^N = \Delta\eta_{11}^N\ , \qquad \Delta\zeta_{11}^\Sigma = -\frac{1}{2}\Delta\eta_{11}^\Sigma - \frac{3}{2}\Delta\eta_{11}^\Lambda\ , \tag{4.115c}$$

$$\Delta\zeta_{11}^\Xi = \frac{3}{2}\Delta\eta_{11}^\Lambda + \frac{1}{2}\Delta\eta_{11}^\Sigma - \Delta\eta_{11}^N\ , \qquad \Delta\zeta_{10}^\Lambda = -\frac{1}{2}\Delta\eta_{10}^\Lambda - \frac{3}{2}\Delta\eta_{10}^\Sigma\ , \tag{4.115d}$$

$$\Delta\upsilon_{10}^N = \Delta\xi_{10}^N\ , \qquad \Delta\upsilon_{10}^\Sigma = -\frac{1}{2}\Delta\xi_{10}^\Sigma - \frac{3}{2}\Delta\xi_{10}^\Lambda\ , \tag{4.115e}$$

$$\Delta\upsilon_{10}^\Xi = \frac{3}{2}\Delta\xi_{10}^\Lambda + \frac{1}{2}\Delta\xi_{10}^\Sigma - \Delta\xi_{10}^N\ , \qquad \Delta\upsilon_{10}^\Lambda = -\frac{1}{2}\Delta\xi_{10}^\Lambda - \frac{3}{2}\Delta\xi_{10}^\Sigma\ . \tag{4.115f}$$

The Wandzura–Wilczek contributions take the form

$$\Pi_4^{B,WW_3} = -\sum_{\substack{n,k\leq n\\ p_{nk}=(-1)_B}} \frac{240\pi_{nk}^B}{(n+2)(n+3)}\left(n+2-\frac{\partial}{\partial x_3}\right)x_1x_2x_3\mathcal{P}_{nk}(x_1,x_2,x_3)\ , \tag{4.116a}$$

$$\Pi_5^{B,WW_3} = \sum_{\substack{n,k\leq n\\ p_{nk}=(-1)_B}} \frac{240\pi_{nk}^B}{(n+2)(n+3)}\left[\left(n+2-\frac{\partial}{\partial x_1}\right)\left(n+1-\frac{\partial}{\partial x_2}\right)-(n+2)^2\right] \times x_1x_2x_3\mathcal{P}_{nk}(x_1,x_2,x_3)\ , \tag{4.116b}$$

$$\Pi_5^{B\neq\Lambda,WW_4} = 4x_3\Big(5(x_1^2+2x_2x_3-x_3^2)\zeta_{11}^B+\dots\Big)\ , \tag{4.116c}$$

$$\Pi_5^{\Lambda,WW_4} = 4x_3(1-x_2)\Big(2\zeta_{00}^\Lambda+3(1-5x_2)\zeta_{10}^\Lambda+\dots\Big)\ , \tag{4.116d}$$

$$\Upsilon_5^{B\neq\Lambda,WW_4} = 4x_1(1+x_1)\upsilon_{00}^B - \frac{27}{2}(4-4x_1+x_1^2-5x_1^3)\upsilon_{10}^B+\dots\ , \tag{4.116e}$$

$$\Upsilon_5^{\Lambda,WW_4} = -12x_1(x_2-x_3)\upsilon_{00}^\Lambda + \frac{27}{2}(5-x_1+5x_1^2)(x_2-x_3)\upsilon_{10}^\Lambda+\dots\ . \tag{4.116f}$$

Let us conclude this section with a short summary. First of all, we found that the behavior under chiral extrapolation of a certain moment correlates to its parity in the sense of eq. (4.104). Therefore it is advantageous to normalize the odd moments of the leading twist DA with λ_1^B instead of f^B. Quantitatively more important, however, is the significant reduction of parameters: we find that (within the approximation used above) we only need 43 parameters to describe the complete set of baryon octet three-quark DAs (including their dependence on the quark mass

splitting). In contrast, an ad hoc linear extrapolation without the knowledge of $\mathrm{SU}(3)_f$ symmetry breaking would require 72 parameters for the given setup, since one cannot make use of eqs. (4.89), (4.91), (4.110) and (4.115). In the latter case we have assumed that the constraints at the flavor symmetric point are taken into account. Otherwise, the number of parameters would be even larger.

4.6 Analysis of lattice QCD data

In this section we analyze lattice QCD data for the normalization constants and first moments of the leading twist distribution amplitudes, corresponding to the small transverse distance limit of the associated S-wave light-cone wave functions (compare eqs. (4.76) and (4.77)). The (higher twist) coupling constants, which normalize the P-wave contribution, are evaluated as well. The calculation is done using $N_f = 2 + 1$ flavors of dynamical (clover) fermions, which are an ideal setup to study SU(3) flavor symmetry violation effects. The results presented here have been published in our work [75]. It is the first ab initio calculation of distribution amplitudes for the full baryon octet using lattice QCD. The main analysis of the lattice data has been performed in collaboration with M. Gruber and F. Hutzler.

4.6.1 Correlation functions

On the lattice the direct calculation of operators with quarks at lightlike separations is impossible, since one is bound to use a Euclidean spacetime[6] in order to have a real action exponent that allows to calculate the path integral via importance sampling. Instead, one calculates moments of DAs, e.g.,

$$V^B_{i,lmn} = \int [dx]\; x_1^l x_2^m x_3^n V_i^B(x_1, x_2, x_3) \;, \tag{4.117}$$

which are linked to the matrix elements of local operators. These can be extracted from two-point correlation functions between a smeared baryon interpolator $\mathcal{N}^B$ and the local current one is interested in at the sink:

$$\langle 0|\mathcal{O}_\tau(t)_{\mathbf{p}}\; \bar{\mathcal{N}}^B_{\tau'}(0,\mathbf{0})|0\rangle = a^3 \sum_{\mathbf{x}} e^{i\mathbf{p}\mathbf{x}} \langle 0|\mathcal{O}_\tau(t,\mathbf{x})\; \bar{\mathcal{N}}^B_{\tau'}(0,\mathbf{0})|0\rangle \;, \tag{4.118}$$

where a is the lattice spacing. The Fourier transform fixes the momentum to $\mathbf{p}$. As source currents we use

$$\mathcal{N}^N = \big(u^T C\gamma_5 d\big)u \;, \tag{4.119a}$$
$$\mathcal{N}^\Sigma = \big(d^T C\gamma_5 s\big)d \;, \tag{4.119b}$$
$$\mathcal{N}^\Xi = \big(s^T C\gamma_5 u\big)s \;, \tag{4.119c}$$
$$\mathcal{N}^\Lambda = \tfrac{1}{\sqrt{6}}\big(2\big(u^T C\gamma_5 d\big)s + \big(u^T C\gamma_5 s\big)d + \big(s^T C\gamma_5 d\big)u\big) \;, \tag{4.119d}$$

[6] Within section 4.6 all equations refer to Euclidean spacetime; we use the gamma matrix convention of [118].

where color antisymmetrization is tacitly assumed. Since we work with degenerate light quark masses we can make use of exact isospin symmetry and only calculate the result for the representatives $N \equiv p$, $\Sigma \equiv \Sigma^-$, $\Xi \equiv \Xi^0$ and Λ. The results for the remaining members of the multiplet are redundant owing to eq. (4.73). From the general decomposition (4.2) one obtains that the baryon-to-vacuum matrix element of the source currents is proportional to the baryon spinor times a combination of normalization constants. However, for the smeared currents the coupling is a priori unknown, which means that we have to model it by the introduction of a coupling constant $\sqrt{Z_B(\mathbf{p})}$:

$$\langle 0|\mathcal{N}^B_\tau(0,\mathbf{0})|B(p,s)\rangle = \sqrt{Z_B(\mathbf{p})}u^B_\tau(p,s)\ . \tag{4.120}$$

This factor depends on various parameters, like the smearing (method and number of steps), the type of baryon and the momentum. Using a symmetric smearing we assume that the smearing factor does not depend on the spin. The (unphysical) phase of $\sqrt{Z_B(\mathbf{p})}$ is trivially fixed to 1 by our conventional choice that the leading twist coupling of the nucleon f^N should be real and positive. The coupling to the smeared interpolators can be obtained from the correlation function of two smeared currents:

$$\begin{aligned}(\gamma_+)_{\tau'\tau}\langle 0|\mathcal{N}^B_\tau(t)_{\mathbf{p}}\ \bar{\mathcal{N}}^B_{\tau'}(0,\mathbf{0})|0\rangle &\approx \sum_s \frac{Z_B(\mathbf{p})}{2E(\mathbf{p})}e^{-E(\mathbf{p})t}\frac{(1+\gamma_0)_{\tau'\tau}}{2}u^B_\tau(p,s)\bar{u}^B_{\tau'}(p,s)\\ &= \frac{Z_B(\mathbf{p})}{4E(\mathbf{p})}e^{-E(\mathbf{p})t}\,\mathrm{tr}\left\{(\mathbb{1}+\gamma_0)(\not{p}+m_B)\right\} = Z_B(\mathbf{p})\frac{E(\mathbf{p})+m_B}{E(\mathbf{p})}e^{-E(\mathbf{p})t}\ ,\end{aligned} \tag{4.121}$$

where we have neglected exponentially suppressed states of higher energy in the first step. $\gamma_\pm = (1\pm\gamma_0)/2$ eliminates the leading negative/positive parity contribution to the correlation function. At nonzero momentum one has to modify the projection operator in order to achieve a complete annihilation of the leading positive/negative parity contribution (see refs. [37, 168]). However, being interested in the positive parity states the parity projection is not a really crucial point for us, since eventual negative parity contaminations are anyway exponentially suppressed in the correlation function due to their higher mass. For the calculation of the normalization constants we define five different local operators

$$\mathcal{S}^B_\tau = (q^a C q^b)(\gamma_5 q^c)_\tau\ , \qquad \mathcal{P}^B_\tau = (q^a C\gamma_5 q^b)q^c_\tau\ , \tag{4.122a}$$

$$\mathcal{V}^B_{\rho,\tau} = (q^a C\gamma_\rho q^b)(\gamma_5 q^c)_\tau\ , \qquad \mathcal{A}^B_{\rho,\tau} = (q^a C\gamma_\rho\gamma_5 q^b)q^c_\tau\ , \tag{4.122b}$$

$$\mathcal{T}^B_{\rho\sigma,\tau} = (q^a C i\sigma_{\rho\sigma} q^b)(\gamma_5 q^c)_\tau\ , \tag{4.122c}$$

where the flavors a, b, c on the r.h.s. are chosen as described below eq. (4.10) at the end of section 4.2 and color antisymmetrization is tacitly assumed. For notational purposes we also define

$$\mathcal{T}^B_{\rho,\tau} = \left(\gamma_\sigma \mathcal{T}^B_{\rho\sigma}\right)_\tau\ , \tag{4.123}$$

and

$$\mathcal{V}^B_\tau = \left(\gamma_\rho \mathcal{V}^B_\rho\right)_\tau\ , \qquad \mathcal{A}^B_\tau = \left(\gamma_\rho \mathcal{A}^B_\rho\right)_\tau\ , \qquad \mathcal{T}^B_\tau = \left(\gamma_\rho \mathcal{T}^B_\rho\right)_\tau = \left(-i\sigma_{\rho\sigma}\mathcal{T}^B_{\rho\sigma}\right)_\tau\ . \tag{4.124}$$

The interpolators $-\mathcal{V}_\tau^B$ and $\mathcal{T}_\tau^B$ are known as Ioffe and Dosch currents. For the calculation of the leading twist normalization constants f^B and f_T^B one has to use specific combinations of $\mathcal{V}_{\rho,\tau}^B$, $\mathcal{A}_{\rho,\tau}^B$ and $\mathcal{T}_{\rho,\tau}^B$ to implement the twist projection. Additionally, these combinations have to be chosen in such a way that they transform under irreducible representations of the spinorial hypercubic group $\overline{\mathrm{H}(4)}$ to avoid operator mixing under renormalization in the RI′/SMOM scheme, see refs. [169–171]. The latter is a regularization independent renormalization scheme using a symmetric (nonexceptional) momentum configuration. We call these specific combinations A, B and C and they are defined for $\mathcal{O} \in \{\mathcal{V}, \mathcal{A}, \mathcal{T}\}$ as

$$\mathcal{O}_{\mathrm{A}}^B = -\gamma_1 \mathcal{O}_1^B + \gamma_2 \mathcal{O}_2^B \ , \tag{4.125a}$$

$$\mathcal{O}_{\mathrm{B}}^B = -\gamma_3 \mathcal{O}_3^B + \gamma_4 \mathcal{O}_4^B \ , \tag{4.125b}$$

$$\mathcal{O}_{\mathrm{C}}^B = -\gamma_1 \mathcal{O}_1^B - \gamma_2 \mathcal{O}_2^B + \gamma_3 \mathcal{O}_4^B + \gamma_4 \mathcal{O}_4^B \ . \tag{4.125c}$$

$\mathcal{O}_{\mathrm{A}}^B$ will not be used since one finds that it only contributes to correlation functions at nonzero momentum and is thus by far not measurable as accurately as $\mathcal{O}_{\mathrm{B}}^B$ and $\mathcal{O}_{\mathrm{C}}^B$. For the correlation functions at zero momentum one finds

$$(\gamma_+)_{\tau'\tau} \langle 0 | \mathcal{V}_{\mathrm{B/C},\tau}^B(t)_{\mathbf{0}} \, \bar{\mathcal{N}}_{\tau'}^B(0,\mathbf{0}) | 0 \rangle \approx \sqrt{Z_B(\mathbf{0})} 2 m_B \, e^{-m_B t} \times \begin{cases} f^B \ , & B \neq \Lambda \ , \\ 0 \ , & B = \Lambda \ , \end{cases} \tag{4.126a}$$

$$(\gamma_+)_{\tau'\tau} \langle 0 | \mathcal{A}_{\mathrm{B/C},\tau}^B(t)_{\mathbf{0}} \, \bar{\mathcal{N}}_{\tau'}^B(0,\mathbf{0}) | 0 \rangle \approx \sqrt{Z_B(\mathbf{0})} 2 m_B \, e^{-m_B t} \times \begin{cases} 0 \ , & B \neq \Lambda \ , \\ \sqrt{\frac{3}{2}} f^\Lambda \ , & B = \Lambda \ , \end{cases} \tag{4.126b}$$

$$(\gamma_+)_{\tau'\tau} \langle 0 | \mathcal{T}_{\mathrm{B/C},\tau}^B(t)_{\mathbf{0}} \, \bar{\mathcal{N}}_{\tau'}^B(0,\mathbf{0}) | 0 \rangle \approx \sqrt{Z_B(\mathbf{0})} 2 m_B \, e^{-m_B t} \times \begin{cases} -2 f_T^B \ , & B \neq \Lambda \ , \\ 0 \ , & B = \Lambda \ , \end{cases} \tag{4.126c}$$

where $f_T^N = f^N$ due to isospin symmetry. We have used that the normalization constants are related to the zeroth moments via

$$f^{B\neq\Lambda} \equiv \varphi_{00}^B = V_{1,000}^B \ , \qquad f^\Lambda \equiv \varphi_{00}^\Lambda = -\sqrt{\tfrac{2}{3}} A_{1,000}^\Lambda \ , \qquad f_T^{B\neq\Lambda} \equiv \pi_{00}^B = T_{1,000}^B \ , \tag{4.127}$$

and that the remaining zeroth moments of the leading twist DAs V_1^B, A_1^B and T_1^B vanish according to eq. (4.10):

$$V_{1,000}^\Lambda = A_{1,000}^{B\neq\Lambda} = T_{1,000}^\Lambda = 0 \ . \tag{4.128}$$

For the calculation of higher moments of the leading twist distribution amplitudes one has to analyze matrix elements of (specific combinations of) the operators $\mathcal{V}_{\rho,\tau}^B$, $\mathcal{A}_{\rho,\tau}^B$ and $\mathcal{T}_{\rho,\tau}^B$ with additional derivatives acting on the quark fields. This introduces some complications: one has to make sure that the operators are chosen from multiplets that do not mix with lower-dimensional operators (see refs. [169–171]). Additionally all correlation functions involving these specific operators vanish at zero momentum, such that one has to use a nontrivial momentum configuration. As discussed above, this complicates parity projection (see [37]) and, generally, leads to less precise results. A detailed discussion of all peculiarities lies beyond the scope of this

work and can be found in our article [75]. The shape parameters defined in section 4.5.4 can be expressed as linear combinations of $S^B_{i,lmn}$, $P^B_{i,lmn}$, $V^B_{i,lmn}$, $A^B_{i,lmn}$ and $T^B_{i,lmn}$ via eqs. (4.70) and (4.72). For the shape parameters that correspond to the first moments of the leading twist distribution amplitude of the N, Σ and Ξ baryons one finds

$$\varphi_{11}^{B\neq\Lambda} = \tfrac{1}{2}\big([V_1-A_1]^B_{100} - 2[V_1-A_1]^B_{010} + [V_1-A_1]^B_{001}\big)\ , \tag{4.129a}$$

$$\varphi_{10}^{B\neq\Lambda} = \tfrac{1}{2}\big([V_1-A_1]^B_{100} - [V_1-A_1]^B_{001}\big)\ , \tag{4.129b}$$

$$\pi_{11}^{B\neq\Lambda} = \tfrac{1}{2}\big(T^B_{1,100} + T^B_{1,010} - 2T^B_{1,001}\big)\ , \tag{4.129c}$$

where $\pi^N_{11} = \varphi^N_{11}$ due to isospin symmetry. For the Λ baryon the result reads

$$\varphi_{11}^{\Lambda} = \tfrac{1}{\sqrt{6}}\big([V_1-A_1]^\Lambda_{100} - 2[V_1-A_1]^\Lambda_{010} + [V_1-A_1]^\Lambda_{001}\big)\ , \tag{4.130a}$$

$$\varphi_{10}^{\Lambda} = -\sqrt{\tfrac{3}{2}}\big([V_1-A_1]^\Lambda_{100} - [V_1-A_1]^\Lambda_{001}\big)\ , \tag{4.130b}$$

$$\pi_{10}^{\Lambda} = \sqrt{\tfrac{3}{2}}\big(T^\Lambda_{1,100} - T^\Lambda_{1,010}\big)\ . \tag{4.130c}$$

In addition one has to define combinations of moments corresponding to the sum of contributions with the derivative acting on each of the three quarks:

$$\varphi_{00,(1)}^{B\neq\Lambda} = [V_1-A_1]^B_{100} + [V_1-A_1]^B_{010} + [V_1-A_1]^B_{001}\ , \tag{4.131a}$$

$$\pi_{00,(1)}^{B\neq\Lambda} = T^B_{1,100} + T^B_{1,010} + T^B_{1,001}\ , \tag{4.131b}$$

$$\varphi_{00,(1)}^{\Lambda} = \sqrt{\tfrac{2}{3}}\big([V_1-A_1]^\Lambda_{100} + [V_1-A_1]^\Lambda_{010} + [V_1-A_1]^\Lambda_{001}\big)\ , \tag{4.131c}$$

where $\pi^N_{00,(1)} = \varphi^N_{00,(1)}$ due to isospin symmetry. In the continuum these moments are equivalent to the normalization constants

$$\varphi^B_{00,(1)} = \varphi^B_{00}\ , \qquad\qquad \pi^{B\neq\Lambda}_{00,(1)} = \pi^B_{00}\ , \tag{4.132}$$

by virtue of the condition $x_1+x_2+x_3=1$ in the integration measure (4.9). On the lattice these relations are violated by discretization effects and one has to take into account mixing of $\varphi^B_{00,(1)}$ and $\pi^{B\neq\Lambda}_{00,(1)}$ with the other first moments under renormalization. A detailed description of this issue is given in ref. [75].

The 21 higher-twist DAs altogether involve only up to three new normalization constants (just two for N, Σ and Ξ), cf. section 4.5.2. They are, e.g., relevant for baryon decays in generic GUT models [172] and as input parameters for QCD sum rule calculations (cf., e.g., refs. [173–175]). For their determination we use the matrix elements

$$(\gamma_+)_{\tau'\tau}\langle 0|\mathcal{O}^B_\tau(t)_{\mathbf{0}}\ \bar{\mathcal{N}}^B_{\tau'}(0,\mathbf{0})|0\rangle \approx c^B_{\mathcal{O}}\sqrt{Z_B(\mathbf{0})}2m_B\, e^{-m_B t} \tag{4.133}$$

Table 4.8: List of the ensembles used in this chapter, labeled by their CLS identifier. The pion and kaon masses have been obtained from two-point functions. $\beta = 3.4$ corresponds to the lattice spacing $a \approx 0.0857$ fm. The lattice spacing was determined from the Wilson flow method as described in ref. [180], where also an in-depth description of the lattices can be found.

id	β	N_s	N_t	κ_l	κ_s	m_π [MeV]	m_K [MeV]	$m_\pi L$	#conf.
H101	3.40	32	96	0.13675962	0.13675962	420	420	5.8	2000
H102	3.40	32	96	0.136865	0.136549339	355	440	4.9	1997
H105	3.40	32	96	0.136970	0.136340790	280	465	3.9	2833
C101	3.40	48	96	0.137030	0.136222041	222	474	4.6	1552

of the operators $\mathcal{O} \in \{\mathcal{S}, \mathcal{P}, \mathcal{V}, \mathcal{A}, \mathcal{T}\}$. These operators are local and do not contain derivatives acting on the quark fields. The coefficients $c_\mathcal{O}^B$ are

$$c_\mathcal{S}^B = \begin{cases} 0\,, & B \neq \Lambda\,, \\ \frac{-\lambda_2^\Lambda - 2\lambda_T^\Lambda}{4\sqrt{6}}\,, & B = \Lambda\,, \end{cases} \qquad c_\mathcal{P}^B = \begin{cases} 0\,, & B \neq \Lambda\,, \\ \frac{-\lambda_2^\Lambda + 2\lambda_T^\Lambda}{4\sqrt{6}}\,, & B = \Lambda\,, \end{cases} \tag{4.134a}$$

$$c_\mathcal{V}^B = \begin{cases} -\lambda_1^B\,, & B \neq \Lambda\,, \\ 0\,, & B = \Lambda\,, \end{cases} \qquad c_\mathcal{A}^B = \begin{cases} 0\,, & B \neq \Lambda\,, \\ \frac{-\lambda_1^B}{\sqrt{6}}\,, & B = \Lambda\,, \end{cases} \tag{4.134b}$$

$$c_\mathcal{T}^B = \begin{cases} \lambda_2^B\,, & B \neq \Lambda\,, \\ 0\,, & B = \Lambda\,. \end{cases} \tag{4.134c}$$

4.6.2 Details on the data

In this analysis we use lattice data of the coordinated lattice simulations (CLS) effort. They are obtained from simulations with $N_f = 2 + 1$ dynamical quark flavors described by a nonperturbatively first order improved Wilson action. The gauge action is tree-level Symanzik improved. A peculiarity is the use of open boundary conditions in time direction, which yields nontrivial boundary effects and thus requires that all measurements are carried out at sufficient distance to the boundary [176, 177]. The advantage of the open boundary conditions is the possibility to carry out simulations at smaller lattice spacing without facing the problem of topological freezing, which leads to large autocorrelation times at lattice spacings $a \lesssim 0.05$ fm [178]. In the future this will allow us to explore the continuum limit with higher precision. The latter is important, since the continuum extrapolation has been identified as a major source of systematic uncertainty in ref. [37]. More simulation details can be found in our work [75] and in ref. [179], where the latter also contains a first analysis of the baryon spectrum for these data points.

A list of the CLS ensembles used in this work is given in table 4.8. One should note that all of them have rather large spatial volumes ($L > 2.7$ fm, with $m_\pi L \gtrsim 4$) and high statistics. As schematically represented in figure 4.3, these ensembles are tuned such that the average quark mass reproduces (approximately) the physical value. They therefore provide a perfect setup to study flavor symmetry breaking. At the flavor symmetric point hadrons form SU(3) multiplets and their properties are related by symmetry. The real world is then approached in such a way that u and d quark masses decrease and simultaneously the s quark mass increases so that their

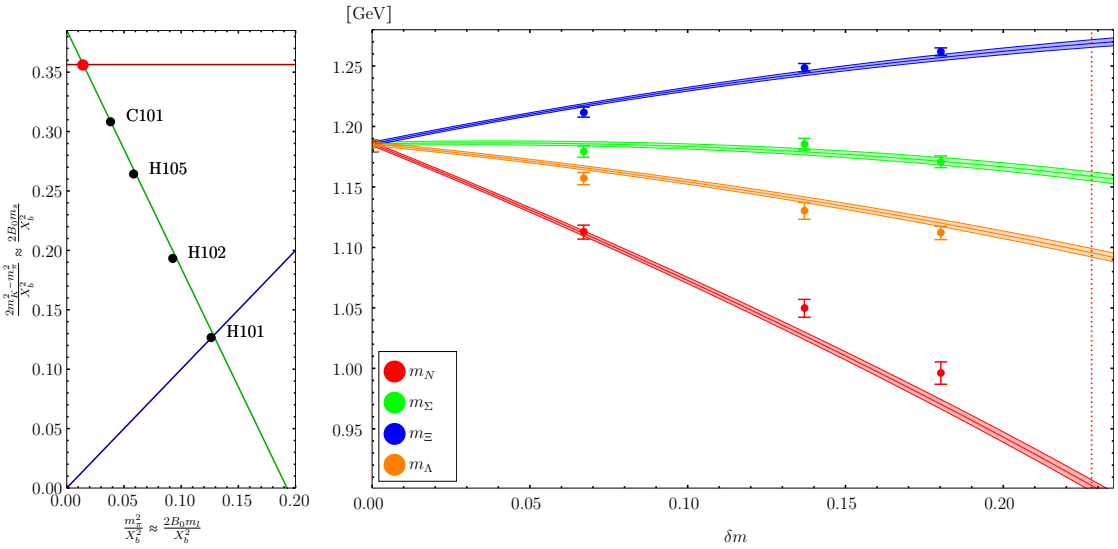

Figure 4.3: (left) Plot showing the meson masses of the lattice ensembles used in this study. All quantities are made dimensionless using the average octet baryon mass X_b defined in eq. (4.66). Along the flavor symmetric line (blue) all pseudoscalar mesons have equal mass ($m_K^2 = m_\pi^2$), which is equivalent to equal quark masses ($m_l = m_s$). The (green) line of physical normalized average quadratic meson mass ($(2m_K^2 + m_\pi^2)/X_b^2 =$ phys.) corresponds to an approximately physical mean quark mass ($2m_l + m_s \approx$ phys.). The red line is defined by $(2m_K^2 - m_\pi^2)/X_b^2 =$ phys. and indicates an approximately physical strange quark mass ($m_s \approx$ phys.). The red dot marks the physical point.

Figure 4.4: (right) The figure shows a combined fit to the octet baryon masses using leading one-loop baryon chiral perturbation theory. (For a detailed study of baryon mass ratios at full one-loop order see [135].) The horizontal axis corresponds to the green line in figure 4.3, which is parametrized using the dimensionless quantity δm defined in eq. (4.65). The leftmost data point ($\delta m = 0$), where all baryon masses are identical, stems from the ensemble H101 at the symmetric point. The red dotted line marks the physical point at $\delta m = 0.228$.

average is kept constant. This leads to the typical fanlike splitting illustrated in figure 4.4 for the octet masses. This figure shows a combined fit using leading one-loop chiral perturbation theory, where (in addition to the effective couplings D and F) only three free parameters occur due to SU(3) constraints. In section 4.6.3 we will perform similar extrapolations for the couplings and the first moments.

The bare lattice results have to be renormalized. In phenomenological calculations the preferred renormalization scheme is $\overline{\text{MS}}$, which is inherently bound to dimensional regularization. Lattice calculations are, however, automatically regularized by the finite lattice spacing. To obtain final results in the $\overline{\text{MS}}$ scheme we proceed as follows: first, we (nonperturbatively) renormalize our results in a regularization independent scheme with a symmetric momentum configuration (the RI′/SMOM scheme). In a second step, we convert our results to the $\overline{\text{MS}}$ scheme using one-loop continuum perturbation theory. The procedure is sketched in ref. [75]. A detailed description will be presented in ref. [181].

4.6.3 Flavor symmetry breaking and chiral extrapolation

For the chiral extrapolation we use the three-flavor baryon chiral perturbation theory expressions presented in section 4.5 (published in ref. [139]). All data points that are used have approximately physical average quark mass. Therefore, we use the simplified version of the extrapolation formulas (4.85), where the mean quark mass is kept fixed and all quantities are expanded around the flavor symmetric point. This scenario corresponds to the green line of figure 4.3.

We start with the analysis of the combinations of distribution amplitudes with minimal SU(3) breaking given in eqs. (4.94) and (4.95). The explicit formulas for the normalization constants read:

$$0 + \mathcal{O}(\delta m^2) = f^\Sigma - f_T^\Sigma + f^\Xi - f_T^\Xi \ , \tag{4.135a}$$

$$8 \cdot 3f^\star + \mathcal{O}(\delta m^2) = 2 \cdot 3f^N + 3 \cdot (f^\Sigma + 2f_T^\Sigma) + 2 \cdot (f^\Xi + 2f_T^\Xi) + 1 \cdot 3f^\Lambda \ , \tag{4.135b}$$

$$8 \cdot 3\lambda_1^\star + \mathcal{O}(\delta m^2) = 2 \cdot 3\lambda_1^N + 3 \cdot 3\lambda_1^\Sigma + 2 \cdot 3\lambda_1^\Xi + 1 \cdot (\lambda_1^\Lambda + 2\lambda_T^\Lambda) \ , \tag{4.135c}$$

$$8\lambda_2^\star + \mathcal{O}(\delta m^2) = 2\lambda_2^N + 3\lambda_2^\Sigma + 2\lambda_2^\Xi + \lambda_2^\Lambda \ , \tag{4.135d}$$

which follow from eqs. (4.94a), (4.94b), (4.94c) and (4.95b), respectively. From eqs. (4.94) and (4.95) one can derive similar relations for the higher moments of the DAs. To visualize the size of the higher order SU(3) breaking terms it is convenient to form dimensionless expressions that vanish in the flavor symmetric limit ($\delta m \to 0$):

$$\delta_1 f = 1 - \frac{f^\Sigma + f^\Xi}{f_T^\Sigma + f_T^\Xi} \ , \tag{4.136a}$$

$$\delta_2 f = 1 - \frac{1}{8 \cdot 3f^\star}\big(2 \cdot 3f^N + 3 \cdot (f^\Sigma + 2f_T^\Sigma) + 2 \cdot (f^\Xi + 2f_T^\Xi) + 1 \cdot 3f^\Lambda\big) \ , \tag{4.136b}$$

$$\delta\lambda_1 = 1 - \frac{1}{8 \cdot 3\lambda_1^\star}\big(2 \cdot 3\lambda_1^N + 3 \cdot 3\lambda_1^\Sigma + 2 \cdot 3\lambda_1^\Xi + 1 \cdot (\lambda_1^\Lambda + 2\lambda_T^\Lambda)\big) \ , \tag{4.136c}$$

$$\delta\lambda_2 = 1 - \frac{1}{8\lambda_2^\star}\big(2\lambda_2^N + 3\lambda_2^\Sigma + 2\lambda_2^\Xi + \lambda_2^\Lambda\big) \ . \tag{4.136d}$$

In figure 4.5 we show linear and quadratic fits to the data. Even though for all these combinations the expected δm dependence is quadratic, we find that a linear dependence cannot be excluded. The largest deviation at the physical point is found for $\delta_2 f$ (up to $\approx 15\%$). Most remarkably, the deviation from the GMO-like relation for the normalization of the leading twist DAs, $\delta_1 f$, is very small ($|\delta_1 f| \approx 1\%$ at the physical point). For comparison, the violation of the GMO sum rule (4.93a) using the experimental values of baryon masses is

$$\delta_{\text{GMO}} = 1 - \frac{2m_N + 2m_\Xi}{m_\Sigma + 3m_\Lambda} \approx 0.57\% \ . \tag{4.137}$$

The formulas we use for the chiral extrapolation (see eqs. (4.85)) already incorporate all relations between different distribution amplitudes at the flavor symmetric point (cf. eq. (4.74)). Note that these relations will be fulfilled to all orders in BChPT. We find for the ensemble H101 which simulates the flavor symmetric case (see table 4.8), that the corresponding relations for the normalization constants and higher moments are fulfilled down to machine precision for each

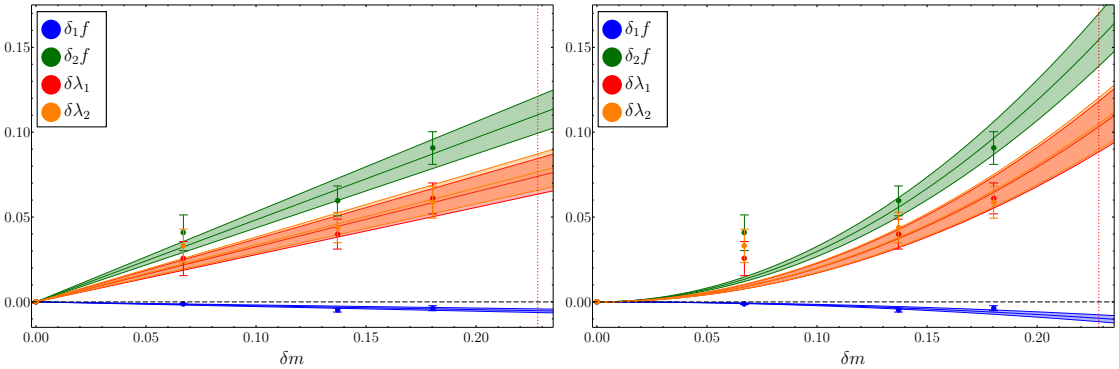

Figure 4.5: Results for the quantities defined in eq. (4.136) are shown, along with linear and quadratic fits. Note that the curves for $\delta\lambda_1$ and $\delta\lambda_2$ lie almost on top of each other.

configuration. In addition to that the SU(3) breaking is (at leading one-loop accuracy in BChPT) constrained by the relations (4.80) and (4.81). To check how good the constraints on the flavor breaking are satisfied by our lattice ensembles we perform two combined fits to the lattice data: a *constrained* fit, where the constraints are enforced, and an *unconstrained* one, where we ignore them. Note that both versions take into account the constraints at the flavor symmetric point.

In figures 4.6–4.11 we show the constrained (left) and the unconstrained (right) combined fits to the lattice data for the normalization constants and the first moments of the leading twist DAs. We use $F_\star = 112$ MeV (cf. ref. [135]), $D = 0.72$ and $F = 0.54$ as input values. The latter lie within the range of typical estimates used in the literature, see, e.g., refs. [182–187]. For most of the measured quantities we find that the SU(3) breaking constraints are fulfilled reasonably well. This manifests itself in comparable values of χ^2 per degree of freedom for both the unconstrained fit, where the symmetry constraints are ignored, and the constrained fit, where the symmetry relations are enforced. Especially for λ_1^B and λ_T^Λ, as well as for the first moments of Φ_-^B and Π^Λ (φ_{10}^B and π_{10}^Λ), which have the same chiral behavior as λ_1^B and λ_T^Λ, one finds an extraordinarily good agreement with the lattice data (cf. figures 4.7 and 4.11). Also for the first moments φ_{11}^B and $\pi_{11}^{B\neq\Lambda}$, which appear in Φ_+^B and $\Pi^{B\neq\Lambda}$, and are predicted to have the same chiral logarithms as the couplings f^B and $f_T^{B\neq\Lambda}$, the constraints are fulfilled within errors (cf. figure 4.10). In contrast, for the leading twist normalization constants f^B and $f_T^{B\neq\Lambda}$, as well as for $\varphi_{00,(1)}^B$ and $\pi_{00,(1)}^{B\neq\Lambda}$ (which have to coincide with f^B and $f_T^{B\neq\Lambda}$ in the continuum), these relations seem to be broken rather badly (cf. figures 4.6 and 4.9). Also for λ_2^B the agreement is not really flawless (cf. figure 4.8).

We can summarize that leading one-loop BChPT can qualitatively describe our data, even though in some cases the observed SU(3) breaking cannot be reproduced by the constrained fit. This might indicate that for these quantities higher order BChPT effects are particularly large. However, the observed discrepancies could also be caused by systematic errors in the lattice data, for which finite volume and discretization effects are prominent candidates. In particular lattice spacing effects have already been identified as a major source of systematic uncertainty in the two-flavor calculation of ref. [37], where it was also argued that for the leading twist

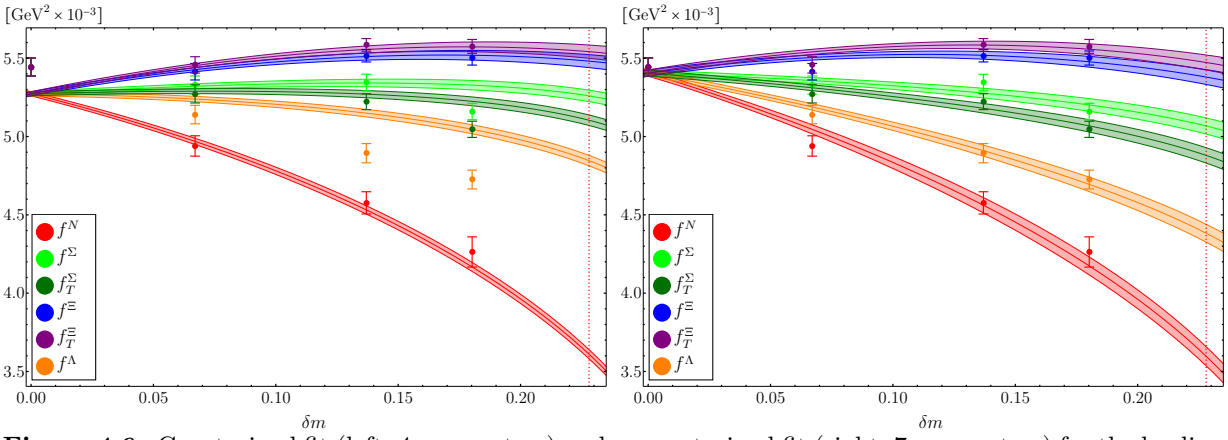

Figure 4.6: Constrained fit (left, 4 parameters) and unconstrained fit (right, 7 parameters) for the leading twist normalization constants f^N, f^Σ, f_T^Σ, f^Ξ, f_T^Ξ and f^Λ.

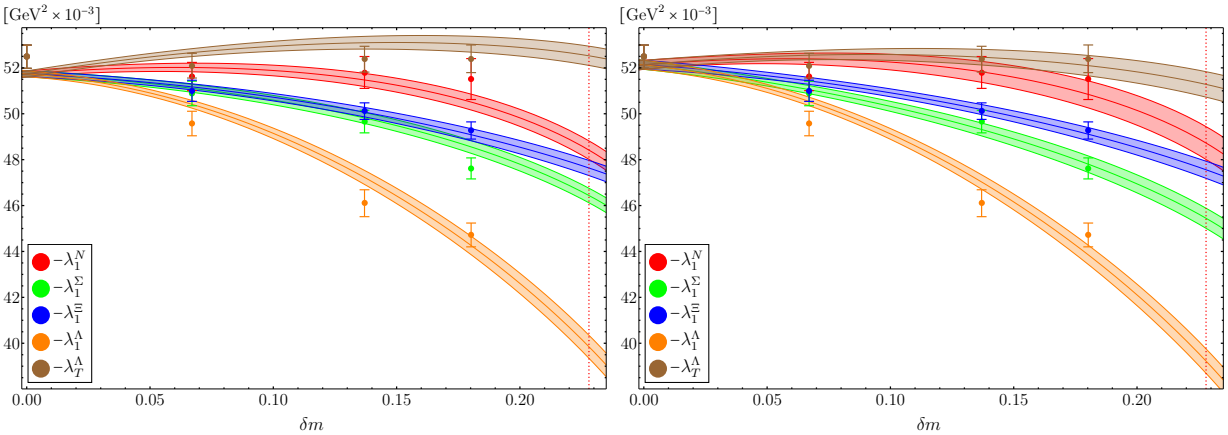

Figure 4.7: Constrained fit (left, 4 parameters) and unconstrained fit (right, 6 parameters) for the chiral-odd higher twist normalization constants λ_1^N, λ_1^Σ, λ_1^Ξ, λ_1^Λ and λ_T^Λ.

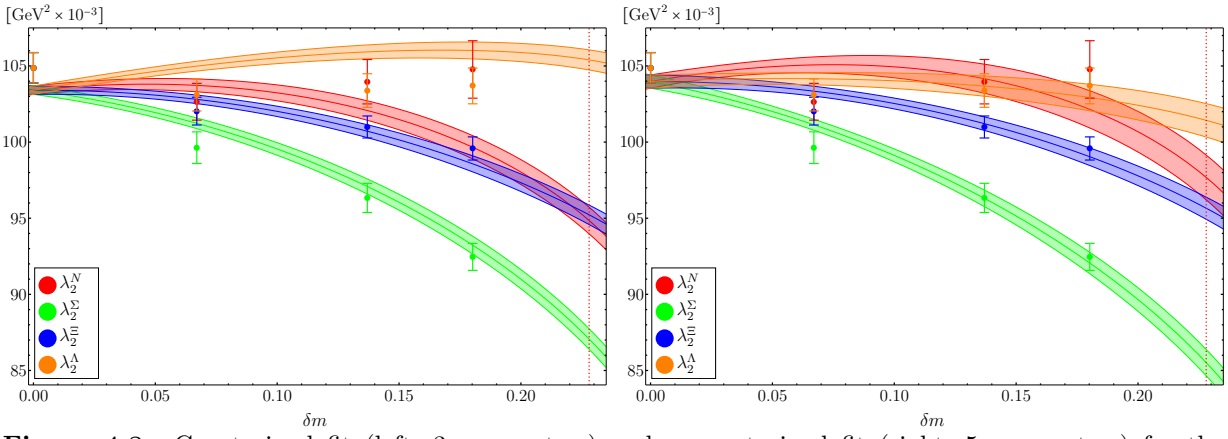

Figure 4.8: Constrained fit (left, 3 parameters) and unconstrained fit (right, 5 parameters) for the chiral-even higher twist normalization constants λ_2^N, λ_2^Σ, λ_2^Ξ and λ_2^Λ.

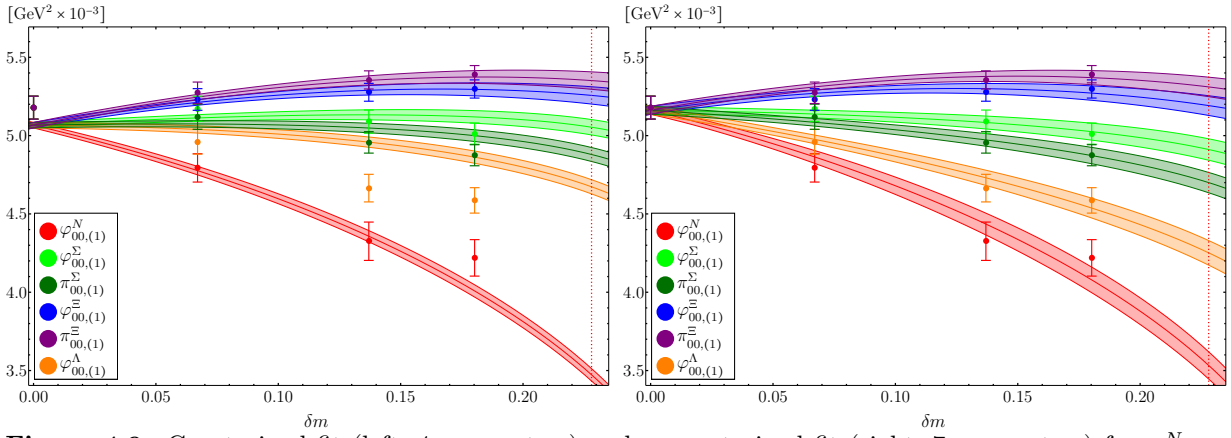

Figure 4.9: Constrained fit (left, 4 parameters) and unconstrained fit (right, 7 parameters) for $\varphi^N_{00,(1)}$, $\varphi^\Sigma_{00,(1)}$, $\pi^\Sigma_{00,(1)}$, $\varphi^\Xi_{00,(1)}$, $\pi^\Xi_{00,(1)}$ and $\varphi^\Lambda_{00,(1)}$ of the leading twist DAs Φ^B_+ and $\Pi^{B\neq\Lambda}$. These moments should be equivalent to the leading twist normalization constants f^B and $f_T^{B\neq\Lambda}$ in the continuum (cf. figure 4.6).

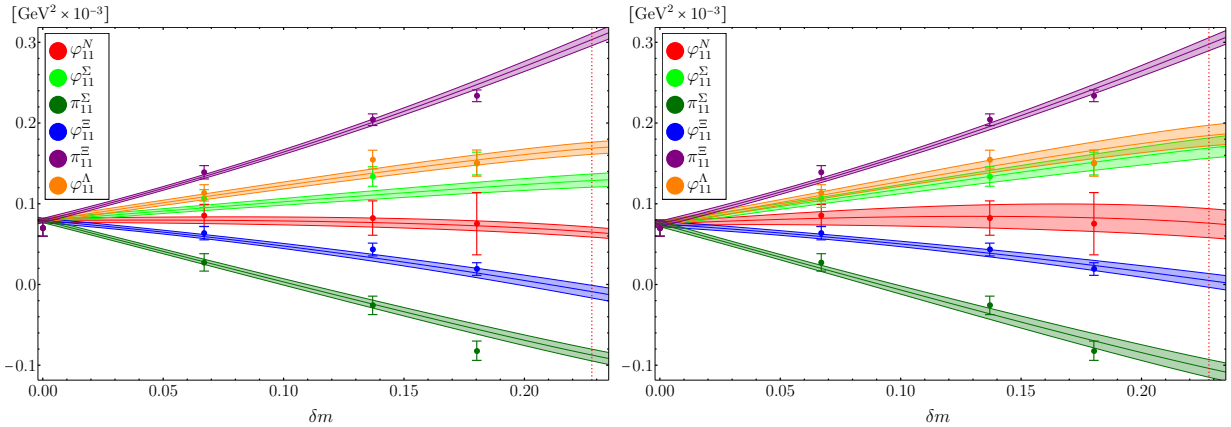

Figure 4.10: Constrained fit (left, 4 parameters) and unconstrained fit (right, 7 parameters) for the first moments φ^N_{11}, φ^Σ_{11}, π^Σ_{11}, φ^Ξ_{11}, π^Ξ_{11} and φ^Λ_{11} of the leading twist DAs Φ^B_+ and $\Pi^{B\neq\Lambda}$.

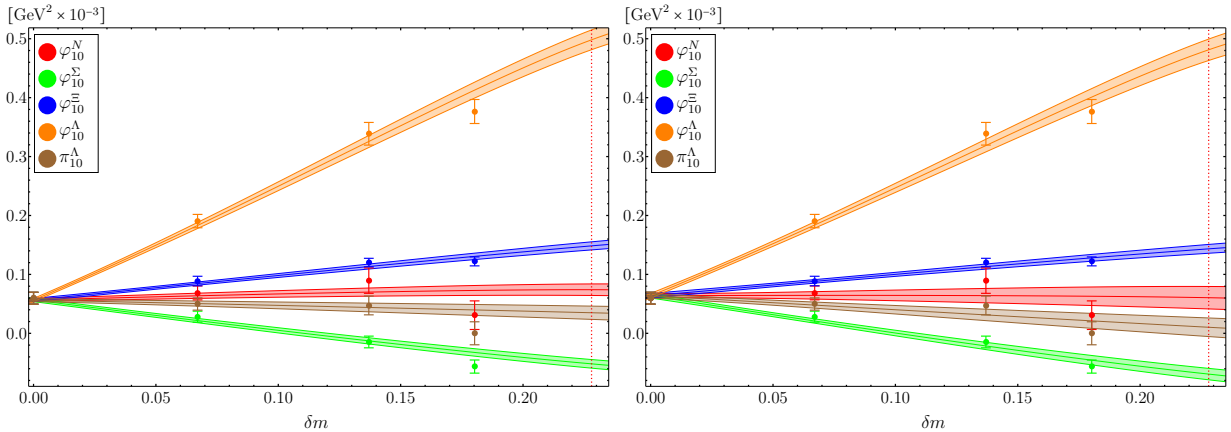

Figure 4.11: Constrained fit (left, 4 parameters) and unconstrained fit (right, 6 parameters) for the first moments φ^N_{10}, φ^Σ_{10}, φ^Ξ_{10}, φ^Λ_{10} and π^Λ_{10} of the leading twist DAs Φ^B_- and Π^Λ.

normalization constants discretization effects are expected to be larger than for the higher twist couplings.

A heuristic parametrization of the leading discretization effects can be constructed by introducing a multiplicative factor into the extrapolation formulas. The leading corrections are linear in the lattice spacing, since the operators we use are not $\mathcal{O}(a)$ improved. At fixed mean quark mass this would yield, for instance, for the leading twist couplings:

$$f^B = g^B_{\Phi+}(\delta m)\big(1 + aC + a\delta m D^B\big)\big(f^\star + \delta m \Delta f^B\big) \;, \tag{4.138a}$$

$$f_T^{B\neq\Lambda} = g^B_{\Pi}(\delta m)\big(1 + aC + a\delta m D^B_T\big)\big(f^\star + \delta m \Delta f^B_T\big) \;. \tag{4.138b}$$

The constant C has to be equal for all baryons in the octet while the $D^B_{(T)}$ can be different and are not necessarily subject to the same constraints as $\Delta f^B_{(T)}$. One can easily convince oneself that, at nonzero lattice spacing, terms $\mathcal{O}(a\delta m)$ can override the effect of the constraints on SU(3) flavor symmetry breaking given in eqs. (4.80) and (4.81).

In the present context we cannot study discretization effects, since we only analyze data at a single lattice spacing. Therefore, for the time being, the difference between chiral extrapolations using constrained and unconstrained fits has to be interpreted as evidence for systematic uncertainties.

4.6.4 Numerical results

The results of the chiral extrapolations as shown in figures 4.6–4.11 are summarized in table 4.9 (constrained fit) and table 4.10 (unconstrained fit). For all quantities the error refers to a combined statistical and extrapolation error. We neither give an estimate of the uncertainty due to the renormalization procedure (see ref. [75]) nor do we provide an estimate for the systematic uncertainty of the chiral extrapolation due to higher order effects (which could be obtained by a variation of the chiral renormalization scale and by a variation of input parameters), since both effects are small compared to the systematic uncertainty due to discretization effects. These errors will become relevant for future studies, if they contain ensembles with multiple lattice spacings allowing for a controlled continuum extrapolation. Note, however, that our results for the momentum sums $\varphi^B_{00,(1)}$ and $\pi^B_{00,(1)}$ defined in eq. (4.131) are within 5% of the corresponding couplings, cf. eq. (4.132), indicating that discretization errors in the derivatives are under control. We do not expect significant finite volume effects [36, 37, 188], since all our ensembles have values of $m_\pi L \gtrsim 4$ and at the same time $L > 2.7$ fm, cf. table 4.8. As discussed above, for some quantities the difference between constrained and unconstrained chiral extrapolations is sizable and can be viewed as part of the systematic uncertainty. Since the overall quality of the unconstrained fit is better (χ^2 per degree of freedom is smaller than 1.5 for all unconstrained fits), we present the corresponding numbers as our final results for this lattice spacing (see table 4.10). All further tables and figures in this section are generated using these values.

In table 4.11 we compare the central values of our $N_f = 2 + 1$ results (unconstrained fit, see table 4.10) with the $N_f = 2$ lattice study for the nucleon [37] and the Chernyak–Ogloblin–Zhitnitsky (COZ) model [150]. In the lattice study [37] the continuum extrapolation has been

Table 4.9: Couplings and shape parameters obtained by the constrained fit method. All values are given in units of GeV^2 in the $\overline{\mathrm{MS}}$ scheme at a scale $\mu^2 = 4\,\mathrm{GeV}^2$. The number in the parentheses gives a combined statistical and chiral extrapolation error.

B	N	Σ	Ξ	Λ
$f^B \times 10^3$	3.61(3)	5.26(4)	5.48(4)	4.85(3)
$f_T^B \times 10^3$	3.61(3)	5.10(3)	5.54(4)	—
$\varphi_{11}^B \times 10^3$	0.06(1)	0.13(1)	−0.01(1)	0.17(1)
$\pi_{11}^B \times 10^3$	0.06(1)	−0.09(1)	0.30(1)	—
$\varphi_{10}^B \times 10^3$	0.074(10)	−0.052(7)	0.15(1)	0.50(2)
$\pi_{10}^B \times 10^3$	—	—	—	0.035(11)
$\varphi_{00,(1)}^B \times 10^3$	3.47(4)	5.05(5)	5.26(6)	4.67(5)
$\pi_{00,(1)}^B \times 10^3$	3.47(4)	4.88(4)	5.35(6)	—
$\lambda_1^B \times 10^3$	−48.4(4)	−46.4(3)	−47.6(3)	−40(1)
$\lambda_T^B \times 10^3$	—	—	—	−52.5(4)
$\lambda_2^B \times 10^3$	95(1)	87(1)	95(1)	105(1)

Table 4.10: Couplings and shape parameters obtained from the unconstrained fits. All values are given in units of GeV^2 in the $\overline{\mathrm{MS}}$ scheme at a scale $\mu^2 = 4\,\mathrm{GeV}^2$. The number in the parentheses gives a combined statistical and chiral extrapolation error. The numbers from this table should be quoted as the final results at our lattice spacing.

B	N	Σ	Ξ	Λ
$f^B \times 10^3$	3.60(6)	5.07(5)	5.38(5)	4.38(6)
$f_T^B \times 10^3$	3.60(6)	4.88(5)	5.47(5)	—
$\varphi_{11}^B \times 10^3$	0.08(2)	0.17(1)	0.01(1)	0.18(1)
$\pi_{11}^B \times 10^3$	0.08(2)	−0.10(1)	0.30(1)	—
$\varphi_{10}^B \times 10^3$	0.06(2)	−0.07(1)	0.14(1)	0.48(2)
$\pi_{10}^B \times 10^3$	—	—	—	0.01(2)
$\varphi_{00,(1)}^B \times 10^3$	3.53(9)	4.91(7)	5.19(6)	4.25(8)
$\pi_{00,(1)}^B \times 10^3$	3.53(9)	4.70(6)	5.31(6)	—
$\lambda_1^B \times 10^3$	−49(1)	−45.4(4)	−47.6(4)	−39(1)
$\lambda_T^B \times 10^3$	—	—	—	−51(1)
$\lambda_2^B \times 10^3$	98(1)	86(1)	96(1)	101(1)

carried out for the normalization constants and resulted in a decrease of f^N by $\approx 30\%$ and a somewhat smaller decrease for $\lambda_{1,2}^N$ for lattice spacings $a \approx 0.06 - 0.08$ fm. Since we use a similar lattice action, we have to expect discretization effects of the same magnitude. This is compatible with the fact that our $N_f = 2 + 1$ results for the nucleon normalization constants (at $a \approx 0.0857$ fm) are approximately 30% larger for f^N and about 20% larger in the case of λ_1^N and λ_2^N compared to the final results of ref. [37]. Nevertheless, this shows that a thorough continuum extrapolation will be of utmost importance and is a primary goal for future studies.

For the first order shape parameters of the leading twist DA of the nucleon, $\varphi_{11}^N = \pi_{11}^N$ and φ_{10}^N, our results agree within errors with the values obtained from two-flavor lattice QCD [37] and with

Table 4.11: Comparison of the central values of our $N_f = 2 + 1$ results (unconstrained fit, see table 4.10) with the $N_f = 2$ lattice study for the nucleon [37] and the Chernyak–Ogloblin–Zhitnitsky (COZ) model [150]. All values are given in units of GeV^2. All quantities have been converted to the conventions established in this work and rescaled to $\mu^2 = 4\,\text{GeV}^2$, cf. ref. [75]. Note that f_Λ^T in ref. [150] is proportional to the first moment π_{10}^Λ in our nomenclature.

B	work	method	$f^B \times 10^3$	$f_T^B \times 10^3$	$\varphi_{11}^B \times 10^3$	$\pi_{11}^B \times 10^3$	$\varphi_{10}^B \times 10^3$	$\pi_{10}^B \times 10^3$
N	ours	$N_f = 2+1$	3.60	3.60	0.08	0.08	0.06	—
	[37]	$N_f = 2$	2.84	2.84	0.085	0.085	0.082	—
	[150]	COZ	4.55	4.55	0.885	0.885	0.748	—
Σ	ours	$N_f = 2+1$	5.07	4.88	0.17	−0.10	−0.069	—
	[150]	COZ	4.65	4.46	1.11	0.511	0.523	—
Ξ	ours	$N_f = 2+1$	5.38	5.47	0.01	0.30	0.14	—
	[150]	COZ	4.83	4.92	0.685	1.10	0.883	—
Λ	ours	$N_f = 2+1$	4.38	—	0.18	—	0.48	0.01
	[150]	COZ	4.69	—	1.05	—	1.39	1.32

results extracted from light-cone sum rules for the nucleon electromagnetic form factors [153].[7] In particular we confirm the approximate equality $\varphi_{10}^N \approx \varphi_{11}^N$. As reported in ref. [37], modern lattice simulations and light-cone sum rule calculations yield estimates of the first moments of the nucleon DA that are one order of magnitude smaller than values obtained from traditional SVZ sum rules, cf. refs. [150, 189]. Comparing our measurements to the values used in the COZ model [150] (see table 4.11) one finds that this observation is not only true for nucleons but also for hyperons.

Interestingly, the SU(3) breaking in the shape parameters of the octet baryons turns out to be very large, e.g., $\pi_{11}^\Xi \gtrsim 3\varphi_{11}^N$ and $\varphi_{10}^\Lambda \gtrsim 7\varphi_{10}^N$, and some parameters even change their sign. The effect is much stronger than in QCD sum rule calculations [150], even though the absolute values are much smaller. This large flavor symmetry breaking is somewhat surprising and is in stark contrast to the situation for the normalization constants where the differences between octet baryons are at most 50%. As a consequence, SU(3) breaking in hard exclusive reactions that are sensitive to the deviations of the DAs from their asymptotic form can be enhanced.

The SU(3) breaking in the shape of the leading twist DAs can be represented in many ways. Consider, e.g., normalized combinations of symmetric and antisymmetric DAs

$$\phi^B = \frac{\Phi_+^B + \Phi_-^B}{f^B}\,, \qquad \varpi^{B\neq\Lambda} = \frac{\Pi^B + \Phi_-^B}{f_T^B}\,, \qquad \varpi^\Lambda = \frac{\Phi_+^\Lambda + \Pi^\Lambda}{f^\Lambda}\,, \tag{4.139}$$

all of which are equal both in the asymptotic limit, $\phi^{\text{as}} \equiv \phi^{B,\text{as}} = \varpi^{B,\text{as}} = 120x_1x_2x_3$, and in the limit of exact flavor symmetry, $\phi^\star \equiv \phi^{B\star} = \varpi^{B\star}$. Due to isospin symmetry $\varpi^N = \phi^N$. Hence, there are seven independent functions that can be used to visualize the deviations from the DA $\phi^\star$ in the SU(3) flavor symmetry limit. These seven functions, $\phi^N - \phi^*$, etc., are shown

[7] Our φ_{nk}^N correspond to $f_N\varphi_{nk}^N$ in refs. [37, 153]. In contrast to the normalization constants, the shape parameters have not been extrapolated to the continuum in ref. [37].

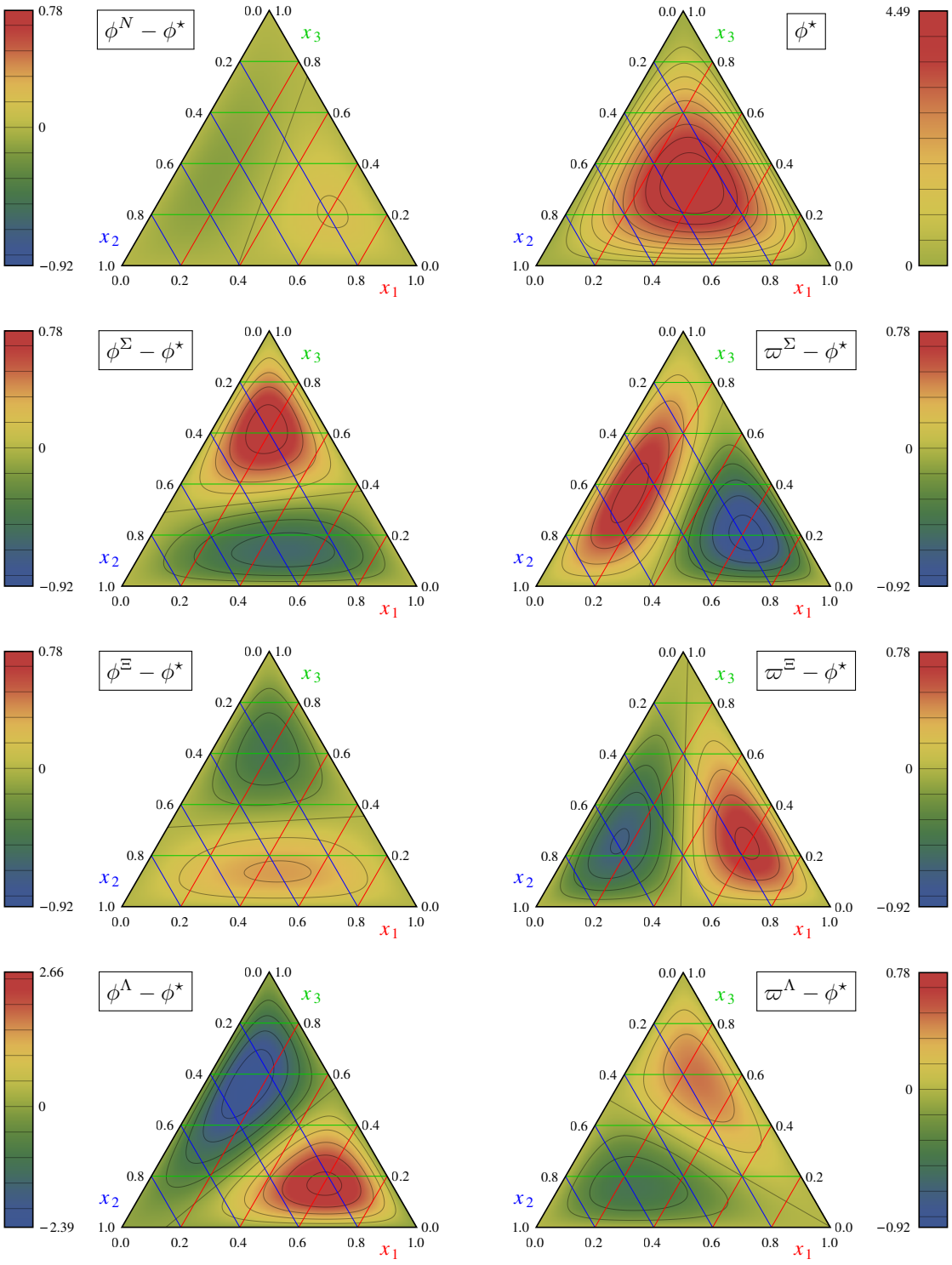

Figure 4.12: Barycentric plots ($x_1 + x_2 + x_3 = 1$) visualizing the SU(3) breaking in the shape functions (4.139). The top right figure displays the momentum distribution for the flavor symmetric case, while the others show the deviations from it at the physical point.

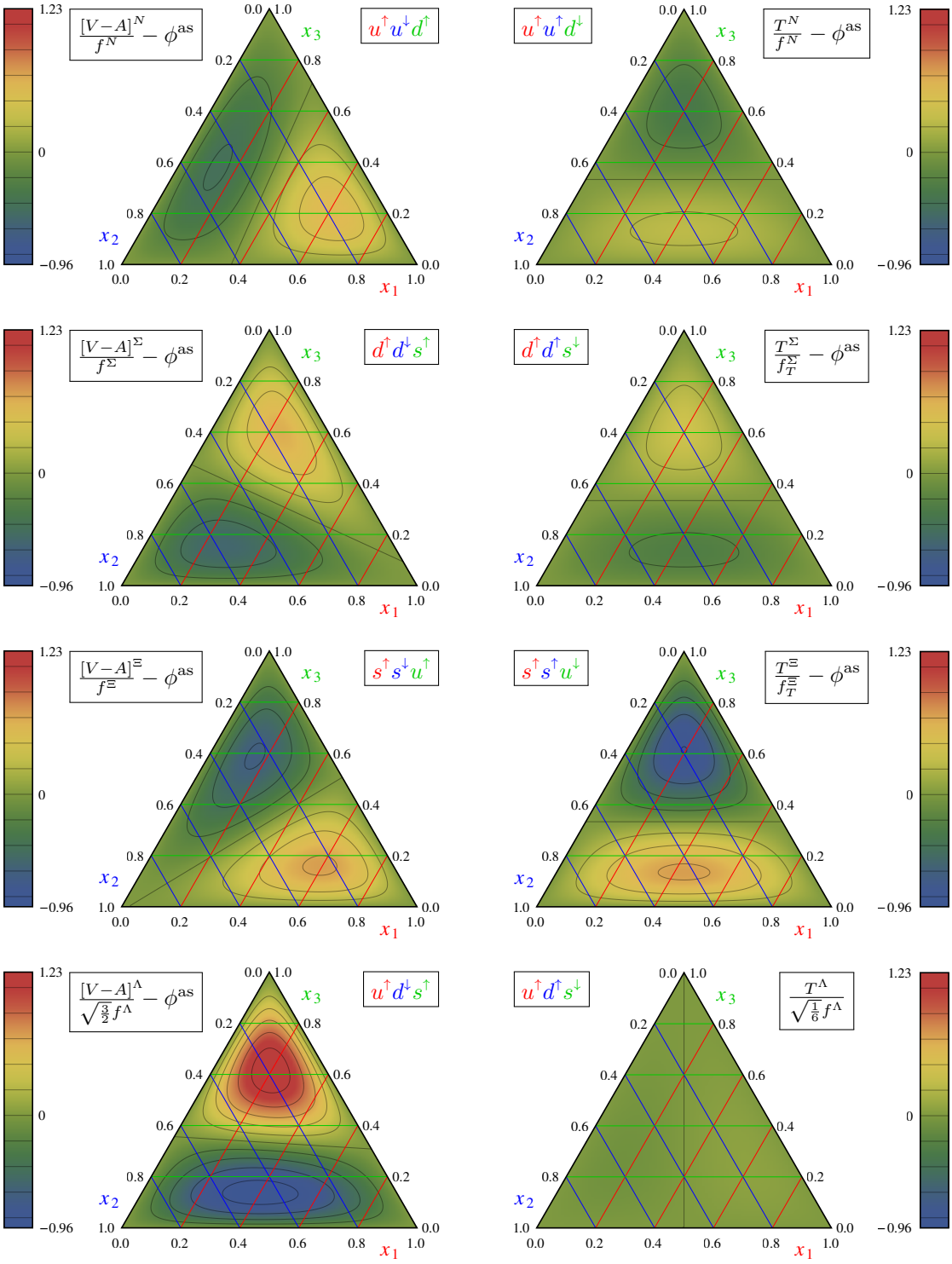

Figure 4.13: Barycentric plots ($x_1 + x_2 + x_3 = 1$) showing the deviations of the DAs $[V-A]^B$ and T^B from the asymptotic shape $\phi^{\rm as} \equiv 120 x_1 x_2 x_3$. T^Λ vanishes in the asymptotic limit. In this representation the coordinates x_i directly correspond to quarks of definite flavor and helicity.

in figure 4.12 together with $\phi^\star$ itself, which is almost (but not exactly) symmetric in x_1, x_2, x_3 due to small (but nonvanishing) values of $\varphi_{11}^\star$ and $\varphi_{10}^\star$ (cf. figures 4.10 and 4.11).

In phenomenological applications it is more convenient to consider the standard representation of DAs in terms of $[V-A]^B$ and T^B. In this way also the physical interpretation is more straightforward as every momentum fraction can be attributed to a quark of definite helicity and flavor. $[V-A]^B$ and T^B do not coincide, however, at the flavor symmetric point, so that for these DAs it is more natural to show the deviations from the asymptotic shape ϕ^{as} rather than from ϕ^*, see figure 4.13. The plots in the left and in the right column show normalized DAs $[V-A]^B$ and T^B after the subtraction of the asymptotic DA. Note that the amplitudes $T^{B\neq\Lambda}$ are symmetric under the interchange of x_1 and x_2 by construction. The approximate symmetry of $[V-A]^N$ under the exchange of x_2 and x_3 is, in contrast, nontrivial. It is due to the approximate equality of the two nucleon shape parameters $\varphi_{10}^N \approx \varphi_{11}^N$ mentioned above. In the nucleon Fock state $u^\uparrow u^\downarrow d^\uparrow$ this is equivalent to a symmetric distribution of momentum between the second and third quark. In agreement with earlier studies [37, 150, 190], we observe that the "leading" $u^\uparrow$ quark, which has the same helicity as the nucleon, carries a larger momentum fraction. In the $u^\uparrow u^\uparrow d^\downarrow$ nucleon state, which is described by T^N, the peak of the distribution is shifted towards the two u quarks in a symmetric manner. T^N, however, is not an independent DA. Taking into account the isospin relation (4.68a), the spin-flavor structure of the nucleon light-cone wave function (4.76) can be presented, schematically, as $[V-A]^N u^\uparrow(u^\downarrow d^\uparrow - d^\downarrow u^\uparrow)$. In this picture our result for $[V-A]^N$ corresponds to a shift of the momentum distribution towards the $u^\uparrow$ quark, which carries the nucleon helicity, and the symmetry under $x_2 \leftrightarrow x_3$ may be interpreted as an indication for the remaining valence quarks forming a dynamical scalar "diquark" (scalar in this context means that the diquark does not carry helicity), which is assumed in many models.

For the isospin-nonsinglet baryons one can identify two competing patterns: first, the strange quarks carry, in general, a larger fraction of the momentum. Second, in the $|\uparrow\downarrow\uparrow\rangle$ state the first quark has a larger momentum fraction than the second, while in the $|\uparrow\uparrow\downarrow\rangle$ state the first two quarks behave identically. These rules do not apply to the Λ baryon due to its reversed symmetry properties, see eq. (4.10): in the $u^\uparrow d^\downarrow s^\uparrow$ state the maximum of the distribution is shifted towards the s quark. T^Λ is a special case, since it does not contain the leading asymptotic part due to the antisymmetry under exchange of x_1 and x_2. Our result shows, that also the next-to-leading asymptotic contribution determined by the shape parameter π_{10}^Λ is very small. Hence, for the Λ baryon, the Fock state $u^\uparrow d^\uparrow s^\downarrow$ is expected to be highly suppressed. Taking this result into account (i.e., neglecting T^Λ), the spin-flavor structure of the lambda light-cone wave function (4.77) reads, schematically, $[V-A]^\Lambda(u^\uparrow d^\downarrow - d^\uparrow u^\downarrow)s^\uparrow$. The approximate symmetry of $[V-A]^\Lambda$ under exchange of x_1 and x_2 indicates that the light quarks flavors form a dynamical scalar "diquark". The momentum distribution is shifted towards the helicity-carrying $s^\uparrow$ quark. The similarity to the nucleon case is striking.

Table 4.12: Normalized first moments of the DAs $[V-A]^B$ and $T^{B\neq\Lambda}$ in the $\overline{\text{MS}}$ scheme at a scale $\mu^2 = 4\ \text{GeV}^2$, obtained via eq. (4.141).

B	N		Σ		Ξ		Λ	
$\langle x_1\rangle^B$	$u^\uparrow$	0.358	$d^\uparrow$	0.331	$s^\uparrow$	0.361	$u^\uparrow$	0.310
$\langle x_2\rangle^B$	$u^\downarrow$	0.319	$d^\downarrow$	0.310	$s^\downarrow$	0.333	$d^\downarrow$	0.304
$\langle x_3\rangle^B$	$d^\uparrow$	0.323	$s^\uparrow$	0.359	$u^\uparrow$	0.306	$s^\uparrow$	0.386
$\langle x_1\rangle_T^B$	$u^\uparrow$	0.340	$d^\uparrow$	0.326	$s^\uparrow$	0.352	—	
$\langle x_2\rangle_T^B$	$u^\uparrow$	0.340	$d^\uparrow$	0.326	$s^\uparrow$	0.352	—	
$\langle x_3\rangle_T^B$	$d^\downarrow$	0.319	$s^\downarrow$	0.348	$u^\downarrow$	0.296	—	

To quantify this picture, one can consider normalized first moments of $[V-A]^B$ and T^B defined as

$$\langle x_i\rangle^B = \frac{1}{\varphi^B_{00,(1)}}\int[dx]\ x_i[V-A]^B\,, \qquad \langle x_i\rangle_T^{B\neq\Lambda} = \frac{1}{\pi^B_{00,(1)}}\int[dx]\ x_i T^B\,, \tag{4.140}$$

which are usually referred to as momentum fractions in the literature. Note that this name is imprecise since the averaging is done with the DA and not a wave function squared, and, in particular, for T^Λ, which has no asymptotic part, the interpretation as momentum fractions breaks down completely. The $\langle x_i\rangle$ can be calculated in terms of the shape parameters as follows:

$$\langle x_1\rangle^{B\neq\Lambda} = \frac{1}{3}+\frac{1}{3}\widehat{\varphi}^B_{11}+\widehat{\varphi}^B_{10}\,, \quad \langle x_2\rangle^{B\neq\Lambda} = \frac{1}{3}-\frac{2}{3}\widehat{\varphi}^B_{11}\,, \quad \langle x_3\rangle^{B\neq\Lambda} = \frac{1}{3}+\frac{1}{3}\widehat{\varphi}^B_{11}-\widehat{\varphi}^B_{10}\,, \tag{4.141a}$$

$$\langle x_1\rangle_T^{B\neq\Lambda} = \frac{1}{3}+\frac{1}{3}\widehat{\pi}^B_{11}\,, \quad \langle x_2\rangle_T^{B\neq\Lambda} = \frac{1}{3}+\frac{1}{3}\widehat{\pi}^B_{11}\,, \quad \langle x_3\rangle_T^{B\neq\Lambda} = \frac{1}{3}-\frac{2}{3}\widehat{\pi}^B_{11}\,, \tag{4.141b}$$

$$\langle x_1\rangle^{\Lambda} = \frac{1}{3}+\frac{1}{3}\widehat{\varphi}^\Lambda_{11}-\frac{1}{3}\widehat{\varphi}^\Lambda_{10}\,, \quad \langle x_2\rangle^{\Lambda} = \frac{1}{3}-\frac{2}{3}\widehat{\varphi}^\Lambda_{11}\,, \quad \langle x_3\rangle^{\Lambda} = \frac{1}{3}+\frac{1}{3}\widehat{\varphi}^\Lambda_{11}+\frac{1}{3}\widehat{\varphi}^\Lambda_{10}\,, \tag{4.141c}$$

where

$$\widehat{\varphi}^B_{nk} = \frac{\varphi^B_{nk}}{\varphi^B_{00,(1)}}\,, \qquad \widehat{\pi}^{B\neq\Lambda}_{11} = \frac{\pi^B_{11}}{\pi^B_{00,(1)}}\,. \tag{4.142}$$

The results are summarized in table 4.12. They support the qualitative picture suggested by the discussion of figure 4.13.

Finally, we consider the higher twist matrix elements that are related to the normalization of the P-wave light-cone wave functions and also appear as low-energy constants in effective theories for generic GUT models [172]. We obtain, for the nucleon, $\lambda_2^N \approx -2\lambda_1^N$, which is well known, see, e.g., refs. [118, 191, 192]. The same relation also holds for the Σ and Ξ hyperons (for the Σ it is not fulfilled as accurately as for the others), but not for the Λ baryon. Instead, we find $\lambda_2^\Lambda \approx -2\lambda_T^\Lambda$. Actually, all these relations hold, since matrix elements of operators containing $q^a C\mathbb{1} q^b$ are approximately zero for arbitrary quark flavors a and b. As pointed out in ref. [191] these matrix elements vanish exactly in the nonrelativistic quark model limit and it is noteworthy that we find only very small corrections to it at the hadronic scale $\mu = 2$ GeV, in particular for the nucleons, the Ξ and the Λ baryons.

4.7 Summary

In this chapter we have presented the first analysis of baryon octet light-cone DAs in the framework of three-flavor BChPT (see also our work [139]). At next-to-leading order accuracy in the chiral counting scheme, we obtain the leading quark mass dependence and (automatically) the leading $\mathrm{SU}(3)_f$ breaking effects. Describing the baryon octet simultaneously we are able to unify and systemize the efforts made in refs. [76, 150–152, 193].

An important insight to be gained from our results is of qualitative nature: in the chiral-odd sector the chiral behavior (i.e., the contained chiral logarithms) of a specific moment does not depend on its twist, but on whether it contributes to the $\Phi^B_{+,i}$ or $\Phi^B_{-,i}$ amplitudes (see eq. (4.70)). Those contributing to the "+" ("−") amplitudes have the same chiral logarithms as f^B (λ_1^B). Therefore the odd moments of the leading twist DA behave like λ_1^B instead of (as one might have expected) f^B. This result is consistent with an earlier two-flavor calculation, where it was found that the odd first and second moments of the leading twist DA have the same chiral logarithms as λ_1^N (see appendix of ref. [37]).

In section 4.5 we provide a set of DAs that parametrize the complete baryon octet (including the Λ baryon) in a minimal way and do not mix under chiral extrapolation. Eqs. (4.85) and (4.102) are our main results. They describe the quark mass dependence of the baryon octet DAs (including all higher twist amplitudes) in a very compact manner. The results are of particular importance for the interpretation and extrapolation of lattice QCD data performed in section 4.6, due to the significant decrease in number of parameters. For the same reason our results are relevant for QCD sum rule analyses and for model building. In particular the relations (4.74), that have to be fulfilled exactly in the flavor symmetric limit, provide helpful consistency checks for both lattice QCD and sum rule calculations.

In section 4.6 we have presented the first $N_f = 2{+}1$ lattice QCD analysis of the normalization constants and (leading twist) first moments of the octet baryon distribution amplitudes with pion masses down to 222 MeV (published in [75]). The results are extrapolated to the physical point using three-flavor BChPT formulas given eq. (4.85). Numerical values are given in table 4.10. Note, however, that our analysis lacks a continuum extrapolation which can have a large impact on the DAs (cf. ref. [37]). Nevertheless our analysis yields first qualitative insights on the octet DAs that will be discussed in the following paragraphs.

We find significant SU(3) flavor breaking effects for the leading twist normalization constants

$$\frac{f^\Sigma}{f^N} = 1.41(4)\ , \quad \frac{f_T^\Sigma}{f^N} = 1.36(4)\ , \quad \frac{f^\Xi}{f^N} = 1.50(4)\ , \quad \frac{f_T^\Xi}{f^N} = 1.52(4)\ , \quad \frac{f^\Lambda}{f^N} = 1.22(4)\ , \tag{4.143}$$

and somewhat smaller symmetry breaking for the higher twist couplings

$$\frac{\lambda_1^\Sigma}{\lambda_1^N} = 0.93(2)\ , \qquad \frac{\lambda_1^\Xi}{\lambda_1^N} = 0.98(2)\ , \qquad \frac{\lambda_1^\Lambda}{\lambda_1^N} = 0.81(2)\ , \qquad \frac{\lambda_T^\Lambda}{\lambda_1^N} = 1.05(3)\ , \tag{4.144}$$

where the number in parentheses gives a combined statistical and chiral extrapolation error. It is likely that these ratios are less sensitive to discretization effects than the couplings themselves.

To first order in the SU(3) symmetry breaking parameter we have derived the following relation between the DAs of the Σ and Ξ hyperons (see eq. (4.94)):

$$\Phi^{\Sigma}_{+,i}(x_1,x_2,x_3) - \Pi^{\Sigma}_{i}(x_1,x_2,x_3) = \Pi^{\Xi}_{i}(x_1,x_2,x_3) - \Phi^{\Xi}_{+,i}(x_1,x_2,x_3)\ , \tag{4.145}$$

which has the same theory status as the renowned Gell-Mann–Okubo relation for the masses. It is satisfied with similarly high accuracy $\sim 1\%$ in our data for the leading twist DAs.

We find that deviations from the asymptotic DAs (quantified by the values of shape parameters) are small for all baryons in the octet. This result is in agreement with the findings of ref. [37] for the nucleon, but it differs from old QCD sum rule calculations [150], which favor larger deviations. The SU(3) breaking in the shape parameters is, however, very large, see table 4.10. For the isospin-nonsinglet baryons one can identify two competing patterns: first, the strange quarks carry, in general, a larger fraction of the momentum. Second, in the $f^{\uparrow}g^{\downarrow}h^{\uparrow}$ state (using our flavor conventions (4.12)) the first quark is favored over the second, while in the $f^{\uparrow}g^{\uparrow}h^{\downarrow}$ state the first two quarks behave identically. These rules do not apply to the Λ baryon due to its reversed symmetry properties, see eq. (4.10). The interplay of these two patterns leads to the rather elaborate structure shown in figure 4.13. For the proton, the neutron and the Λ, our results for the leading twist DAs at the scale $\mu = 2$ GeV are consistent with quark-diquark models that approximate the baryon by a leading quark (up for the proton, down for the neutron and strange for the Λ), which carries the helicity and a disproportionately large fraction of the momentum, and a scalar diquark formed from one up and one down quark.

CHAPTER 5

Conclusion and outlook

In the following we will highlight selected main results of this work. For more details the reader may consult the individual summary sections in the respective chapters.

In chapter 3 we have extended the calculation performed in ref. [34] for first moments of chiral-even nucleon GPDs to full one-loop order in two-flavor BChPT. The resulting extrapolation formulas are summarized in section 3.5. In contrast to its predecessor, the increased accuracy allows for a correct reproduction of the leading chiral logarithms (known from older heavy baryon ChPT calculations) also for the B-type form factors. The preliminary analysis of $N_f = 2$ lattice data, described in section 3.6, shows that the tradeoff fit ansatz is in agreement with the heavy baryon version, at least for isovector generalized form factors. However, this is hardly surprising, since the problematic triangle diagram (cf. ref. [86]) does not contribute to these quantities. Accordingly, our results do not allow to draw a similar conclusion for isoscalar GFFs, since these may exhibit a nontrivial chiral behavior due to the admixture of the pion GPD via the said Feynman diagram. Therefore, lattice QCD data on the isoscalar form factors would be highly interesting. Unfortunately, the simulation of three-point functions with isoscalar operator insertions is computationally very challenging due to the contribution of disconnected diagrams. For the usual benchmark quantity $\langle x \rangle^{u-d}$ our preliminary analysis leads to a numeric result that overshoots the values extracted from global PDF fits to QCD world data by roughly 20%, in agreement with ref. [128]. As discussed in some detail this discrepancy occurs most likely due to discretization effects, and, until this issue is resolved, one has to expect similarly large deviations also for the nonforward observables.

In chapter 4 we have presented the first analysis of three-quark light-cone DAs (including all higher twist amplitudes) within three-flavor BChPT at leading one-loop accuracy. The results on flavor symmetry and its breaking allow a systematic study of the baryon octet as a whole, unifying efforts made in refs. [76, 150–152, 193], compare section 4.5. The understanding of the underlying symmetry formed the backbone of the analysis of $N_f = 2 + 1$ CLS lattice data described in section 4.6, which provides a first qualitative insight on baryon octet DAs from lattice

QCD. Quantitative results can be obtained in the near future, after the inclusion of upcoming data at smaller lattice spacings, which will enable us to take the continuum limit. In particular, we find that eq. (4.94a), which relates Σ and Ξ DAs and is the theoretical analogue for DAs of the famous Gell-Mann–Okubo mass formula, is fulfilled to high accuracy. In accordance with earlier results for the nucleon (cf. ref. [37]), we find only very modest deviations of the DAs from their asymptotic shape. Nevertheless, we observe that flavor symmetry breaking is pronounced in case of the normalization constants, and even larger for the shape parameters. This leads to the rather elaborate shape of the DAs depicted in the barycentric plots in figure 4.13 on page 110. Interestingly, our results for proton, neutron and Λ leading twist DAs at the scale $\mu = 2$ GeV are consistent with simple quark-diquark models. The latter describe the baryon as a compound of a leading quark (up, down and strange, for proton, neutron and Λ, respectively), which carries the helicity and a disproportionally large fraction of the momentum, and a scalar diquark formed from one up and one down quark of opposite helicity.

Besides the beautiful results it yields, the method used to construct the effective operators in chapter 4 is also interesting from a technical perspective: the nonlocal operator is parametrized as a product of a distribution amplitude with a hadronic operator integrated over all momentum configurations, where the hadronic operator at a specific momentum configuration only contains hadrons at a single spacetime position (cf. eq. (4.18)). This novel proceeding yields the best possible disentanglement of the light-cone dynamics of the internal partons (parametrized in the DAs) from the chiral dynamics of the hadrons. As an outlook, we therefore will only advertise the one most promising of the numerous possible extensions of this work: the treatment of GPDs based on the very same method for operator construction and with the same generality (open Dirac and flavor indices) as the one we have performed for baryon DAs. Such a project is certainly worth the effort, since it would not only yield results for all moments simultaneously (including ordinary form factors), but would also provide information about transversity GPDs. Due to the above stated locality of the hadronic operators, the calculation would (by construction) not suffer from the problems concerning regularization reported in ref. [112] (in said reference the problem has been overcome by the choice of a specific suitable regularization procedure, that cures the deficiencies of the usual operator construction). In particular a calculation within three-flavor BChPT can provide valuable information on flavor symmetry and its breaking, which would simplify a consistent treatment of the numerous (transition) GPDs of the baryon octet considerably. Thus, the results of such a calculation would be a mighty tool, especially in the hands of the lattice analyst who has the pleasure to extract the wealth of information contained in the upcoming CLS data on three-point functions.

Acknowledgements

I am indebted to my colleagues from the Regensburg QCD group and the SFB/TR55. In particular, I want to thank R. Rödl for the joint work on GPD fits, and F. Hutzler and M. Gruber for our close collaboration on baryon DAs. Furthermore, I want to express my gratitude to P. Bruns, who has always found convincing answers for my questions concerning ChPT and physics in general – even for the most heretic and far-fetched ones. I am much obliged to A. Schäfer for his theoretical guidance and physical overview: under his supervision I was always free to follow every emerging and interesting research topic, and I was supported whenever it was necessary. I am deeply grateful to D. Ostermeier, P. Bruns and M. Gruber for their invaluable and tireless proofreading. Last but not least, I want to thank my parents and my beloved girlfriend Michaela for their unconditional and immeasurable support in all imaginable situations.

Appendices

APPENDIX A

General definitions

A.1 Pauli matrices

The Pauli matrices, denoted by σ^i $(i = 1, 2, 3)$, are defined as

$$\sigma^1 = \begin{pmatrix} 0 & 1 \\ 1 & 0 \end{pmatrix}, \qquad \sigma^2 = \begin{pmatrix} 0 & -i \\ i & 0 \end{pmatrix}, \qquad \sigma^3 = \begin{pmatrix} 1 & 0 \\ 0 & -1 \end{pmatrix} . \tag{A.1}$$

They differ from the generators of the SU(2) Lie algebra τ^i by a factor of 2 ($\sigma^i = 2\tau^i$) and obey the commutation relation

$$[\sigma^i, \sigma^j] = 2i\varepsilon^{ijk}\sigma^k , \tag{A.2}$$

where

$$\varepsilon^{ijk} = \begin{cases} +1 , & \text{if } (i,j,k) \text{ is a cyclic permutation of } (1,2,3) , \\ -1 , & \text{if } (i,j,k) \text{ is an anticyclic permutation of } (1,2,3) , \\ 0 , & \text{else .} \end{cases} \tag{A.3}$$

Together with the two-dimensional unity matrix the Pauli matrices yield a basis for the complex 2×2 matrices. One easily finds that they have the following basic properties:

$$\sigma^{i\dagger} = \sigma^i , \qquad \operatorname{tr}\{\sigma^i\} = 0 , \tag{A.4a}$$

$$\det \sigma^i = -1 , \qquad \sigma^i\sigma^j = \delta^{ij}\mathbb{1} + i\varepsilon^{ijk}\sigma^k . \tag{A.4b}$$

Using these properties one can derive eq. (A.2) and the following useful relations:

$$\sigma^{i\,2} = \mathbb{1} , \qquad \operatorname{tr}\{\sigma^i\sigma^j\} = 2\delta^{ij} , \tag{A.5a}$$

$$\{\sigma^i, \sigma^j\} = 2\delta^{ij}\mathbb{1} , \qquad \operatorname{tr}\{\sigma^i\sigma^j\sigma^k\} = 2i\varepsilon^{ijk} . \tag{A.5b}$$

A.2 Gell-Mann matrices

The Gell-Mann matrices λ^i $(i = 1, \ldots, 8)$ are a set of traceless Hermitian 3×3 matrices, which fulfill the commutation relation

$$[\lambda^i, \lambda^j] = 2if^{ijk}\lambda^k \ , \tag{A.6}$$

where the f^{ijk} are the structure constants of the SU(3) group. These are totally antisymmetric and the nonzero elements are given by

$$\begin{aligned} f^{123} &= 1 \ , & f^{147} = f^{246} = f^{257} = f^{345} &= \frac{1}{2} \ , \\ f^{156} = f^{367} &= -\frac{1}{2} \ , & f^{458} = f^{678} &= \frac{\sqrt{3}}{2} \ . \end{aligned} \tag{A.7}$$

The Gell-Mann matrices differ only by a factor of 2 from the usual generators $t^i = \frac{\lambda^i}{2}$, and are defined as

$$\begin{aligned} \lambda^1 &= \begin{pmatrix} 0 & 1 & 0 \\ 1 & 0 & 0 \\ 0 & 0 & 0 \end{pmatrix} \ , & \lambda^2 &= \begin{pmatrix} 0 & -\mathrm{i} & 0 \\ \mathrm{i} & 0 & 0 \\ 0 & 0 & 0 \end{pmatrix} \ , & \lambda^3 &= \begin{pmatrix} 1 & 0 & 0 \\ 0 & -1 & 0 \\ 0 & 0 & 0 \end{pmatrix} \ , \\ \lambda^4 &= \begin{pmatrix} 0 & 0 & 1 \\ 0 & 0 & 0 \\ 1 & 0 & 0 \end{pmatrix} \ , & \lambda^5 &= \begin{pmatrix} 0 & 0 & -\mathrm{i} \\ 0 & 0 & 0 \\ \mathrm{i} & 0 & 0 \end{pmatrix} \ , & & \\ \lambda^6 &= \begin{pmatrix} 0 & 0 & 0 \\ 0 & 0 & 1 \\ 0 & 1 & 0 \end{pmatrix} \ , & \lambda^7 &= \begin{pmatrix} 0 & 0 & 0 \\ 0 & 0 & -\mathrm{i} \\ 0 & \mathrm{i} & 0 \end{pmatrix} \ , & \lambda^8 &= \frac{1}{\sqrt{3}} \begin{pmatrix} 1 & 0 & 0 \\ 0 & 1 & 0 \\ 0 & 0 & -2 \end{pmatrix} \ . \end{aligned} \tag{A.8}$$

They fulfill the following useful relations

$$\begin{aligned} \mathrm{tr}\left\{\lambda^i\lambda^j\right\} &= 2\delta^{ij} \ , & \{\lambda^i, \lambda^j\} &= \frac{4}{3}\delta^{ij}\mathbb{1} + 2d^{ijk}\lambda^k \ , \\ \mathrm{tr}\left\{\lambda^i\lambda^j\lambda^k\right\} &= 2(d^{ijk} + if^{ijk}) \ , & & \end{aligned} \tag{A.9}$$

where d^{ijk} is totally symmetric. Its nonzero components are

$$\begin{aligned} d^{118} = d^{228} = d^{338} = -d^{888} &= \frac{1}{\sqrt{3}} \ , & d^{448} = d^{558} = d^{668} = d^{778} &= -\frac{1}{2\sqrt{3}} \ , \\ d^{146} = d^{157} = d^{256} = d^{344} = d^{355} &= \frac{1}{2} \ , & d^{247} = d^{366} = d^{377} &= -\frac{1}{2} \ . \end{aligned} \tag{A.10}$$

A.3 Dirac algebra

The Dirac matrices are a set of four 4×4 matrices that obey the anticommutation relation

$$\{\gamma^\mu, \gamma^\nu\} = 2g^{\mu\nu}\mathbb{1} \ , \tag{A.11}$$

where $g = \mathrm{diag}(1,-1,-1,-1)$ is the Minkowski metric. They can be chosen such that the following hermiticity condition is fulfilled:

$$(\gamma^\mu)^\dagger = \gamma^0\gamma^\mu\gamma^0 \ . \tag{A.12}$$

It is useful to define a fifth matrix $\gamma_5 \equiv \gamma^5$ as

$$\gamma_5 \equiv \gamma^5 \equiv i\gamma^0\gamma^1\gamma^2\gamma^3 = -\frac{i}{4!}\varepsilon_{\mu\nu\rho\sigma}\gamma^\mu\gamma^\nu\gamma^\rho\gamma^\sigma \ , \tag{A.13}$$

where the Levi-Civita symbol in four dimensions is defined as

$$\varepsilon^{\mu\nu\rho\sigma} = \begin{cases} +1 \ , & \text{if } (\mu,\nu,\rho,\sigma) \text{ is a cyclic permutation of } (0,1,2,3) \ , \\ -1 \ , & \text{if } (\mu,\nu,\rho,\sigma) \text{ is an anticyclic permutation of } (0,1,2,3) \ , \\ 0 \ , & \text{else .} \end{cases} \tag{A.14}$$

Since the indices have to be raised/lowered by the use of the Minkowski metric $\varepsilon_{0123} = -\varepsilon^{0123} = -1$. The choice, whether the Levi–Civita tensor with upper or lower indices has the value $+1$ or -1 is pure convention and corresponds to a minus sign in eq. (A.13). The γ^5 matrix has the following properties:

$$\left(\gamma^5\right)^2 = \mathbb{1} \ , \qquad \left(\gamma^5\right)^\dagger = \gamma^5 \ , \qquad \left\{\gamma^\mu,\gamma^5\right\} = 0 \ . \tag{A.15}$$

Furthermore we define

$$\sigma^{\mu\nu} \equiv \frac{i}{2}\left[\gamma^\mu,\gamma^\nu\right] \ , \tag{A.16}$$

which is antisymmetric by construction. The following identity turns out to be useful:

$$\gamma^5\sigma^{\mu\nu} = \frac{i}{2}\varepsilon^{\mu\nu\rho\sigma}\sigma_{\rho\sigma} \ . \tag{A.17}$$

Since the four Dirac matrices are not defined uniquely by eq. (A.11) and eq. (A.12) one can choose from various explicit representations. Two common choices are the Dirac and the Weyl representation, which both have their advantages: in the Dirac representation the upper and lower half of the bispinor correspond to negative and positive parity, while in the Weyl representation they correspond to parts of left and right chirality. Since the latter transform under $\mathrm{SL}(2,\mathbb{C})$, which is associated with restricted Lorentz transformations, the Weyl representation is sometimes said to be more fundamental than other representations. In the Weyl representation the contravariant γ matrices and γ_5 take the form

$$\gamma^0 = \begin{pmatrix} 0 & \mathbb{1} \\ \mathbb{1} & 0 \end{pmatrix} \ , \qquad \gamma^i = \begin{pmatrix} 0 & \sigma^i \\ -\sigma^i & 0 \end{pmatrix} \ , \qquad \gamma^5 = \begin{pmatrix} -\mathbb{1} & 0 \\ 0 & \mathbb{1} \end{pmatrix} \ . \tag{A.18}$$

In order to separate components of different chirality one introduces the left- and right-handed projectors $\gamma_{L/R}$ as

$$\gamma_L \equiv \frac{\mathbb{1}-\gamma^5}{2} \ , \qquad \gamma_R \equiv \frac{\mathbb{1}+\gamma^5}{2} \ , \tag{A.19}$$

Table A.1: The constants η_Γ^P, η_Γ^C, η_Γ^H and η_Γ^5 characterizing the symmetry properties of the elements of the Clifford algebra.

Γ	η_Γ^P	η_Γ^C	η_Γ^H	η_Γ^5
$\mathbb{1}$	1	-1	1	1
γ_5	-1	-1	-1	1
γ_μ	1	1	1	-1
$\gamma_\mu\gamma_5$	-1	-1	1	-1
$\sigma_{\mu\nu}$	1	1	1	1

which have the following properties:

$$\left(\gamma_{L/R}\right)^2 = \gamma_{L/R} \ , \qquad \gamma_R + \gamma_L = \mathbb{1} \ , \tag{A.20a}$$

$$\gamma_L\gamma_R = \gamma_R\gamma_L = 0 \ , \qquad \gamma_R - \gamma_L = \gamma_5 \ . \tag{A.20b}$$

The charge conjugation matrix C is defined such that

$$(\gamma^\mu)^T = -C^{-1}\gamma^\mu C \ . \tag{A.21}$$

In the Weyl representation one can choose it as a specific combination of gamma matrices, which induces some additional, convenient properties:

$$C = i\gamma^2\gamma^0 \ , \tag{A.22a}$$

$$C = -C^T = -C^\dagger = -C^{-1} \ . \tag{A.22b}$$

The set of 16 matrices

$$\left\{\mathbb{1}, \gamma^5, \gamma^\mu, \gamma^\mu\gamma^5, \sigma^{\mu\nu}\right\} \quad \text{with} \quad \mu < \nu \ , \tag{A.23}$$

is called Clifford algebra and forms a basis of the space of complex 4×4 matrices. For the operator construction it is convenient to define for the elements of the Clifford algebra

$$\Gamma = \begin{cases} \eta_\Gamma^P \gamma_0\Gamma\gamma_0 \ , & \text{for } \Gamma \in \{\mathbb{1}, \gamma^5\} \ , \\ (-1)_\mu \eta_\Gamma^P \gamma_0\Gamma\gamma_0 \ , & \text{for } \Gamma \in \{\gamma^\mu, \gamma^\mu\gamma^5\} \ , \\ (-1)_\mu(-1)_\nu \eta_\Gamma^P \gamma_0\Gamma\gamma_0 \ , & \text{for } \Gamma = \sigma^{\mu\nu} \ , \end{cases} \tag{A.24a}$$

$$\Gamma^T = \eta_\Gamma^C C\Gamma C \ , \tag{A.24b}$$

$$\Gamma^\dagger = \eta_\Gamma^H \gamma_0\Gamma\gamma_0 \ , \tag{A.24c}$$

$$\Gamma = \eta_\Gamma^5 \gamma_5\Gamma\gamma_5 \ , \tag{A.24d}$$

where $(-1)_\mu$ is 1 for $\mu = 0$ and -1 for $\mu = 1, 2, 3$. The different ηs are collected in table A.1. Since complex conjugation can be written as the transposed of the Hermitian conjugate one has

$$\Gamma^* = \eta_\Gamma^H \eta_\Gamma^C \gamma_0 C\Gamma C\gamma_0 \ . \tag{A.25}$$

A.4 Standard integrals

A.4.1 Definition of standard two-point integrals

The standard d-dimensional integrals that occur when one applies infrared regularization [86] are defined as

$$I_{k,l} = \frac{1}{i}\int_{\mathrm{IR}} \frac{d^dq}{(2\pi)^d} \frac{1}{\left(m^2-q^2-i\epsilon\right)^k \left(M^2-(p-q)^2-i\epsilon\right)^l} \ , \tag{A.26}$$

where p is an external momentum, m is a meson mass, M a baryon mass and IR indicates that the integration over the Feynman parameter connecting the meson and baryon propagators is extended to infinity, cf. section 2.1.5. Loop integrals containing only heavy particles (baryons) are set to zero, while those containing only light ones (pseudoscalar mesons) are kept as they are. One obtains

$$I_{1,0} = 2m^2\left(L + \frac{1}{32\pi^2}\ln\frac{m^2}{\mu^2}\right) + \mathcal{O}(d-4) \ , \tag{A.27a}$$

$$I_{0,1} = 0 \ , \tag{A.27b}$$

$$\begin{aligned} I_{1,1} = &-\frac{m^2-M^2+p^2}{p^2}\left(L + \frac{1}{32\pi^2}\left(\ln\frac{m^2}{\mu^2}-1\right)\right) \\ &- \frac{1}{8\pi^2}\sqrt{\frac{m^2}{p^2} - \frac{\left(m^2-M^2+p^2\right)^2}{4p^4}}\arccos\frac{-\left(m^2-M^2+p^2\right)}{\sqrt{4m^2p^2}} + \mathcal{O}(d-4) \ , \end{aligned} \tag{A.27c}$$

where L contains the pole term and the typical constants for the minimal subtraction scheme

$$L \equiv \frac{-\mu^{-\epsilon}}{(4\pi)^2}\left(\frac{1}{\epsilon} + \frac{1}{2}\left(1+\ln 4\pi - \gamma_E\right)\right) \ , \tag{A.28}$$

with $\epsilon \equiv 4-d$. Due to the uniqueness of the decomposition into regular and infrared singular part [86] one can utilize the identities derived for standard dimensional regularization ($k, l \geq 1$):

$$I_{k+1,l} = -\frac{1}{k}\frac{\partial}{\partial m^2}I_{k,l} = -\frac{1}{2mk}\frac{\partial}{\partial m}I_{k,l} \ , \tag{A.29a}$$

$$I_{k,l+1} = -\frac{1}{l}\frac{\partial}{\partial M^2}I_{k,l} = -\frac{1}{2Ml}\frac{\partial}{\partial M}I_{k,l} \ . \tag{A.29b}$$

A.4.2 Reduction of three-point integrals

In the following we express the two specific three-point integrals, which are needed for the full one-loop calculation presented in chapter 3, in terms of standard integrals ($\bar{p} \equiv \frac{1}{2}(p'+p)$, $\Delta \equiv p'-p$). For the integral with two baryon propagators we find

$$\begin{aligned} &\frac{1}{i}\int_{\mathrm{IR}} \frac{d^dq}{(2\pi)^d} \frac{f(q)}{\left(m^2-q^2-i\epsilon\right)^k \left(M^2-(p'-q)^2-i\epsilon\right)\left(M^2-(p-q)^2-i\epsilon\right)} = \\ &\quad = \int_{-\frac{1}{2}}^{\frac{1}{2}} du\ \frac{1}{i}\int_{\mathrm{IR}} \frac{d^dq}{(2\pi)^d} \frac{f(q)}{\left(m^2-q^2-i\epsilon\right)^k \left(\tilde{M}^2-(\tilde{p}-q)^2-i\epsilon\right)^2} \\ &\quad = \int_{-\frac{1}{2}}^{\frac{1}{2}} du\ I_{k,2}(m^2, \tilde{M}^2, \tilde{p}^2=\tilde{M}^2) \ , \quad \text{if } f(q)=1 \ , \end{aligned} \tag{A.30}$$

where $\tilde{M}^2 = M^2+(u^2-\frac{1}{4})\Delta^2 = \bar{p}^2+u^2\Delta^2$ and $\tilde{p} = \bar{p}+u\Delta$. For nontrivial $f(q)$ one has to proceed with a tensor decomposition (see section A.4.3). For the integral with two pion propagators we find

$$\begin{aligned}\frac{1}{i}\int_{\mathrm{IR}}\frac{d^dq}{(2\pi)^d}\frac{f(q)}{(m^2-q^2-i\epsilon)\,(m^2-(q+\Delta)^2-i\epsilon)\,(M^2-(p-q)^2-i\epsilon)^l} &= \\ = \int_{-\frac{1}{2}}^{\frac{1}{2}} du\;\frac{1}{i}\int_{\mathrm{IR}}\frac{d^dq}{(2\pi)^d}\frac{f(q-(u+\frac{1}{2})\Delta)}{(\tilde{m}^2-q^2-i\epsilon)^2\,(M^2-(\tilde{p}-q)^2-i\epsilon)^l} &\qquad (A.31)\\ = \int_{-\frac{1}{2}}^{\frac{1}{2}} du\; I_{2,l}(\tilde{m}^2,M^2,\tilde{p}^2=\tilde{M}^2)\;, \quad \text{if } f(q)=1\;, &\end{aligned}$$

where $\tilde{m}^2 = m^2+(u^2-\frac{1}{4})\Delta^2$. The remaining integration over the Feynman parameter u is carried out numerically.

A.4.3 Tensor decomposition

If the loop momentum occurs in the numerator of the integrand one has to perform a tensor decomposition in order to express the integral in terms of standard integrals. We define

$$I^{\mu\nu\cdots}_{k,l} \equiv \frac{1}{i}\int_{\mathrm{IR}}\frac{d^dq}{(2\pi)^d}\frac{q^\mu q^\nu\cdots}{(m^2-q^2-i\epsilon)^k(M^2-(p-q)^2-i\epsilon)^l}\;. \qquad (A.32)$$

Lorentz decomposition yields

$$I^{\mu}_{k,l} \equiv p^\mu I^{(1)}_{k,l}\;, \qquad (A.33a)$$

$$I^{\mu\nu}_{k,l} \equiv p^2 g^{\mu\nu} I^{(2)}_{k,l} + p^\mu p^\nu I^{(3)}_{k,l}\;, \qquad (A.33b)$$

$$I^{\mu\nu\rho}_{k,l} \equiv p^2(g^{\mu\nu}p^\rho + g^{\nu\rho}p^\mu + g^{\rho\mu}p^\nu) I^{(4)}_{k,l} + p^\mu p^\nu p^\rho I^{(5)}_{k,l}\;, \qquad (A.33c)$$

$$\begin{aligned}I^{\mu\nu\rho\sigma}_{k,l} \equiv\; & p^4(g^{\mu\nu}g^{\rho\sigma}+g^{\mu\rho}g^{\nu\sigma}+g^{\mu\sigma}g^{\nu\rho}) I^{(6)}_{k,l}\\ & + p^2(p^\mu p^\nu g^{\rho\sigma}+p^\mu p^\rho g^{\nu\sigma}+p^\mu p^\sigma g^{\nu\rho}+p^\nu p^\rho g^{\mu\sigma}+p^\nu p^\sigma g^{\mu\rho}+p^\rho p^\sigma g^{\mu\nu}) I^{(7)}_{k,l} \qquad (A.33d)\\ & + p^\mu p^\nu p^\rho p^\sigma I^{(8)}_{k,l}\;.\end{aligned}$$

Since we use infrared regularization all integrals that do not involve at least one meson propagator are zero, i.e., $I_{0,l} = I^{(i)}_{0,l} = 0$. For the integrals which only contain propagators of pseudoscalar mesons the decomposition is actually simpler, since they do not depend on the external momentum p. Therefore

$$I^{(1)}_{k,0} = I^{(3)}_{k,0} = I^{(4)}_{k,0} = I^{(5)}_{k,0} = I^{(7)}_{k,0} = I^{(8)}_{k,0} = 0\;, \qquad (A.34a)$$

$$I^{(2)}_{k,0} = \frac{1}{dp^2}\left(-I_{k-1,0}+m^2 I_{k,0}\right)\;, \qquad (A.34b)$$

$$I^{(6)}_{k,0} = \frac{1}{(d+2)p^2}\left(-I^{(2)}_{k-1,0}+m^2 I^{(2)}_{k,0}\right)\;, \qquad (A.34c)$$

such that the decomposition is independent of p in this case. With the definitions

$$T^{(i)}_{k,l} \equiv -I^{(i)}_{k-1,l} + m^2 I^{(i)}_{k,l}\;, \qquad (A.35)$$

$$U^{(i)}_{k,l} \equiv I^{(i)}_{k,l-1} - I^{(i)}_{k-1,l} + (m^2-M^2+p^2) I^{(i)}_{k,l}\;, \qquad (A.36)$$

we find the following result for the case containing both meson and baryon propagators:

$$I^{(1)}_{k,l} = \frac{1}{2p^2} U^{(0)}_{k,l} \ , \tag{A.37a}$$

$$I^{(2)}_{k,l} = \frac{1}{(d-1)p^2} \left(T^{(0)}_{k,l} - \frac{1}{2} U^{(1)}_{k,l} \right) \ , \tag{A.37b}$$

$$I^{(3)}_{k,l} = \frac{-1}{(d-1)p^2} \left(T^{(0)}_{k,l} - \frac{d}{2} U^{(1)}_{k,l} \right) \ , \tag{A.37c}$$

$$I^{(4)}_{k,l} = \frac{1}{(d-1)p^2} \left(T^{(1)}_{k,l} - \frac{1}{2} \left(U^{(2)}_{k,l} + U^{(3)}_{k,l} \right) \right) \ , \tag{A.37d}$$

$$I^{(5)}_{k,l} = \frac{-1}{(d-1)p^2} \left(3T^{(1)}_{k,l} - \frac{d+2}{2} \left(U^{(2)}_{k,l} + U^{(3)}_{k,l} \right) \right) \ , \tag{A.37e}$$

$$I^{(6)}_{k,l} = \frac{1}{(d+1)p^2} \left(T^{(2)}_{k,l} - \frac{1}{2} U^{(4)}_{k,l} \right) \ , \tag{A.37f}$$

$$I^{(7)}_{k,l} = \frac{-1}{(d+1)p^2} \left(T^{(2)}_{k,l} - \frac{d+2}{2} U^{(4)}_{k,l} \right) \ , \tag{A.37g}$$

$$\begin{aligned} I^{(8)}_{k,l} &= \frac{1}{p^2} T^{(3)}_{k,l} - (d+4) I^{(7)}_{k,l} \\ &= \frac{-1}{(d+1)p^2} \left(3T^{(3)}_{k,l} - \frac{d+4}{2} U^{(5)}_{k,l} \right) \ . \end{aligned} \tag{A.37h}$$

APPENDIX B

Supplements: GPDs

B.1 Low-energy constants and fit parameters

The divergences occurring in the loop calculation for $4-d=\epsilon\to 0$ have to be absorbed in LECs:

$$l_{i,j}=l_{i,j}^{(r)}(\mu)+\gamma_{i,j}L\ , \qquad\qquad l_{i,j}^{s}=l_{i,j}^{s,(r)}(\mu)+\gamma_{i,j}^{s}L\ , \tag{B.1}$$

where L contains the pole term plus the typical constants for the modified minimal subtraction scheme (see eq. (A.28)). The renormalized constants pick up a scale dependence:

$$\mu\frac{\partial}{\partial\mu}l_{i,j}^{(r)}(\mu)=\frac{-\gamma_{i,j}}{(4\pi)^2}\ , \qquad\qquad \mu\frac{\partial}{\partial\mu}l_{i,j}^{s,(r)}(\mu)=\frac{-\gamma_{i,j}^{s}}{(4\pi)^2}\ . \tag{B.2}$$

For the nonzero $\gamma_{i,j}$ and $\gamma_{i,j}^{s}$ we find

$$\gamma_{2,2}=\frac{1+3g_A^2}{2F_\pi^2}l_{0,1}\ , \tag{B.3a}$$

$$\gamma_{2,4}=\frac{1+2g_A^2}{2F_\pi^2}l_{0,2}\ , \tag{B.3b}$$

$$\gamma_{3,1}=\frac{1+2g_A^2}{2F_\pi^2}l_{1,1}-\frac{g_A^2}{12m_0F_\pi^2}l_{0,2}\ , \tag{B.3c}$$

$$\gamma_{3,3}=\frac{1+2g_A^2}{2F_\pi^2}l_{1,2}-\frac{g_A^2}{4m_0F_\pi^2}l_{0,1}\ , \tag{B.3d}$$

$$\gamma_{2,4}^{s}=\frac{3g_A^2}{2F_\pi^2}l_{0,2}^{s}\ , \tag{B.3e}$$

$$\gamma_{3,1}^{s}=\frac{g_A^2}{4m_0F_\pi^2}l_{0,2}^{s}+\frac{3g_A^2}{2F_\pi^2}l_{1,1}^{s}\ , \tag{B.3f}$$

$$\gamma_{3,3}^{s}=\frac{3g_A^2}{4m_0F_\pi^2}l_{0,1}^{s}+\frac{3g_A^2}{2F_\pi^2}l_{1,2}^{s}-\frac{3g_A^2}{4m_0F_\pi^4}l^{s}\ , \tag{B.3g}$$

$$\gamma_{3,4}^{s}=\frac{-g_A^2}{2F_\pi^4m_0}l^{s}\ . \tag{B.3h}$$

The combined fit parameters used in the heavy baryon reduced results for the isoscalar form factors (3.43) are related to the LECs defined in section 3.3 by

$$A_{2,0}^{s,(0)} = 8l_{0,1}^s \ , \tag{B.4a}$$

$$A_{2,0}^{s,(m2)} = 32l_{2,2}^s \ , \tag{B.4b}$$

$$A_{2,0}^{s,(m3)} = \frac{7g_A^2 l^s}{8F_\pi^4 m_0 \pi} - \frac{3g_A^2 l_{0,1}^s}{4F_\pi^2 m_0 \pi} - \frac{g_A l_{1,6}^s}{F_\pi^2 m_0 \pi} - \frac{12 g_A m_0 l_{1,15}^s}{F_\pi^2 \pi} - \frac{12 g_A l_{1,18}^s}{F_\pi^2 \pi} \ , \tag{B.4c}$$

$$A_{2,0}^{s,(t)} = -8l_{2,3}^s \ , \tag{B.4d}$$

$$B_{2,0}^{s,(0)} = 16 m_0 l_{1,2}^s \ , \tag{B.4e}$$

$$B_{2,0}^{s,(m2)}(\mu) = -\frac{2g_A^2 l^s}{F_\pi^4 \pi^2} + 64 m_0 l_{3,3}^{s,(r)}(\mu) - 64 l_{1,2}^s c_1 \ , \tag{B.4f}$$

$$B_{2,0}^{s,(t)}(\mu) = -16 m_0 l_{3,4}^{s,(r)}(\mu) + \frac{5g_A^2 l^s}{12F_\pi^4 \pi^2} \ , \tag{B.4g}$$

$$C_2^{s,(0)} = -4 m_0 l_{2,1}^s \ , \tag{B.4h}$$

$$\tilde{A}_{2,0}^{s,(0)} = 8l_{0,2}^s \ , \tag{B.4i}$$

$$\tilde{A}_{2,0}^{s,(m2)}(\mu) = -\frac{3g_A^2 l_{0,2}^s}{2F_\pi^2 \pi^2} + 32 l_{2,4}^{s,(r)}(\mu) \ , \tag{B.4j}$$

$$\tilde{A}_{2,0}^{s,(m3)} = \frac{7g_A^2 l_{0,2}^s}{4F_\pi^2 m_0 \pi} - \frac{g_A l_{1,4}^s}{F_\pi^2 m_0 \pi} \ , \tag{B.4k}$$

$$\tilde{A}_{2,0}^{s,(t)} = -8l_{2,5}^s \ , \tag{B.4l}$$

$$\tilde{B}_{2,0}^{s,(0)} = 16 m_0 l_{1,1}^s \ , \tag{B.4m}$$

$$\tilde{B}_{2,0}^{s,(m2)}(\mu) = -\frac{3g_A^2 m_0 l_{1,1}^s}{F_\pi^2 \pi^2} + 64 m_0 l_{3,1}^{s,(r)}(\mu) - 64 l_{1,1}^s c_1 \ , \tag{B.4n}$$

$$\tilde{B}_{2,0}^{s,(t)} = -16 m_0 l_{3,2}^s \ , \tag{B.4o}$$

$$A_{2,0}^{\pi,s,(0)} = \frac{8l^s}{F_\pi^2} \ , \tag{B.4p}$$

and those occurring in the isovector form factors (3.45) by

$$A_{2,0}^{v,(0)} = 4l_{0,1} \ , \tag{B.5a}$$

$$A_{2,0}^{v,(m2)}(\mu) = -\frac{g_A^2 l_{0,1}}{2F_\pi^2 \pi^2} + 16 l_{2,2}^{(r)}(\mu) \ , \tag{B.5b}$$

$$\begin{aligned} A_{2,0}^{v,(m3)} = {} & \frac{7g_A^2 l_{0,1}}{8F_\pi^2 m_0 \pi} + \frac{g_A l_{0,2}}{3F_\pi^2 m_0 \pi} - \frac{g_A (l_{1,6} + l_{1,7})}{6F_\pi^2 m_0 \pi} - \frac{2 g_A m_0 (l_{1,15} + l_{1,16})}{F_\pi^2 \pi} \\ & - \frac{2 g_A (l_{1,18} + l_{1,19})}{F_\pi^2 \pi} \ , \end{aligned} \tag{B.5c}$$

$$A_{2,0}^{v,(t)} = -4l_{2,3} \ , \tag{B.5d}$$

$$B_{2,0}^{v,(0)} = 8m_0 l_{1,2} \ , \tag{B.5e}$$

$$B_{2,0}^{v,(m2)}(\mu) = -\frac{g_A^2 m_0 l_{1,2}}{F_\pi^2 \pi^2} + 32 m_0 l_{3,3}^{(r)}(\mu) - 32 l_{1,2} c_1 \ , \tag{B.5f}$$

$$B_{2,0}^{v,(t)} = -8m_0 l_{3,4} \ , \tag{B.5g}$$

$$C_2^{v,(0)} = -2m_0 l_{2,1} \ , \tag{B.5h}$$

$$\tilde{A}_{2,0}^{v,(0)} = 4l_{0,2} \ , \tag{B.5i}$$

$$\tilde{A}_{2,0}^{v,(m2)}(\mu) = -\frac{g_A^2 l_{0,2}}{4F_\pi^2 \pi^2} + 16 l_{2,4}^{(r)}(\mu) \ , \tag{B.5j}$$

$$\tilde{A}_{2,0}^{v,(m3)} = \frac{g_A l_{0,1}}{3F_\pi^2 m_0 \pi} + \frac{11 g_A^2 l_{0,2}}{24 F_\pi^2 m_0 \pi} + \frac{g_A l_{1,2}}{3F_\pi^2 \pi} + \frac{2 g_A l_{1,17}}{3F_\pi^2 \pi} - \frac{g_A (l_{1,4} + l_{1,5})}{6F_\pi^2 m_0 \pi} \ , \tag{B.5k}$$

$$\tilde{A}_{2,0}^{v,(t)} = -4l_{2,5} \ , \tag{B.5l}$$

$$\tilde{B}_{2,0}^{v,(0)} = 8m_0 l_{1,1} \ , \tag{B.5m}$$

$$\tilde{B}_{2,0}^{v,(m2)}(\mu) = -\frac{g_A^2 m_0 l_{1,1}}{2F_\pi^2 \pi^2} + 32 m_0 l_{3,1}^{(r)}(\mu) - 32 l_{1,1} c_1 \ , \tag{B.5n}$$

$$\tilde{B}_{2,0}^{v,(t)} = -8m_0 l_{3,2} \ . \tag{B.5o}$$

B.2 Full results by diagram

In this appendix we present the outcome of the full one-loop calculation for the generalized form factors as explained in section 3.5.1. The results are given by diagram in terms of standard integrals (see appendix A.4), with the exception of diagrams (d) and (e) (see figure 3.1) that only are compatible with the form factor decomposition if they are treated together:

$$X^{s/v} = X_{(a)}^{s/v} + X_{(b)}^{s/v} + X_{(de)}^{s/v} + \int_{-\frac{1}{2}}^{\frac{1}{2}} du \, \left(X_{(c)}^{s/v} + X_{(f)}^{s/v} \right) \ . \tag{B.6}$$

For the massive three-point integrals the remaining integration over the Feynman parameter u has to be carried out numerically. In the following the arguments of the standard integrals are not written down explicitly:

$$\begin{aligned} I_{1,0} &\equiv I_{1,0}(m_\pi^2) \ , \\ I_{2,0} &\equiv I_{2,0}(m_\pi^2) \ , \\ I_{1,1}^{(i)} &\equiv I_{1,1}^{(i)}(m_\pi^2, m_N^2, m_N^2) \ , \\ I_{1,2}^{(i)} &\equiv I_{1,2}^{(i)}(m_\pi^2, \tilde{m}_N^2, \tilde{m}_N^2) \ , \\ I_{2,1}^{(i)} &\equiv I_{2,1}^{(i)}(\tilde{m}_\pi^2, m_N^2, \tilde{m}_N^2) \ . \end{aligned} \tag{B.7}$$

The mass parameters $\tilde{m}_\pi^2$ and $\tilde{m}_N^2$ depend on the remaining integration parameter u and are defined as

$$\tilde{m}_N^2 \equiv m_N^2 + (u^2 - \tfrac{1}{4})\Delta^2 = \bar{p}^2 + u^2\Delta^2 \ , \tag{B.8a}$$

$$\tilde{m}_\pi^2 \equiv m_\pi^2 + (u^2 - \tfrac{1}{4})\Delta^2 \ . \tag{B.8b}$$

In the results presented below we have appended the Z-factor to the leading and next-to-leading tree-level contributions only. Yet, as long as one is not truncating the results, one could equitably argue that the Z-factor has to be appended as an overall prefactor to all diagrams. Note, however, that the results obtained from these two approaches would only differ by terms of higher order.

B.2.1 Isoscalar GFFs for the vector current

$\mathbf{A^s_{2,0}}$

$$\begin{aligned}
A^s_{2,0,(a)} &= 8l^s_{0,1}Z + 32l^s_{2,2}m_\pi^2 - 8l^s_{2,3}t \ , \\
A^s_{2,0,(c)} &= 6l^s_{0,1}\frac{g_A^2}{F_\pi^2}\Big[I_{1,0} - 4m_N^2\big(I^{(1)}_{1,1} - I^{(3)}_{1,1}\big) - 4(d-2)m_N^2\tilde{m}_N^2\big(I^{(2)}_{1,2} - I^{(4)}_{1,2}\big) \\
&\qquad + 4m_N^2(2m_N^2 - \tilde{m}_N^2)\big(I^{(3)}_{1,2} - I^{(5)}_{1,2}\big)\Big] \\
&\quad + 24l^s_{1,2}\frac{g_A^2}{F_\pi^2}m_N^3 t\big(I^{(3)}_{1,2} - I^{(5)}_{1,2}\big) \ , \\
A^s_{2,0,(de)} &= 48\frac{g_A}{F_\pi^2}\Big[- l^s_{1,6}m_N^2 I^{(3)}_{1,1} + l^s_{1,15}m_N^2\big(2I^{(2)}_{1,0} + m_\pi^2\big(4I_{1,1} - 4I^{(1)}_{1,1} + I^{(3)}_{1,1}\big)\big) \\
&\qquad + l^s_{1,13}\big(m_\pi^2 I_{1,0} + m_N^2 m_\pi^2\big(I^{(3)}_{1,1} - 2I^{(1)}_{1,1}\big) + m_N^2 I^{(2)}_{1,0} \\
&\qquad\quad + 4m_N^4\big(I^{(2)}_{1,1} - I^{(4)}_{1,1}\big) + 2m_N^2\bar{p}^2\big(2I^{(3)}_{1,1} - I^{(5)}_{1,1}\big)\big) \\
&\qquad + 2l^s_{1,18}m_N^3\big(2(d-1)I^{(2)}_{1,1} - dI^{(4)}_{1,1}\big)\Big] \ , \\
A^s_{2,0,(f)} &= -48l^s\frac{g_A^2}{F_\pi^4}m_N^2\Big[2\tilde{m}_N^2 I^{(4)}_{2,1} + m_N^2 I^{(5)}_{2,1}\Big] \ .
\end{aligned}$$

$\mathbf{B^s_{2,0}}$

$$\begin{aligned}
B^s_{2,0,(a)} &= 2m_N\Big[8l^s_{1,2}Z + 32l^s_{3,3}m_\pi^2 - 8l^s_{3,4}t\Big] \ , \\
B^s_{2,0,(c)} &= -48l^s_{0,1}\frac{g_A^2}{F_\pi^2}m_N^4\big(I^{(3)}_{1,2} - I^{(5)}_{1,2}\big) \\
&\quad - 12l^s_{1,2}\frac{g_A^2}{F_\pi^2}m_N\Big[I_{1,0} - 4m_N^2\big(I^{(1)}_{1,1} - I^{(3)}_{1,1}\big) + 4(d-4)m_N^2\tilde{m}_N^2\big(I^{(2)}_{1,2} - I^{(4)}_{1,2}\big) \\
&\qquad + 4m_N^2(2m_N^2 - \tilde{m}_N^2)\big(I^{(3)}_{1,2} - I^{(5)}_{1,2}\big)\Big] \ , \\
B^s_{2,0,(de)} &= -48\frac{g_A}{F_\pi^2}m_N^2\Big[2l^s_{1,13}m_N^2\big(2I^{(2)}_{1,1} - I^{(4)}_{1,1}\big) + l^s_{1,15}m_\pi^2\big(4I_{1,1} - 4I^{(1)}_{1,1} + I^{(3)}_{1,1}\big) \\
&\qquad + 2l^s_{1,18}m_N\big(I^{(5)}_{1,1} - 2I^{(3)}_{1,1}\big)\Big] \ , \\
B^s_{2,0,(f)} &= 48l^s\frac{g_A^2}{F_\pi^4}m_N^4 I^{(5)}_{2,1} \ .
\end{aligned}$$

$\mathbf{C^s_2}$

$$
\begin{aligned}
C^s_{2,(a)} &= -4l^s_{2,1}m_N \ , \\
C^s_{2,(c)} &= -48l^s_{0,1}\frac{g_A^2}{F_\pi^2}m_N^4u^2I^{(5)}_{1,2} + 24l^s_{1,2}\frac{g_A^2}{F_\pi^2}m_N^3\tilde{m}_N^2I^{(4)}_{1,2} \ , \\
C^s_{2,(de)} &= 12\frac{g_A}{F_\pi^2}m_N^2\Big[2l^s_{1,13}m_N^2I^{(4)}_{1,1} + l^s_{1,15}m_\pi^2I^{(3)}_{1,1} + 2l^s_{1,18}m_NI^{(5)}_{1,1}\Big] \ , \\
C^s_{2,(f)} &= 24l^s\frac{g_A^2}{F_\pi^4}m_N^2\Big[(u^2-\tfrac{1}{4})\big(I_{2,0} - 2m_N^2I^{(1)}_{2,1}\big) + 2m_N^2u^2\big(2I^{(3)}_{2,1} - I^{(5)}_{2,1}\big)\Big] \ .
\end{aligned}
$$

B.2.2 Isoscalar GFFs for the axial current

$\mathbf{\tilde{A}^s_{2,0}}$

$$
\begin{aligned}
\tilde{A}^s_{2,0,(a)} &= 8l^s_{0,2}Z + 32l^s_{2,4}m_\pi^2 - 8l^s_{2,5}t \ , \\
\tilde{A}^s_{2,0,(c)} &= 6l^s_{0,2}\frac{g_A^2}{F_\pi^2}\Big[I_{1,0} - 4m_N^2\big(I^{(1)}_{1,1} - I^{(3)}_{1,1}\big) + 4(d-2)m_N^2\tilde{m}_N^2\big(I^{(2)}_{1,2} - I^{(4)}_{1,2}\big) \\
&\qquad + 4m_N^2\tilde{m}_N^2\big(I^{(3)}_{1,2} - I^{(5)}_{1,2}\big)\Big] \ , \\
\tilde{A}^s_{2,0,(de)} &= 48\frac{g_A}{F_\pi^2}\Big[- l^s_{1,4}m_N^2I^{(3)}_{1,1} + 2l^s_{1,11}m_N^2I^{(2)}_{1,0} \\
&\qquad + l^s_{1,9}\big(m_\pi^2I_{1,0} + m_N^2I^{(2)}_{1,0} + 4m_N^4\big(I^{(2)}_{1,1} - I^{(4)}_{1,1}\big) \\
&\qquad\quad + m_N^2m_\pi^2\big(I^{(3)}_{1,1} - 2I^{(1)}_{1,1}\big) - 2m_N^2\bar{p}^2\big(I^{(5)}_{1,1} - 2I^{(3)}_{1,1}\big)\big)\Big] \ .
\end{aligned}
$$

$\mathbf{\tilde{B}^s_{2,0}}$

$$
\begin{aligned}
\tilde{B}^s_{2,0,(a)} &= 2m_N\Big[8l^s_{1,1}Z + 32l^s_{3,1}m_\pi^2 - 8l^s_{3,2}t\Big] \ , \\
\tilde{B}^s_{2,0,(c)} &= -192l^s_{0,2}\frac{g_A^2}{F_\pi^2}m_N^4u^2\big(I^{(3)}_{1,2} - 2I^{(5)}_{1,2}\big) \\
&\qquad - 12l^s_{1,1}\frac{g_A^2}{F_\pi^2}m_N\Big[I_{1,0} - 4m_N^2\big(I^{(1)}_{1,1} - I^{(3)}_{1,1}\big) - 4dm_N^2\tilde{m}_N^2\big(I^{(2)}_{1,2} - I^{(4)}_{1,2}\big) \\
&\qquad\qquad - 4m_N^2\tilde{m}_N^2\big(I^{(3)}_{1,2} - I^{(5)}_{1,2}\big) + 8m_N^2\tilde{m}_N^2I^{(4)}_{1,2}\Big] \ , \\
\tilde{B}^s_{2,0,(de)} &= 96\frac{g_A}{F_\pi^2}m_N^2\Big[-2l^s_{1,9}m_N^2I^{(2)}_{1,1} + l^s_{1,11}m_\pi^2\big(I^{(3)}_{1,1} - 2I^{(1)}_{1,1}\big)\Big] \ .
\end{aligned}
$$

B.2.3 Isovector GFFs for the vector current

$\mathbf{A^v_{2,0}}$

$$
\begin{aligned}
A^v_{2,0,(a)} &= 4l_{0,1}Z + 16l_{2,2}m_\pi^2 - 4l_{2,3}t \ , \\
A^v_{2,0,(b)} &= -\frac{4}{F_\pi^2}l_{0,1}I_{1,0} \ ,
\end{aligned}
$$

$$
\begin{aligned}
A^v_{2,0,(c)} &= -l_{0,1}\frac{g_A^2}{F_\pi^2}\Big[I_{1,0} - 4m_N^2\big(I^{(1)}_{1,1} - I^{(3)}_{1,1}\big) - 4(d-2)m_N^2\tilde{m}_N^2\big(I^{(2)}_{1,2} - I^{(4)}_{1,2}\big) \\
&\qquad + 4m_N^2(2m_N^2 - \tilde{m}_N^2)\big(I^{(3)}_{1,2} - I^{(5)}_{1,2}\big)\Big] - 4l_{1,2}\frac{g_A^2}{F_\pi^2}m_N^3 t\big(I^{(3)}_{1,2} - I^{(5)}_{1,2}\big)\ , \\
A^v_{2,0,(de)} &= 4\frac{g_A}{F_\pi^2}\Big[l_{0,2}\big(I_{1,0} - 2m_N^2 I^{(1)}_{1,1} + m_N^2 I^{(3)}_{1,1}\big) - 2(l_{1,6}+l_{1,7})m_N^2 I^{(3)}_{1,1} \\
&\qquad + (l_{1,1} - 2l_{1,3})m_N^3\big(-2I^{(2)}_{1,1} - 2I^{(3)}_{1,1} + 2I^{(4)}_{1,1} + I^{(5)}_{1,1}\big) \\
&\qquad - 2l_{1,8}\big(2m_N m_\pi^2 I_{1,0} + 4m_N^3 I^{(2)}_{1,0} + 2m_N^5\big(4I^{(2)}_{1,1} - 8I^{(4)}_{1,1} + 2I^{(6)}_{1,1} + 3I^{(7)}_{1,1}\big) \\
&\qquad\quad - m_N^3 m_\pi^2\big(4I^{(1)}_{1,1} - 4I^{(2)}_{1,1} - 4I^{(3)}_{1,1} + 2I^{(4)}_{1,1} + I^{(5)}_{1,1}\big) \\
&\qquad\quad + 2m_N^3\bar{p}^2\big(4I^{(3)}_{1,1} - 4I^{(4)}_{1,1} - 4I^{(5)}_{1,1} + 2I^{(7)}_{1,1} + I^{(8)}_{1,1}\big)\big) \\
&\qquad + 2(l_{1,13}+l_{1,14})\big(m_\pi^2 I_{1,0} + m_N^2 m_\pi^2\big(I^{(3)}_{1,1} - 2I^{(1)}_{1,1}\big) + m_N^2 I^{(2)}_{1,0} \\
&\qquad\quad + 4m_N^4\big(I^{(2)}_{1,1} - I^{(4)}_{1,1}\big) + 2m_N^2\bar{p}^2\big(2I^{(3)}_{1,1} - I^{(5)}_{1,1}\big)\big) \\
&\qquad + 2(l_{1,15}+l_{1,16})m_N^2\big(2I^{(2)}_{1,0} + m_\pi^2\big(4I_{1,1} - 4I^{(1)}_{1,1} + I^{(3)}_{1,1}\big)\big) \\
&\qquad + 4(l_{1,18}+l_{1,19})m_N^3\big(2(d-1)I^{(2)}_{1,1} - dI^{(4)}_{1,1}\big)\Big]\ .
\end{aligned}
$$

$\mathbf{B^v_{2,0}}$

$$
\begin{aligned}
B^v_{2,0,(a)} &= 2m_N\Big[4l_{1,2}Z + 16l_{3,3}m_\pi^2 - 4l_{3,4}t\Big]\ , \\
B^v_{2,0,(b)} &= -\frac{8}{F_\pi^2}l_{1,2}m_N I_{1,0}\ , \\
B^v_{2,0,(c)} &= 8l_{0,1}\frac{g_A^2}{F_\pi^2}m_N^4\big(I^{(3)}_{1,2} - I^{(5)}_{1,2}\big) \\
&\qquad + 2l_{1,2}\frac{g_A^2}{F_\pi^2}m_N\Big[I_{1,0} - 4m_N^2\big(I^{(1)}_{1,1} - I^{(3)}_{1,1}\big) + 4(d-4)m_N^2\tilde{m}_N^2\big(I^{(2)}_{1,2} - I^{(4)}_{1,2}\big) \\
&\qquad\qquad + 4m_N^2(2m_N^2 - \tilde{m}_N^2)\big(I^{(3)}_{1,2} - I^{(5)}_{1,2}\big)\Big]\ , \\
B^v_{2,0,(de)} &= 4\frac{g_A}{F_\pi^2}m_N\Big[(l_{1,1} - 2l_{1,3})m_N^2\big(2I^{(3)}_{1,1} + I^{(5)}_{1,1}\big) - 2(l_{1,15}+l_{1,16})m_N m_\pi^2\big(4I_{1,1} - 4I^{(1)}_{1,1} + I^{(3)}_{1,1}\big) \\
&\qquad + 2l_{1,8}\big(2m_\pi^2 I_{1,0} + 4m_N^2 I^{(2)}_{1,0} + 2m_N^4\big(4I^{(2)}_{1,1} - 8I^{(4)}_{1,1} + 3I^{(7)}_{1,1}\big) \\
&\qquad\quad - m_N^2 m_\pi^2\big(4I^{(1)}_{1,1} - 4I^{(3)}_{1,1} + I^{(5)}_{1,1}\big) + 2m_N^2\bar{p}^2\big(4I^{(3)}_{1,1} - 4I^{(5)}_{1,1} + I^{(8)}_{1,1}\big)\big) \\
&\qquad - 4(l_{1,13}+l_{1,14})m_N^3\big(2I^{(2)}_{1,1} - I^{(4)}_{1,1}\big) + 4(l_{1,18}+l_{1,19})m_N^2\big(2I^{(3)}_{1,1} - I^{(5)}_{1,1}\big)\Big]\ .
\end{aligned}
$$

$\mathbf{C^v_2}$

$$
\begin{aligned}
C^v_{2,(a)} &= -2l_{2,1}m_N\ , \\
C^v_{2,(c)} &= 8l_{0,1}\frac{g_A^2}{F_\pi^2}m_N^4 u^2 I^{(5)}_{1,2} - 4l_{1,2}\frac{g_A^2}{F_\pi^2}m_N^3\tilde{m}_N^2 I^{(4)}_{1,2}\ , \\
C^v_{2,(de)} &= \frac{g_A}{F_\pi^2}m_N\Big[-2l_{1,1}m_N^2 I^{(3)}_{1,1} + (l_{1,1} - 2l_{1,3})m_N^2 I^{(5)}_{1,1} + 2l_{1,8}m_N^2\big(m_\pi^2 I^{(5)}_{1,1} - 2m_N^2 I^{(7)}_{1,1} - 2\bar{p}^2 I^{(8)}_{1,1}\big) \\
&\qquad + 4(l_{1,13}+l_{1,14})m_N^3 I^{(4)}_{1,1} + 2(l_{1,15}+l_{1,16})m_N m_\pi^2 I^{(3)}_{1,1} + 4(l_{1,18}+l_{1,19})m_N^2 I^{(5)}_{1,1}\Big]\ .
\end{aligned}
$$

B.2.4 Isovector GFFs for the axial current

$\tilde{\mathbf{A}}^{\mathbf{v}}_{\mathbf{2,0}}$

$$
\begin{aligned}
\tilde{A}^{v}_{2,0,(a)} &= 4l_{0,2}Z + 16l_{2,4}m_\pi^2 - 4l_{2,5}t \ , \\
\tilde{A}^{v}_{2,0,(b)} &= -\frac{4}{F_\pi^2}l_{0,2}I_{1,0} \ , \\
\tilde{A}^{v}_{2,0,(c)} &= -l_{0,2}\frac{g_A^2}{F_\pi^2}\Big[I_{1,0} - 4m_N^2\big(I^{(1)}_{1,1} - I^{(3)}_{1,1}\big) + 4(d-2)m_N^2\tilde{m}_N^2\big(I^{(2)}_{1,2} - I^{(4)}_{1,2}\big) \\
&\qquad + 4m_N^2\tilde{m}_N^2\big(I^{(3)}_{1,2} - I^{(5)}_{1,2}\big)\Big] \ , \\
\tilde{A}^{v}_{2,0,(de)} &= 4\frac{g_A}{F_\pi^2}\Big[l_{0,1}\big(I_{1,0} - 2m_N^2 I^{(1)}_{1,1} + m_N^2 I^{(3)}_{1,1}\big) - l_{1,2}m_N^3\big(2(d-1)I^{(2)}_{1,1} + 2I^{(3)}_{1,1} - dI^{(4)}_{1,1} - I^{(5)}_{1,1}\big) \\
&\qquad - 2(l_{1,4}+l_{1,5})m_N^2 I^{(3)}_{1,1} + 4(l_{1,11}+l_{1,12})m_N^2 I^{(2)}_{1,0} \\
&\qquad + 2(l_{1,9}+l_{1,10})\big(m_\pi^2 I_{1,0} + m_N^2 I^{(2)}_{1,0} + 4m_N^4\big(I^{(2)}_{1,1} - I^{(4)}_{1,1}\big) \\
&\qquad\quad + m_N^2 m_\pi^2\big(I^{(3)}_{1,1} - 2I^{(1)}_{1,1}\big) - 2m_N^2\bar{p}^2\big(I^{(5)}_{1,1} - 2I^{(3)}_{1,1}\big)\big) \\
&\qquad + 2l_{1,17}m_N^3\big(-2(d-1)I^{(2)}_{1,1} - 2I^{(3)}_{1,1} + dI^{(4)}_{1,1} + I^{(5)}_{1,1}\big)\Big] \ .
\end{aligned}
$$

$\tilde{\mathbf{B}}^{\mathbf{v}}_{\mathbf{2,0}}$

$$
\begin{aligned}
\tilde{B}^{v}_{2,0,(a)} &= 2m_N\Big[4l_{1,1}Z + 16l_{3,1}m_\pi^2 - 4l_{3,2}t\Big] \ , \\
\tilde{B}^{v}_{2,0,(b)} &= -\frac{8}{F_\pi^2}l_{1,1}m_N I_{1,0} \ , \\
\tilde{B}^{v}_{2,0,(c)} &= 32l_{0,2}\frac{g_A^2}{F_\pi^2}m_N^4 u^2\big(I^{(3)}_{1,2} - 2I^{(5)}_{1,2}\big) \\
&\qquad + 2l_{1,1}\frac{g_A^2}{F_\pi^2}m_N\Big[I_{1,0} - 4m_N^2\big(I^{(1)}_{1,1} - I^{(3)}_{1,1}\big) \\
&\qquad\qquad - 4m_N^2\tilde{m}_N^2\big(dI^{(2)}_{1,2} + I^{(3)}_{1,2} - (d+2)I^{(4)}_{1,2} - I^{(5)}_{1,2}\big)\Big] \ , \\
\tilde{B}^{v}_{2,0,(de)} &= 8\frac{g_A}{F_\pi^2}m_N^2\Big[l_{1,2}m_N\big(2I^{(3)}_{1,1} - I^{(5)}_{1,1}\big) - 4(l_{1,9}+l_{1,10})m_N^2 I^{(2)}_{1,1} \\
&\qquad\qquad + 2(l_{1,11}+l_{1,12})m_\pi^2\big(I^{(3)}_{1,1} - 2I^{(1)}_{1,1}\big) + 2l_{1,17}m_N\big(I^{(3)}_{1,1} - I^{(5)}_{1,1}\big)\Big] \ .
\end{aligned}
$$

APPENDIX C

Supplements: BDAs

C.1 Loop contributions

The functions $g^{\star}_{\rm DA}$ and $\Delta g^{B}_{\rm DA}$ are given by

$$
\begin{aligned}
6F_\star^2 g^\star_{\Phi+} &= -19\,\mathrm{H}_1(m^\star_m) + 2(5D+6F)\,\mathrm{H}_2(m^\star_m)\ ,\\
6F_\star^2 g^\star_{\Phi-} &= -7\,\mathrm{H}_1(m^\star_m) - 10D\,\mathrm{H}_2(m^\star_m)\ ,\\
6F_\star^2 g^\star_{\Xi} &= -9\,\mathrm{H}_1(m^\star_m) - 18F\,\mathrm{H}_2(m^\star_m)\ ,
\end{aligned}
\tag{C.1}
$$

$$
\begin{aligned}
24F_\star^2\Delta g^N_{\Phi+} &= -57\,\Delta\mathrm{H}_1(m_\pi) - 18\,\Delta\mathrm{H}_1(m_K) - \Delta\mathrm{H}_1(m_\eta)\\
&\quad + 30(D+F)\,\Delta\mathrm{H}_2(m_\pi) + 12(D+F)\,\Delta\mathrm{H}_2(m_K) + (-2D+6F)\,\Delta\mathrm{H}_2(m_\eta)\ ,\\
24F_\star^2\Delta g^\Sigma_{\Phi+} &= -12\,\Delta\mathrm{H}_1(m_\pi) - 60\,\Delta\mathrm{H}_1(m_K) - 4\,\Delta\mathrm{H}_1(m_\eta)\\
&\quad + 24D\,\Delta\mathrm{H}_2(m_\pi) + 24(D+2F)\,\Delta\mathrm{H}_2(m_K) - 8D\,\Delta\mathrm{H}_2(m_\eta)\ ,\\
24F_\star^2\Delta g^\Xi_{\Phi+} &= -9\,\Delta\mathrm{H}_1(m_\pi) - 66\,\Delta\mathrm{H}_1(m_K) - \Delta\mathrm{H}_1(m_\eta)\\
&\quad + 18(-D+F)\,\Delta\mathrm{H}_2(m_\pi) + (60D+36F)\,\Delta\mathrm{H}_2(m_K) - 2(D+3F)\,\Delta\mathrm{H}_2(m_\eta)\ ,\\
24F_\star^2\Delta g^\Lambda_{\Phi+} &= -36\,\Delta\mathrm{H}_1(m_\pi) - 36\,\Delta\mathrm{H}_1(m_K) - 4\,\Delta\mathrm{H}_1(m_\eta)\\
&\quad + 24D\,\Delta\mathrm{H}_2(m_\pi) + 8(D+6F)\,\Delta\mathrm{H}_2(m_K) + 8D\,\Delta\mathrm{H}_2(m_\eta)\ ,\\
24F_\star^2\Delta g^N_{\Phi-} &= -9\,\Delta\mathrm{H}_1(m_\pi) - 18\,\Delta\mathrm{H}_1(m_K) - \Delta\mathrm{H}_1(m_\eta)\\
&\quad - 18(D+F)\,\Delta\mathrm{H}_2(m_\pi) + (-20D+12F)\,\Delta\mathrm{H}_2(m_K) + (-2D+6F)\,\Delta\mathrm{H}_2(m_\eta)\ ,\\
24F_\star^2\Delta g^\Sigma_{\Phi-} &= -12\,\Delta\mathrm{H}_1(m_\pi) - 12\,\Delta\mathrm{H}_1(m_K) - 4\,\Delta\mathrm{H}_1(m_\eta)\\
&\quad - 8D\,\Delta\mathrm{H}_2(m_\pi) - 24D\,\Delta\mathrm{H}_2(m_K) - 8D\,\Delta\mathrm{H}_2(m_\eta)\ ,\\
24F_\star^2\Delta g^\Xi_{\Phi-} &= -9\,\Delta\mathrm{H}_1(m_\pi) - 18\,\Delta\mathrm{H}_1(m_K) - \Delta\mathrm{H}_1(m_\eta)\\
&\quad + 18(-D+F)\,\Delta\mathrm{H}_2(m_\pi) - 4(5D+3F)\,\Delta\mathrm{H}_2(m_K) - 2(D+3F)\,\Delta\mathrm{H}_2(m_\eta)\ ,\\
24F_\star^2\Delta g^\Lambda_{\Phi-} &= -36\,\Delta\mathrm{H}_1(m_\pi) + 12\,\Delta\mathrm{H}_1(m_K) - 4\,\Delta\mathrm{H}_1(m_\eta)\\
&\quad - 72D\,\Delta\mathrm{H}_2(m_\pi) + 24D\,\Delta\mathrm{H}_2(m_K) + 8D\,\Delta\mathrm{H}_2(m_\eta)\ ,
\end{aligned}
$$

$$
\begin{aligned}
\Delta g_{\Pi}^{N} &= \Delta g_{\Phi+}^{N} \ , \\
24F_\star^2 \Delta g_{\Pi}^{\Sigma} &= -24\,\Delta\mathrm{H}_1(m_\pi) - 36\,\Delta\mathrm{H}_1(m_K) - 16\,\Delta\mathrm{H}_1(m_\eta) \\
&\quad + 48F\,\Delta\mathrm{H}_2(m_\pi) + 24D\,\Delta\mathrm{H}_2(m_K) + 16D\,\Delta\mathrm{H}_2(m_\eta) \ , \\
24F_\star^2 \Delta g_{\Pi}^{\Xi} &= -9\,\Delta\mathrm{H}_1(m_\pi) - 42\,\Delta\mathrm{H}_1(m_K) - 25\,\Delta\mathrm{H}_1(m_\eta) \\
&\quad + 18(D-F)\,\Delta\mathrm{H}_2(m_\pi) + 12(D+3F)\,\Delta\mathrm{H}_2(m_K) + 10(D+3F)\,\Delta\mathrm{H}_2(m_\eta) \ , \\
24F_\star^2 \Delta g_{\Pi}^{\Lambda} &= -12\,\Delta\mathrm{H}_1(m_K) - 16\,\Delta\mathrm{H}_1(m_\eta) - 24D\,\Delta\mathrm{H}_2(m_K) - 16D\,\Delta\mathrm{H}_2(m_\eta) \ , \\
24F_\star^2 \Delta g_{\Xi}^{N} &= -9\,\Delta\mathrm{H}_1(m_\pi) - 18\,\Delta\mathrm{H}_1(m_K) - 9\,\Delta\mathrm{H}_1(m_\eta) \\
&\quad - 18(D+F)\,\Delta\mathrm{H}_2(m_\pi) + 12(D-3F)\,\Delta\mathrm{H}_2(m_K) + 6(D-3F)\,\Delta\mathrm{H}_2(m_\eta) \ , \\
24F_\star^2 \Delta g_{\Xi}^{\Sigma} &= -24\,\Delta\mathrm{H}_1(m_\pi) - 12\,\Delta\mathrm{H}_1(m_K) - 48F\,\Delta\mathrm{H}_2(m_\pi) - 24F\,\Delta\mathrm{H}_2(m_K) \ , \\
24F_\star^2 \Delta g_{\Xi}^{\Xi} &= -9\,\Delta\mathrm{H}_1(m_\pi) - 18\,\Delta\mathrm{H}_1(m_K) - 9\,\Delta\mathrm{H}_1(m_\eta) \\
&\quad + 18(D-F)\,\Delta\mathrm{H}_2(m_\pi) - 12(D+3F)\,\Delta\mathrm{H}_2(m_K) - 6(D+3F)\,\Delta\mathrm{H}_2(m_\eta) \ , \\
24F_\star^2 \Delta g_{\Xi}^{\Lambda} &= -36\,\Delta\mathrm{H}_1(m_K) - 72F\,\Delta\mathrm{H}_2(m_K) \ .
\end{aligned}
\tag{C.2}
$$

The Z-factor contributions are given by

$$
\begin{aligned}
\Sigma'^{\star} &= \frac{4}{3}(5D^2+9F^2)\,\mathrm{H}_3(m_m^\star) \ , \\
\Delta\Sigma'_B &= 3g_{B,\pi}\,\Delta\mathrm{H}_3(m_\pi) + 4g_{B,K}\,\Delta\mathrm{H}_3(m_K) + g_{B,\eta}\,\Delta\mathrm{H}_3(m_\eta) \ ,
\end{aligned}
\tag{C.3}
$$

where the coefficients $g_{B,M}$ are defined in eq. (4.49). The auxiliary functions $\Delta\mathrm{H}_k$ are defined as

$$
\Delta\mathrm{H}_k(m) = \mathrm{H}_k(m) - \mathrm{H}_k(m_m^\star) \ , \tag{C.4}
$$

with

$$
\mathrm{H}_1(m) = 2m^2\left[L + \frac{1}{32\pi^2}\ln\frac{m^2}{\mu^2}\right] \ , \tag{C.5a}
$$

$$
\mathrm{H}_2(m) = \frac{m^4}{m_b^{\star 2}}\left[L + \frac{1}{32\pi^2}\ln\frac{m^2}{\mu^2}\right] - \frac{m^4}{32\pi^2 m_b^{\star 2}} + \frac{m^3}{8\pi^2 m_b^\star}\sqrt{1-\frac{m^2}{4m_b^{\star 2}}}\arccos\left(-\frac{m}{2m_b^\star}\right) \ , \tag{C.5b}
$$

$$
\begin{aligned}
\mathrm{H}_3(m) &= -\frac{3m^2}{2F_\star^2}\left(1-\frac{2m^2}{3m_b^{\star 2}}\right)\left[L + \frac{1}{32\pi^2}\ln\frac{m^2}{\mu^2}\right] - \frac{m^2}{32F_\star^2\pi^2} \\
&\quad + \frac{3m^3}{32F_\star^2 m_b^\star \pi^2}\frac{\left(1-\frac{m^2}{3m_b^{\star 2}}\right)}{\sqrt{1-\frac{m^2}{4m_b^{\star 2}}}}\arccos\left(-\frac{m^2}{2m_b^{\star 2}}\right) \ .
\end{aligned}
\tag{C.5c}
$$

L contains the divergence and the finite constants typical for the modified minimal subtraction scheme in $d = 4-\epsilon$ dimensions (see eq. (A.28)). Note that we have shown that the divergences of leading one-loop order can be canceled. For practical purposes one can therefore set L to zero everywhere if one simultaneously replaces the corresponding DAs by the renormalized ones (compare section 4.5). Within our level of accuracy it is legitimate to replace $m_b^\star$ and $F_\star$ by their values at the symmetric point, where $\bar{m}_q = \bar{m}_q^{\mathrm{phys}}$.

C.2 Handbook of distribution amplitudes

In this section we express the 24 standard DAs occurring in the general decomposition derived in ref. [76] (S_i^B, P_i^B, V_i^B, A_i^B, T_i^B) in terms of the DAs defined in section 4.5. The equations given below follow directly from the definition of the DAs in eqs. (4.70) and (4.72) together with the symmetry properties of the standard DAs under exchange of the first and the second variable given in eq. (4.10). For the twist-three and twist-six amplitudes one finds

$$\begin{aligned}
V_{1/6}^B &= \frac{1}{2}\left(\frac{\Phi_{+,3/6}^B}{c_B^+}+\frac{\Phi_{-,3/6}^B}{c_B^-}\right)(x_1,x_2,x_3)+\frac{(-1)_B}{2}\left(\frac{\Phi_{+,3/6}^B}{c_B^+}+\frac{\Phi_{-,3/6}^B}{c_B^-}\right)(x_2,x_1,x_3)\,,\\
A_{1/6}^B &= -\frac{1}{2}\left(\frac{\Phi_{+,3/6}^B}{c_B^+}+\frac{\Phi_{-,3/6}^B}{c_B^-}\right)(x_1,x_2,x_3)+\frac{(-1)_B}{2}\left(\frac{\Phi_{+,3/6}^B}{c_B^+}+\frac{\Phi_{-,3/6}^B}{c_B^-}\right)(x_2,x_1,x_3)\,,\\
T_{1/6}^B &= (-1)_B\frac{\Pi_{3/6}^B(x_1,x_3,x_2)}{c_B^-}\,,
\end{aligned}\tag{C.6}$$

where the DAs on the l.h.s. are functions of (x_1,x_2,x_3). The twist-four and twist-five amplitudes read

$$\begin{aligned}
S_{1/2}^B &= \frac{(-1)_B}{24}\left(\frac{\Xi_{+,4/5}^B}{c_B^+}+\frac{\Xi_{-,4/5}^B}{c_B^-}\right)(x_1,x_2,x_3)-\frac{1}{24}\left(\frac{\Xi_{+,4/5}^B}{c_B^+}+\frac{\Xi_{-,4/5}^B}{c_B^-}\right)(x_2,x_1,x_3)\\
&\quad+\frac{1}{4}\left(\frac{\Pi_{4/5}^B(x_2,x_3,x_1)}{c_B^-}-(-1)_B\frac{\Pi_{4/5}^B(x_1,x_3,x_2)}{c_B^-}\right)\,,\\
P_{1/2}^B &= \frac{(-1)_B}{24}\left(\frac{\Xi_{+,4/5}^B}{c_B^+}+\frac{\Xi_{-,4/5}^B}{c_B^-}\right)(x_1,x_2,x_3)-\frac{1}{24}\left(\frac{\Xi_{+,4/5}^B}{c_B^+}+\frac{\Xi_{-,4/5}^B}{c_B^-}\right)(x_2,x_1,x_3)\\
&\quad-\frac{1}{4}\left(\frac{\Pi_{4/5}^B(x_2,x_3,x_1)}{c_B^-}-(-1)_B\frac{\Pi_{4/5}^B(x_1,x_3,x_2)}{c_B^-}\right)\,,\\
V_{2/5}^B &= \frac{1}{4}\left(\frac{\Phi_{+,4/5}^B}{c_B^+}+\frac{\Phi_{-,4/5}^B}{c_B^-}\right)(x_1,x_2,x_3)+\frac{(-1)_B}{4}\left(\frac{\Phi_{+,4/5}^B}{c_B^+}+\frac{\Phi_{-,4/5}^B}{c_B^-}\right)(x_2,x_1,x_3)\,,\\
A_{2/5}^B &= -\frac{1}{4}\left(\frac{\Phi_{+,4/5}^B}{c_B^+}+\frac{\Phi_{-,4/5}^B}{c_B^-}\right)(x_1,x_2,x_3)+\frac{(-1)_B}{4}\left(\frac{\Phi_{+,4/5}^B}{c_B^+}+\frac{\Phi_{-,4/5}^B}{c_B^-}\right)(x_2,x_1,x_3)\,,\\
V_{3/4}^B &= \frac{(-1)_B}{4}\left(\frac{\Phi_{+,4/5}^B}{c_B^+}-\frac{\Phi_{-,4/5}^B}{c_B^-}\right)(x_3,x_1,x_2)+\frac{1}{4}\left(\frac{\Phi_{+,4/5}^B}{c_B^+}-\frac{\Phi_{-,4/5}^B}{c_B^-}\right)(x_3,x_2,x_1)\,,\\
A_{3/4}^B &= -\frac{(-1)_B}{4}\left(\frac{\Phi_{+,4/5}^B}{c_B^+}-\frac{\Phi_{-,4/5}^B}{c_B^-}\right)(x_3,x_1,x_2)+\frac{1}{4}\left(\frac{\Phi_{+,4/5}^B}{c_B^+}-\frac{\Phi_{-,4/5}^B}{c_B^-}\right)(x_3,x_2,x_1)\,,\\
T_{2/5}^B &= \frac{\Upsilon_{4/5}^B(x_3,x_2,x_1)}{6c_B^-}\,,\\
T_{3/4}^B &= \frac{(-1)_B}{24}\left(\frac{\Xi_{+,4/5}^B}{c_B^+}+\frac{\Xi_{-,4/5}^B}{c_B^-}\right)(x_1,x_2,x_3)+\frac{1}{24}\left(\frac{\Xi_{+,4/5}^B}{c_B^+}+\frac{\Xi_{-,4/5}^B}{c_B^-}\right)(x_2,x_1,x_3)\\
&\quad+\frac{1}{4}\left(\frac{\Pi_{4/5}^B(x_2,x_3,x_1)}{c_B^-}+(-1)_B\frac{\Pi_{4/5}^B(x_1,x_3,x_2)}{c_B^-}\right)\,,
\end{aligned}$$

$$T^B_{7/8} = -\frac{(-1)_B}{24}\left(\frac{\Xi^B_{+,4/5}}{c^+_B} + \frac{\Xi^B_{-,4/5}}{c^-_B}\right)(x_1,x_2,x_3) - \frac{1}{24}\left(\frac{\Xi^B_{+,4/5}}{c^+_B} + \frac{\Xi^B_{-,4/5}}{c^-_B}\right)(x_2,x_1,x_3)$$
$$+ \frac{1}{4}\left(\frac{\Pi^B_{4/5}(x_2,x_3,x_1)}{c^-_B} + (-1)_B\frac{\Pi^B_{4/5}(x_1,x_3,x_2)}{c^-_B}\right) . \tag{C.7}$$

C.3 Matching to other definitions in the literature

Since we use the same definitions as ref. [76] it is no surprise that

$$f^N = f_N([76]) , \qquad \lambda_1^N = \lambda_1([76]) , \qquad \lambda_2^N = \lambda_2([76]) . \tag{C.8}$$

We can also match some of our constants to the leading twist normalization constants given in ref. [150]. Note that for the Σ and Ξ a relative minus sign originates from the fact that ref. [150] uses Σ^+ and Ξ^- for the definition, while our choice is Σ^- and Ξ^0 in order to have the same sign as for the proton.

$$f^N = f_N([150]) , \tag{C.9a}$$
$$f^\Sigma = -f_\Sigma([150]) , \qquad f_T^\Sigma = -f_\Sigma^T([150]) , \tag{C.9b}$$
$$f^\Xi = -f_\Xi([150]) , \qquad f_T^\Xi = -f_\Xi^T([150]) , \tag{C.9c}$$
$$f^\Lambda = \sqrt{\frac{2}{3}} f_\Lambda([150]) , \qquad \int [dx] x_1 \Phi^\Lambda_{-,3}(x_1,x_2,x_3) = \sqrt{6} f_\Lambda^T([150]) . \tag{C.9d}$$

Due to some misprints and inconsistencies within refs. [151, 152, 193] we are not able to give reliable matching formulas for their definitions.

C.4 Details on the operator construction

Derivatives acting on the baryon field

In the first part of this section we will describe why we can trade covariant derivatives acting on the baryon field for normal derivatives acting on the complete current. This choice is very convenient since the external derivatives (in contrast to the covariant derivatives acting on the baryon field) do not lead to additional loop momenta in the integrals. To show that this formulation only differs in higher order contributions we use the identities

$$\varepsilon^{abc} = u_{aa'}u_{bb'}u_{cc'}\varepsilon^{a'b'c'} , \tag{C.10a}$$
$$\varepsilon^{abc} = (u^\dagger)_{aa'}(u^\dagger)_{bb'}(u^\dagger)_{cc'}\varepsilon^{a'b'c'} , \tag{C.10b}$$

and

$$0 = \big((\partial_\mu u)_{aa'}u_{bb'}u_{cc'} + u_{aa'}(\partial_\mu u)_{bb'}u_{cc'} + u_{aa'}u_{bb'}(\partial_\mu u)_{cc'}\big)\varepsilon^{a'b'c'} , \tag{C.10c}$$
$$0 = \big((\partial_\mu u^\dagger)_{aa'}(u^\dagger)_{bb'}(u^\dagger)_{cc'} + (u^\dagger)_{aa'}(\partial_\mu u^\dagger)_{bb'}(u^\dagger)_{cc'} + (u^\dagger)_{aa'}(u^\dagger)_{bb'}(\partial_\mu u^\dagger)_{cc'}\big)\varepsilon^{a'b'c'} , \tag{C.10d}$$

which follow from $\det(u) = 1$. From these one obtains

$$\begin{aligned}(D_\mu B)_{aa'}\varepsilon^{a'bc} &= \big((\partial_\mu B)_{aa'}\delta_{bb'}\delta_{cc'} + (\Gamma_\mu B)_{aa'}\delta_{bb'}\delta_{cc'} - (B\Gamma_\mu)_{aa'}\delta_{bb'}\delta_{cc'}\big)\varepsilon^{a'b'c'} \\ &= \big((\partial_\mu B)_{aa'}\delta_{bb'}\delta_{cc'} + (\Gamma_\mu B)_{aa'}\delta_{bb'}\delta_{cc'} + (B)_{aa'}(\Gamma_\mu)_{bb'}\delta_{cc'} \\ &\quad + (B)_{aa'}\delta_{bb'}(\Gamma_\mu)_{cc'}\big)\varepsilon^{a'b'c'} \ . \end{aligned} \tag{C.11}$$

Additionally we need

$$\partial_\mu u_X = u_X(u_{\bar{X}}\partial_\mu u_X) = u_X\Big(\Gamma_\mu - (-1)_X\frac{i}{2}u_\mu\Big) \doteq u_X\Gamma_\mu \ , \tag{C.12a}$$

$$\partial_\mu X_M = D_\mu X_M - [\Gamma_\mu, X_M] \doteq -[\Gamma_\mu, X_M] \ , \quad \text{for } X_M \in \{u_\nu, \chi_\pm\} \ . \tag{C.12b}$$

Putting everything together we find for a general structure with arbitrary mesonic building blocks $X_1, X_2, X_3 \in \{u_\nu, \chi_\pm\}$

$$\begin{aligned}&(u_X X_1 D_\mu B)_{aa'}(u_Y X_2)_{bb'}(u_Z X_3)_{cc'}\varepsilon^{a'b'c'} = \\ &\quad = \big((u_X X_1\partial_\mu B)_{aa'}(u_Y X_2)_{bb'}(u_Z X_3)_{cc'} + (u_X X_1\Gamma_\mu B)_{aa'}(u_Y X_2)_{bb'}(u_Z X_3)_{cc'} \\ &\qquad + (u_X X_1 B)_{aa'}(u_Y X_2\Gamma_\mu)_{bb'}(u_Z X_3)_{cc'} + (u_X X_1 B)_{aa'}(u_Y X_2)_{bb'}(u_Z X_3\Gamma_\mu)_{cc'}\big)\varepsilon^{a'b'c'} \\ &\quad \doteq \partial_\mu\big((u_X X_1 B)_{aa'}(u_Y X_2)_{bb'}(u_Z X_3)_{cc'}\big)\varepsilon^{a'b'c'} \ . \end{aligned} \tag{C.13}$$

In the last step we have used

$$u_X X_1\Gamma_\mu \doteq u_X\partial_\mu X_1 + u_X\Gamma_\mu X_1 \doteq u_X\partial_\mu X_1 + (\partial_\mu u_X)X_1 = \partial_\mu(u_X X_1) \ , \tag{C.14}$$

and the same for $u_Y X_2$ and $u_Z X_3$.

Locality of the low-energy operator

In the following we will argue that structures involving baryon and meson fields at different positions can be dropped. We can choose the structure containing the baryon to be situated at x, while we call the second position y such that we can write schematically $B(x, y) = f(x)g(y)$, where g only contains mesonic building blocks. Every derivative acting on g therefore has to be counted as first order in the chiral power counting. It follows trivially that

$$f(x)g(y) = f(x)\big(g(x) + (x-y)\cdot\partial g(x) + \dots\big) \doteq f(x)g(x) \ . \tag{C.15}$$

Properties of the Γ structures

For the construction of the low-energy effective operator in section 4.3.2 we define in eq. (4.19) an object which depends on 4 Dirac indices

$$\Gamma^{i,XYZ}_{\alpha\beta\gamma\delta} = (\gamma_X\Gamma^i_A\gamma_Y C)_{\alpha\beta}(\gamma_Z\Gamma^i_B(i\partial\!\!\!/)^{d_i^m})_{\gamma\delta}(n\cdot\partial)^{d_i^n} \ , \tag{C.16}$$

where the derivatives act on hadron fields. Γ^i_A and Γ^i_B are both elements of the Clifford algebra, where all open Lorentz indices are either contracted between Γ^i_A and Γ^i_B or with a derivative ∂^μ

or with the light-cone vector n^μ. For the explicit expressions which finally enter the construction refer to table 4.2. Analogous to eq. (A.24) we define

$$\Gamma_A^i \otimes \Gamma_B^i = \eta_{\Gamma,i}^P \ \gamma_0\Gamma_A^i\gamma_0 \otimes \gamma_0\Gamma_B^i\gamma_0\Big|_{\substack{\mathbf{n}\to-\mathbf{n}\\ \boldsymbol{\partial}\to-\boldsymbol{\partial}}} , \tag{C.17a}$$

$$\Gamma_A^{i\,\dagger} \otimes \Gamma_B^{i\,\dagger} = \eta_{\Gamma,i}^H \ \gamma_0\Gamma_A^i\gamma_0 \otimes \gamma_0\Gamma_B^i\gamma_0 , \tag{C.17b}$$

$$\Gamma_A^{i\,T} \otimes \Gamma_B^{i\,T} = \eta_{\Gamma,i}^C \ C\Gamma_A^i C \otimes C\Gamma_B^i C , \tag{C.17c}$$

such that

$$\Gamma_A^{i\,*} \otimes \Gamma_B^{i\,*} = \eta_{\Gamma,i}^H\eta_{\Gamma,i}^C \ \gamma_0 C\Gamma_A^i C\gamma_0 \otimes \gamma_0 C\Gamma_B^i C\gamma_0 , \tag{C.18}$$

and

$$\begin{aligned}\Gamma_A^i \otimes \Gamma_B^i\Big|_{\substack{n_0\to-n_0\\ \partial_0\to-\partial_0}} &= (-1)^{\#\text{cont.}} \ \eta_{\Gamma,i}^P \ \gamma_0\Gamma_A^i\gamma_0 \otimes \gamma_0\Gamma_B^i\gamma_0 \\ &= \eta_{\Gamma,i}^P \ \gamma_0\gamma_5\Gamma_A^i\gamma_5\gamma_0 \otimes \gamma_0\gamma_5\Gamma_B^i\gamma_5\gamma_0 ,\end{aligned} \tag{C.19}$$

where #cont. is the number of Lorentz indices within Γ_A^i and Γ_B^i that are contracted with a derivative or a light-cone vector. Using these relations one finds for the complete object

$$\left(\Gamma_{\alpha\beta\gamma\delta}^{i,XYZ}\right)^* = -\eta_{\Gamma,i}^H\eta_{\Gamma,i}^C \ (C\gamma_0)_{\alpha\alpha'}(C\gamma_0)_{\beta\beta'}(C\gamma_0)_{\gamma\gamma'}\Gamma_{\alpha'\beta'\gamma'\delta'}^{i,XYZ}(C\gamma_0)_{\delta'\delta} . \tag{C.20}$$

Under parity transformation the spacelike components of the derivatives change their sign, which leads to

$$\begin{aligned}\mathcal{P}\Gamma_{\alpha\beta\gamma\delta}^{i,XYZ}\mathcal{P}^\dagger &= \Gamma_{\alpha\beta\gamma\delta}^{i,XYZ}\Big|_{\boldsymbol{\partial}\to-\boldsymbol{\partial}} \\ &= \eta_{\Gamma,i}^P \ (\gamma_X\gamma_0\Gamma_A^i\gamma_0\gamma_Y C)_{\alpha\beta}(\gamma_Z\gamma_0\Gamma_B^i\gamma_0(i\gamma_0\partial\!\!\!/\gamma_0)^{d_i^m})_{\gamma\delta}(n\cdot\partial)^{d_i^n}\Big|_{\mathbf{n}\to-\mathbf{n}} \\ &= -\eta_{\Gamma,i}^P \ (\gamma_0)_{\alpha\alpha'}(\gamma_0)_{\beta\beta'}(\gamma_0)_{\gamma\gamma'}\Gamma_{\alpha'\beta'\gamma'\delta'}^{i,\bar{X}\bar{Y}\bar{Z}}(\gamma_0)_{\delta'\delta}\Big|_{\mathbf{n}\to-\mathbf{n}} ,\end{aligned} \tag{C.21}$$

where we have used eq. (C.17a) in the step from the first to the second line. Charge conjugation has no effect on the Γ structure such that one obtains the same result for $\mathcal{CP}$ as for $\mathcal{P}$. But if we take a look at eq. (4.16b) it becomes clear that we have to relate it to its complex conjugate. Using eq. (C.20) one finds

$$\mathcal{CP}\Gamma_{\alpha\beta\gamma\delta}^{i,XYZ}\mathcal{P}^\dagger\mathcal{C}^\dagger = \mathcal{P}\Gamma_{\alpha\beta\gamma\delta}^{i,XYZ}\mathcal{P}^\dagger = -\eta_{\Gamma,i}^C\eta_{\Gamma,i}^P\eta_{\Gamma,i}^H \ C_{\alpha\alpha'}C_{\beta\beta'}C_{\gamma\gamma'}\left(\Gamma_{\alpha'\beta'\gamma'\delta'}^{i,XYZ}\right)^* C_{\delta'\delta}\Big|_{\mathbf{n}\to-\mathbf{n}} . \tag{C.22}$$

Under time reversal the time component of the derivative gets a minus sign. Additionally the complete structure becomes subject to complex conjugation since time reversal is described by an antiunitary operator. By the use of eqs. (C.19) and (C.20) one finds

$$\begin{aligned}\mathcal{T}\Gamma_{\alpha\beta\gamma\delta}^{i,XYZ}\mathcal{T}^\dagger &= \left(\Gamma_{\alpha\beta\gamma\delta}^{i,XYZ}\right)^*\Big|_{\partial_0\to-\partial_0} \\ &= -\eta_{\Gamma,i}^C\eta_{\Gamma,i}^P\eta_{\Gamma,i}^H \ (-1)_X(-1)_Y(-1)_Z C_{\alpha\alpha'}C_{\beta\beta'}C_{\gamma\gamma'}\Gamma_{\alpha'\beta'\gamma'\delta'}^{i,XYZ}(C\gamma_5)_{\delta'\delta}\Big|_{n_0\to-n_0} .\end{aligned} \tag{C.23}$$

C.5 Matching relations

In this section we provide the result of the matching described in section 4.4.3, which is needed in intermediate steps of our calculation (in practical applications one can always use the readily evaluated expressions shown in appendix C.2). For the twist projected amplitudes introduced in ref. [76] one finds

$$
\begin{aligned}
S_1^B(x_1,x_2,x_3) &= \big(2h_{B,\text{even}}^{2,abc} + 2h_{B,\text{odd}}^{2,abc}\big)(x_1,x_2,x_3)\ ,\\
S_2^B(x_1,x_2,x_3) &= \big(-4h_{B,\text{even}}^{1,abc} + 2h_{B,\text{even}}^{2,abc} - 4h_{B,\text{odd}}^{1,abc} + 2h_{B,\text{odd}}^{2,abc}\big)(x_1,x_2,x_3)\ ,\\
P_1^B(x_1,x_2,x_3) &= \big(2h_{B,\text{even}}^{2,abc} - 2h_{B,\text{odd}}^{2,abc}\big)(x_1,x_2,x_3)\ ,\\
P_2^B(x_1,x_2,x_3) &= \big(-4h_{B,\text{even}}^{1,abc} + 2h_{B,\text{even}}^{2,abc} + 4h_{B,\text{odd}}^{1,abc} - 2h_{B,\text{odd}}^{2,abc}\big)(x_1,x_2,x_3)\ ,\\
V_1^B(x_1,x_2,x_3) &= -4h_{B,\text{odd}}^{8,bca}(x_2,x_3,x_1) - 4h_{B,\text{odd}}^{8,cab}(x_3,x_1,x_2)\ ,\\
V_2^B(x_1,x_2,x_3) &= \big(2h_{B,\text{odd}}^{2,bca} + 2h_{B,\text{odd}}^{7,bca} - 2h_{B,\text{odd}}^{8,bca}\big)(x_2,x_3,x_1)\\
&\quad + \big(-2h_{B,\text{odd}}^{2,cab} + 2h_{B,\text{odd}}^{7,cab} - 2h_{B,\text{odd}}^{8,cab}\big)(x_3,x_1,x_2)\ ,\\
V_3^B(x_1,x_2,x_3) &= \big(-2h_{B,\text{odd}}^{2,bca} + 2h_{B,\text{odd}}^{7,bca} - 2h_{B,\text{odd}}^{8,bca}\big)(x_2,x_3,x_1)\\
&\quad + \big(2h_{B,\text{odd}}^{2,cab} + 2h_{B,\text{odd}}^{7,cab} - 2h_{B,\text{odd}}^{8,cab}\big)(x_3,x_1,x_2)\ ,\\
V_4^B(x_1,x_2,x_3) &= \big(4h_{B,\text{odd}}^{1,bca} - 2h_{B,\text{odd}}^{2,bca} + 4h_{B,\text{odd}}^{4,bca} + 2h_{B,\text{odd}}^{7,bca} - 2h_{B,\text{odd}}^{8,bca}\big)(x_2,x_3,x_1)\\
&\quad + \big(-4h_{B,\text{odd}}^{1,cab} + 2h_{B,\text{odd}}^{2,cab} + 4h_{B,\text{odd}}^{4,cab} + 2h_{B,\text{odd}}^{7,cab} - 2h_{B,\text{odd}}^{8,cab}\big)(x_3,x_1,x_2)\ ,\\
V_5^B(x_1,x_2,x_3) &= \big(-4h_{B,\text{odd}}^{1,bca} + 2h_{B,\text{odd}}^{2,bca} + 4h_{B,\text{odd}}^{4,bca} + 2h_{B,\text{odd}}^{7,bca} - 2h_{B,\text{odd}}^{8,bca}\big)(x_2,x_3,x_1)\\
&\quad + \big(4h_{B,\text{odd}}^{1,cab} - 2h_{B,\text{odd}}^{2,cab} + 4h_{B,\text{odd}}^{4,cab} + 2h_{B,\text{odd}}^{7,cab} - 2h_{B,\text{odd}}^{8,cab}\big)(x_3,x_1,x_2)\ ,\\
V_6^B(x_1,x_2,x_3) &= \big(8h_{B,\text{odd}}^{4,bca} + 8h_{B,\text{odd}}^{7,bca} - 4h_{B,\text{odd}}^{8,bca} - 16h_{B,\text{odd}}^{9,bca}\big)(x_2,x_3,x_1)\\
&\quad + \big(8h_{B,\text{odd}}^{4,cab} + 8h_{B,\text{odd}}^{7,cab} - 4h_{B,\text{odd}}^{8,cab} - 16h_{B,\text{odd}}^{9,cab}\big)(x_3,x_1,x_2)\ ,\\
A_1^B(x_1,x_2,x_3) &= -4h_{B,\text{odd}}^{8,bca}(x_2,x_3,x_1) + 4h_{B,\text{odd}}^{8,cab}(x_3,x_1,x_2)\ ,\\
A_2^B(x_1,x_2,x_3) &= \big(2h_{B,\text{odd}}^{2,bca} + 2h_{B,\text{odd}}^{7,bca} - 2h_{B,\text{odd}}^{8,bca}\big)(x_2,x_3,x_1)\\
&\quad + \big(2h_{B,\text{odd}}^{2,cab} - 2h_{B,\text{odd}}^{7,cab} + 2h_{B,\text{odd}}^{8,cab}\big)(x_3,x_1,x_2)\ ,\\
A_3^B(x_1,x_2,x_3) &= \big(2h_{B,\text{odd}}^{2,bca} - 2h_{B,\text{odd}}^{7,bca} + 2h_{B,\text{odd}}^{8,bca}\big)(x_2,x_3,x_1)\\
&\quad + \big(2h_{B,\text{odd}}^{2,cab} + 2h_{B,\text{odd}}^{7,cab} - 2h_{B,\text{odd}}^{8,cab}\big)(x_3,x_1,x_2)\ ,\\
A_4^B(x_1,x_2,x_3) &= \big(-4h_{B,\text{odd}}^{1,bca} + 2h_{B,\text{odd}}^{2,bca} - 4h_{B,\text{odd}}^{4,bca} - 2h_{B,\text{odd}}^{7,bca} + 2h_{B,\text{odd}}^{8,bca}\big)(x_2,x_3,x_1)\\
&\quad + \big(-4h_{B,\text{odd}}^{1,cab} + 2h_{B,\text{odd}}^{2,cab} + 4h_{B,\text{odd}}^{4,cab} + 2h_{B,\text{odd}}^{7,cab} - 2h_{B,\text{odd}}^{8,cab}\big)(x_3,x_1,x_2)\ ,\\
A_5^B(x_1,x_2,x_3) &= \big(-4h_{B,\text{odd}}^{1,bca} + 2h_{B,\text{odd}}^{2,bca} + 4h_{B,\text{odd}}^{4,bca} + 2h_{B,\text{odd}}^{7,bca} - 2h_{B,\text{odd}}^{8,bca}\big)(x_2,x_3,x_1)\\
&\quad + \big(-4h_{B,\text{odd}}^{1,cab} + 2h_{B,\text{odd}}^{2,cab} - 4h_{B,\text{odd}}^{4,cab} - 2h_{B,\text{odd}}^{7,cab} + 2h_{B,\text{odd}}^{8,cab}\big)(x_3,x_1,x_2)\ ,\\
A_6^B(x_1,x_2,x_3) &= \big(8h_{B,\text{odd}}^{4,bca} + 8h_{B,\text{odd}}^{7,bca} - 4h_{B,\text{odd}}^{8,bca} - 16h_{B,\text{odd}}^{9,bca}\big)(x_2,x_3,x_1)\\
&\quad + \big(-8h_{B,\text{odd}}^{4,cab} - 8h_{B,\text{odd}}^{7,cab} + 4h_{B,\text{odd}}^{8,cab} + 16h_{B,\text{odd}}^{9,cab}\big)(x_3,x_1,x_2)\ ,
\end{aligned}
$$

$$
\begin{aligned}
T_1^B(x_1,x_2,x_3) &= 4h_{B,\text{odd}}^{8,abc}(x_1,x_2,x_3)\ ,\\
T_2^B(x_1,x_2,x_3) &= -16h_{B,\text{even}}^{5,abc}(x_1,x_2,x_3)\ ,\\
T_3^B(x_1,x_2,x_3) &= \big(-8h_{B,\text{even}}^{5,abc}+2h_{B,\text{even}}^{6,abc}-2h_{B,\text{odd}}^{7,abc}+2h_{B,\text{odd}}^{8,abc}\big)(x_1,x_2,x_3)\ ,\\
T_4^B(x_1,x_2,x_3) &= \big(-4h_{B,\text{even}}^{3,abc}-4h_{B,\text{even}}^{4,abc}-8h_{B,\text{even}}^{5,abc}-2h_{B,\text{even}}^{6,abc}\\
&\qquad -4h_{B,\text{odd}}^{4,abc}-2h_{B,\text{odd}}^{7,abc}+2h_{B,\text{odd}}^{8,abc}\big)(x_1,x_2,x_3)\ ,\\
T_5^B(x_1,x_2,x_3) &= \big(-8h_{B,\text{even}}^{4,abc}-16h_{B,\text{even}}^{5,abc}\big)(x_1,x_2,x_3)\ ,\\
T_6^B(x_1,x_2,x_3) &= \big(-8h_{B,\text{odd}}^{4,abc}-8h_{B,\text{odd}}^{7,abc}+4h_{B,\text{odd}}^{8,abc}+16h_{B,\text{odd}}^{9,abc}\big)(x_1,x_2,x_3)\ ,\\
T_7^B(x_1,x_2,x_3) &= \big(8h_{B,\text{even}}^{5,abc}-2h_{B,\text{even}}^{6,abc}-2h_{B,\text{odd}}^{7,abc}+2h_{B,\text{odd}}^{8,abc}\big)(x_1,x_2,x_3)\ ,\\
T_8^B(x_1,x_2,x_3) &= \big(4h_{B,\text{even}}^{3,abc}+4h_{B,\text{even}}^{4,abc}+8h_{B,\text{even}}^{5,abc}+2h_{B,\text{even}}^{6,abc}\\
&\qquad -4h_{B,\text{odd}}^{4,abc}-2h_{B,\text{odd}}^{7,abc}+2h_{B,\text{odd}}^{8,abc}\big)(x_1,x_2,x_3)\ .
\end{aligned}
\tag{C.24}
$$

The functions on the r.h.s. are given in eq. (4.59). For the flavor indices a,b,c on the r.h.s. one has to insert the flavors of the operators for which the l.h.s. is defined. Our choice is $p \mathrel{\hat{=}} uud$, $n \mathrel{\hat{=}} ddu$, $\Sigma^+ \mathrel{\hat{=}} uus$, $\Sigma^0 \mathrel{\hat{=}} uds$, $\Sigma^- \mathrel{\hat{=}} dds$, $\Xi^0 \mathrel{\hat{=}} ssu$, $\Xi^- \mathrel{\hat{=}} ssd$, $\Lambda \mathrel{\hat{=}} uds$, where the order of the flavors is relevant for the symmetry properties of the DAs (cf. eq. (4.12)).

Bibliography

[1] S. L. Glashow, *Partial Symmetries of Weak Interactions*, *Nucl. Phys.* **22** (1961) 579.

[2] S. Weinberg, *A Model of Leptons*, *Phys. Rev. Lett.* **19** (1967) 1264.

[3] A. Salam, *Weak and Electromagnetic Interactions*, in *Proceedings of the 8th Nobel Symposium, Lerum (Sweden), May 19-25, 1968, eConf* **C680519** (1968) 367.

[4] P. W. Higgs, *Broken Symmetries and the Masses of Gauge Bosons*, *Phys. Rev. Lett.* **13** (1964) 508.

[5] C. N. Yang and R. L. Mills, *Conservation of Isotopic Spin and Isotopic Gauge Invariance*, *Phys. Rev.* **96** (1954) 191.

[6] Y. L. Dokshitzer, D. I. Dyakonov, and S. I. Troyan, *Hard Processes in Quantum Chromodynamics*, *Phys. Rept.* **58** (1980) 269.

[7] J. C. Collins, D. E. Soper, and G. Sterman, *Factorization of Hard Processes in QCD*, *Adv. Ser. Direct. High Energy Phys.* **5** (1989) 1, `arXiv:hep-ph/0409313`.

[8] G. P. Lepage and S. J. Brodsky, *Exclusive processes in quantum chromodynamics: Evolution equations for hadronic wavefunctions and the form factors of mesons*, *Phys. Lett.* **87B** (1979) 359.

[9] G. P. Lepage and S. J. Brodsky, *Exclusive processes in perturbative quantum chromodynamics*, *Phys. Rev.* **D22** (1980) 2157.

[10] A. V. Efremov and A. V. Radyushkin, *Factorization and Asymptotic Behaviour of Pion Form Factor in QCD*, *Phys. Lett.* **94B** (1980) 245.

[11] Y. L. Dokshitzer, *Calculation of the structure functions for deep-inelastic scattering and e^+e^- annihilation by perturbation theory in quantum chromodynamics*, *Sov. Phys. JETP* **46** (1977) 641.

[12] V. N. Gribov and L. N. Lipatov, *Deep inelastic e p scattering in perturbation theory*, *Sov. J. Nucl. Phys.* **15** (1972) 438.

[13] G. Altarelli and G. Parisi, *Asymptotic freedom in parton language*, *Nucl. Phys.* **B126** (1977) 298.

[14] J. Collins, *Foundations of perturbative QCD*. Cambridge University Press, Cambridge (UK), 2011.

[15] X. Ji, *Gauge-Invariant Decomposition of Nucleon Spin*, *Phys. Rev. Lett.* **78** (1997) 610, arXiv:hep-ph/9603249.

[16] X. Ji, W. Melnitchouk, and X. Song, *A Study of off forward parton distributions*, *Phys. Rev.* **D56** (1997) 5511, arXiv:hep-ph/9702379.

[17] A. V. Radyushkin, *Nonforward parton distributions*, *Phys. Rev.* **D56** (1997) 5524, arXiv:hep-ph/9704207.

[18] M. Diehl, *Generalized parton distributions*, *Phys. Rept.* **388** (2003) 41, arXiv:hep-ph/0307382.

[19] **EM** Collaboration, J. Ashman et al., *A measurement of the spin asymmetry and determination of the structure function g_1 in deep inelastic muon-proton scattering*, *Phys. Lett.* **B206** (1988) 364.

[20] C. Lorcé, B. Pasquini, and M. Vanderhaeghen, *Unified framework for generalized and transverse-momentum dependent parton distributions within a 3Q light-cone picture of the nucleon*, *JHEP* **05** (2011) 041, arXiv:1102.4704 [hep-ph].

[21] V. M. Braun and I. E. Filyanov, *QCD sum rules in exclusive kinematics and pion wave function*, *Z. Phys.* **C44** (1989) 157.

[22] I. I. Balitsky, V. M. Braun, and A. V. Kolesnichenko, *Radiative decay $\Sigma^+ \to p\gamma$ in quantum chromodynamics*, *Nucl. Phys.* **B312** (1989) 509.

[23] V. L. Chernyak and I. R. Zhitnitsky, *B-meson exclusive decays into baryons*, *Nucl. Phys.* **B345** (1990) 137.

[24] V. M. Braun, *Light cone sum rules*, in *Proceedings of the 4th International Workshop on Progress in Heavy Quark Physics, Rostock (Germany), September 20-22, 1997*, arXiv:hep-ph/9801222.

[25] V. M. Braun, A. Lenz, and M. Wittmann, *Nucleon Form Factors in QCD*, *Phys. Rev.* **D73** (2006) 094019, arXiv:hep-ph/0604050.

[26] M. A. Shifman, A. I. Vainshtein, and V. I. Zakharov, *QCD and Resonance Physics. Theoretical Foundations*, *Nucl. Phys.* **B147** (1979) 385.

[27] M. A. Shifman, A. I. Vainshtein, and V. I. Zakharov, *QCD and Resonance Physics. Applications*, *Nucl. Phys.* **B147** (1979) 448.

[28] M. A. Shifman, *Snapshots of hadrons*, *Prog. Theor. Phys. Suppl.* **131** (1998) 1, arXiv:hep-ph/9802214.

[29] M. A. Shifman, *The Quark-Hadron Duality*, in *Proceedings of QCD@Work 2003 – International Workshop on Quantum Chromodynamics, Conversano (Italy), June 14-18, 2003, eConf* **C030614** (2003) 1.

[30] C. Gattringer and C. B. Lang, *Quantum chromodynamics on the lattice*, *Lect. Notes Phys.* **788** (2010) 1.

[31] K. G. Wilson, *Confinement of Quarks*, *Phys. Rev.* **D10** (1974) 2445.

[32] S. Borsanyi et al., *Ab initio calculation of the neutron-proton mass difference*, *Science* **347** (2015) 1452, arXiv:1406.4088 [hep-lat].

[33] P. C. Bruns, L. Greil, R. Rödl, and A. Schäfer, *Can Baryon Chiral Perturbation Theory be used to extrapolate lattice data for the moment $\langle x \rangle_{u-d}$ of the nucleon?*, arXiv:1411.7528 [hep-lat].

[34] M. Dorati, T. A. Gail, and T. R. Hemmert, *Chiral perturbation theory and the first moments of the generalized parton distributions in a nucleon*, *Nucl. Phys.* **A798** (2008) 96, arXiv:nucl-th/0703073.

[35] P. Wein, *Chiral extrapolation of nucleon wave function normalization constants*. Diploma thesis, Universität Regensburg (Germany), 2011.

[36] P. Wein, P. C. Bruns, T. R. Hemmert, and A. Schäfer, *Chiral extrapolation of nucleon wave function normalization constants*, *Eur. Phys. J.* **A47** (2011) 149, arXiv:1106.3440 [hep-ph].

[37] V. M. Braun, S. Collins, B. Gläßle, M. Göckeler, A. Schäfer, R. W. Schiel, W. Söldner, A. Sternbeck, and P. Wein, *Light-cone distribution amplitudes of the nucleon and negative parity nucleon resonances from lattice QCD*, *Phys. Rev.* **D89** (2014) 094511, arXiv:1403.4189 [hep-lat].

[38] S. Weinberg, *Phenomenological Lagrangians*, *Physica* **A96** (1979) 327.

[39] M. E. Peskin and D. V. Schroeder, *An Introduction to Quantum Field Theory*. Westview Press, Boulder (Colorado, USA), 1995.

[40] S. Weinberg, *The quantum theory of fields. Vol. 2: Modern applications*. Cambridge University Press, Cambridge (UK), 1996.

[41] L. D. Faddeev and V. N. Popov, *Feynman Diagrams for the Yang–Mills Field*, *Phys. Lett.* **25B** (1967) 29.

[42] C. Becchi, A. Rouet, and R. Stora, *Renormalization of Gauge Theories*, *Annals Phys.* **98** (1976) 287.

[43] I. V. Tyutin, *Gauge Invariance in Field Theory and Statistical Physics in Operator Formalism*, *LEBEDEV-75-39* (1975) , arXiv:0812.0580 [hep-th].

[44] G. 't Hooft and M. Veltman, *Regularization and Renormalization of Gauge Fields*, *Nucl. Phys.* **B44** (1972) 189.

[45] F. Olness and R. Scalise, *Regularization, Renormalization, and Dimensional Analysis: Dimensional Regularization meets Freshman E&M*, *Am. J. Phys.* **79** (2011) 306, arXiv:0812.3578 [hep-ph].

[46] W. A. Bardeen, A. J. Buras, D. W. Duke, and T. Muta, *Deep-inelastic scattering beyond the leading order in asymptotically free gauge theories*, *Phys. Rev.* **D18** (1978) 3998.

[47] M. Pospelov and A. Ritz, *Theta vacua, QCD sum rules, and the neutron electric dipole moment*, *Nucl. Phys.* **B573** (2000) 177, arXiv:hep-ph/9908508.

[48] **PDG** Collaboration, K. A. Olive et al., *Review of Particle Physics*, *Chin. Phys.* **C38** (2014) 090001.

[49] **CMS** Collaboration, V. Khachatryan et al., *Measurement of the inclusive* 3*-jet production differential cross section in proton-proton collisions at* 7 TeV *and determination of the strong coupling constant in the* TeV *range*, *Eur. Phys. J.* **C75** (2015) 186, arXiv:1412.1633 [hep-ex].

[50] V. M. Braun, G. P. Korchemsky, and D. Müller, *The Uses of conformal symmetry in QCD*, *Prog. Part. Nucl. Phys.* **51** (2003) 311, arXiv:hep-ph/0306057.

[51] E. Noether, *Invariante Variationsprobleme*, *Nachr. v. d. Ges. d. Wiss. zu Göttingen* (1918) 235, arXiv:physics/0503066 [physics.hist-ph]. (arXiv version translated to English).

[52] S. L. Adler, *Axial-Vector Vertex in Spinor Electrodynamics*, *Phys. Rev.* **177** (1969) 2426.

[53] U. Mosel, *Fields, symmetries, and quarks*. Springer, Berlin (Germany), 2nd ed., 1999.

[54] J. Goldstone, *Field Theories with Superconductor Solutions*, *Nuovo Cim.* **19** (1961) 154.

[55] J. Goldstone, A. Salam, and S. Weinberg, *Broken Symmetries*, *Phys. Rev.* **127** (1962) 965.

[56] C. Vafa and E. Witten, *Restrictions on symmetry breaking in vector-like gauge theories*, *Nucl. Phys.* **B234** (1984) 173.

[57] J. Sivardière, *A simple mechanical model exhibiting a spontaneous symmetry breaking*, *Am. J. Phys.* **51** (1983) 1016.

[58] B. Holstein, *Chiral perturbation theory: An Introduction*, in *Phenomenology and Lattice QCD: Proceedings of the 1993 Uehling Summer School, Seattle (Washington, USA), June 21 - July 2, 1993,* World Scientific, Singapore, 1995.

[59] H. Watanabe and H. Murayama, *Unified Description of Nambu–Goldstone Bosons without Lorentz Invariance*, *Phys. Rev. Lett.* **108** (2012) 251602, arXiv:1203.0609 [hep-th].

[60] P. W. Higgs, *Broken symmetries, massless particles and gauge fields*, *Phys. Lett.* **12** (1964) 132.

[61] P. W. Higgs, *Spontaneous Symmetry Breakdown without Massless Bosons*, *Phys. Rev.* **145** (1966) 1156.

[62] H. Leutwyler, *Chiral effective Lagrangians*, *Lect. Notes Phys.* **396** (1991) 1.

[63] H. Leutwyler, *On the Foundations of Chiral Perturbation Theory*, *Annals Phys.* **235** (1994) 165, arXiv:hep-ph/9311274.

[64] S. Scherer and M. R. Schindler, *A Primer for Chiral Perturbation Theory*, *Lect. Notes Phys.* **830** (2012) 1.

[65] W.-K. Tung, *Group theory in physics*. World Scientific, Singapore, 1985.

[66] S. R. Coleman, J. Wess, and B. Zumino, *Structure of Phenomenological Lagrangians. 1.*, *Phys. Rev.* **177** (1969) 2239.

[67] J. Gasser and H. Leutwyler, *Chiral Perturbation Theory to One Loop*, *Annals Phys.* **158** (1984) 142.

[68] S. Weinberg, *Nonlinear realizations of chiral symmetry*, *Phys. Rev.* **166** (1968) 1568.

[69] J. F. Donoghue and H. Leutwyler, *Energy and momentum in chiral theories*, *Z. Phys.* **C52** (1991) 343.

[70] A. Manohar and H. Georgi, *Chiral quarks and the non-relativistic quark model*, *Nucl. Phys.* **B234** (1984) 189.

[71] J. Gasser and H. Leutwyler, *Chiral perturbation theory: Expansions in the mass of the strange quark*, *Nucl. Phys.* **B250** (1985) 465.

[72] J. Bijnens, *Chiral perturbation theory beyond one loop*, *Prog. Part. Nucl. Phys.* **58** (2007) 521, arXiv:hep-ph/0604043.

[73] C. W. Bernard and M. F. L. Golterman, *Chiral perturbation theory for the quenched approximation of QCD*, *Phys. Rev.* **D46** (1992) 853, arXiv:hep-lat/9204007.

[74] H. Georgi, *Weak Interactions and Modern Particle Theory*. Benjamin Cummings, Menlo Park (California, USA), 1984.

[75] G. S. Bali, V. M. Braun, M. Göckeler, M. Gruber, F. Hutzler, A. Schäfer, R. W. Schiel, J. Simeth, W. Söldner, A. Sternbeck, and P. Wein, *Light-cone distribution amplitudes of the baryon octet*, *JHEP* **02** (2016) 070, arXiv:1512.02050.

[76] V. M. Braun, R. J. Fries, N. Mahnke, and E. Stein, *Higher twist distribution amplitudes of the nucleon in QCD*, *Nucl. Phys.* **B589** (2000) 381, arXiv:hep-ph/0007279. [Erratum: *Nucl. Phys.* **B607** (2001) 433].

[77] S. Scherer, *Introduction to chiral perturbation theory*, *Adv. Nucl. Phys.* **27** (2003) 277, arXiv:hep-ph/0210398.

[78] J. Gasser, M. E. Sainio, and A. Švarc, *Nucleons with Chiral Loops*, *Nucl. Phys.* **B307** (1988) 779.

[79] P. C. Bruns, L. Greil, and A. Schäfer, *The first PDF moments for three dynamical flavors in BChPT*, *Eur. Phys. J.* **A48** (2012) 16, arXiv:1105.6000 [hep-ph].

[80] A. Krause, *Baryon Matrix Elements of the Vector Current in Chiral Perturbation Theory*, *Helv. Phys. Acta* **63** (1990) 3.

[81] N. Fettes, U.-G. Meißner, M. Mojžiš, and S. Steininger, *The Chiral Effective Pion-Nucleon Lagrangian of Order p^4*, *Annals Phys.* **283** (2000) 273, arXiv:hep-ph/0001308. [Erratum: *Annals Phys.* **288** (2001) 249].

[82] J. A. Oller, M. Verbeni, and J. Prades, *Meson-baryon effective chiral Lagrangians to $\mathcal{O}(q^3)$*, *JHEP* **09** (2006) 079, arXiv:hep-ph/0608204. arXiv:hep-ph/0701096.

[83] S. Weinberg, *Effective chiral Lagrangians for nucleon-pion interactions and nuclear forces*, *Nucl. Phys.* **B363** (1991) 3.

[84] V. Bernard, N. Kaiser, J. Kambor, and U.-G. Meißner, *Chiral structure of the nucleon*, *Nucl. Phys.* **B388** (1992) 315.

[85] V. Bernard, N. Kaiser, and U.-G. Meißner, *Chiral dynamics in nucleons and nuclei*, *Int. J. Mod. Phys.* **E4** (1995) 193, arXiv:hep-ph/9501384.

[86] T. Becher and H. Leutwyler, *Baryon chiral perturbation theory in manifestly Lorentz invariant form*, *Eur. Phys. J.* **C9** (1999) 643, arXiv:hep-ph/9901384.

[87] T. A. Gail, *Chiral Analysis of Baryon Form Factors*. PhD thesis, Technische Universität München (Germany), 2007.

[88] T. Fuchs, J. Gegelia, G. Japaridze, and S. Scherer, *Renormalization of relativistic baryon chiral perturbation theory and power counting*, *Phys. Rev.* **D68** (2003) 056005, arXiv:hep-ph/0302117.

[89] M. R. Schindler, J. Gegelia, and S. Scherer, *Infrared and extended on-mass-shell renormalization of two-loop diagrams*, *Nucl. Phys.* **B682** (2004) 367, arXiv:hep-ph/0310207.

[90] S. Weinberg, *The Quantum theory of fields. Vol. 1: Foundations*. Cambridge University Press, Cambridge (UK), 1995.

[91] M. Maggiore, *A modern introduction to quantum field theory*. Oxford University Press, Oxford (UK), 2005.

[92] R. F. Streater and A. S. Wightman, *PCT, spin and statistics, and all that*. Princeton University Press, Princeton (New Jersey, USA), revised ed., 2000.

[93] G. Lüders, *Proof of the TCP theorem*, *Annals Phys.* **2** (1957) 1.

[94] M. Fierz, *Zur Fermischen Theorie des β-Zerfalls*, *Z. Phys.* **104** (1937) 553.

[95] C. Itzykson and J.-B. Zuber, *Quantum Field Theory*. McGraw–Hill, New York (USA), 1980.

[96] C. C. Nishi, *Simple derivation of general Fierz-like identities*, *Am. J. Phys.* **73** (2005) 1160, arXiv:hep-ph/0412245.

[97] P. Wein, P. C. Bruns, and A. Schäfer, *First moments of nucleon generalized parton distributions in chiral perturbation theory at full one-loop order*, *Phys. Rev.* **D89** (2014) 116002, arXiv:1402.4979 [hep-ph].

[98] D. Müller, D. Robaschik, B. Geyer, F.-M. Dittes, and J. Hořejši, *Wave functions, evolution equations and evolution kernels from light-ray operators of QCD*, *Fortsch. Phys.* **42** (1994) 101, arXiv:hep-ph/9812448.

[99] X. Ji, *Generalized parton distributions*, *Ann. Rev. Nucl. Part. Sci.* **54** (2004) 413.

[100] A. V. Belitsky and A. V. Radyushkin, *Unraveling hadron structure with generalized parton distributions*, *Phys. Rept.* **418** (2005) 1, arXiv:hep-ph/0504030.

[101] B. Z. Kopeliovich, I. Schmidt, and M. Siddikov, *Flavor structure of generalized parton distributions from neutrino experiments*, *Phys. Rev.* **D86** (2012) 113018, arXiv:1210.4825 [hep-ph].

[102] K. Kumerički, S. Liuti, and H. Moutarde, *GPD phenomenology and DVCS fitting – Entering the high-precision era*, arXiv:1602.02763 [hep-ph].

[103] L. Favart, M. Guidal, T. Horn, and P. Kroll, *Deeply Virtual Meson Production on the nucleon*, arXiv:1511.04535 [hep-ph].

[104] C. Lorcé, *Spin-orbit correlations in the nucleon*, *Phys. Lett.* **B735** (2014) 344, arXiv:1401.7784 [hep-ph].

[105] D. Arndt and M. J. Savage, *Chiral corrections to matrix elements of twist-2 operators*, *Nucl. Phys.* **A697** (2002) 429–439, arXiv:nucl-th/0105045.

[106] A. V. Belitsky and X. Ji, *Chiral structure of nucleon gravitational form factors*, *Phys. Lett.* **B538** (2002) 289, arXiv:hep-ph/0203276.

[107] M. Diehl, A. N. Manashov, and A. Schäfer, *Chiral perturbation theory for nucleon generalized parton distributions*, *Eur. Phys. J.* **A29** (2006) 315, arXiv:hep-ph/0608113.

[108] M. Diehl, A. N. Manashov, and A. Schäfer, *Generalized parton distributions for the nucleon in chiral perturbation theory*, *Eur. Phys. J.* **A31** (2007) 335, arXiv:hep-ph/0611101.

[109] S.-i. Ando, J.-W. Chen, and C.-W. Kao, *Leading chiral corrections to the nucleon generalized parton distributions*, *Phys. Rev.* **D74** (2006) 094013, arXiv:hep-ph/0602200.

[110] P. Wang and A. W. Thomas, *The First Moments of Nucleon Generalized Parton Distributions*, *Phys. Rev.* **D81** (2010) 114015, arXiv:1003.0957 [hep-ph].

[111] W. Detmold and C. J. D. Lin, *Twist-two matrix elements at finite and infinite volume*, *Phys. Rev.* **D71** (2005) 054510, arXiv:hep-lat/0501007.

[112] A. M. Moiseeva and A. A. Vladimirov, *On chiral corrections to nucleon GPD*, *Eur. Phys. J.* **A49** (2013) 23, arXiv:1208.1714 [hep-ph].

[113] X. Ji, *Breakup of hadron masses and the energy-momentum tensor of QCD*, *Phys. Rev.* **D52** (1995) 271, arXiv:hep-ph/9502213.

[114] R. Baur and J. Kambor, *Generalized heavy baryon chiral perturbation theory*, *Eur. Phys. J.* **C7** (1999) 507, arXiv:hep-ph/9803311.

[115] A. Lacour, B. Kubis, and U.-G. Meißner, *Hyperon decay form-factors in chiral perturbation theory*, *JHEP* **10** (2007) 083, arXiv:0708.3957 [hep-ph].

[116] M. Diehl, A. N. Manashov, and A. Schäfer, *Generalized parton distributions for the pion in chiral perturbation theory*, *Phys. Lett.* **B622** (2005) 69, arXiv:hep-ph/0505269.

[117] N. Kivel and M. V. Polyakov, *One loop chiral corrections to hard exclusive processes: 1. Pion case*, arXiv:hep-ph/0203264.

[118] **QCDSF** Collaboration, V. M. Braun et al., *Nucleon distribution amplitudes and proton decay matrix elements on the lattice*, *Phys. Rev.* **D79** (2009) 034504, arXiv:0811.2712 [hep-lat].

[119] S. Güsken, *A study of smearing techniques for hadron correlation functions*, *Nucl. Phys. B (Proc. Suppl.)* **17** (1990) 361.

[120] M. Falcioni, M. L. Paciello, G. Parisi, and B. Taglienti, *Again on SU(3) glueball mass*, *Nucl. Phys.* **B251** (1985) 624.

[121] J. S. S. Najjar, *Nucleon structure from stochastic estimators*. PhD thesis, Universität Regensburg (Germany), 2014. http://nbn-resolving.de/urn:nbn:de:bvb:355-epub-306948.

[122] G. Bali, S. Collins, M. Göckeler, R. Rödl, A. Schäfer, and A. Sternbeck, *Nucleon generalized form factors from lattice QCD with nearly physical quark masses*, *PoS* **LATTICE2015** (2016) 118, arXiv:1601.04818 [hep-lat].

[123] B. Sheikholeslami and R. Wohlert, *Improved Continuum Limit Lattice Action for QCD with Wilson Fermions*, *Nucl. Phys.* **B259** (1985) 572.

[124] **QCDSF** Collaboration, G. S. Bali et al., *Nucleon mass and sigma term from lattice QCD with two light fermion flavors*, *Nucl. Phys.* **B866** (2013) 1, arXiv:1206.7034 [hep-lat].

[125] R. Sommer, *A New way to set the energy scale in lattice gauge theories and its applications to the static force and α_s in SU(2) Yang–Mills theory*, *Nucl. Phys.* **B411** (1994) 839, arXiv:hep-lat/9310022.

[126] G. S. Bali et al., *Nucleon isovector couplings from $N_f = 2$ lattice QCD*, *Phys. Rev.* **D91** (2015) 054501, arXiv:1412.7336 [hep-lat].

[127] **QCDSF/UKQCD** Collaboration, M. Göckeler et al., *Perturbative and Nonperturbative Renormalization in Lattice QCD*, *Phys. Rev.* **D82** (2010) 114511, arXiv:1003.5756 [hep-lat]. [Erratum: *Phys. Rev.* **D86** (2012) 099903].

[128] G. S. Bali, S. Collins, B. Gläßle, M. Göckeler, J. Najjar, R. H. Rödl, A. Schäfer, R. W. Schiel, A. Sternbeck, and W. Söldner, *The moment $\langle x \rangle_{u-d}$ of the nucleon from $N_f = 2$ lattice QCD down to nearly physical quark masses*, *Phys. Rev.* **D90** (2014) 074510, arXiv:1408.6850 [hep-lat].

[129] G. S. Bali et al., *Nucleon generalized form factors and sigma term from lattice QCD near the physical quark mass*, *PoS* **LATTICE2013** (2014) 291, arXiv:1312.0828 [hep-lat].

[130] J. Gao et al., *CT10 next-to-next-to-leading order global analysis of QCD*, *Phys. Rev.* **D89** (2014) 033009, arXiv:1302.6246 [hep-ph].

[131] S. Alekhin, J. Blümlein, and S. Moch, *The ABM parton distributions tuned to LHC data*, *Phys. Rev.* **D89** (2014) 054028, arXiv:1310.3059 [hep-ph].

[132] **NNPDF** Collaboration, R. D. Ball et al., *Parton distributions with LHC data*, *Nucl. Phys.* **B867** (2013) 244, arXiv:1207.1303 [hep-ph].

[133] A. D. Martin, W. J. Stirling, R. S. Thorne, and G. Watt, *Uncertainties on α_S in global PDF analyses and implications for predicted hadronic cross sections*, *Eur. Phys. J.* **C64** (2009) 653, arXiv:0905.3531 [hep-ph].

[134] L. Greil, P. Wein, P. C. Bruns, and A. Schäfer, *Finite Volume corrections to $\langle x \rangle_{u \pm d}$*, *Phys. Rev.* **D90** (2014) 114002, arXiv:1406.6866 [hep-lat].

[135] P. C. Bruns, L. Greil, and A. Schäfer, *Chiral extrapolation of baryon mass ratios*, *Phys. Rev.* **D87** (2013) 054021, arXiv:1209.0980 [hep-ph].

[136] S. Dürr, *Validity of ChPT – is $M_\pi = 135$ MeV small enough?*, *PoS* **LATTICE2014** (2015) 006, arXiv:1412.6434 [hep-lat].

[137] M. Burkardt, *Transverse deformation of parton distributions and transversity decomposition of angular momentum*, *Phys. Rev.* **D72** (2005) 094020, arXiv:hep-ph/0505189.

[138] M. Burkardt, *Transversity decomposition of quark angular momentum*, *Phys. Lett.* **B639** (2006) 462.

[139] P. Wein and A. Schäfer, *Model-independent calculation of SU(3)$_f$ violation in baryon octet light-cone distribution amplitudes*, *JHEP* **05** (2015) 073, arXiv:1501.07218 [hep-ph].

[140] **WA89** Collaboration, M. I. Adamovich et al., *Ξ^- production by Σ^-, π^- and neutrons in the hyperon beam experiment at CERN*, *Z. Phys.* **C76** (1997) 35.

[141] Y. A. Aleksandrov et al., *The high-intensity hyperon beam at CERN*, *Nucl. Instrum. Meth.* **A408** (1998) 359, arXiv:physics/9801006 [physics.acc-ph].

[142] **LHCb** Collaboration, R. Aaij et al., *Measurement of Form-Factor-Independent Observables in the Decay $B^0 \to K^{*0}\mu^+\mu^-$*, *Phys. Rev. Lett.* **111** (2013) 191801, arXiv:1308.1707 [hep-ex].

[143] T. M. Aliev, A. Özpineci, and M. Savcı, *Model independent analysis of Λ baryon polarizations in $\Lambda_b \to \Lambda\ell^+\ell^-$ decay*, *Phys. Rev.* **D67** (2003) 035007, arXiv:hep-ph/0211447.

[144] T. M. Aliev, A. Özpineci, and M. Savcı, *Exclusive $\Lambda_b \to \Lambda\ell^+\ell^-$ decay beyond standard model*, *Nucl. Phys.* **B649** (2003) 168, arXiv:hep-ph/0202120.

[145] T. Feldmann and M. W. Y. Yip, *Form factors for $\Lambda_b \to \Lambda$ transitions in the soft-collinear effective theory*, *Phys. Rev.* **D85** (2012) 014035, arXiv:1111.1844 [hep-ph]. [Erratum: *Phys. Rev.* **D86** (2012) 079901].

[146] Y.-M. Wang and Y.-L. Shen, *Perturbative Corrections to $\Lambda_b \to \Lambda$ Form Factors from QCD Light-Cone Sum Rules*, arXiv:1511.09036 [hep-ph].

[147] **CDF** Collaboration, T. Aaltonen et al., *Observation of the Baryonic Flavor-Changing Neutral Current Decay $\Lambda_b \to \Lambda\mu^+\mu^-$*, *Phys. Rev. Lett.* **107** (2011) 201802, arXiv:1107.3753 [hep-ex].

[148] **LHCb** Collaboration, R. Aaij et al., *Measurement of the differential branching fraction of the decay $\Lambda_b^0 \to \Lambda\mu^+\mu^-$*, *Phys. Lett.* **B725** (2013) 25, arXiv:1306.2577 [hep-ex].

[149] Y.-M. Wang, Y. Li, and C.-D. Lu, *Rare decays of $\Lambda_b \to \Lambda\gamma$ and $\Lambda_b \to \Lambda\ell^+\ell^-$ in the light-cone sum rules*, *Eur. Phys. J.* **C59** (2009) 861, arXiv:0804.0648 [hep-ph].

[150] V. L. Chernyak, A. A. Ogloblin, and I. R. Zhitnitsky, *Wave functions of octet baryons*, *Z. Phys.* **C42** (1989) 569.

[151] Y.-L. Liu and M.-Q. Huang, *Distribution amplitudes of Σ and Λ and their electromagnetic form factors*, *Nucl. Phys.* **A821** (2009) 80, arXiv:0811.1812 [hep-ph].

[152] Y.-L. Liu and M.-Q. Huang, *Light-cone distribution amplitudes of Ξ and their applications*, *Phys. Rev.* **D80** (2009) 055015, arXiv:0909.0372 [hep-ph].

[153] I. V. Anikin, V. M. Braun, and N. Offen, *Nucleon form factors and distribution amplitudes in QCD*, *Phys. Rev.* **D88** (2013) 114021, arXiv:1310.1375 [hep-ph].

[154] I. V. Anikin and A. N. Manashov, *Higher twist nucleon distribution amplitudes in Wandzura-Wilczek approximation*, *Phys. Rev.* **D89** (2014) 014011, arXiv:1311.3584 [hep-ph].

[155] V. M. Braun, A. N. Manashov, and J. Rohrwild, *Baryon operators of higher twist in QCD and nucleon distribution amplitudes*, *Nucl. Phys.* **B807** (2009) 89, arXiv:0806.2531 [hep-ph].

[156] S. Wandzura and F. Wilczek, *Sum Rules for Spin-Dependent Electroproduction: Test of Relativistic Constituent Quarks*, *Phys. Lett.* **72B** (1977) 195.

[157] J. Lach and P. Zenczykowski, *Hyperon radiative decays*, *Int. J. Mod. Phys.* **A10** (1995) 3817.

[158] **QCDSF/UKQCD** Collaboration, W. Bietenholz et al., *Flavour blindness and patterns of flavour symmetry breaking in lattice simulations of up, down and strange quarks*, *Phys. Rev.* **D84** (2011) 054509, arXiv:1102.5300 [hep-lat].

[159] **QCDSF/UKQCD** Collaboration, M. Göckeler et al., *Baryon Axial Charges and Momentum Fractions with $N_f = 2 + 1$ Dynamical Fermions*, *PoS* **LATTICE2010** (2010) 163, arXiv:1102.3407 [hep-lat].

[160] **QCDSF/UKQCD** Collaboration, A. N. Cooke et al., *SU(3) flavour breaking and baryon structure*, *PoS* **LATTICE2013** (2014) 278, arXiv:1311.4916 [hep-lat].

[161] X. Ji, J.-P. Ma, and F. Yuan, *Three quark light cone amplitudes of the proton and quark orbital motion dependent observables*, *Nucl. Phys.* **B652** (2003) 383, arXiv:hep-ph/0210430.

[162] J.-W. Chen and I. W. Stewart, *Model-independent results for SU(3) violation in light-cone distribution functions*, *Phys. Rev. Lett.* **92** (2004) 202001, arXiv:hep-ph/0311285.

[163] J.-W. Chen, H.-M. Tsai, and K.-C. Weng, *Model-independent results for SU(3) violation in twist-3 light-cone distribution functions*, *Phys. Rev.* **D73** (2006) 054010, arXiv:hep-ph/0511036.

[164] M. Gell-Mann, *The Eightfold Way: A Theory of strong interaction symmetry*, *CTSL-20, TID-12608* (1961) .

[165] I. V. Anikin and A. N. Manashov, *Baryon octet distribution amplitudes in Wandzura-Wilczek approximation*, arXiv:1512.07141 [hep-ph].

[166] P. Ball, V. M. Braun, Y. Koike, and K. Tanaka, *Higher twist distribution amplitudes of vector mesons in QCD: Formalism and twist 3 distributions*, *Nucl. Phys.* **B529** (1998) 323, arXiv:hep-ph/9802299.

[167] V. M. Braun and A. Lenz, *SU(3) symmetry-breaking corrections to meson distribution amplitudes*, *Phys. Rev.* **D70** (2004) 074020, arXiv:hep-ph/0407282.

[168] F. X. Lee and D. B. Leinweber, *Negative-parity baryon spectroscopy*, *Nucl. Phys. B (Proc. Suppl.)* **73** (1999) 258, arXiv:hep-lat/9809095.

[169] **QCDSF/UKQCD** Collaboration, M. Göckeler et al., *Non-perturbative renormalization of three-quark operators*, *Nucl. Phys.* **B812** (2009) 205, arXiv:0810.3762 [hep-lat].

[170] T. Kaltenbrunner, M. Göckeler, and A. Schäfer, *Irreducible multiplets of three-quark operators on the lattice: Controlling mixing under renormalization*, *Eur. Phys. J.* **C55** (2008) 387, arXiv:0801.3932 [hep-lat].

[171] T. Kaltenbrunner, *Renormalization of three-quark operators for the nucleon distribution amplitude*. PhD thesis, Universität Regensburg (Germany), 2008. http://nbn-resolving.de/urn:nbn:de:bvb:355-opus-11093.

[172] M. Claudson, M. B. Wise, and L. J. Hall, *Chiral Lagrangian for Deep Mine Physics*, *Nucl. Phys.* **B195** (1982) 297.

[173] V. M. Belyaev and B. L. Ioffe, *Determination of the baryon mass and baryon resonances from the quantum-chromodynamics sum rule. Strange baryons*, *Sov. Phys. JETP* **57** (1983) 716.

[174] B. L. Ioffe and A. V. Smilga, *Hyperon magnetic moments in QCD*, *Phys. Lett.* **133B** (1983) 436.

[175] T. M. Aliev and M. Savcı, *Octet negative parity to octet positive parity electromagnetic transitions in light cone QCD*, *J. Phys.* **G41** (2014) 075007, arXiv:1403.0096 [hep-ph].

[176] M. Lüscher and S. Schaefer, *Lattice QCD without topology barriers*, *JHEP* **07** (2011) 036, arXiv:1105.4749 [hep-lat].

[177] M. Lüscher and S. Schaefer, *Lattice QCD with open boundary conditions and twisted-mass reweighting*, *Comput. Phys. Commun.* **184** (2013) 519, arXiv:1206.2809 [hep-lat].

[178] **ALPHA** Collaboration, M. Bruno, S. Schaefer, and R. Sommer, *Topological susceptibility and the sampling of field space in $N_f = 2$ lattice QCD simulations*, *JHEP* **08** (2014) 150, arXiv:1406.5363 [hep-lat].

[179] **RQCD** Collaboration, W. Söldner, *Lattice QCD with $2 + 1$ Flavors and Open Boundaries: First Results of the Baryon Spectrum*, *PoS* **LATTICE2014** (2015) 099, arXiv:1502.05481 [hep-lat].

[180] M. Bruno et al., *Simulation of QCD with $N_f = 2 + 1$ flavors of non-perturbatively improved Wilson fermions*, *JHEP* **02** (2015) 043, arXiv:1411.3982 [hep-lat].

[181] M. Gruber, *Renormalization of three-quark operators for baryon distribution amplitudes*. PhD thesis, Universität Regensburg (Germany), 2016.

[182] E. Jenkins and A. V. Manohar, *Chiral corrections to the baryon axial currents*, *Phys. Lett.* **B259** (1991) 353.

[183] F. E. Close and R. G. Roberts, *Consistent analysis of the spin content of the nucleon*, *Phys. Lett.* **B316** (1993) 165, arXiv:hep-ph/9306289.

[184] B. Borasoy, *Baryon axial vector currents*, *Phys. Rev.* **D59** (1999) 054021, arXiv:hep-ph/9811411.

[185] S.-L. Zhu, S. Puglia, and M. J. Ramsey-Musolf, *Recoil order chiral corrections to baryon octet axial vector currents*, *Phys. Rev.* **D63** (2001) 034002, arXiv:hep-ph/0009159.

[186] H.-W. Lin and K. Orginos, *Calculation of hyperon axial couplings from lattice QCD*, *Phys. Rev.* **D79** (2009) 034507, arXiv:0712.1214 [hep-lat].

[187] A. Walker-Loud, *Evidence for nonanalytic light quark mass dependence in the baryon spectrum*, *Phys. Rev.* **D86** (2012) 074509, arXiv:1112.2658 [hep-lat].

[188] **QCDSF** Collaboration, R. W. Schiel, G. S. Bali, V. M. Braun, S. Collins, M. Göckeler, C. Hagen, R. Horsley, Y. Nakamura, D. Pleiter, P. E. L. Rakow, A. Schäfer, G. Schierholz, H. Stüben, P. Wein, and J. M. Zanotti, *An Update on Distribution Amplitudes of the Nucleon and its Parity Partner*, *PoS* **LATTICE2011** (2011) 175, arXiv:1112.0473 [hep-lat].

[189] V. L. Chernyak and A. R. Zhitnitsky, *Asymptotic Behaviour of Exclusive Processes in QCD*, *Phys. Rept.* **112** (1984) 173.

[190] V. L. Chernyak and I. R. Zhitnitsky, *Nucleon Wave Function and Nucleon Form Factors in QCD*, *Nucl. Phys.* **B246** (1984) 52.

[191] D. B. Leinweber, W. Melnitchouk, D. G. Richards, A. G. Williams, and J. M. Zanotti, *Baryon spectroscopy in lattice QCD*, *Lect. Notes Phys.* **663** (2005) 71, arXiv:nucl-th/0406032.

[192] **RBC/UKQCD** Collaboration, Y. Aoki, P. Boyle, P. Cooney, L. Del Debbio, R. Kenway, C. M. Maynard, A. Soni, and R. Tweedie, *Proton lifetime bounds from chirally symmetric lattice QCD*, *Phys. Rev.* **D78** (2008) 054505, arXiv:0806.1031 [hep-lat].

[193] Y.-L. Liu, C.-Y. Cui, and M.-Q. Huang, *Higher order light-cone distribution amplitudes of the Lambda baryon*, *Eur. Phys. J.* **C74** (2014) 3041, arXiv:1407.4889 [hep-ph].